Identifying novel molecules controlling CD4+ T cell - dendritic cell interactions

Caio Santos Bonilha

BSc, MSc

Submitted in fulfilment of the requirements for the Degree of Doctor of Philosophy

Institute of Infection, Immunity, and Inflammation

College of Medical, Veterinary & Life Sciences

University of Glasgow

November 2020

Abstract

CD4+ T cell interactions with dendritic cells (DC) are pivotal in adaptive immune responses and play an important role in both protective immunity (e.g. infection) and autoimmune diseases (e.g. rheumatoid arthritis). As such, there is increasing interest in discovering molecules that would promote/disrupt this interaction. Taking advantage of transcriptomic data generated in our lab using a murine model of inflammatory arthritis, we aimed to identify molecules that can control these interactions. We hypothesised that blockade of some of these molecules will disrupt these interactions, affecting T cell activation and/or migration of immune cells that promote pathology. This will not only further our basic understanding of disease processes but may also highlight potential therapeutic targets for human disease.

The F11 receptor (*F11R*) gene, which encodes the junctional adhesion molecule-A (JAM-A), was identified in a gene list previously generated in the laboratory. *F11R* was upregulated in non-migratory leukocytes from inflamed joints in comparison to migratory immune cells. To investigate the role of JAM-A on CD4+ T cell activation, we employed *in vitro* and *in vivo* assays with cells from transgenic T cell receptor (TCR) mice (OTII). Treatment with an antagonistic anti-JAM-A monoclonal antibody (mAb) *in vitro* attenuated CD4+ T cell activation and proliferation and decreased T cell differentiation towards the Th1 subset in comparison with cells treated with its isotype control. *In vivo*, anti-JAM-A mAb treatment impaired CD4+ T cell proliferation in comparison with cells from mice treated with its isotype control. However, prophylactic treatment with anti-JAM-A mAb did not impact clinical disease in an acute, breach of self-tolerance model of arthritis.

These findings are the first to describe a role for JAM-A during CD4+ T cell-DC interactions, but do not support JAM-A as a therapeutic target for rheumatoid arthritis (RA). Future work to evaluate the effects of treatment with JAM-A antagonists in late models of RA, in which autoimmune components may play a bigger role in clinical arthritis, or in models of other autoimmune diseases will further our understanding on JAM-A contribution to human disease.

Acknowledgments

Firstly, I would like to thank my parents for all the love and support since my childhood in a small wood house built by my dad's hands in the middle of the Brazilian Atlantic Forest.

Secondly, I have no words to thank Paul. You believed in my potential more than anyone. Your trust motivated me to work harder day by day. Thanks to you, I'm making an old dream come true of graduating in one of the best universities in the world in this exciting field that is immunology.

Third, I would like to dedicate some words to my other supervisors. Jim, for his amazing support during the whole PhD, and Bob, for… everything. Besides the countless outstanding talks about the theory, Bob was the one who taught me the most inside the lab. Because of you, I know I've been trained well. Your daily support and incredible guidance made everything easier.

I would also like to show my appreciation to all other members of the LIVE group, from the PIs (Megan, Vicky, Pasquale) to postdocs and PhD students. Thanks Hannah and Gavin for the support in the lab and Hannah and Larissa for helping to review this work. Thanks to lab technicians in L5 and L4, to members of the 3I's flow cytometry facility for the constant assistance, especially Alana and Diane, and to members of the CRF staff (a special thanks to Tony, for his outstanding support).

Together, you all made me feel like home and directly or indirectly contributed for everything that was produced in this thesis.

Thanks to the CAPES Foundation (Ministry of Education, Brazil) for funding this PhD.

Author's Declaration

I declare that, except where reference is made to the contribution of others, this thesis is the result of my own work and has not been submitted for any other degree at the University of Glasgow or any other institution.

Signature:

Name: Caio Santos Bonilha

Table of Contents

List of Tables

List of Figures

Abbreviations

Ahr	Aryl hydrocarbon receptor
APC	Antigen presenting cells
APOE	Apolipoprotein E
Batf3	Basic leucine zipper transcription factor ATF-like 3
BCL6	B-cell lymphoma 6 protein
BCR	B cell receptors
BMDCs	Bone marrow-derived dendritic cells
CCL	C-C motif chemokine ligand
CCR	C-C motif chemokine receptor
CD	Cluster of differentiation
CD62L	L-selectin
cDC	Conventional dendritic cell
cDNA	Complementary Deoxyribonucleic Acid
CFA	Complete Freund's Adjuvant
CFSE	Carboxyfluorescein succinimidyl ester
CIA	Collagen-induced arthritis
CII	Collagen II
Con A	Concanavalin A
CRF	Central Research Facility
CTLA-4	Cytotoxic T-lymphocyte associated protein 4
CXCR	C-X-C-chemokine receptor
DC	Dendritic cell
DMARD	Disease-modifying antirheumatic drugs
DR3	Death receptor 3
DSS	Dextran sulphate sodium
Eα	Eα52–68 peptide
F11R	F11 receptor
FBS	Fetal bovine serum
FcεRII	IgE receptors
FDA	Food and Drug Administration
Flt3L	Fms-like tyrosine kinase ligand
FMO	Fluorescence minus one
FOXO1	Forkhead box O1
FoxP3	Forkhead box P3
GAL9	Galectin-9

GATA3	GATA binding protein 3
GC	Germinal centres
GITR	Glucocorticoid-Induced TNF receptor-related protein
GITRL	GITR ligand
GM-CSF	Granulocyte-macrophage colony-stimulating factor
HAO	Heat aggregated OVA
HEV	High endothelial venules
HLA	Human leucocyte antigens
HRP	Horseradish peroxidase
HVEM	Herpesvirus entry mediator
ICAM1	Intercellular adhesion molecule 1
ICOS	Inducible T cell co-stimulator
IFN-I	Type I interferon
IFN-γ	Interferon gamma
IFNGR1	IFN-γ receptor 1
Ig	Immunoglobulin
IgSF	Immunoglobulin superfamily
IL	Interleukin
IL17RA	IL-17 receptor A
IRF4	Interferon response factor 4
IRF8	Interferon regulatory factor 8
iTreg	Induced regulatory T
JAK	Janus kinase
JAM-A	Junctional adhesion molecule-A
KO	Knockout
LAG3	Lymphocyte Activating 3
LAIR1	Leukocyte-associated immunoglobulin-like receptor 1
LDLR	Low density lipoprotein receptor
LFA	Lymphocyte function-associated antigen
LN	Lymph nodes
LPS	Lipopolysaccharides
LTB4	Leukotriene B4
LYVE1	Lymphatic vessel endothelial receptor 1
mAb	Monoclonal antibody
MFI	Median fluorescence intensity
MHC	Major histocompatibility complex
MOC	Manders' overlap coefficient
moDC	Monocyte derived dendritic cell

MS	Multiple sclerosis
NHS	National Health Service
NK	Natural killer
NSAID	Non-steroidal anti-inflammatory drugs
nTreg	Natural T regulatory
OVA	Chicken ovalbumin
PAF	Platelet-activating factor
PBS	Phosphate-Buffered Saline
PBS-T	0.05% Tween 20 in Phosphate-Buffered Saline
PCC	Pearson's correlation index
PD1	Programmed cell death-protein 1
pDC	Plasmacytoid DCs
PDL	Programmed cell death-ligand
PEG	Polyethylene glycol
pLN	Popliteal LNs
PMA	Phorbol myristate acetate
pOVA	OVA peptide 323-339
RA	Rheumatoid arthritis
RANKL	Receptor activator of nuclear factor kappa-B ligand
RBC	Red blood cell
RNA	Ribonucleic acid
RORγt	Retinoic acid-related orphan receptor gamma t
S1P	Sphingosine-1-phosphate
S1PR1	S1P receptor 1
SAP	SLAM-associated protein
SD	Standard deviation
SEMA	Semaphorin
SI	Site of interaction
siRNA	Small Interfering RNA
SLAM	Signaling lymphocytic activation molecule
SLC	Secondary lymphoid-tissue chemokine
SLE	Lupus erythematosus
SOCS1	Suppressor of cytokine signalling 1
STAT	Transducer and activator of transcription molecules
TCR	T cell receptor
Tfh	T follicular helper
TGFß	Transforming growth factor beta
Th	T helper

TIGIT	T cell immunoglobulin and ITIM domain
TIM	T cell immunoglobulin and mucin domain
TL1A	TNF-like ligand 1A
TLR	Toll-like receptors
TNBS	2,4,6-trinitrobenzene sulfonic acid
TNF	Tumour necrosis factor
TNF-α	TNF alpha
TNFRSF	TNF receptor superfamily
tolDCs	Tolerogenic DCs
Treg	T regulatory
VCAM1	Vascular cell adhesion molecule-1
WT	Wild-type mice
αß	Alpha beta
γδ	Gamma delta

Chapter 1 Introduction

1.1 The Immune System

The immune system is composed of a collection of cells, chemicals and processes with the capacity to protect tissues and organs from foreign antigens, such as bacteria, viruses, fungi, parasites, toxins and tumour cells[1]. The immune system can be divided in two categories: the innate and the adaptive immune systems. The innate immune system is traditionally known as the first line of defence, as it induces nonspecific responses immediately or within hours of contact with antigens, aiming for pathogen clearance before they can start an active infection. These responses are mediated by mechanisms that include physical barriers, such as the skin; chemicals, such as proteins and protein fragments of the complement system, coagulation factors and acute-phase proteins; and the participation of immune cells, such as natural killer (NK) cells, macrophages, dendritic cells (DC), mast cells and granulocytes (neutrophils, basophils and eosinophils)[2]. On the other hand, a key feature of the adaptive immune system is the ability to learn and remember specific pathogens to provide long-lasting protection against possible recurrent infections[3]. This protection is dependent on the ability of lymphocytes to recognize specific antigens.

1.2 The Adaptive Immune System

Immunological memory is the main feature of the adaptive immune system, in which specific antigens can be memorized aiming a strong specific response in subsequent encounters with pathogens[4]. Adaptive immune responses in the first encounter with the antigen are called primary response, and often takes days to develop. Lymphocytes need to proliferate and differentiate to become specialised immune cells that will later secrete cytokines (proteins that mediate and regulate the immune system) and antibodies. Memory cells are also induced during this process and remain ready to respond rapidly upon a second encounter with the antigen in a phase called secondary immune response[5]. This shorter delay between antigen exposure and maximal immune response makes the adaptive immune system an efficient protective system upon a second exposure to the antigen,

often clearing the pathogen before considerable damage is caused. The main lineages of lymphocytes responsible for adaptive immune responses are B cells and T cells. Memory cells, specific subsets of B and T cells, are responsible to maintain memory of the adaptive immune system. Nevertheless, participation of DCs, a cell type characteristic of the innate immune system, is essential for generation of memory cells and optimal adaptive immune responses against pathogens[6,7].

DCs are part of a group called antigen presenting cells (APC) that is also composed by B cells and macrophages, cells with the capacity to internalise antigens, process them into peptides and expose these fragments on their cell surface in the context of major histocompatibility complex (MHC) class II molecules[8]. Although some authors consider B cells and macrophages as professional APCs[9], it is consensus that DCs are professional APCs[6,9]. These cells are driven by their surface receptors and chemokines present in the environment that can induce its maturation and facilitate its migration from affected tissues, where they can uptake antigen, to specialised lymphoid organs, where most of antigen presentation to T cells occurs[10]. In addition, DCs are one of the main promoters of central and immune tolerance. In the thymus, DCs promote negative selection of autoreactive T cells and generation of natural T regulatory (Treg) cells[11,12]. In peripheral tissues and lymphoid organs, DCs can also lead to T cell tolerance, preventing responsiveness against foreign or self-antigens that might be subsequently encountered. In the centre of immune tolerance mechanisms are steady-state DCs, cells that express low levels of T cell co-stimulatory molecules. Intercellular interactions between DCs and T cells exemplify the importance of the synergy between the innate and the adaptive immune systems for protective immunity against foreign antigens.

T cells are derived from hematopoietic stem cells in the bone marrow and need to migrate to the thymus to complete their maturation[13,14]. Thymic progenitors that are negative for the surface molecules CD4 and CD8 recombine T cell receptor (TCR) genes in an important event that enables T cells to recognise a diverse range of antigens and that induces expression of both CD4 and CD8 in the surface of these cells. The CD4+ CD8+ cells then go through appropriate thymic selection to control undesirable generation of auto-reactive T cells[12]. These cells can mature

into two functionally distinct sub-lineages that can be distinguished by their TCR, alpha beta (αß) T cells that express TCR comprised of a α and a ß chain, and gamma delta (γδ) T cells that have a γ and a δ chain in its TCR composition[15], although the correlation between TCR type in thymocytes and sub-lineage fate is not always perfect[16]. The TCR α chain is formed of three segments: constant (C) that is common to several TCRs and extends from the cytoplasm to the exterior of the cell membrane, variable (V) that gets in direct contact with the peptide/MHCII complex and joining (J) that connects the C and V regions but also gets in contact with the antigen[17,18]. Simultaneously, the ß chain has a fourth segment called diversity (D), that connects the V and J regions in a process called V(D)J recombination. Their complexity dictates the diversity of T cell clonality, ruled by numerous rearrangements of TCR genes that result in an extensive TCR repertoire randomly generated[19].

T cells enter lymph nodes (LN) via lymphatic vessels or from blood through high endothelial venules (HEV)[20]. Cells from these venules/vessels express surface molecules that allow T cell homing. This process is constituted by three steps: rolling, chemokine activation and arrest, in mechanisms dependent on T cell surface molecules, such as L-selectin (CD62L) and CC-chemokine receptor 7 (CCR7). The T cell then enters the T cell area in a CCR7 dependent way, where they can interact with other immune cells, such as DCs, before finally leaving the LN and re-enter the circulation. γδ T cells are more frequently found in mucosal tissues in comparison with blood or lymphoid tissues. These cells are known to have an important role in immune responses against infections and disruption of the epithelial barrier. Due to the gain of an effector phenotype during its maturation in the thymus, γδ T cells preferentially secrete the cytokines interferon gamma (IFN-γ) and interleukin (IL) 17[21]. On the other hand, αß T cells require activation followed by cell expansion to differentiate and secrete optimal levels of cytokines. When matured, αß T cells conventionally become CD4+CD8- or CD4-CD8+ T cells. Although the TCR is antigen-specific, it can only interact with antigen when it is bound to MHC molecules from the surface of other cells. CD8+ T cells, also called cytotoxic T cells, recognize antigen bound to MHC class I (MHCI), a molecule found on the surface of all nucleated cells. Due to the broad range of cell types possible, cytotoxic T cells are important not only in the immune defence against microbes, but also in the immune surveillance to directly avoid

propagation of abnormal cells. On the other hand, the TCR in CD4+ T cells can only interact with antigen bound to MHC class II (MHCII), a protein found on the surface of APCs[8]. These interactions can lead to CD4+ T cell activation, proliferation, and generation of effector and/or memory T cells[22]. While memory T cells are a long-term survival cell that will remain ready for a secondary exposure to the antigen, cells that can promote effector functions during primary exposure to antigens and are optimal secretors of cytokines are called T helper (Th) cells.

B cells that are generated in the bone marrow will later migrate to the blood and specialized lymphoid organs, such as LN and the spleen, where they will complete their maturation[23]. Both immature and mature B cells are known to express antigen-specific receptors on their surface, called B cell receptors (BCR). While some types of antigens (T cell independent type 2) can activate both immature and mature B cells, others can activate only mature B cells (T cell independent type 1)[24,25]. In the centre of the BCR is a membrane-bound monomeric form of immunoglobulin M (IgM), that is co-expressed with immunoglobulin (Ig) D and the associated proteins cluster of differentiation (CD) 79A and 79B[26], molecules that have relevant signalling functions upon antigen stimulation. B cell responses to antigen can be dependent or independent of T cells[27]. While molecules like polysaccharides and lipopolysaccharides are considered T cell independent antigens, protein antigens generally require the assistance of T cells that respond to the same antigen for full B cell activation. Upon activation with a T dependent antigen, the B cell undergoes clonal expansion and differentiation, which will ultimately generate high-affinity plasma cells that are fated to produce and secrete large amounts of antibodies. Whereas during primary adaptive immune responses the overall level of antibodies secreted by plasma cells is low and can take weeks to reach its peak, secondary responses take less time, and more antibodies are released. Furthermore, this higher secretion is sustained for a longer period of time and these antibodies have greater affinity for its specific antigen when compared with the antibodies produced in the primary adaptive immune response[5]. This higher affinity is due to affinity maturation, a process that involves hyper-mutation of B cell gene segments that encode the antigen-binding site of the antibodies, inducing production of antibodies with higher affinity, avidity and anti-pathogen activity[28]. Therefore, although antibodies have

a strong role in pathogen clearance in secondary adaptive immune responses, they show low effectiveness in responses in which the antigen is being recognized for the first time. Although the main role of B cells in immunity is to produce antibodies, these cells can also present antigen to CD4+ T cells, in interactions that can not only assist T cells differentiation to a specific subset, but also promote B cells survival, generation of high affinity antibodies and differentiation into certain B cell memory subsets[29].

The adaptive immune system is responsible for acquiring tolerance against self-antigens in intercellular mechanisms involving MHC molecules, and to mediate destruction and elimination of pathogens in primary and secondary responses. Mechanisms of induction of CD4+ T cells activation and differentiation that will lead to inflammatory conditions or that control it are essential for the homeostasis and maintenance of tissues and organs. Therefore, the way a naïve CD4+ T cell interacts with a DC in the context of MHCII molecules dictates the fate of important pathways of the adaptive immune system.

1.3 Dendritic Cells (DC)

Among APCs, DCs are the most efficient cells to present antigen to CD4+ T lymphocytes[6]. DCs are cells, derived from hematopoietic stem cells in the bone marrow and integrate the innate and adaptive immune systems. Fms-like tyrosine kinase ligand (Flt3L) and Flt3L receptor signalling can induce differentiation of these stem cells into plasmacytoid DCs (pDC), conventional DCs (cDC) or other DC subsets. Meanwhile, signalling of some factors, such as interferon regulatory factor 8 (IRF8), basic leucine zipper transcription factor ATF-like 3 (Batf3), and type I interferon (IFN-I), strongly restricts the development of common lymphoid or myeloid progenitor lineages into pDCs[30]. In mice, DCs can be classified into five lineages: cDC type 1 (cDC1), cDC type 2 (cDC2), pDC, monocyte derived DC (moDC) and Langerhans cells[6,31]. Conventional DC subtypes can be distinguished by the expression of markers like CD8, present in cDC1, and CD11b, present on cDC2. Both cDC1 and cDC2 express high levels of MHC molecules, and therefore are the main subtypes involved in antigen presentation in both steady state and during inflammation, although the two can induce CD4+ T cell activation or tolerance.

cDC1 are essential for differentiation of CD4+ T cells into Th1 cells. On the other hand, cDC2 appears to more relevant for Th2 differentiation[32].

pDCs are distinguished from cDCs by production of IFN-I and expression of markers such as PDCA1 and low levels of MHCII[6,32]. These cells are rarely found in healthy skin, but in inflammatory conditions, LN and splenic pDCs upregulate CCR6 and CCR10 that facilitate their traffic to the inflamed skin through blood vessels[33]. The entrance of pDCs in LNs is facilitated by the expression of CD62L on its surface. Although pDCs do not normally migrate from the gut to mesenteric LNs, they assist the migration of cDCs in a toll-like receptors (TLR) and tumour necrosis factor (TNF)-dependent manner[34]. Lamina propria as well as lung pDCs have also been found to play a role in the induction of oral tolerance[35]. These cells play an important tolerogenic role in allergic diseases like asthma[36]. pDCs and cDCs are derived from a common DC progenitor cell, while moDCs and Langerhans cells are part of a monocyte/macrophage lineage[32,37]. MoDCs are directly involved in the defence against microbial pathogens and other roles seem to be dependent on the tissue where they are normally found. Lung moDCs secret relatively large amounts of pro-inflammatory cytokines, while dermal moDCs preferentially secrete IL-10[38], suggesting a tolerogenic role in the skin. Langerhans cells are mainly found on the epidermis and in the epithelia of the respiratory, digestive and urogenital tracts and their development *in vivo* is dependent on granulocyte-macrophage colony-stimulating factor (GM-CSF)[37] and IL-34[39]. Langerhans cells act as APCs in many infections and are known to be an optimal driver of Th17 differentiation[40,41].

The development of techniques for generation of mouse DCs induced by GM-CSF *in vitro*, such as bone marrow-derived DCs (BMDCs)[42,43], facilitated the study of T cell-DC interactions and the development of DC immunotherapies. *In vitro* generated tolerogenic DCs (tolDCs), for instance, hold a tolerogenic trait similar to steady-state DCs. TolDCs are being extensively studied for the treatment of autoimmune diseases due to their anti-inflammatory capacity to induce tolerance[44,45]. TolDCs are cells that exhibit resistance to maturation in the presence of stimulatory signals. In vitro induction of tolDCs requires IL-10[46]. These IL-10-induced cells acquire the ability to secrete IL-10, that is known to be essential in the generation of Treg cells. IL-10-induced tolDCs display a semi-mature phenotype, expressing intermediate levels of CD80 and CD86, and low

levels of MHCII. Both BMDCs and tolDCs express different levels of surface proteins in comparison to endogenous equivalent subtypes of DCs found in the spleen, LN or tissue resident DCs[31,47]. However, studies using these cells allowed us to understand better about mechanisms of DC antigen uptake, migration and antigen presentation, essential DC immunomodulatory roles.

1.3.1 DC Activation and Maturation

Immature DCs express a number of receptors that respond to chemokines, such as C-C motif chemokine receptor (CCR) 1, CCR2, CCR6, and assist their migration from the bone marrow to inflamed tissues[48]. When an immature DC captures antigen, stimulation of DC cytokine receptors by inflammatory cytokines (e.g. IL-1) or agonism of TLR receptors by non-bacterial (e.g. DNA/RNA from viruses) or bacteria-derived (e.g. lipopolysaccharides, LPS) antigens trigger DC activation[49]. DC activation induces its transition from immature to mature antigen-presenting DC, in processes that involve loss of endocytic/phagocytic receptors, upregulation of co-stimulatory molecules, change in MHCII compartments and change in morphology. Several surface molecules that actively participate in the crosstalk with CD4+ T cells are upregulated in mature DCs and give an enhanced T cell activation capability to these cells. These are CD80, CD83, CD86, CD40 and MHCII[42,43]. In addition, a profile of proinflammatory cytokine production, characteristic of mature DCs, assures delivery of signal 3 to naïve T cells during priming. In this context, different DC subtypes are specialized in priming T cells that preferentially differentiate into distinct subsets[32]. Changes in morphology increase the motility of the DC[50], an essential feature of DC in the context of the adaptive immune system.

1.3.2 DC Migration to Lymphoid Tissues

DCs are the most efficient APCs for the initial activation of naïve T cells. This function is not only related to the direct crosstalk with the T cell but also to the highly efficient migratory properties of DCs in comparison to other APCs, as they can migrate in a high number from inflamed tissues to lymphoid tissues within hours[51,52]. DCs take up pathogens in affected sites (Figure 1-1), in a process that will often induce their maturation[53,54] and internalize it to carry it through

lymphatic vessels to the LN. DC migration to lymphoid organs requires coordinated action of a number of chemokines. Mature DCs downregulate CCR6 and other chemokine receptors and upregulate CCR7. Agonism of this receptor by chemokines in lymphatic vessels, such as C-C motif chemokine ligand (CCL) 19 and secondary lymphoid-tissue chemokine (SLC), facilitates DC migration to the LN[49]. After entering the LN through afferent lymphatic vessels, the DC reaches the T cell area, where it will present the antigen to naïve CD4+ T cells. Costimulatory signals are delivered by the DCs to the CD4+ T cell, along with the MHCII-peptide complex, and assisted by several cytokines that will stimulate receptors on the surface of the T cell. This will lead to CD4+ T cell activation, clonal expansion and differentiation into Th cells. These effector T cells, thus, egress the LN to migrate to the affected site to assist in pathogen clearance and recruit more immune cells. These coordinated steps are fundamental not only for the immediate response against microbes but also for acquisition of immunological memory by memory T cells[6].

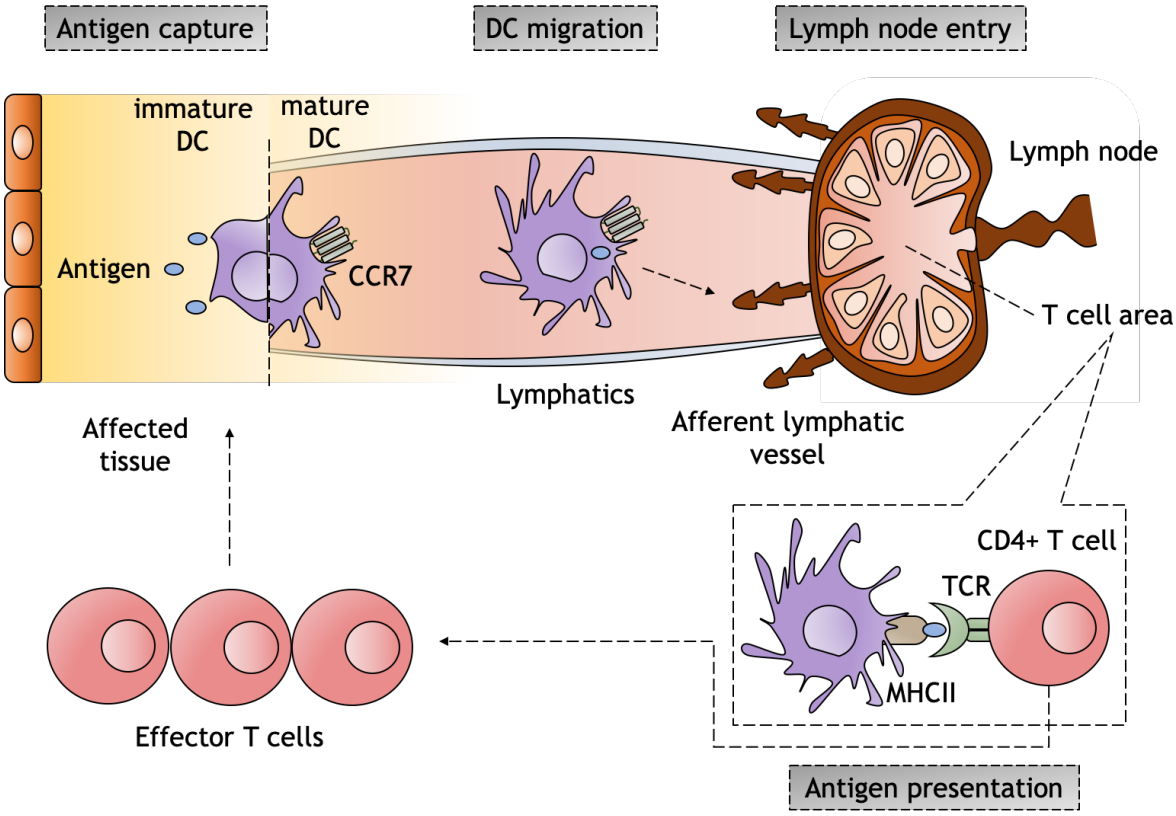

Figure 1-1. Dendritic cell functions in the adaptive immune system upon encounter with a pathogen
Immature dendritic cells (DC) capture potential pathogenic antigens and internalising it in a process that induces its maturation. Mature DC upregulates C-C chemokine receptor 7 (CCR7) that assists DC migration through the lymphatic vascular network to the draining lymph nodes (LN), via afferent lymphatic vessels. In the T cell area of the LN, the antigen is presented through major histocompatibility complex class II (MHCII) molecule to the T cell receptor (TCR) with specificity for this antigen, leading to activation of CD4+ T cells, clonal expansion and differentiation into effector cells that will later execute fundamental functions aiming clearance of the foreign peptide.

1.4 CD4+ T Cell-Antigen Presenting Cell (APC) Interactions in Lymphoid Tissues

While primary lymphoid organs are responsible for generation (bone marrow) and maturation (thymus) of T cells, secondary lymphoid organs, such as LNs and spleen, are a critical location for encounter of leukocytes and its interactions. Several cell types express MHCII and work as APCs to deliver antigen to CD4+ T cells, such as macrophages, B cells and DCs. B cells play an important role in the adaptive immune system not only by differentiating into plasma cells after being activated and secreting antibodies, but also by working as APCs[29]. These cells express high levels of MHCII as a mechanism to present antigen to CD4+ T cells and obtain

feedback from these cells for the production of antibodies with high affinity to the specific antigen involved in these processes.

The TCR is an essential part of the T cell that allows recognition of cognate antigen in the context of MHC molecules. The TCR complex is composed of both TCR chains and an auxiliary protein called CD3, essential for T cell signalling. Many anti-CD3 antibody clones can trigger TCR signalling by directly crosslinking CD3 co-receptors[55,56]. Other transmembrane proteins also bind to MHC molecules and act as a co-receptors for T cell activation, such as CD4[57,58]. This surface molecule is known to contribute to signalling functions, exert intercellular adhesion functions, and stabilize the interaction between the TCR and the MHCII.

1.4.1 CD4+ T Cell-DC Interactions and T Cell Outcomes

The activation of CD4+ T cells induces T cell clonal expansion and differentiation into effector and memory cells that will assist adaptive immune responses. Upon DC migration to the LNs, these cells interact with CD4+ T cells in the T cell area in a complex crosstalk involving several pathways that are described later in this Chapter. Mature recirculating T cells that have not yet encountered an antigen are known as naïve T cells. Naïve CD4+ T cells are found in high proportion in specialized lymphoid organs, where most of antigen presentation occurs. The way a naïve CD4+ T cell encounters an antigen for the first time determines its subsequent phenotype: activated, apoptotic or anergic (Figure 1-2). For optimal T cell activation, three signals are required: the antigen needs to be presented bound by MHCII molecules to the TCR (signal 1), co-stimulation needs to be delivered by intercellular interaction of surface molecules (signal 2), such as CD28-CD80/CD86, and cytokines receptors must be stimulated by proteins released by the APC or other cell types in the immunological environment (signal 3)[59]. In case signal 1 is present but not signal 2, for instance, the T cell will undergo apoptosis or anergy. Tolerance mechanisms such as apoptosis and anergy are essential to keep tissues intact from potential damage caused by self-reactive T cells that escaped the appropriate selection in the thymus. Anergy is a hyporesponsive state of T cells in which they remain inactive, whereas apoptosis is a form of programmed cell death, that will lead to clonal deletion. On the other hand, when an effector state is desirable for assistance of the adaptive immune

system, the T cell will undergo activation. Both the TCR and CD4+ T cells co-receptors are essential for the activation of T cells under the first contact with antigen presented by APCs. This process is called priming.

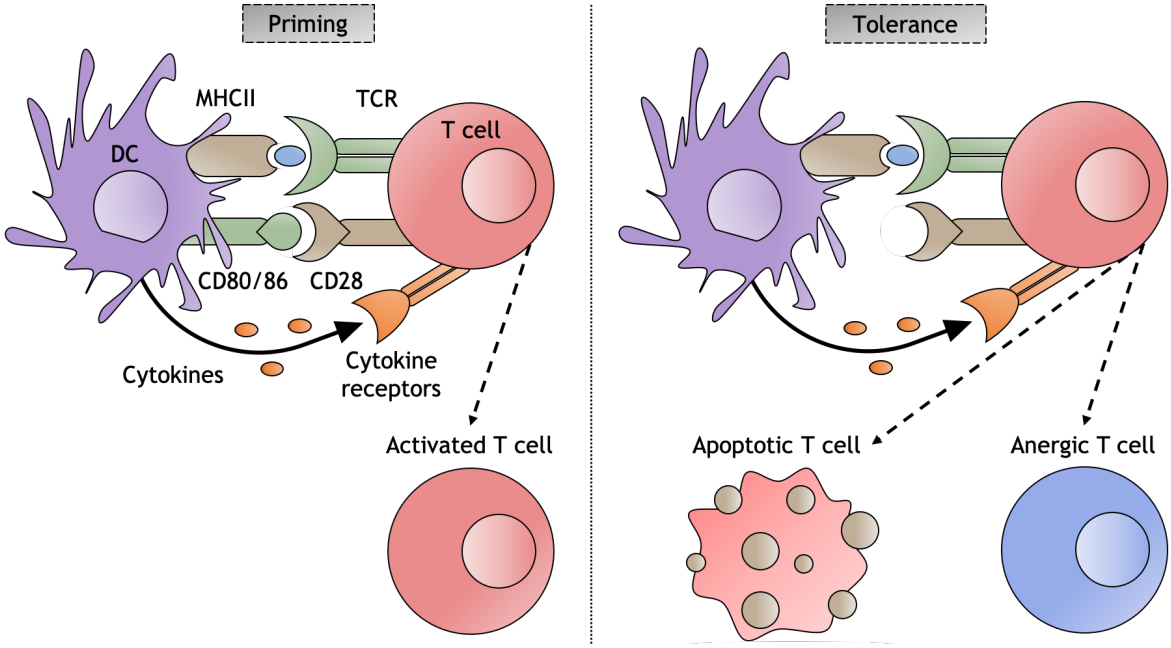

Figure 1-2. Priming vs tolerance on CD4+ T cells
Adapted from[9]. Three signals are required for optimal activation of naïve CD4+ T cells, antigen presentation (signal 1), co-stimulation (signal 2) and stimulation of cytokine receptors (signal 3). On CD4+ T cells, signal 1 is delivered by the professional antigen presenting cell (APC) through presentation of the antigen bound to the surface molecule major histocompatibility complex class II (MHCII) to the T cell receptor (TCR) and is specific. Signal 2 is a non-specific and antigen independent signal that is induced by the interaction of the costimulatory receptor for T cell activation CD28 and the molecules CD80 and CD86 (B7), expressed on the surface of dendritic cells (DC). If costimulatory signal is absent, the cell will undergo apoptosis (deletion) or anergy (unresponsiveness). The stimulation of cytokine receptors on the CD4+ T cell surface triggers pathways that affect T cell activation and proliferation and will dictate T cell differentiation.

Once primed, T cells undergo physical changes, consisting of cell enlargement, an increase in their total ribonucleic acid (RNA) content and a differential regulation of the expression of hundreds of genes[60,61]. This change in gene expression assures a higher expression of surface proteins essential for effector functions of activated CD4+ T cells, as well as a decrease in molecules that prevent achievement of appropriate functions. At this stage, CD62L and CCR7 that functioned as homing receptors to mediate extravasation of naïve T cells migration from the thymus to the LNs through the afferent lymph vessel are no longer necessary[20]. In addition, the type II C-lectin CD69 is upregulated. This molecule forms a complex with the sphingosine-1-phosphate (S1P) receptor 1 (S1PR1), that has a role in the egress of T cells from the LN to inflamed tissues, leading to S1PR1 internalisation and

degradation and inhibiting temporarily T cell egress by local detection of its ligand S1P[62]. After reaching its peak of expression, CD69 starts to downregulate, allowing S1P to interact with its ligand present on the surface of lymphatic endothelial cells, triggering a series of other interactions that end with the CD4+ T cell leaving the LN through the efferent lymph vessel. CD44 is another molecule that is upregulated in activated CD4+ T cells and is widely used as an antigen experienced cell marker. CD44 assists LN egress by regulating tethering and rolling interactions between activated CD4+ T cells and the endothelia[63] ultimately allowing these cells to exert their effector functions in the affected tissues. The many changes promoted by activation of CD4+ T cells, such as the increase in cell metabolism, are essential for its proliferation and differentiation. On average, a CD4+ T cell undergo 7 divisions, but there are reports of up to 10 divisions[64]. The division of activated CD4+ T cells usually starts 24 hours after antigen presentation[65], reaching its peak 1-2 days later. T cell clonal expansion assists the adaptive immune system by increasing the "army" of T memory and Th cells.

Following activation, and depending on the way the cell gets activated, CD4+ T cells can differentiate into different subsets of Th cells (Figure 1-3) that play supportive and immunomodulatory roles in the adaptive immune system. This differentiation is regulated not only by the crosstalk with the APC, but also by cytokines released by this or other immune cells. Th1 cells, for instance, are induced in an environment with abundant IL-12 produced by APCs[66] and IFN-γ that subsequently comes from IL-12 stimulation of NK cells[67,68]. Th cells express different transcription factors that are necessary for the synthesis of distinct cytokines. Transcription factors are proteins that bind to specific regions of the DNA and lead to a regulation of the production of mRNA, leading to protein expression. Th1 cells, in comparison with other Th cells, intracellularly express high levels of a T-box transcription factor known as T-bet. T-bet is not only required for optimal production of IFN-γ, one of the key cytokines that drive Th1 effector functions, but it is also required for survival of effector and memory cells in the sites of inflammation[69]. Th1 cells are mainly involved in pathogen clearance. IFN-γ activates macrophages[70], cells that engulf and digest cellular debris, foreign substances, microbes and cancer cells. However, Th1 cells are also usually the most frequent pathogenic subset found in organ-specific autoimmune diseases[70,71]. Besides IFN-γ, TNF alpha (TNF-α), another cell signalling protein produced in high

levels by Th1 cells, is also a pro-inflammatory cytokine implicated in the pathogenesis of connective tissue autoimmune disorders, such as rheumatoid arthritis (RA), an autoimmune disease that mainly affect joints[72].

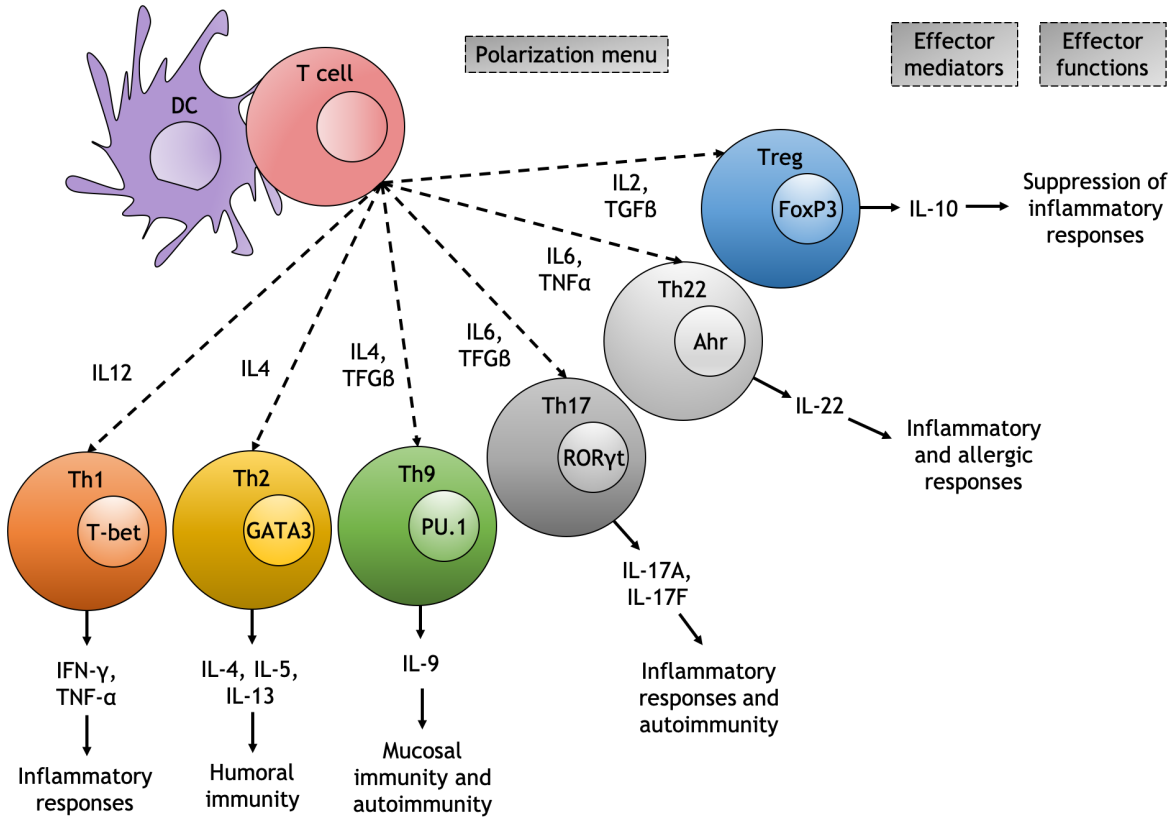

Figure 1-3. CD4+ T cell subsets based on T cell differentiation and its effector functions
Adapted from[73,74]. Following recognition of cognate antigen and induction of CD4+ T cell activation, T cells can differentiate into different Th subtypes, depending on the cytokines that they may encounter. Interleukin (IL) 12 induces T helper (Th) 1 differentiation, that express T-bet and leads to secretion of interferon gamma (IFN-γ) and tumour necrosis factor alpha (TNF-α). IL-4 promotes Th2 differentiation. These cells express GATA binding protein 3 (GATA3) and are optimal secretors of IL-4, IL-5 and IL-13 and play an essential role in humoral immunity. Th9 cells are induced under concomitant presence of IL-4 and transforming growth factor beta (TGFß) and are IL-9 secretors. These cells are important in mucosal immunity and autoimmunity and express the transcription factor PU.1. Th17 cells undergo differentiation in the presence of IL-6 and TGFß, and express retinoic acid-related orphan receptor gamma t (RORγt) that is required for the production of IL-17A and IL-17F. Th22 differentiation is more likely to happen in an environment rich in IL-6 and TNF-α. This cell subset expresses the aryl hydrocarbon receptor (Ahr), that is related to the production of IL-22. In the context of CD4+ T cell activation, regulatory T (Treg) cells differentiation can be induced in the presence of IL-2 and TGFß. Treg cells secret optimal amounts of IL-10 that is assisted by the transcript factor Forkhead box P3 (FoxP3). Th1, Th17 and Th22 cells play important roles in inflammatory responses, while Treg cells induce its suppression.

It is important to note that induction towards a single CD4+ T cell subset usually inhibits differentiation to other subsets. This can be seen in observations that showed that T-bet suppresses the development of Th2 cells by inhibiting the main

IL-4 gene and impairing the function of the main Th2 transcription factor, GATA binding protein 3 (GATA3)[75]. In addition, T-bet interacts with promoters of the RORC gene, responsible for encoding the retinoic acid-related orphan receptor gamma t (RORγt)[76], the master transcript factor of Th17 cells. Th2 cells also express transducer and activator of transcription molecules (STAT), such as STAT5. STAT5 is not exclusively expressed by Th2, but its coordinated activity associated with GATA3 is necessary for production of IL-4[77], one of Th2 cells most expressed cytokines which is also necessary for its initial differentiation[78], along with IL-2[79]. IL-6 was also found to promote Th2 differentiation. The presence of IL-6 at high levels inhibits Th1 development through upregulation of suppressor of cytokine signalling 1 (SOCS1)[80], a direct inhibitor of Janus kinase (JAK) activity that transduces cytokine-mediated signals, being a potent inhibitor of IFN-γ pathway. Th2 cells help the adaptive immune system in the response against multicellular parasites, a role sustained by IL-13 and assisted by IL-10, a cytokine that helps achievement of homeostasis after the pathogen is eliminated[81]. IL-25 is another cytokine that assists the induction of differentiation towards Th2 cells by supressing Th17 responses and consequently inhibiting the secretion of cytokines that drive Th17 differentiation[82]. In the context of allergic reactions, IL-4 upregulates especially high-affinity immunoglobulin E (IgE) receptors (FcεRII) on the surface of mast cells and basophils[83], facilitating degranulation of these cells with release of large amounts of histamine, a potent vasodilator that increases vascular permeability, heart rate, cardiac contraction, and glandular secretion and can lead to severe complications, such as anaphylaxis. IL-4 is also important in the differentiation of Th9 cells[84]. This subset was initially characterised as a subtype of Th2 cells. Th9 cells can be distinguished from Th2 by the expression of transcription factors such as PU.1, interferon response factor 4 (IRF4) and forkhead box O1 (FOXO1), all necessary for IL-9 protein coding[85,86]. IL-9 participates in many inflammatory conditions, such as asthma in which it promotes hypersecretion of mucus[87,88] and in RA, where it not only facilitates Th17 differentiation but also assists neutrophil survival that play a definitive role in the pathogenesis of the disease[89].

Th22 cells are optimal secretors of IL-22, a cytokine that is involved in mucosal host defence against bacteria, and also plays a part in the development and pathogenesis of autoimmune diseases such as RA, systemic lupus erythematosus

(SLE), multiple sclerosis (MS) and psoriasis[90,91]. Th22 cells require IL-6 and TNF-α to develop[92] and express the aryl hydrocarbon receptor (Ahr), that regulates IL-22 production and Th17 differentiation. Th17 cells express RORγt which is necessary for the secretion of IL-17A and IL-17F. IL-17A and IL-17F bind to the IL-17 receptor A (IL17RA) and are involved in the development of autoimmune diseases. IL-17 is important in the response against bacteria and fungi and leads to indirect increase of other pro-inflammatory cytokines that recruit immune cells to the affected site, such as IL-6 and TNF-α[93].

Although regulatory CD4+ T cells (Treg) expressing forkhead box P3 (FoxP3) and CD25 are naturally released from the thymus (nTreg), induced regulatory T (iTreg) cells can also be developed upon TCR stimulation of naïve CD4+ T cells[94], where IL-2 and transforming growth factor beta (TGFß) are of major importance. Even though TGFß is needed for both Treg and Th17 differentiation, the absence of proinflammatory cytokines signalling, such as IL-6, inhibits RORγt function and induces Treg differentiation[95]. In addition, the transcription factor responsible for the production of IL-10, FoxP3, can also inhibit Th17 differentiation by direct interaction with RORγt[96]. IL-10 plays a definitive role in supressing inflammation and autoimmune processes. In addition to these CD4+ T cell subsets that can differentiate exclusively upon antigen presentation by DCs and stimulation with specific cytokines, another subset requires B cell signals to differentiate. This subset is called T follicular helper (Tfh) cell.

1.4.2 CD4+ T Cell-B Cell Interactions and T Follicular Helper (Tfh) Differentiation

Tfh cells are frequently found in follicular areas of lymphoid tissues, playing an immunomodulatory role in the humoral immunity assisting formation of effective memory B cell and antibody responses through interaction with B cells[97-99]. After a naïve CD4+ T cell is primed in the T cell area of LNs by DCs in conditions to promote differentiation into pre-Tfh cells, these T cells upregulate CXC-chemokine receptor 5 (CXCR5) and B-cell lymphoma 6 protein (BCL6)[100]. In association to downregulation of CCR7, a T cell zone homing chemokine receptor, upregulation of CXCR5 allows initial migration of these Tfh precursor cells toward the B cell zone. In the T cell-B cell border, these cells interact with cognate B

cells that provide co-stimulation by surface molecules ligation and activation of cytokines receptors, such as IL-6R, by secreting high levels of IL-6, an essential cytokine for Tfh differentiation[101]. Tfh cells express high levels of BCL6[102], known to be essential for the production of IL-21. This cytokine is key for Tfh feedback to B cells during their interactions and assistance of formation of germinal centres (GC)[100]. IL-21, IL-4 and IL-10 are secreted by Tfh cells and stimulate B cell cytokines receptors, stimulating B cells differentiation into plasma cells that will later produce and secrete antigen-specific antibodies, which will assist adaptive immune responses against antigen of a specific pathogen.

1.5 CD4+ T Cell-APC Interactions in Peripheral Tissues

CD4+ T cell-APC interactions in peripheral tissues participate in the immunopathology of several inflammatory conditions. Macrophages are one of the earliest leukocytes to contact antigen in sites of injury[7]. These cells play important roles in sites of inflammation by clearing necrotic and apoptotic material and may also work as APCs[103,104]. These APCs secrete considerable levels of inflammatory cytokines, such as IFN-γ, assisting the recruitment of other immune cells to inflammatory sites. However, depending on the way they get activated, macrophages can also secrete IL-10, a cytokine that regulates inflammation and is important for maintaining integrity of epithelial barriers[105]. DCs can present antigen and activate CD4+ T cells in the synovium of RA[106,107]. In addition, during certain states, such as chronic inflammation, immune cells accumulate in peripheral tissues and form tertiary lymphoid organs that share common structural and functional features with secondary lymphoid tissues, including T cell areas, B cell follicles, GCs, and vascularization with HEVs[7,108,109]. These similarities may suggest that these tertiary organs could support not only CD4+ T cell-DC interactions in the T cell areas, but also CD4+ T cell-B cell interactions in T cell-B cell intermediate areas, which could promote B cell differentiation and support local production of specific antibodies proximal to the site of inflammation.

1.6 Molecules Controlling CD4+ T Cell-APC Interactions

Depending on the phase of T cell-DC interactions, different molecules are recruited to the site of interaction and play distinct roles in the cells' crosstalk. Whereas interactions within the first 8 hours of contact with antigen are usually short (<5 minutes), later interactions, up to 20 hours after antigen presentation starts, are long-term (>10 minutes)[107]. Behind all this are the interactions between surface molecules, such as adhesion molecules, that ensure a strong cell-cell interaction and trigger pathways that will decide the fate of naïve CD4+ T cells. Several molecule ligations have been described to control T cell-APC interactions. These pathways can be classified as co-stimulatory or co-inhibitory, depending on the outcome of the cells' crosstalk upon disruption of these ligations in different time points, especially during priming.

1.6.1 T Cell Co-Stimulatory Interactions

Several molecules present on the surface of T cells and APCs have been described as contributing to CD4+ T cell co-stimulation (Figure 1-4). Co-stimulatory interactions can promote enhanced T cell activation, cell growth, differentiation and can be important for T cell effector functions, survival and memory. Several members of the immunoglobulin superfamily (IgSF) participate in that. CD80, also known as B7-1, and CD86, also known as B7-2, are well characterized co-signalling molecules from the B7-CD28 family[110]. When binding to CD28, a transmembrane protein expressed by T cells, CD80 and CD86 trigger a pathway that optimises priming outcomes. CD28 is also required for both natural development of Treg cells in the thymus, contributing to their survival and homeostasis in the periphery,[111]and *in vivo* differentiation of naïve CD4+ T cells into Treg cells, a mechanism dependent on IL-2. The inducible T cell co-stimulator (ICOS) receptor is another member of the B7-CD28 family expressed on activated CD4+ T cells and is essential for T cell survival and critical during the effector phase of the adaptive immune response[112]. This molecule is also expressed on Tregs and its ligation facilitates FoxP3 transcription, subsequently optimizing the production of IL-10[113].

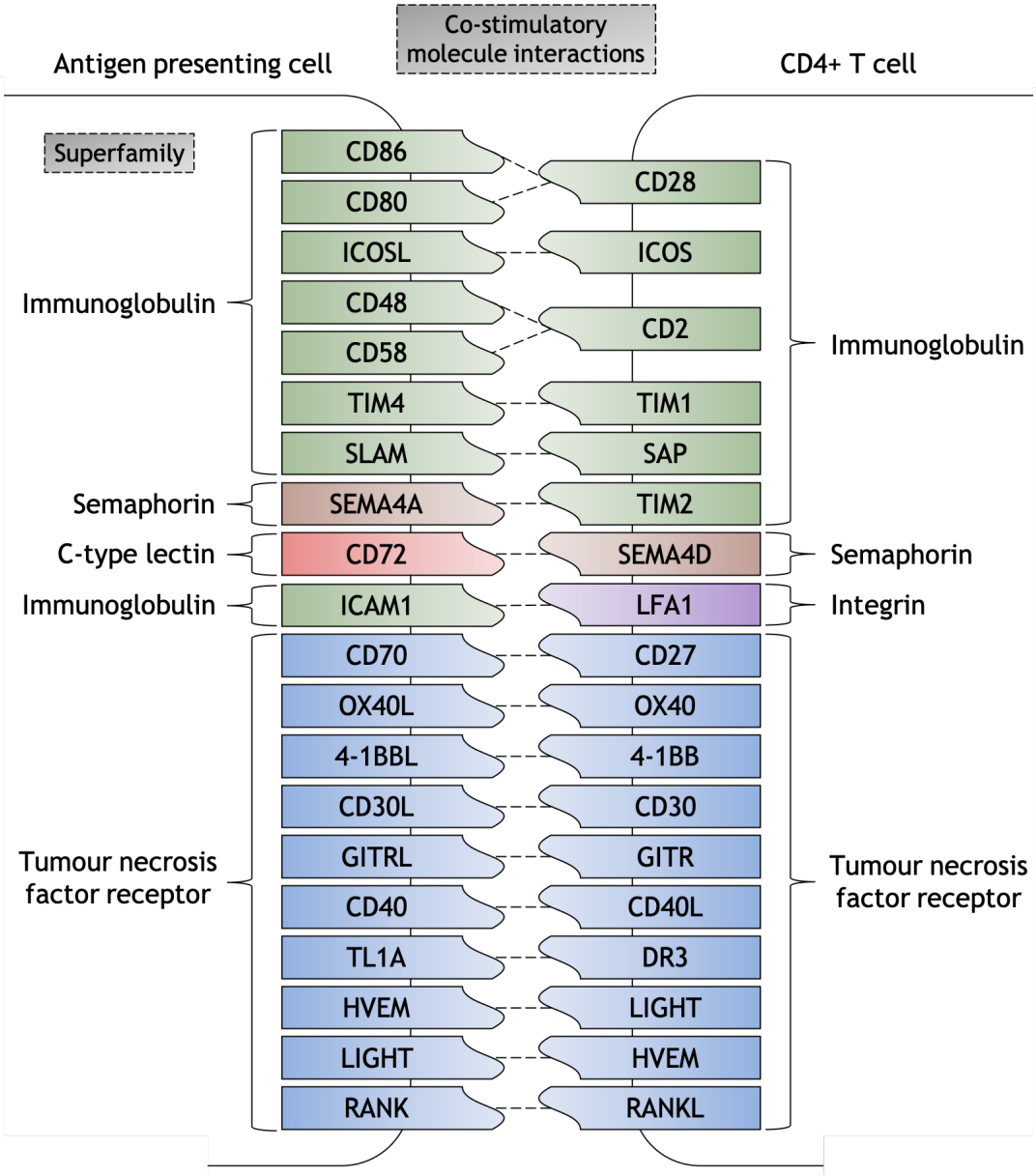

Figure 1-4. CD4+ T cell co-stimulation pathways
Adapted from[114,115]. Co-stimulatory molecules on the surface of CD4+ T cells are engaged by ligands expressed by antigen presenting cells (APC) and control the outcome of these cell-cell interactions. Interactions between members of the immunoglobulin superfamily (IgSF) can be seen with CD28 binding to CD80 and CD86 (B7), the inducible T cell co-stimulator (ICOS) binding by its ligand on the APC surface (ICOSL), CD2 binding to CD58 and CD48, the T-cell immunoglobulin and mucin domain 1 (TIM) 1 binding to TIM4 and the signalling lymphocytic activation molecule (SLAM) being engaged by SLAM-associated proteins (SAP) present on the surface of APCs, leading to optimal T cell activation. Members of the IgSF expressed by CD4+ T cells can also bind to other superfamilies, such as TIM2, that binds to Semaphorin (SEMA) 4A. SEMA4D can bind to CD72, another member of the C-type lectin superfamily. Lymphocyte function-associated antigen 1 (LFA1) is an integrin that binds to the member of the IgSF, ICAM1. Most of the CD4+ T cell co-stimulatory molecules described in the literature are part of the Tumour necrosis factor receptor superfamily (TNFRSF). Within this superfamily, CD27 binds to CD70. OX40, 4-1BB, CD30 and the glucocorticoid-Induced TNF receptor-Related protein (GITR) are engaged by OX40L, 4-1BBL, CD30L and GITRL, respectively. CD40 ligand (CD40L) interacts with the CD40 receptor expressed by APCs. The death receptor 3 (DR3) binds to TL1A. The herpesvirus entry mediator (HVEM) and the LIGHT protein are both expressed by T cells and APCs and interactions can occur on both ways, although it was not described to occur at the same time. Furthermore, the receptor activator of nuclear factor kappa-B ligand (RANKL) expressed on T cells binds to the surface molecule RANK delivering co-stimulatory signals to the CD4+ T cell during its interaction with APCs.

The CD2-signaling lymphocytic activation molecule (SLAM) family of proteins is also part of the IgSF. CD2 is a transmembrane molecule that is widely expressed in different T cell subsets and binds to lymphocyte function-associated antigen (LFA) 3, also known as CD58, and SLAMF2, also known as CD48, to promote stimulatory responses[116]. Within this same family is the SLAM-associated protein (SAP), highly expressed on Th cells. SAPs were found to contribute to differentiation of Th17 cells through interaction with SLAM molecules on the surface of APCs[117]. Other co-stimulatory roles, such as enhanced proliferation, were described upon activation of pathways involving members of the T cell immunoglobulin and mucin domain (TIM) family. TIM-1 interacts with TIM-4 and regulates T cell proliferation and is associated with the regulation of Th2 responses. This pathway enhances Th2 cells proliferation and IL-4 production[118]. TIM-2 binds to the protein Semaphorin (SEMA) 4A on the surface of DCs and is implicated in co-simulation of T cells and Th1 differentiation[119]. LFA1 is an integrin composed of an α (CD11a) and a ß chain (CD18) and is highly expressed on the surface of naïve CD4+ T cells. Its interaction with intercellular adhesion molecule 1 (ICAM1), also known as CD54, was found to support firm arrest during antigen recognition promoting long-lived contacts, thereby enhancing T cells activation and contributing to Th1 differentiation[120,121]. In addition, the ligation between SEMA4D, a protein expressed on the surface of T cells, and CD72 is also important for proliferation and enhances the activation of DCs[122]. Plexin-B1 was described to possibly be involved in some of the interactions with CD72 that contribute to proliferation of T cells, although this has not been proved yet[123].

The TNF receptor superfamily (TNFRSF) is characterised by the ability to bind to TNFs but also comprises a large family of T cell co-stimulatory molecules with different roles[124], of which the CD27-CD70 pathway is the most extensively described. CD27 and CD70 are molecules from the type V family and this pathway enhances T cell activation, proliferation, induces Th1 differentiation[125], inhibits Th17 differentiation[126], promotes survival[127] and contributes to effector memory T cell formation[128]. The ligation between OX40, also known as CD134, found on the surface of T cells, and its ligand, named OX40L or CD252, also potentiates TCR signalling, and is known to be important in T cell activation and survival[129] and to contribute to Th9 differentiation[130]. In the same family the 4-1BB protein, also known as CD137, and its ligand 4-1BBL (or CD137L), a pathway that when activated,

promotes T cell clonal expansion and secretion of pro-inflammatory cytokines[131]. Both OX40 and 4-1BB have been shown to be important for memory T cell responses, to increase Treg cell expansion and to enhance its production of the proinflammatory cytokine IFN-γ[132,133]. CD30 is another member of the type V family expressed by CD4+ T cells and upon interaction with its ligand located on the surface of DCs (CD30L) promotes T cell growth and differentiation towards a Th17 phenotype[124]. Finally, the glucocorticoid-Induced TNF receptor-related protein (GITR) is related to CD4+ T cell proliferation of both effector and regulatory subtypes, when associated with its ligand present on the DCs' surface, GITR ligand (GITRL)[134,135].

Within the TNFRSF, members of the type L family have also been described to have co-stimulatory roles. CD40 is a widely used marker to detect maturation of DCs. Its ligand is present on the surface of activated CD4+ T cells (CD40L), and this pathway induces release of pro-inflammatory cytokines, including IL-17[136]. The expression of other molecules from the same family also co-stimulate T cell activation and induces cytokine secretion. This is the case of the pathway triggered by the ligation between the death receptor 3 (DR3) and the TNF-like ligand 1A (TL1A) and between the Herpesvirus entry mediator (HVEM) and another protein called LIGHT. HVEM and LIGHT are both expressed by T cells and DCs, although concomitant expression on the same cell has not been observed, due to an unexplained mechanism that is suggested to avoid cis interactions on the surface of T cells[114]. This is exemplified by the fact that HVEM is highly expressed by naïve CD4+ T cells, downregulated upon activation but re-expressed later on[137]. On the other hand, LIGHT is upregulated on activated CD4+ T cells but downregulated on effector and memory T cells. The Receptor activator of nuclear factor kappa-B ligand (RANKL) is another member of the TNFRSF that binds to the RANK molecule, also known as CD265. This signal , delivered by the T cell to the DC, assists cDC survival and ensures T cells priming, enhancing the effectiveness of T cell activation[138].

1.6.2 T Cell Co-Inhibitory Interactions

In the context of immune tolerance, T cells are targets for the induction of anergy or apoptosis, and co-inhibitory interactions between surface molecules are

essential for this (Figure 1-5). Co-signalling through members of the same family of molecules can promote opposite outcomes on CD4+ T cells. Although CD80 and CD86 are highly expressed on mature DCs and less in TolDCs, these B7 molecules have a co-inhibitory role when binding to the cytotoxic T-lymphocyte associated protein 4 (CTLA-4), expressed by activated CD4+ T cells[139]. CD80/CD86-CTLA-4 ligation has higher affinity in comparison to CD80/CD86-CD28 interaction[140]. Upon TCR stimulation and under recruitment of CTLA-4, T cell CTLA-4 captures DC co-stimulatory molecules, such as CD86, that is internalised by the CD4+ T cell, possibly decreasing the availability of surface CD86 that could be recruited by CD28[141,142]. Within the same family is the programmed cell death-protein 1 (PD1), or CD279, a protein expressed on CD4+ T cells that binds to the molecules programmed cell death-ligand (PDL) 1 and 2 in interactions that prevent CD28-induced changes in the T cell gene profile under TCR signalling[143]. This inhibition leads to a control in T cell activation.

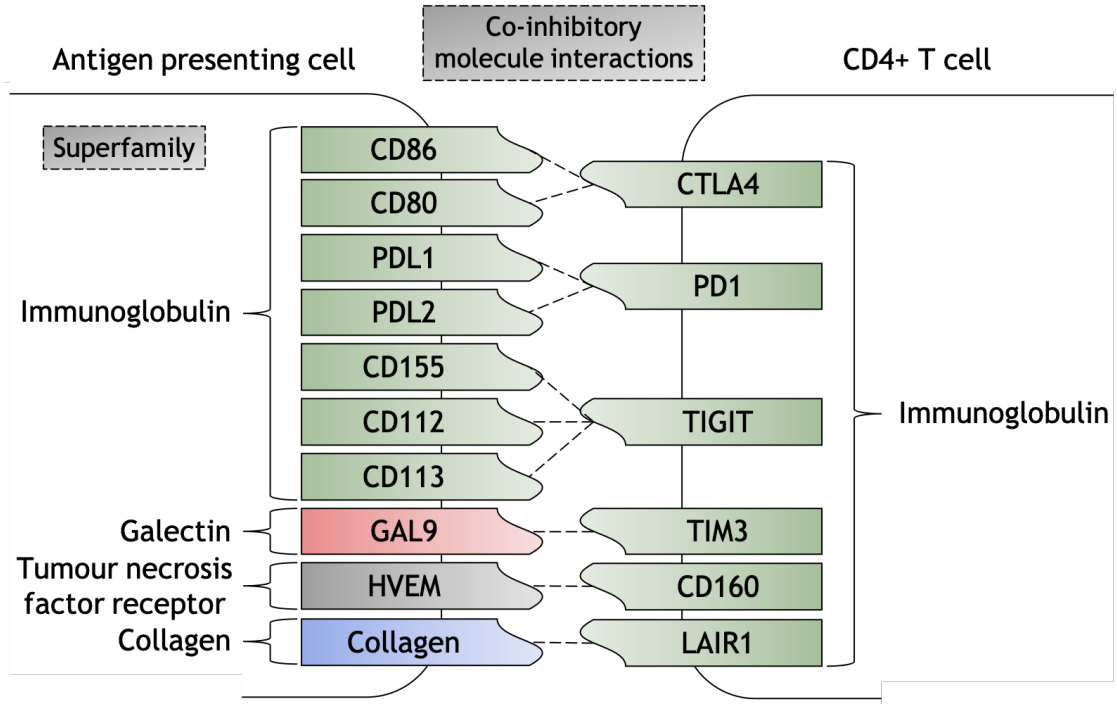

Figure 1-5. CD4+ T cell co-inhibition pathways
Adapted from[114,115]. Co-inhibitory molecules expressed by CD4+ T cells are engaged by ligands present on the surface of antigen presenting cells (APC) and control the outcome of these cell-cell interactions. Interactions between members of the immunoglobulin superfamily (IgSF) are the vast majority of co-signalling molecules found to have inhibition effects on CD4+ T cells. The Cytotoxic T-Lymphocyte Associated Protein 4 (CTLA4) is a well characterised co-inhibition receptor that binds to CD80 and CD86. Programmed cell death protein 1 (PD1) also has inhibitory effects when engaged by the programmed death-ligand 1 (PDL1) or PDL2. The T cell immunoglobulin and ITIM domain (TIGIT) expressed on CD4+ T cells can bind to CD155, CD112 and CD113. Besides the interactions between molecules of the same superfamily, other co-inhibitory pathways were described of proteins from the IgSF binding to proteins from different superfamilies. This is case of the T cell immunoglobulin and mucin domain-containing protein 3 (TIM3) that interacts with the Galectin 9 (GAL9), CD160 that binds to the herpesvirus entry mediator (HVEM) and the Leukocyte Associated Immunoglobulin Like Receptor 1 (LAIR1) that is engaged by molecules of Collagen, present on the APCs' membrane surface.

The T cell immunoglobulin and ITIM domain (TIGIT) coreceptor is also part of the IgSF and binds to CD155 and different members of the Nectin family, CD112 and CD113, to control T cell activation and proliferation[144-146]. Although TIM-1 shows function of a co-stimulatory receptor, a ligation between two other members of the TIM family promotes a different outcome. TIM-3, expressed on the surface of T cells, binds to galectin-9 (GAL9) to promote inhibitory effects[147]. Similarly, HVEM that have co-stimulatory functions when binding to LIGHT modulates immune responses by controlling T cell proliferation when binding to CD160 expressed on DCs[137]. Leukocyte-associated immunoglobulin-like receptor 1 (LAIR1) is a protein found on the surface of T cells that binds to collagen from the surface of other immune cells such as DCs and also negatively regulate T cell activation[148,149]. Subtypes of collagen molecules are relevant in the context of

several autoimmune disorders, such as collagen II (CII) that is one of the autoantigens in RA and SLE[150,151]. Interestingly, autoantibodies against collagen in these pathologies could potentially interfere in the LAIR1-Collagen pathway, leading to an augmented auto-reactivity by inhibition of this pathway[148]. This rationale highlights the importance of considering the different mechanisms involved in these diseases when developing drugs targeting T cell co-stimulatory or co-inhibitory molecules for therapeutic use in distinct medical conditions.

1.7 The Role of CD4+ T Cells-APC Interactions in Pathological Conditions

The interactions between CD4+ T cells and APCs participate in the immunopathogenesis of a number of inflammatory conditions and cancer, through modulation of effector and memory T cell responses. In normal conditions, upon maturation, DCs migrate to LNs and present tumour antigens to antigen specific CD4+ (via MHCII) and CD8+ (via MHCI) T cells[152]. Primed CD4+ T cell are required for generation and maintenance of effector and memory CD8+ T cells, T cells subtypes that have a major contribution to anti-tumour mechanisms[153]. Treg cells directly and effectively supress tumour responses[97]. In addition, Tfh cells are essential for a more efficient tumour eradication, as these increase CD8+ T cells expansion and activity[154,155]. However, abnormal cells that escape immune surveillance to recognise and destroy them can lead to tumour formation. This is evidenced by DCs infiltrated in tumours of cancer patients that have phenotypes with low levels of co-stimulatory molecules and MHCII, suggesting impaired tumour-specific CD4+ T cell priming functions[156,157].

1.7.1 Rheumatoid Arthritis (RA)

The interactions between CD4+ T cells and DCs play a dominant role in RA. CD4+ In autoimmune diseases such as RA, a breach of self-tolerance led by failure in immune regulatory mechanisms results in activation of immune responses that leads to the production and secretion of several autoantibodies[158]. T cell priming following a primary recognition of specific antigen-MHCII complexes induces T cell activation, proliferation and differentiation into Th cells and underlies the breach

of self-tolerance required for the initiation of RA[107]. In addition, a second or next recognition of cognate antigen by antigen experienced CD4+ T cells can lead to re-activation and re-expansion of resting memory cells, playing a fundamental part in propagation of RA pathogenesis[106]. Antibodies against cartilage components (e.g. collagen), nuclear proteins, stress proteins, citrullinated proteins and the Fc portion of IgG antibodies (rheumatoid factor) can be found in the serum of RA patients[159–161]. These autoantibodies mediate adaptive immune responses against articular cartilage and bone, leading to deposition of immune complexes that can increase tissue damage and persistent synovial inflammation[159,162]. CXCR5+ Tfh cells that originate from the interactions of B cells with antigen experienced CD4+ T cells are required for the production of antibodies against type II collage (CII) and for the development of RA[163–165]. Patients with specific polymorphisms in MHCII genes, which encode human leucocyte antigens (HLA) that mediate antigen presentation to CD4+ T cells, have differential risks for developing RA[166], and associations between these and autoantibodies are reported. MHCII-expressing DCs are essential on discriminating self-antigen from foreign antigens and found in high numbers in joints tissues and synovial fluids of RA patients[167]. As such, these polymorphisms associated with other genes that encode molecules involved in T-cell signalling may contribute to the development of a more autoimmune phenotype[107].

A number of animal models of RA are used to study possible therapeutic intervention in this disease, such as the collagen-induced arthritis (CIA) model or the K/BxN model[168]. The CIA model is induced by immunisation of mice with collagen injections and an adjuvant (e.g. CFA), therefore directly stimulating adaptive immune responses against collagen. On the other hand, the K/BxN model is induced upon transferring serum from arthritic mice that contain autoantibodies that will induce joint inflammation[169]. In addition to these models, there is the breach of self-tolerance model of RA[170], utilised in this thesis. In this model, joint inflammation is mediated by antigen specific Th1 cells, that ultimately leads to adaptive immune responses against self-antigens like collagen. The breach of self-tolerance model allows clear distinction in the effects of the used treatment in adaptive immune responses mediated by antigen-experienced T cells, that can be measured by the analysis adoptively transferred Th1 cells and anti-OVA antibodies, and adaptive immune responses by recently primed T cells, that can be measured

by analysing endogenous T cells and production of autoantibodies. However, it is important to note that none of these animal models reliably simulate human disease, as RA in humans is a complex autoimmune disease in which several immune components may play a major role, such as the undiscovered antigen that initiates RA[171].

1.8 Therapeutic Targeting of T Cell Co-Signalling Pathways

The expression of T cell co-signalling molecules has been studied in many pathological tissues and their manipulation in preclinical and clinical trials has established their use for medical conditions. In general terms, blockade of co-stimulatory interactions can be targeted for inflammatory conditions and blockade of co-inhibitory interactions has been used for the treatment of cancer. In addition, while some reagents may block these interactions, others may promote them. It is also important to consider the affinity of these reagents, since the target molecules may compete with other ligands that perhaps have not yet been described. Furthermore, each disease has its peculiarities, and the blockade of these molecules can have distinct outcomes not only on T cell-DC interactions, but on the interactions between other immune cell types. Therefore, studies to analyse clinical effects and involved mechanisms in different disease models are essential for the development of prospective successful drugs.

1.8.1 Agonists of T Cell Co-Stimulatory Molecules

Agonists of co-stimulatory molecules from the IgSF and TNFRSF have been used in several preclinical cancer models. A bioinformatic tool called High-Throughput Systematic Evolution of Ligands by EXponential Enrichment (HT-SELEX) was used to engineer an ICOS agonistic aptamer that although not able to independently induce a potent antitumor response, was able to potentiate CTLA-4 blockade efficacy to inhibit tumour growth[172]. In the TNFRSF, anti-CD27 agonistic antibodies enhanced survival of mice in a B cell lymphoma model[173] and improved tumour control in melanoma models[174], with mechanisms that seem to involve CD8+ T cells more than CD4+ T cells. In addition, multiple lymphoma models have shown

that treatment with agonistic anti-CD27 antibody concomitantly with an anti-CD20 antibody treatment induced cure of all treated mice beyond 100 days[175]. The authors have also demonstrated the essential role of T cells on the therapeutic effect by showing that deletion of either CD4+ or CD8+ T cells alone had minimal impact, but deletion of both T cells types considerably reduced the therapeutic effect of the combined treatment. A phase 2 clinical trial has been recently completed using Varlilumab, an anti-CD27 agonistic antibody, in combination with Nivolumab, a PD1 blocker, on the treatment of colorectal and ovarian cancer[176]. This study showed that Varlilumab induced tumoral changes that led to better outcomes, with patients safely tolerating the drugs.

The potential for OX40 agonistic targeting has been analysed in some preclinical and clinical studies[177]. However, the results between *in vitro* and *in vivo* studies are conflicting and the mechanisms are yet not well understood. A few clinical trials are still underway, while others have been terminated early[178] or finished with good results of remission[179]. The most promising study showed an increase in survival of patients treated with an agonistic target of OX40[180]. The amelioration in clinical condition was mediated by antigen processing related to MHCI, and differences in the expression of genes associated with MHCI were correlated to clinical responsiveness. 4-1BB is a T cell co-stimulatory molecule, also from the TNFRSF, that is targeted for agonistic drugs. They are also being studied in clinical trials due to their capacity to stimulate the 4-1BB pathway and activate T cells that will help on cancer cells clearance. Utomilumab and Urelumab are 4-1BB agonists that are being tested in combination with other drugs for treatment of leukaemia, multiple myeloma, solid tumours and B cell non-Hodgkin's lymphoma[181]. Brentuximab is a well-established drug approved by the U.S. Food and Drug Administration (FDA) and used within the UK's National Health Service (NHS) that targets CD30 and is used for the treatment of relapsed or refractory Hodgkin lymphoma and systemic anaplastic large cell lymphoma[182,183].

Agonistic targeting of other T cell co-stimulatory molecules from the TNFRSF is also being tested in preclinical and clinical phases, such as GITR and CD40L. GITR agonist antibodies were also found to have potential anti-tumour effects in mouse models of cancer by enhancing both CD4+ and CD8+ T cell effector functions and Treg cell apoptosis[184,185]. Furthermore, the combination of GITR agonist with

blockade of CTLA-4 was found to reduce the immune suppression induced by Treg cells and restore the cytokine secretion of effector T cells in human liver tumour *ex vivo*[186]. Currently, a drug targeting GITR in the treatment of advanced or metastatic malignancies is in course (ID NCT03126110) to try to establish efficacy, safety and tolerability of this drug in combination with others. Besides GITR, CD40L is also a target of agonistic drugs on the treatment of cancer. The use of recombinant CD40L molecules and agonistic antibodies against CD40 in early clinical trials show promising results regarding anti-tumour effect and biological safety[187].

1.8.2 Antagonists of T Cell Co-Inhibitory Molecules

CTLA-4 alone has also been a target for treatment of diseases where induction of Th cell activity and inhibition of Treg immunosuppressive functions are desirable. Ipilimumab is a commercially available monoclonal antibody that blocks CTLA-4 binding with CD80/CD86 and prolongs survival in patients with metastatic melanoma, with ongoing clinical trials in many other types of cancer[188–190]. However, this drug was found to show limited effects in tumour cells with genomic defects in the IFN-γ pathway genes. Mice deficient in IFN-γ receptor 1 (IFNGR1) showed high mortality despite treatment with this CTLA-4 blocker[191], IFN-g therefore being a potential marker for predicting responder vs non-responder patients.

PD1-PDL1/PDL2 is another pathway of members from the IgSF. Atezolizumab is a monoclonal antibody anti-PD1L that has been approved by FDA for medical use on the treatment of small cell lung cancer, non-small cell lung cancer, triple-negative breast cancer and urothelial carcinoma[192]. Like any cancer treatment, the importance of detecting non-responders can increase the chances of survival and reduce patient suffering. A study with 51 patients with non-small cell lung carcinoma, who were treated with Atezolizumab, Nivolumab and Pembrolizumab, all drugs targeting the PD1-PDL1 pathway, showed that the therapeutic effects expected by these treatments were compromised in patients with dysfunctional systemic CD4 immunity[193]. In addition, a study of 171 patients with the same kind of cancer showed that the percentage of Tregs in the peripheral blood of patients prior to anti-PD1 therapy was higher in non-responders, while long-term

responders had higher numbers of CD4+ T cells expressing low levels of CD62L prior to the therapy[194].

In mice, blockade of the pathway TIGIT-CD155, also members of the IgSF, with anti-TIGIT monoclonal antibody was found to inhibit tumour growth and prevent T cell exhaustion, enhancing anti-tumour effects[195]. Treatment with anti-TIGIT antibody in combination with Nivolumab, a PD1 blocker, or with an antibody targeting the anti-Lymphocyte Activating 3 (LAG3), a protein expressed by T cells that plays a role on maintenance of CD8+ T cells tolerogenic state[196], are being studied in clinical trials for solid tumours (ID NCT02913313) and multiple myeloma (ID NCT04150965), respectively[179]. In addition, TIM-3 blockade was used in a number of preclinical studies and showed enhancement of anti-tumour immunity, suggesting it may be an effective target for cancer treatment[197].

1.8.3 Antagonists of T Cell Co-Stimulatory Molecules

CTLA4-Ig, a protein synthetized by fusion of extracellular domain of human CTLA4 and a modified human IgG1 heavy chain, binds to CD80/CD86 blocking a possible ligation with T cell CD28[198]. Abatacept, the first FDA-approved co-stimulation blocker and a CTLA4-Ig fusion protein, is widely used in the treatment of autoimmune diseases like RA, juvenile idiopathic arthritis, adult psoriatic arthritis and SLE[199]. Abatacept's mechanism of action includes a limit on the breach of self-tolerance that was demonstrated in a murine model of RA by decreasing maturation and expansion of Tfh cells and reducing the production of inflammatory mediators, such as IFN-γ, IL-17 and CCL3[200]. Similar effects could also be seen in a mice model of collagen-induced arthritis (CIA), in which lower levels of collagen-specific IgG1 and IgG2c antibodies were found in comparison with the control group[201]. A reduction in autoantibodies such as rheumatoid factor could also be seen in the serum of patients treated with abatacept[202]. Although this drug is already in use for treating RA patients, other aspects of the mechanism of action remain unclear, such as the duration of the effect on T cells in vivo and the influence of the drug on the migration of immune cells, such as DCs. Abatacept was also found to reduce the progression and severity of a murine model of heart failure by inhibiting the activation and infiltration of T cells and macrophages[203]. In addition, the use of IL-10-deficient mice in this same study allowed researchers

to identify an important role of IL-10 in the therapeutic effects of abatacept in this model of cardiovascular disease. IL-10 deficient mice were unable to acquire protection against the development of the disease, but abatacept's protective effects were restored upon adoptive transfer of IL-10-sufficient B cells. Clinical trials using abatacept for other immune conditions, such as graft-versus-host disease, the major cause of mortality after allogeneic transplant of hematopoietic stem cells[204,205], are also underway (ID NCT01743131).

Other pathways of molecules from the IgSF play important roles in a number of pathologies, and a few disease models have been tested aiming to evaluate the clinical effects and mechanisms of blockade of these routes. The ICOS-ICOSL pathway was addressed using ICOSL knockout (KO) mice in a murine model of antigen-induced asthma. Mice lacking ICOSL showed less lung eosinophilic infiltration; reduced mucus production and airway hyperresponsiveness upon challenge in comparison with wild-type mice (WT)[206]. This therapeutic effect seems to be related to a decrease in antigen specific antibodies, such as IgG1, IgG2a and IgE. Additionally, CD4+ T cells from the ICOSL KO mice produced less IL-4, IL-5, IL-10, IL-13, but more IL-17 than the WT controls, suggesting a higher differentiation into Th17 cells. Recently, antagonistic anti-ICOSL antibodies were used in a different model of allergic airway disease showing an amelioration in the clinical condition of the treated mice in comparison to the control group[207]. Here, the treatment decreased the differentiation of Tfh cells, cells that are essential in the regulation of allergic airway diseases like asthma[207,208]. The mechanisms of amelioration of the disease were also possibly related to a reduction in the concentration of antigen specific IgE in the serum and pulmonary IL-13. Antigen receptor domains with the ability to block ICOS-ICOSL ligation were used in a murine model of CIA, delayed the disease onset and reduced the disease progression and severity[209]. On the other hand, a model of Th1-driven crescentic glomerulonephritis showed that ICOSL blockade increased glomerular accumulation of CD4+ T cells and macrophages, leading to augmented renal injury[210]. Apolipoprotein E (APOE) KO mice fed with a high-fat diet in a mouse model of atherosclerosis and treated with anti-ICOS antibody showed augmented disease, with an increase by 40% in aortic lesions[211]. In this case, a reduction on the number of Tregs was found in the iliac LNs, which may have contributed to the increase in pathology.

Immunotherapies aiming for disruption of the CD2-CD48/CD58 pathway were used in models of colitis, allergy and arthritis, among others. Prophylactic treatment with anti-CD2 blocking antibody attenuated and delayed the onset of adoptive transfer colitis in mice, with a reduction in T cell proliferation and IL-2 secretion[212]. In a model of allergic eosinophilic airway inflammation, anti-CD48 administration attenuated eosinophilic inflammation by decreasing Th2 responses and secretion of IL-4, IL-5, IL-13 and TNF-α[213]. Anti-CD48 was also used in a model of autoimmune encephalomyelitis where it decreased disease severity by reducing lymphocyte accumulation and the production of IFN-γ, TNF-α and IL-17 by splenic CD4+ T cells[214].

The TIM1-TIM4 pathway has also been tested in a few disease models. In a model of atherosclerosis, low density lipoprotein receptor (LDLR) KO mice treated with anti-TIM1 or anti-TIM4 had increased atherosclerotic lesions when compared to the control group[215]. While the effects on this disease of TIM1 blockade is believed to be due to an accumulation of CD4+ T cells in the lesions, TIM4 blockade reduced the number of circulating Tregs and increased Th1 and Th2 responses. In the context of autoimmune diseases, treatment with anti-TIM4 antibody just before or after the disease onset suppressed the development and progression of arthritis in a CIA model by reduction of proinflammatory cytokines, such as IL-6, TNF-α and IL-1β, although serum levels of anti-CII antibodies were not different in comparison with the control group[216].

SEMA4D has been targeted for a number of inflammatory diseases. SEMA4D KO mice showed reduced lung inflammation in an airway allergic inflammation model[217]. This reduction was associated with a decrease in the levels of IL-5, IL-6, IL-13, IL-17 and TGFβ. Additionally, T cells from the SEMA4D KO mice re-stimulated *in vitro* showed decreased proliferation, and the proportion of Treg cells found in the spleen was higher in comparison to the WT control group. Administration of anti-SEMA4D antibody inhibited neuroinflammation during the development of experimental autoimmune encephalomyelitis[218]. Mice lacking SEMA4D and LDLR simultaneously accumulated less platelets during the induction of thrombus formation in comparison to LDLR KO mice, although they still developed the induced dyslipidaemia[219]. Finally, treatment with anti-SEMA4D

antibody ameliorated severity of arthritis in CIA mice, reducing the level of serum TNF-α, IL-6 and anti-collagen antibodies[220].

The pathway involving ICAM1, also a member of the IgSF, and the integrin LFA1 have been studied in several inflammation models. Simultaneous treatment with peptides that bind to ICAM1 and LFA1 in the first week after disease induction had a beneficial effect in a mouse model of emphysema, preventing lung tissue destruction, reducing leukocyte infiltration and inhibiting the decrease in the ratio of CD4:CD8 T cells that is characteristic in human emphysema[221]. Blockade with anti-ICAM1 or anti-LFA1 antibodies inhibited experimental allergic conjunctivitis[222]. For both treatments, there were a decrease in clinical scores and leukocyte infiltration in the conjunctiva. In a model of adoptive transfer of Crohn's disease, ICAM1 blockade associated with blockade of vascular cell adhesion molecule-1 (VCAM1), a protein upregulated in endothelial cells during inflammation, achieved a 70% resolution of the acute inflammation on the gut[223]. Interestingly, this effect was not seen in treatments with ICAM1 or VCAM1 alone. In a model of arthritis, where the transfer of serum from arthritic transgenic (K/BxN) mice to WT mice to induces inflammation driven by autoantibodies, treatment with anti-ICAM1 antibody was able to delay the disease onset and permitted a faster resolution of the disease[224].

CD27 and CD70 are molecules from the TNFRSF that represent an important pathway in many diseases when binding to each other. Mice lacking APOE and CD70 showed larger atherosclerotic plaques with lower cellularity and a more advanced phenotype in comparison to APOE KO mice[225]. Treatment with anti-CD70 blocking antibody inhibited the induction of allergic lung inflammation in mice by reducing eosinophil infiltration in lung tissue and decreasing the secretion of IL-4, IL-5 and IL-13, cytokines that are characteristic of Th2 cells[226]. An experimental model of inflammatory bowel disease was also used to evaluate the clinical effects of treatment with a different anti-CD70 blocking antibody. The treatment suppressed the induction of 2,4,6-trinitrobenzene sulfonic acid (TNBS)-induced colitis in mice but was not able to inhibit non-T cell mediated colitis[227]. Anti-CD70 treatment both before and after the disease onset was also used in a CIA mouse model that ameliorated arthritis with a reduction in inflammation and a decrease

in bone and cartilage destruction[228]. The treatment significantly decreased the concentration of anti-CII found in the serum.

Blockade of the OX40-OX40L pathway was also addressed in many inflammatory conditions. In a model of allergic conjunctivitis, mice treated with an anti-OX40L blocking antibody, during the induction phase of the disease, showed decreased eosinophil infiltration, with splenocytes re-stimulated *in vitro* with Concanavalin A (Con A) produced less IL-2 and IL-5 but significantly more IFN-γ, characteristic of a Th1 phenotypic differentiation[229]. Blockade of the OX40-OX40L interaction with an OX40-Ig fusion protein ameliorated dextran sulphate sodium (DSS)-induced colitis, with a significant increase in the production of IL-10 and IL-5 by immune cells from the mesenteric LNs[230]. Similarly, IL-10 mRNA levels were increased in colonic tissue, and T-bet expression was significantly decreased. This therapeutic effect was partially inhibited with blockade of IL-10. In the context of cardiovascular diseases, blockade of this pathway also seems beneficial. Anti-OX40L treatment showed a reduction on the number of T cells within cells that formed atherosclerotic plaques, plaque size and cytokines related to Th2 responses in LDLR KO mice[231]. Similarly, treatment with an antagonistic anti-OX40L antibody in APOE KO mice reduced aortic atherosclerotic plaque formation[232]. In a CIA model, an antagonistic anti-OX40 conjugated to a polyethylene glycol molecule and an OX40L-Ig fusion protein reduced arthritic inflammation and restored tissue integrity by an inhibition in the production of inflammatory cytokines by macrophages expressing OX40L[233]. Blockade of OX40 also prevented the development of arthritis in K/BxN mice by reduction of IL-17-secreting Tfh cells[234].

Although only few studies are available in the literature, targeting the 4-1BB-4-1BBL pathway may represent a promising therapeutic strategy for treatment of inflammatory diseases. Two models of hyperlipidaemia were tested in a study that showed that mice lacking APOE or 4-1BB were found to have smaller atherosclerotic plaques compared to the APOE control mice[235]. This same effect was found on mice lacking LDLR and 4-1BB simultaneously. These effects were attributed to a decrease in IFN-γ, TNF-α and CCL2 expression. Treatment with anti-4-1BB antibody in a CIA model inhibited the establishment of arthritis in mice and reduced the concentration of serum anti-CII[236]. This amelioration is believed

to be driven by an increase of IFN-γ-producing-CD11c+ CD8+ T cells, that depleted CD4+ T cells.

Anti-CD30L treatment of LDLR KO mice resulted in a reduction in atherosclerotic lesions, with a decrease in proliferation of splenocytes and T cells, indicating that the therapeutic effect may be driven by T cells[237]. Blockade of this pathway was also tested in a model of enteritis using CD30 KO mice that showed reduced inflammation with a decrease in Th1 and Th17 responses measured by secreted IFN-γ and IL-17, respectively[238]. Mice lacking CD30L were also used in another model of inflammatory bowel disease, in which these animals resisted induction of acute and chronic DSS-induced colitis[239]. Here, levels of IFN-γ and IL-17 were also lower, and T cells from the lamina propria produced higher levels of IL-2. This study also used an antagonistic CD30-Ig fusion protein that ameliorated both acute and chronic models of colitis, associated with an inhibition of Th17 differentiation.

The GITR-GITRL interaction is another pathway from the TNFRSF that was found to have beneficial effects in models of colitis and arthritis. Blockade of this pathway with the use of GITR KO mice or with the treatment of WT mice with soluble GITR protein was able to protect mice against TNBS-induced colitis[240]. CD4+ T cells from the lamina propria of the GITR KO mice with colitis were found to secrete less IFN-γ, TNF-α and IL-2 and more IL-10 and TGFß than the WT mice that were subjected to the same inflammation model. GITR-Ig fusion protein was found to ameliorate CIA pathology in mice. This effect was believed to be due to a supressed Tfh response. The treatment reduced not only the levels of anti-CII IgG1 and IgG2a antibodies but also the number of CII specific IgG-secreting cells in the bone marrow[241].

The pathway DR3-TL1A is also a focus of study for treatment of inflammatory diseases. In a study that analysed the role of this molecular route using two different murine models of arthritis, DR3 KO mice had decreased development both bone pathology in antigen-induced arthritis and subchondral bone erosions in a CIA model. In the same study, the CIA model was also used in WT mice treated with anti-TL1A antibody and these also showed amelioration in the arthritis immunopathology in comparison with the control group[242]. In the context of inflammatory bowel diseases, blockade of TL1A with monoclonal antibody

inhibited DSS-induced colitis in mice by downregulating Th1 and Th17 differentiation[243]. This finding was corroborated by another study that showed that DR3 deficient mice had protection against development of intestinal inflammation in mice upregulating TL1A in T cells and DCs that spontaneously develop IL-13 dependent inflammatory small bowel pathology[244]. In this same study, they also administered anti-TL1A and anti-DR3 blocking antibodies in mice with TNBS-induced colitis, with significant amelioration of the disease. Anti-TL1A treatment also seems to be relevant in the context of allergies. In an antigen-induced model of asthma, treatment with antibody against TL1A significantly reduced the levels of Th2 cytokines, such as IL-4, IL-5 and IL-13, inducing an amelioration in airway inflammation[245].

The CD40L-CD40 pathway has been extensively studied and treatments blockade of this pathway ligation are already being tested in clinical trials, for different diseases. Dapirolizumab pegol is a Polyethylene glycol (PEG)ylated Fab fragment that is being tested for SLE in a Phase 3 clinical trial (ID NCT04294667) but has also potential for use in other autoimmune diseases. VIB4920 is a CD40L binding protein that significantly reduced disease activity in RA patients, with a decrease in autoantibodies such as RF in a Phase 1 clinical trial, whereas results from a Phase 2 trial in RA patients are being currently analysed (ID NCT04163991). Letolizumab is an anti-CD40L antagonistic antibody that is being tested in a phase 2 clinical trial for primary immune thrombocytopenia, with results currently being analysed (ID NCT02273960). Drugs targeting CD40 are also being tested in patients with a number of autoimmune diseases, such as RA, SLE, Sjogren's syndrome, myasthenia gravis, psoriasis, focal segmental glomerulosclerosis, immune thrombocytopenia, lupus nephritis, Chron's disease and primary biliary cirrhosis[246].

1.8.4 Agonists of T Cell Co-Inhibitory Molecules

Disruption of the TIGIT-CD155/CD112/CD113 T cell co-inhibitory pathway with TIGIT agonists has been studied. An anti-TIGIT antagonistic antibody was used in a model of cardiovascular disease in mice. The treatment was able to decrease T cell activation and expansion, but this effect was not enough to see an effect on atherosclerotic lesion development in LDLR KO mice[247]. Additionally, a higher percentage of DCs was also seen in the spleen. These cells had increased

activation and a lower production of IL-10. Nevertheless, although more studies should evaluate the potential of agonistic targeting of T cell co-inhibitory pathways in pre-clinical models, it seems that antagonism of co-stimulatory pathways have better results on manipulating immune responses that promotes amelioration of clinical disease in models of inflammation.

1.9 Aims

Several molecules expressed by CD4+ T cells have been described to have stimulatory or inhibitory effects over their encounter with APCs during antigen presentation. Due to the important role that CD4+ T cells have in the pathogenesis of many diseases, the manipulation of a number of these molecules have been tested in preclinical trials with promising results. As a matter of fact, drugs that target many of these molecules have passed all clinical trials and have been successfully established for the treatment of a number of immunological disorders, such as autoimmune diseases and cancer. For this thesis, transcriptomic data, previously generated in our laboratory, in which a murine model of RA was used to obtain a list of upregulated genes from immune cells that were retained in the joints in comparison to immune cells that migrated to the popliteal LNs (pLN) was used to identify potential candidates to test my hypothesis that blockade of some of these molecules can disrupt CD4+ T cell-DC interactions. Due to the fact that this model is antigen-induced and that antigen presentation has been shown to occur in the synovium of RA joints, we believe that these upregulated genes may translate to an upregulation in surface molecules that can be important for the immune synapses between T cells and APCs in the synovium. Therefore, the following aims will be addressed:

1. To screen candidate molecules from the gene list, based on a literature review and availability of reagents, to evaluate if blockade of the candidate molecules with their potential ligands during antigen presentation is able to manipulate CD4+ T cell activation, proliferation or differentiation *in vitro*, with selection of the most promising candidate for the next aims.

2. To assess if blockade of the most promising candidate molecule with its potential ligands during antigen presentation is able to manipulate CD4+ T cells activation, proliferation or differentiation *in vivo*.

3. To monitor the progress of inflammation in a model of acute murine antigen-induced arthritis during treatment with an antagonist of the most promising candidate molecule and the study of potential involved mechanisms.

Addressing these aims should allow us to identify a new molecule that can control the interactions between CD4+ T cells and DCs and further our understanding on these cells' crosstalk *in vitro* and *in vivo*. In addition, the results of the study on the chosen murine model of inflammation can direct follow up studies on the treatment of RA targeting this new molecule, with or without combined use with other drugs. The elucidation of the mechanisms of the potential effects caused by this prospective treatment may contribute to a better understanding of the immunological mechanisms involved on this disease. Furthermore, the discovery of a novel molecule controlling CD4+ T cell-DC interactions can contribute to the development of drugs aiming the new pathway for prophylaxis or treatment of different types of inflammatory disease, as well as cancer.

Chapter 2 Materials and Methods

2.1 Animals

Six to 12-week-old male and female C57BL/6J mice (substrain C57BL/6JOlaHsd expressing MHC H-2^b haplotype) were purchased from Envigo (formerly Harlan) UK and are considered as WT mice in this thesis. OTII transgenic mice[248] containing CD4+ T cells expressing TCR that recognizes the peptide 323-339 from chicken ovalbumin (OVA) bound to MHCII molecule I-A^b and with all immune cells expressing CD45.1 and Kaede mice[249] expressing a photoconvertible protein in all cell types were bred at the University of Glasgow, Central Research Facility (CRF). All mice were housed at the CRF and all protocols were conducted under licenses issued by the U.K. Home Office under the Animals (Scientific Procedures) Act of 1986 and approved by the University of Glasgow Ethical Review Committee.

2.2 Cell Isolation and Culture

2.2.1 T Cell Stimulation

Spleens were homogenised using a 70 µm EASYstrainer (Greiner-Bio-One) inserted into a 50 mL centrifuge tube (Corning), with help of the flat end of a plunger from a 2 mL syringe (Fisher Scientific). The strainer was washed with Phosphate-Buffered Saline (PBS) (Gibco) and tubes were centrifuged at 400 g for 5 minutes at 4°C. The cell suspension obtained from the spleens was then treated with 1 mL of Red Blood Cell (RBC) Lysis Buffer (eBioscience) per mouse, incubated at room temperature for 3 minutes, washed with PBS and centrifuged once again. $1x10^6$ cells were then stimulated with 1 µg/mL anti-CD3 monoclonal antibody (mAb) 17A2 (BioLegend) and 3 µg/mL anti-CD28 mAb 37.51 (BioLegend) in complete medium (RPMI 1640 (Gibco), 10% foetal bovine serum (FBS) (gibco), 100 IU/ml Penicillin and 100 ug/ml streptomycin, 2 mM L-glutamine) for 72 hours as previously described[250]. Cells were then harvested and stained as described in section 2.4 for flow cytometry analysis.

2.2.2 Isolation of CD4+ T cells

Cells were obtained from peripheral LNs (popliteal, superficial cervical, inguinal, brachial, and axillary), mesenteric LNs and spleens of euthanized OTII transgenic mice and homogenised as described in section 2.2.1. Cells from all tubes were then pooled, counted by trypan blue (Sigma Aldrich) exclusion using a haemocytometer and resuspended in MACS buffer (PBS and 2% FBS) at the required concentration. CD4+ T cells were isolated with a negative antibody selection kit (CD4+ T Cell Isolation Kit Mouse, Miltenyi Biotec) according to the manufacturer's instructions and as previously described[250].

2.2.3 Generation of Bone Marrow-Derived Dendritic Cells (BMDCs)

BMDCs were generated as previously described[251]. Bone marrow of C57BL/6 mice was extracted by flushing RPMI 1640 Medium through the interior of femurs and tibias with a 25G needle and a 5 mL syringe. Cells were centrifuged at 400 g for 5 min at 4ºC and resuspended with 2 mL RBC lysis buffer per mouse, incubated at room temperature for 3 minutes, washed with RPMI and centrifuged again. Viable cells were counted by trypan blue exclusion and haemocytometer and resuspended with complete medium supplemented with 5% GM-CSF (made in house from X63 GM-CSF cell line) at the appropriate cell concentration. $2x10^6$ cells per well were seeded to 6-well non-treated tissue culture plates (Corning) and incubated at 37°C and 5% CO_2. At day 2, cells received additional complete medium, and at day 3 and 6, the entire medium was removed before fresh complete medium was added. At day 6, mature BMDCs were obtained by overnight stimulation with 100 ng/mL Lipopolysaccharide from *Escherichia coli* O111:B4 (LPS) (Sigma-Aldrich) at 37°C and 5% CO_2. BMDCs were harvested on day 7. BMDCs purity was constantly assessed by flow cytometry (Figure 2-1) across the experiments and cells were usually 50-70% double positive for CD11c and MHCII.

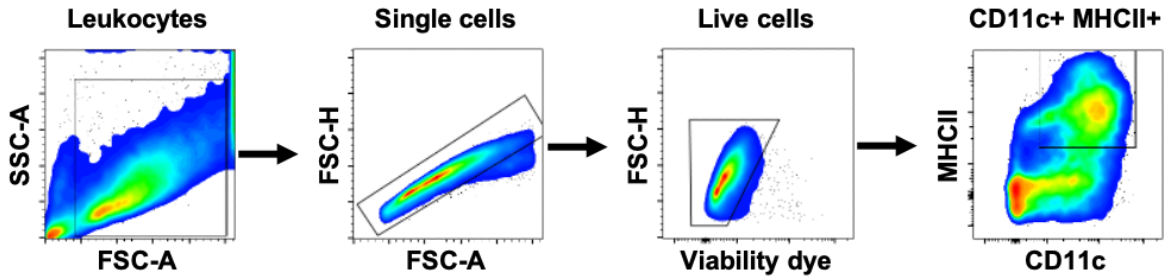

Figure 2-1. Bone marrow-derived dendritic cells (BMDCs) purity analysis by flow cytometry
BMDCs with or without LPS stimulation were harvested on day 7 and analysed for purity by flow cytometry. Events were gated to exclude debris, doublets and dead cells with the use of a Fixable Viability Dye (eBioscience). BMDCs were then identified as CD11c+ MHCII+.

2.2.4 BMDC-T-Cell Co-Culture and Stimulation

BMDCs were pulsed with different concentrations of OVA peptide 323-339 (pOVA) (Sigma-Aldrich) prior to the co-culture set-up as previously described[251]. For proliferation assays, isolated CD4+ T cells were labelled with 1 μM Carboxyfluorescein succinimidyl ester (CFSE) (CFSE Cell Proliferation Kit, Invitrogen) in warm PBS for 20 min at 37ºC 5% CO_2. T cells were then re-incubated for further 10 min in complete medium and washed twice. For flow cytometry analysis or detection of cytokines from the supernatant, pOVA-pulsed BMDCs and CD4+ T cells were cultured at 1:10 BMDC:T cell ratio or at different ratios when indicated in 96-well culture plates (Corning) for different time points (Figure 2-2), according to the objective of the experiment, in a final volume of 200 μL complete medium at 37ºC 5% CO_2. For CEACAM1 targeting, treatments consisted of anti-CEACAM1 mAb CC1 (BioLegend) or Purified Mouse IgG1κ mAb MG1-45 Isotype Control (BioLegend), both at 20 μg/mL. For JAM-A targeting, treatments consisted of anti-JAM-A antibody clone BV11 (Sigma Aldrich) or Ultra-LEAF Purified Rat IgG2bk Isotype Control (BioLegend), both at 20 μg/mL.

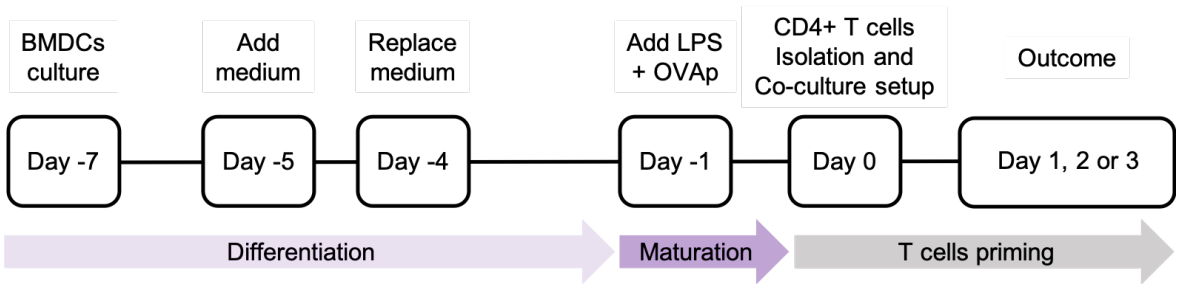

Figure 2-2. Schematic representation of BMDCs culture and BMDC-T cell co-culture set-up
Bone marrow cells were cultured in Granulocyte-macrophage colony-stimulating factor (GM-CSF)-enriched complete RPMI. Fresh medium is added 2 and 3 days after the initial culture. Three days later, the medium is again replaced with Lipopolysaccharides (LPS) and OVA peptide (pOVA). In the following day, BMDCs are harvested and CD4+ T cells from OTII transgenic mice are isolated. Cells are placed together in appropriate plates or slides for different time points. Cells were analysed one, two or three days after the co-culture set-up by fluorescence microscopy, widefield microscopy or flow cytometry, respectively.

2.2.5 Small Interfering RNA (siRNA) in BMDCs

On day 7 of BMDCs culture, immature cells were washed with RPMI, seeded in 6-well non-treated tissue culture plates in serum/antibiotics-free RPMI 1640 Medium (Gibco), to avoid cell death and decrease in transfection efficiency, and incubated for 1 hour at 37ºC, 5% CO_2. Cells were seeded in a total volume of 2 mL but in different cell concentrations to find the most appropriate confluency for the transfection. Lipofectamine 2000 (Invitrogen) and MISSION esiRNA targeting EGFP, CEACAM1 or F11R (Sigma Aldrich) were separately diluted in serum/antibiotics-free RPMI, both at 1:25 or in different concentrations when indicated, and incubated for 15 min at room temperature. Lipofectamine 2000 and the correspondent siRNA were mixed in serum/antibiotics-free RPMI and incubated for another 20 min to allow complexes to form. The volume used for the transfection was 400 µL, that was directly transferred to wells containing BMDCs. Cells were then incubated for 6 hours at 37ºC and 5% CO_2. Following the transfection, cells were fed with 800 µL concentrated complete medium to achieve concentrations of 10% FBS, 1% Penicillin and streptomycin and 1% L-glutamine and re-incubated at 37ºC, 5% CO_2. Prior to harvest, cells were stimulated with 100 ng/mL LPS. Cells were harvested 3 days after the transfection and stained to be analysed by flow cytometry.

2.3 Animal Procedures

2.3.1 Adoptive Transfer of OTII Cells into WT Mice

Adoptive transfer was performed as previously described[10]. Cell suspensions obtained from spleens and LNs of OTII transgenic mice were stained with CFSE as described in section 2.2.3. Cells were resuspended in PBS and a small aliquot was used to estimate the proportion of cells expressing CD4 and the α and ß chains of the transgenic TCR, Vα2 and Vß5 by flow cytometry. $1x10^6$ CD4+ OT-II T cells were transferred intravenously into WT recipients. One day later, different concentrations of Tissue Culture Grade OVA (Code OAC – Worthington Biochemicals) and 8 µg LPS were dissolved in 50 µL PBS and injected into each hind footpad, and 100 µg anti-JAM-A antibody or Rat IgG2b Isotype Control, when indicated, was injected intraperitoneally (200 µL per injection). In the following day, mice were euthanized and the pLNs harvested for flow cytometry analysis.

2.3.2 Breach of Self-Tolerance Arthritis Model

The breach of self-tolerance arthritis model, described by Maffia et. Al.[170], was the chosen inflammatory disease model for this thesis, as the experiment that generated the gene list containing the potential candidates tested in this present work used this model. This model of arthritis was conducted in Kaede mice (Figure 2-3A) for the detection of expression of the marker of interest on migratory immune cells and in WT mice (Figure 2-3B). It was also used as a model to evaluate the effects of disrupting specific molecules and pathways on the development of arthritis in mice.

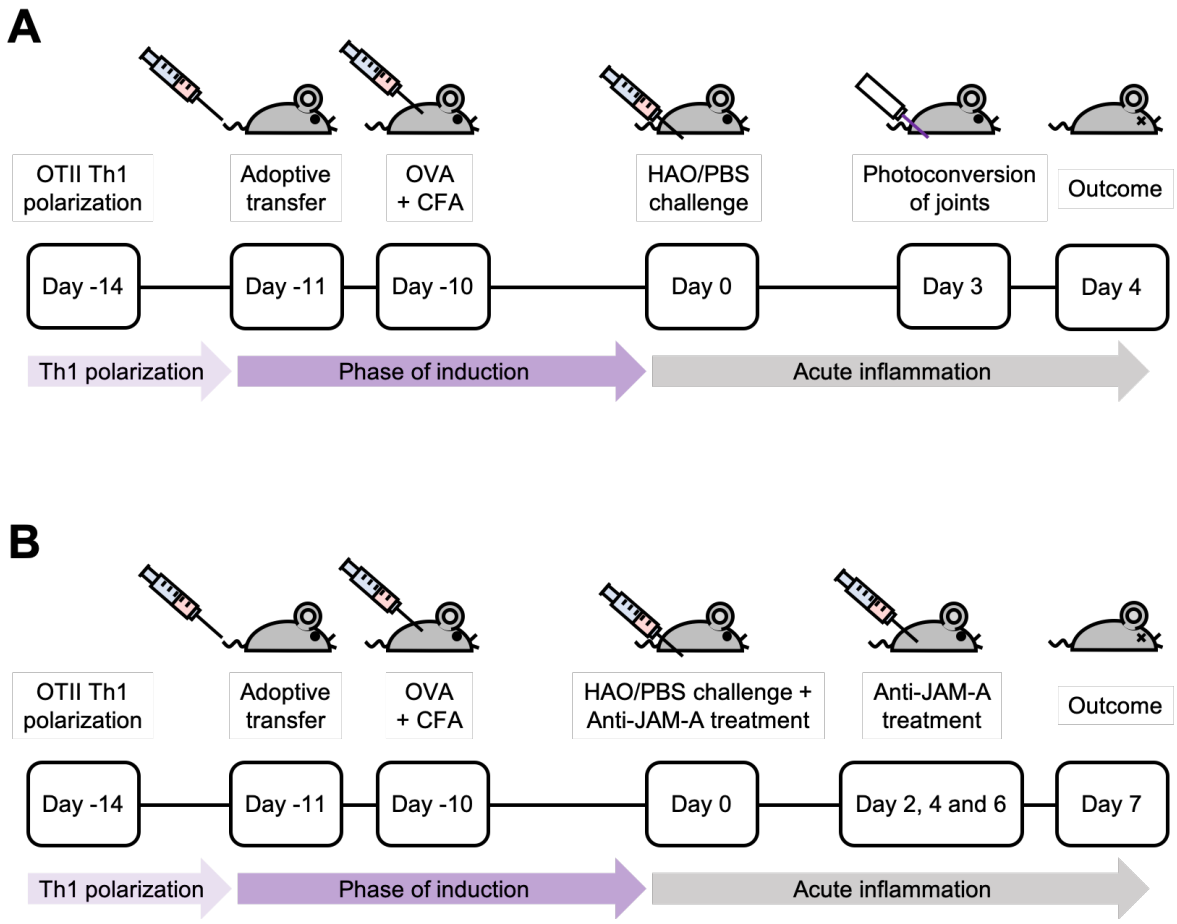

Figure 2-3. Schematic representation of the breach of self-tolerance model of arthritis
The breach of self-tolerance model of arthritis[170] was induced in Kaede and wild-type (WT) mice. Isolated OTII CD4+ T cells were incubated with antigen presenting cells (APC) to induce Th1 polarization (OVA peptide, IL12 and anti-IL4 antibody). After 3 days, Th1 cells were transferred intravenously into Kaede **(A)** or WT **(B)** mice. In both cases, OVA and Complete Freund's Adjuvant (CFA) were injected into the scruff the following day. This induction phase was followed by acute inflammation in the joints triggered by challenge with heat aggregated OVA (HAO) in the footpads. In the experiment with Kaede mice, joints were photoswitched 3 days after challenge and popliteal lymph nodes (pLN) and joints were harvested the next day for flow cytometry analysis. In the experiment with WT mice, treatments with anti-JAM-A mAb BV11 were conducted in days 0, 2, 4 and 6 after HAO injections. The pLNs were harvested on day 7 for flow cytometry analysis.

For Th1 polarization, APCs acquired from leftover cells following CD4+ T cell isolation and from fresh spleens of C57BL/6 mice were initially treated with 50 µg/mL mitomycin (Sigma-Aldrich) diluted in complete medium and incubated for 1 hour at 37ºC and 5% CO_2. APCs were then washed three times in complete medium and incubated with isolated CD4+ T cells from OTII mice in a 1:5 ratio in complete medium containing 1 µg/mL pOVA, 10 ng/mL IL-12 (Bio-Techne), and 5 µg/mL murine monoclonal anti-IL-4 antibody (2BScientific, clone 11B11). Cells were incubated in 75 cm^2 vented flasks (Corning) at 37ºC, 5% CO_2. After 72 hours, the amount of Th1 cells obtained was estimated by the percentage of CD4+ Vα2+ Vß5+ cells obtained in a flow cytometry analysis along with the use of trypan blue

and haemocytometer in which only large cells were counted. The expression of CD45.1 was also confirmed in the flow cytometry analysis. Cells were then re-suspended in PBS and 200 µL of this suspension containing $1x10^6$ Th1 cells was injected intravenously into WT or Kaede mice, depending on the experiment.

Tissue culture grade OVA was diluted in PBS and prepared with Complete Freund's Adjuvant (CFA) (Sigma Aldrich) in a 1:1 ratio to make a 1 µg/µL final concentration of OVA. The emulsion was injected subcutaneously into the scruff in 100 µL 24 hours after the adoptive transfer of Th1 cells. Ten days later, 100 µg heat aggregated OVA (HAO) was injected in the hind footpad. HAO was prepared by dissolving OVA (Sigma Aldrich) at 20 mg/mL in PBS, 200 µL aliquots were placed in 1.5 mL Eppendorf tubes and incubated at 100^{o}C for 2 hours. The suspension was then centrifuged at 10,000 g for 5 min and the supernatant removed. A wash with PBS was performed and the heat-aggregated OVA was resuspended in PBS. Aliquots were stored at –20C until use. Prior to use an aliquot was transferred to a GentleMACS C-tubes (Miltenyi Biotec) and 1.8 mL of PBS added to make a concentration of 2 mg/mL. The HAO was then homogenised using a gentleMACS Dissociator (Miltenyi Biotec) and the suspension was considered as appropriate when it could pass through a 25-gauge needle. WT mice that were subjected to the breach of self-tolerance model of arthritis were treated every 48 hours (days 0, 2, 4 and 6) with 100 µg (200 µL) of anti-JAM-A mAb BV11 or Rat IgG2b Isotype Control. Clinical scores as well as footpad thickness, measured using a C-Series IP67 electronic calliper (Kroeplin GmbH), were measured on a daily basis until the 7th day after the HAO challenge. On day 7, 80 µL peripheral blood from the tail vein was harvested and placed in an Eppendorf with 1 mL FACS Buffer (PBS, 2% FBS and 1 mM EDTA). Peripheral blood mononuclear cells (PBMC) were then stained and analysed by flow cytometry as described in section 2.4. WT mice were then kept housed in the CRF for further analysis of the arthritis clinical response after a second footpad challenge. This analysis is not covered in this present work, as the experiment was still ongoing at the time.

Kaede mice were also subjected to the breach of self-tolerance arthritis model. Cells from Kaede mice express a photoconvertible protein (Kaede green) that can be excited with a 488 nm laser[249]. On the day prior to harvesting, cells from the joints were photoconverted with a 12X S06J blu-ray diode with a 405-G-2-glass

lens (DTR's Laser Shop) emitting at 405 nm with mean power of 600–650 mW. The photoconversion modifies the conformation of the transgenic protein, changing its fluorescence properties. The photoconverted cells are called Kaede red cells and present fluorescent proteins that can be excited with 561 nm lasers. The time of laser exposure was previously optimized in the lab[52]. Each foot was exposed for 5 seconds in three different parts on both the ventral and dorsal sides of the hind paw, in a total of 30 seconds per foot. Photoconversion was only performed once per animal. All Kaede mice were euthanized 4 days after the HAO challenge and had their pLNs and joints harvested. The skin and muscle were removed from the feet, and the ankle and joints teased apart. Joints and pLNs were separately digested with 2.68 mg/mL Collagenase D (Roche) in PBS using a shaker at 110 rpm at 37ºC for 30 min. pLN samples were washed and pooled per mouse, cells obtained from pLNs were enumerated using a haemocytometer and were then stained for subsequent flow cytometry analysis. Joints were homogenised in gentleMACS C tubes using the gentleMACS Dissociator. The tissue was then filtered using a 70 µm strainer and centrifuged at 400 g for 5 min at 4ºC. The pellet was resuspended in PBS and joints were pooled per mouse. An aliquot of the cell suspension was used to count live cells by excluding trypan blue positive cells, whereas the rest was added to a 96-well plate to be stained for flow cytometry analysis.

2.4 Flow Cytometry

2.4.1 Viability Staining

Plates containing cells were centrifuged at 400 g for 5 min at 4ºC. Cells were then resuspended in 100 µL diluted Fixable Viability Dye (eBioscience) and incubated for 15 min at 4ºC. Dilutions were 1:1000 for Viability Dyes eFluor 450 or eFluor 780 and 1:500 for Viability Dye eFluor 506. Cells were washed twice with PBS before extracellular staining was initiated.

2.4.2 Extracellular Staining

After cells were stained with viability dye and washed, the suspensions were incubated with 50 µL Fc receptor (FcR) block (produced in-house using

supernatant from 2.4G2 cell line supplemented with 5% mouse serum) for 10 min at 4ºC to block non-specific binding of antibodies to the Fc receptors. Antibodies (Table 2-1) were diluted in FACS Buffer and 50 µL was added to the cells and incubated for further 30 min at 4ºC. When biotinylated antibodies were used, cells were washed and an extra step of 20 min incubation containing FACS Buffer and Streptavidin was performed at 4ºC. Cells were then washed again in FACS Buffer and re-suspended in 200 µL FACS Buffer before running on BD LSRII, BD LSR Fortessa or BD FACSCelesta.

2.4.3 Intracellular Staining

To detect intracellular cytokines, the supernatant of co-cultures from 96-well plates was removed and 100 µL of a stimulation mixture was added, containing 20 ng/mL phorbol myristate acetate (PMA) (Sigma Aldrich), 1 µg/mL ionomycin (Sigma Aldrich) and 1:1000 GolgiPlug (BD Biosciences) and cells were incubated for 4 hours at 37ºC and 5% CO_2. Cells were then stained for viability and extracellular markers as described in sections 2.4.1 and 2.4.2, respectively, and later fixed in 100 µL Cytofix/Cytoperm (BD Biosciences) for 20 min at 4ºC and washed with 100 µL Perm/Wash Buffer (BD Biosciences). This buffer was also used to dilute the appropriate antibodies in the concentrations stated in Table 2-1. Following addition of antibodies, cells were incubated for 30 min at 4ºC and washed twice with FACS Buffer before being re-suspended in 200 µL FACS Buffer and analysed in the flow cytometers.

For intracellular detection of transcription factors, cells were fixed directly in the 96-well plates with 100 µL FoxP3 Transcription Factor Fixation/Permeabilization buffer (eBioscience) for 1 hour at 4ºC. Cells suspensions were then washed with Permeabilization Buffer (eBioscience) and incubated with a mixture containing appropriate antibodies diluted in Permeabilization Buffer and incubated for 30 min at 4ºC. Before being conducted to flow cytometry analysis, cells were washed with FACS Buffer and re-suspended in 200 µL FACS Buffer.

2.4.4 Data Analysis

Data were analysed using FlowJo 10.6.2 software (Treestar). Gates indicating positive or negative populations were based on the background staining of fluorescence minus one (FMO) controls or FMO controls with addition of the corresponding isotype control antibody, when indicated. To generate tSNE plots, the total population of cells excluding doublets and dead cells was downsized with the plugin DownSample v3.2 to $2x10^5$ events per biological replicate. The biological replicates were concatenated with the marker of interest being selected before the final tSNE analysis was performed.

Table 2-1. Antibodies and other reagents used for flow cytometry

Marker	Fluorochrome	Clone	Concentration	Manufacturer
B220 (CD45R)	PE-Cy7	RA3-6B2	1:200	eBioscience
CD11a	PE	M17/A	1:200	eBioscience
CD11b	Super Bright 600	M1/70	1:200	eBioscience
CD11c	BV421	N418	1:200	BioLegend
CD11c	PE-Cy7	N418	1:200	BioLegend
CD19	Alexa Fluor 700	eBio1D3	1:200	eBioscience
CD3	APC-Cy7	17A2	1:200	BioLegend
CD3	V500	500A2	1:200	BD Biosciences
CD3	FITC	145-2C11	1:200	BioLegend
CD4	APC	RM4.5	1:200	BD Biosciences
CD4	BUV805	GK1.5	1:200	BD Biosciences
CD4	eFluor 450	RM4.5	1:200	eBioscience
CD4	FITC	GK1.5	1:200	eBioscience
CD44	APC	IM7	1:400	eBioscience
CD44	BUV395	IM7	1:200	BD Biosciences
CD44	PE	IM7	1:400	eBioscience
CD45	BUV395	30-F11	1:200	BD Biosciences
CD45.1	APC	A20	1:200	eBioscience
CD45.1	APC-eFluor 780	A20	1:200	eBioscience
CD45.1	PE	A20	1:200	eBioscience
CD62L	APC-eFluor 780	MEL-14	1:200	eBioscience
CD8	Alexa Fluor 700	53-6.7	1:200	BioLegend
CD8	PE-Cy7	53-6.7	1:200	eBioscience
CD86	FITC	GL1	1:200	BD Biosciences
CD86	PE-Cy7	GL1	1:200	BD Biosciences
CEACAM1 (CD66a)	BV421	CC1	1:200	BioLegend
CEACAM1 (CD66a)	PE	CC1	1:200	BioLegend
FoxP3	BV421	MF-14	1:200	BioLegend
IFN-γ	PE	XMG1.2	1:200	BD Biosciences
IFN-γ	PE-Cy7	XMG1.2	1:200	eBioscience
IL10	BV421	JES5-16E3	1:200	BioLegend
IL17	APC	17B7	1:200	eBioscience
JAM-A (CD321)	Biotin	H202-106	1:200	eBioscience
JAM-A (CD321)	PE	H202-106	1:200	BD Biosciences
Ki67	Alexa Fluor 488	SolA15	1:200	eBioscience
Ly6G	APC	RB6-8C5	1:200	eBioscience
MHCII	APC	M5/114.15.2	1:400	eBioscience
MHCII	APC-Cy7	M5/114.15.2	1:400	BioLegend
MHCII	BV510	29G	1:200	BD Biosciences
MHCII	PerCP-Cy5.5	M5/114.15.2	1:400	BioLegend
NK1.1	APC-Cy7	PK136	1:200	BioLegend
PDCA1 (CD317)	APC	eBio129c	1:200	eBioscience
RORγt	APC	AFKJS-9	1:200	eBioscience
Streptavidin	BV421	-	1:100	BioLegend
Streptavidin	PE-Cy7	-	1:100	eBioscience
T-bet	PE-Cy7	4B10	1:200	eBioscience
TIM-3 (CD366)	PE	RMT3-23	1:200	eBioscience
TNF-α	Alexa Fluor 488	MP6-XT22	1:200	eBioscience
YAe	Biotin	eBioY-Ae	1:200	eBioscience

2.5 Enzyme-Linked Immunosorbent Assay (ELISA)

For all ELISAs, High Binding Assay 96-well Plates (Corning) were used. Absorbance measurements were performed using a Sunrise Absorbance Reader (Tecan). The washing buffer in all assays consisted of 0.05% Tween 20 (Sigma Aldrich) in PBS (PBS-T).

2.5.1 Cytokine Measurement

Cytokine concentrations were measured in the co-culture supernatants by ELISA using ELISA MAX Standard Sets for Mouse IL-4, IL-6, IL-10, IL-17 and IFN-γ (BioLegend) according to the manufacturer's instructions. The absorbance was measured at 450 nm with subtraction of wavelengths from readings at 570 nm. Background absorbance was removed from all samples by subtracting the mean of blank wells. Titrations to identify appropriate concentrations of supernatants, aiming for optical density (OD) values between 0.5 and 2.5 to ensure that the cytokine concentrations were within the range of the standard curve, were performed before the final ELISA assays were performed. Standards of the commercial kits were also included in the analysis in order to build a standard curve in GraphPad Prism 7 software. Cytokine concentrations were determined by extrapolating the unknown values from the standard curve.

2.5.2 Anti-Collagen II (CII) and Anti-OVA Antibodies Measurement

ELISA was used to detect anti-OVA and anti-CII antibodies in serum from mice that underwent the breach of self-tolerance arthritis model was conducted as previously described[170]. Blood was collected from mice in 1.5 mL Eppendorf microcentrifuge tubes (Greiner Bio-One) and serum was extracted by allowing the blood to clot at room temperature for 6 hours and centrifuging it at 10,000 g for 5 min. Serum was transferred to new Eppendorf tubes and frozen at -20°C. High binding plates were coated with 50 µL of 20 µg/mL OVA (Sigma Aldrich) or 4 µg/mL bovine collagen II (Sigma Aldrich) diluted in carbonate buffer (Sigma Aldrich) and incubated overnight at 4°C. Plates were washed, blocked with 100 µL animal free serum (Vector Laboratories) for 1 hour at 37°C and washed again. Sera were initially diluted in PBS at 1:50 for anti-CII and 1:200 for anti-OVA detections, added

to the plates in duplicates and serial dilutions were performed. The final volume in each well was 100 µL. The plates were incubated for 1 hour at 37ºC and later washed. In plates for detection of anti-CII antibodies, a positive control from arthritic mice from an experiment previously performed was used, while serum from one of the mice of the present experiment was used in all plates, in order to normalize the data across plates. To detect anti-CII antibodies, plates were incubated with rabbit anti-mouse whole IgG antibody conjugated to horseradish peroxidase (HRP) (Sigma Aldrich) diluted to 1:10000 in PBS for 1 hour at 37ºC. For the detection of anti-OVA antibodies, plates were incubated with biotin-conjugated goat anti-mouse IgG1 (1:5000) or IgG2c (1:10000) for 1 hour at 37ºC, washed and incubated with ExtrAvidin-Peroxidase (Sigma Aldrich) (1:10000) for 30 min at 37ºC. All plates were then washed and 100 µL SigmaFAST OPD solution (Sigma Aldrich) was added before plates were incubated for 5-30 min, protected from light, at room temperature. Sulphuric acid at 10% was used to stop the reactions and the absorbance was read at 492 nm.

2.6 Imaging

Widefield and confocal microscopy were used according to the requirements of the assay. Widefield microscopy is a technique in which the whole sample is illuminated, and light is emitted and gathered from many focal planes, and was used to visualize cell clusters and tissue sections. The moving pinhole in confocal microscopes intercepts most of the out-of-focus light and allows detection of light only in one focal plane, also known as z-stack. Confocal microscopy was used for visualization of individual cell-cell interactions.

2.6.1 Widefield Microscopy

The EVOS FL Auto 2 Imaging System Fluorescence Microscope (Invitrogen) equipped with EVOS LED light cubes equivalent to channels DAPI (357/44 nm excitation, 447/60 nm emission), GFP (470/22 nm excitation, 510/42 nm emission), RFP (531/40 nm excitation, 593/40 nm emission) and Cy5 (628/40 nm excitation, 692/40 nm emission) was used to acquire fluorescence images. Light directly from the condenser was used, to acquire brightfield.

Isolated CD4+ T cells were stained with CFSE as described in section 2.2.3 and BMDCs were stained with 5 µM CellTracker Red CMTPX Dye (Invitrogen) in warm PBS for 30 min at 37ºC 5% CO_2. BMDCs were then re-incubated for further 10 min in complete medium and washed twice. $4x10^3$ BMDCs and $4x10^4$ T cells (1:10 ratio) were co-cultured in 384-well black tissue culture-treated assay plates with flat clear bottom (Corning) in a final volume of 30 µL complete medium and incubated at 37ºC and 5% CO_2. Treatments consisted of anti-JAM-A antibody clone BV11 or its isotype control, both at 20 µg/mL. Cell clusters were visualized one or two days after the co-culture set-up for fluorescence or brightfield images, respectively. For fluorescence images, CFSE fluorescence was detected with the GFP filter and CMTPX fluorescence was detected with the Cy5 filter. Two scans from a 10x objective lens were made per well and exported to be analysed separately. To acquire brightfield images, acquisition was automated and tile scans from a 10x objective lens were merged using the built-in EVOS FL Auto 2 software to obtain the images that were then exported and analysed.

LNs from C57BL/6 mice were harvested in cold PBS and frozen in OCT compound (Tissue-Tek) using a Thermo Shandon Cryotome FE cryostat (Thermo Fisher) and stored at -80ºC. In the cryostat, 8-10 µm sections were cut, adhered to Superfrost Microscope slides (Thermo Fisher) and stored at -20ºC. Before being stained, sections were thawed and fixed in acetone for 10 min at room temperature. Slides were washed with PBS-T. The regions of interest were marked with an ImmEDGE Hydrophobic Barrier Pen (Vector Laboratories) and slides were left to dry at room temperature. Slides were put in a humidity chamber and non-specific binding was blocked with Protein Block Serum-Free (Dako) for 10 min at room temperature. An Avidin/Biotin Blocking Kit (Vector Laboratories) was used to block endogenous biotin by incubating the sections with Avidin D for 15 min at room temperature, washing it and incubating it with Biotin for a further 15 min. Sections were washed and incubated with a mixture containing antibodies against the markers of interest directly conjugated to fluorophores or to biotin diluted in PBS, for 30 min at room temperature. The sections were again washed and incubated with Streptavidin conjugated to a fluorophore for 30 min at room temperature. Sections were dried, mounted in VECTASHIELD® Antifade Mounting Medium (Vector Laboratories) with the addition of a coverslip, sealed in the slide with nail polish, before being analysed using the EVOS microscope.

2.6.2 Confocal Microscopy

BMDCs pre-pulsed with pOVA and CD4+ T cells were cultured in 96-well culture plates in a final volume of 100 µL complete medium at 1:10 BMDC:T cell ratio for 24 hours at 37ºC 5% CO_2. Cells were then fixed directly in the plates with 2% PFA for 20 minutes at room temperature to preserve clusters. Cells were washed in PBS, stained as described in section 2.4.2 and resuspended in FACS Buffer. Antibodies used were: FITC-conjugated anti-CD4 mAb (clone GK1.5), APC-conjugated anti-CD11c mAb (clone N418), BV421-conjugated anti-MHCII mAb (clone HL3) and PE-conjugated anti-JAM-A mAb (H202-106). All antibodies were used at a 1:200 concentration. A volume of 100 µL was then added to uncoated µ-Slide I (Ibidi) and left to settle for 2 hours at 4ºC before being analysed with a ZEISS Cell Observer Spinning Disc Confocal Microscope (Carl Zeiss) using a 63x objective lens and filters capable of detecting DAPI, GFP, RFP and Cy5 channels.

2.6.3 Image Analysis

All images were analysed using Fiji open-source software[252]. For images of cell clusters acquired with EVOS' brightfield, images were converted to 8-bit files, contrast was enhanced in 4% and the plugins Gray Morphology and Sharpen were applied to make clusters more visible. Fiji's Ellipse tool was used to detect the limits of visible cell clusters. The regions of interest were then measured and exported to a spreadsheet. In Microsoft Excel, a formula was used to automate the application of a threshold to exclude cell aggregates smaller than 2000 μm^2, as clusters were defined as cell aggregates with area of at least 2000 μm^2.

Images of cell clusters acquired with EVOS' fluorescence filters were subjected to a colocalization analysis. Images were converted to 8-bit files and a threshold was applied to remove background noise. The Pearson's correlation coefficient and the Mander's overlap coefficient of images from the GFP and Cy5 channels were calculated with the EzColocalization plugin[253]. Immunofluorescence images of LNs were submitted to Fiji's Unsharp filter (2 pixels radius, mask weight 0.6), its pseudo-colours were changed by arranging channels and the graphs for fluorescence intensity were obtained with the Plot Profile tool.

For the analysis of individual BMDC-T cell cluster, the synapse area and the rest of the cell membrane were determined by using the Polygon Selection tool. The fluorescence intensities of both areas were then measured, and the ratio was obtained by dividing the intensity from the synapse area by the rest of the cell membrane.

2.7 Statistical Analysis

Results are expressed as mean ± standard deviation (SD) of technical replicates, or biological replicates when indicated. All statistical analyses were performed using GraphPad Prism 7 software. Appropriate normality tests were performed to detect normal distribution. For comparing 2 groups, a variable for more than 2 groups and two variables for more than 2 groups the Student t test, one-way ANOVA and two-way ANOVA were performed, respectively. P values shown as *$p<0.05$, ** $p<0.01$, ***$p<0.005$, ****$p<0.0001$.

Chapter 3 Selection of Candidate Molecules

3.1 Introduction

CD4+ T cell interactions with DCs are pivotal in adaptive immune responses and there is increasing interest in discovering molecules that would promote or disrupt these interactions. To screen candidate molecules for testing my hypothesis that blockade of their pathways can disrupt CD4+ T cell-DC interactions, I took advantage of transcriptomic data previously generated in our laboratory using a murine model of inflammatory arthritis. To acquire the gene data that was used to select these potential candidates, experiments using the breach of tolerance model of arthritis[170] in Kaede mice[249], as described in Chapter 2 (section 2.3.3) were performed by the former laboratory members Drs Robert Benson and Catriona Prendergast (unpublished data). Immune cells from joints and pLNs obtained four days after footpad challenge were sent for genetic sequencing. Individual transcriptomic data from three biological replicates were processed and analysed, generating a list of 4,507 differentially regulated genes between joints and LNs. In order to generate a list that was joint-specific, the same disease model was conducted in Kaede mice but instead of a footpad challenge, mice were challenged in the ear pinna followed by photoswitching (Figure 3-1). The auricular LN was harvested to detect Kaede red migratory cells in addition to the ear pinna. Viable, Kaede red immune cells from these tissues were sent for sequencing. Finally, a joint-specific differentially regulated gene list containing 217 genes from non-migratory cells was generated by subtracting the genes of the non-specific inflamed site from the list acquired in the previous experiment.

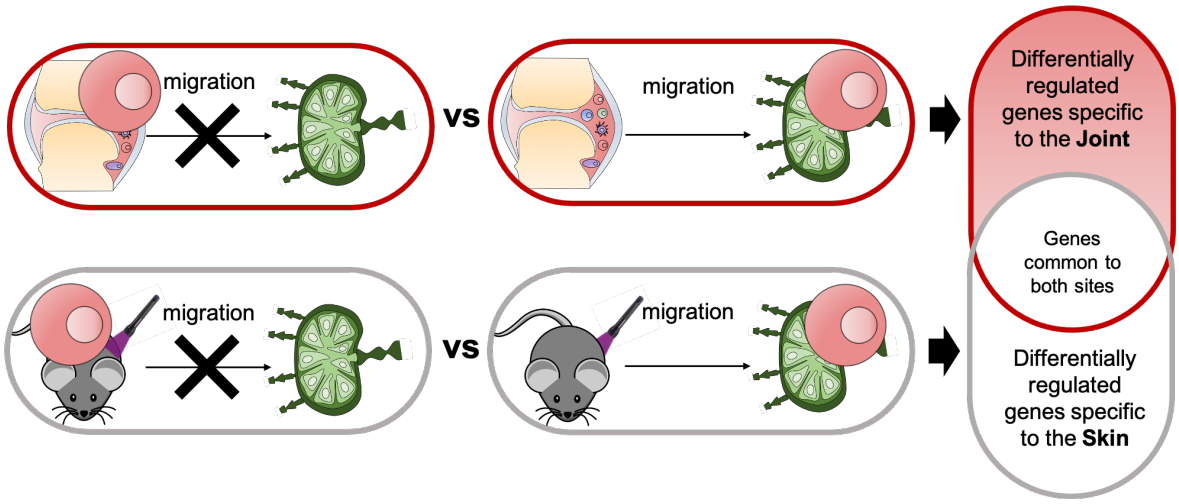

Figure 3-1. Schematic representation of experiments previously performed in the laboratory that generated a joint-specific differentially regulated gene list
Adapted from Robert A. Benson and Catriona Prendergast unpublished data. The breach of self-tolerance model of arthritis was performed in Kaede mice as described in Chapter 2 (section 2.3.3). Upon induction of the disease model experiment, cells from LNs and joints were harvested and sent for gene sequencing. Gene expression between cells that did not migrate to the LNs (joint-retained cells) and cells that migrated to the LNs (LN cells) were compared. In the first experiment (top diagram), gene sequencing generated a list containing 4,507 genes that were upregulated in the joint in comparison to LNs. In the second experiment (bottom part), gene sequencing generated a list of genes that were upregulated in a skin site in comparison to LNs. Then, genes that were present in both lists were excluded from the first gene list to finally generate a joint-specific differentially regulated gene list containing 217 genes.

From the set of 217 genes, pathway analysis revealed lists of genes related to distinct regulatory functions. A small list of 15 genes relevant to leukocyte migration pathways (Figure 3-2) was used to select candidates to test my hypothesis. Focus was given to upregulated genes from cells that were retained in the joints, as I believe that molecules encoded by these genes might be relevant in antigen presentation that occurs in the arthritic joint[106]. In addition, these molecules might play a role in the retention of leukocytes in the inflamed joints that are one of the causes of symptoms in RA patients[171], and therapeutic targeting these molecules might be an useful tool in symptomatic treatment of RA patients, as discussed in Chapters 1 (sections 1.7.1 and 1.8.3) and 6. However, at the time when this Thesis was being written, the data of absolute values of gene expression was not found. As such, it is not possible to know if the expression of these genes was, for example, lower than 100, which would mean a low expression that would possibly not be biologically relevant. Therefore, the interpretation of gene upregulation using only z-scores requires precaution.

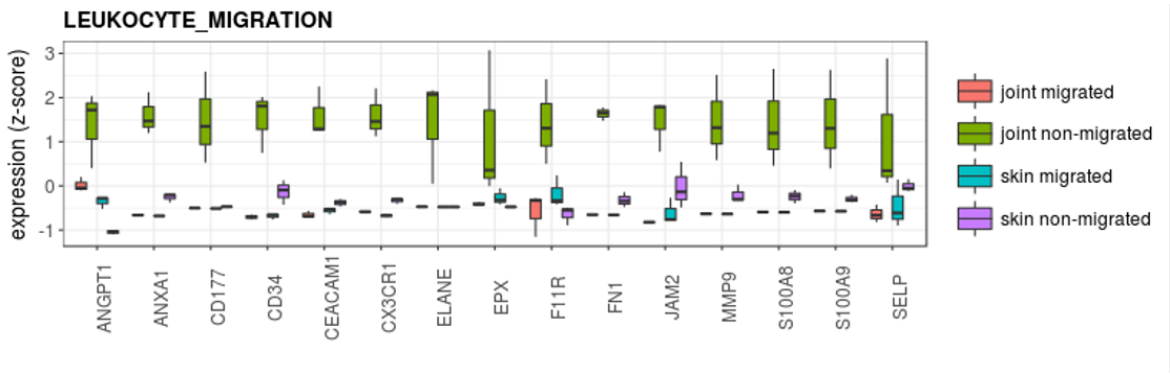

Figure 3-2. Identification of a joint-specific differentially regulated gene related to leukocyte migration
Adapted from Robert A. Benson and Catriona Prendergast unpublished data. The figure shows a graph of relative expression of the 15 genes involved in leukocyte migration in the joint migrated, joint non-migrated, skin migrated and skin non-migrated populations.

To support the foundation of my hypothesis that the upregulation in the 15 genes is related to an upregulation in molecules encoded by these genes on the surface of CD4+ T cells or DCs, I analysed the proportion of different immune cell types in the whole population. By looking at lineage markers for B cells (CD19+), T cells (CD3+), Neutrophils (CD11b+ Ly6G+) and DCs (CD11c+), I concluded that the majority of cells sent for RNAseq analysis were neutrophils, although there was also a considerable population of DCs (data not shown). I therefore gathered information from a gene bank (Immunological Genome Project, Gene Skyline, Microarray)[254] to analyse the expression profiles of the 15 genes related to leukocyte migration in T cells, DCs and neutrophils from spleens and LNs of C57BL/6 mice. Values for gene expression determined by microarray are shown in Table 3-1, where intervals based on the thresholds suggested by the gene bank relative to trace (0-5), very low (5-20) and low (20-80) expression are not highlighted, whereas medium (80-800), high (800-8000) and very high (>8000) intervals are highlighted in green, yellow and red, respectively. The analysis of these expression profiles showed that the genes expressed by DCs or CD4+ T cells at medium, high or very high levels were ANXA1, CD177, CEACAM1, CX3CR1, F11R and MMP9. Noting that neutrophils were the more frequently found cell type, I used the threshold suggested by the gene bank to exclude genes that were more highly expressed in arthritic joint neutrophils than any subtype of DC or CD4+ T cell. These were ANXA1 and MMP9 genes.

Table 3-1. Expression profiles of upregulated genes from joint non-migratory immune cells that are involved in leukocyte migration pathways

Gene Symbol	Cell Type / ProbeSet	Naive CD4+ T cell		Memory CD4+ T cell		CD8+ DC		CD11b+ DC		CD8- pDC	Neutrophil
		Spleen	LN	Spleen	LN	Spleen	LN	Spleen	LN	Spleen	Synovial Fluid
ANGPT1	10428376	17	17	17	20	21	18	35	23	32	24
ANXA1	10466606	27	25	50	36	564	593	240	128	32	1778
CD34	10352905	38	38	40	39	46	47	72	43	41	54
CD177	10560886	79	79	83	91	80	96	109	81	141	410
CEACAM1	10561008	39	37	35	35	83	77	163	246	1103	940
CX3CR1	10597743	80	85	117	103	235	123	297	302	92	134
ELANE	10364535	45	49	42	52	57	49	61	46	57	75
EPX	10389654	32	34	37	37	38	41	42	38	29	48
F11R	10351623	38	40	36	46	57	103	100	810	37	80
FN1	10355403	37	36	34	48	43	51	60	68	40	968
JAM2	10436666	43	48	46	49	47	48	58	57	43	67
MMP9	10478633	50	63	113	64	62	68	218	53	45	4266
S100A8	10493831	27	29	34	35	31	33	44	44	38	7740
S100A9	10499861	49	44	50	53	65	52	78	46	65	11321
SELP	10351206	39	36	51	42	43	38	60	39	33	136

From the list of 4 gene candidates that were left, an analysis of the availability of reagents for molecules encoded by each one of these genes was done. To date, the only candidate that has no commercially available agonist or antagonist reagents offered by the main companies that serve our laboratory (Thermo Fisher, BioLegend, BD Biosciences, Abcam, Sigma Aldrich) is the molecule CD177, also known as NB1. Lastly, a brief literature review was performed to gather information about the 3 candidates that met the established technical requirements: CEACAM1, CX3CR1 and F11R. Final selection was based on existing literature about surface expression by the immune cells of interest, preliminary results on manipulation of these molecules on the context of T cell-DC interactions and effects on manipulation in disease models, such as RA. For the purpose of this chapter, CEACAM1 was studied.

3.1.2 Carcinoembryonic Antigen-Related Cell Adhesion Molecule 1 (CEACAM1)

CEACAM1, also known as CD66a, is a cell-cell adhesion molecule, a member of the carcinoembryonic antigen (CEA) family and part of the IgSF[255,256]. This molecule was first described as a biliary glycoprotein found in human hepatic bile[257,258] and is expressed by several cell types, such as epithelial, endothelial and immune cells[259,260]. CEACAM1 is a transmembrane protein that has a cytoplasmatic tail and an extra-cellular region formed by an amino-terminal variable domain followed by up to three immunoglobulin C2 (IgC2)-like constant domains[261]. In mice and humans, 4 and 11 isoforms of CEACAM1 have been identified, respectively[262]. These variants differ in the number of extracellular domains and length of their cytoplasmatic tail. CEACAM1-4L, for example, contains 4 extracellular domains and a long cytoplasmatic tail, whereas CEACAM1-4S is formed by the same number of extracellular domains but has a short cytoplasmatic tail[261,262].

CEACAM1 can undergo homophilic (CEACAM1-CEACAM1) or heterophilic interactions with other members of the CEA family (CEACAM5, 6 and 8) in humans[257] or TIM-3 in humans[263] and mice[264]. In addition, CEACAM1 was also shown to function as an innate receptor for a number of pathogens in humans and mice, such as bacteria and viruses[265-274]. CEACAM1-4L and -4S are the isoforms capable of mediating homophilic binding[275-277], and the short form was shown to bind less avidly to immobilized CEACAM1 molecules in comparison to the long form[278]. Variants containing a long cytoplasmatic tail are reported to generally have inhibitory functions[261], whereas those with a short tail have been implicated in interactions with the cytoskeleton[279,280]. However, distinct cellular responses are promoted by CEACAM1 isoforms that play a role in signalling functions. This is suggested to be dependent on the balance between monomeric and dimeric forms[281], as many of these variants undergo dimerization. Additionally, the expression profile of isoforms varies according to cell type, phase of growth and activation status and may also dictate the fate of cellular outcomes driven by CEACAM1 binding as stimulation or inhibition[260,282,283].

CEACAM1 extra-cellular domains are essential for its intercellular functions in leukocytes. In B cells, CEACAM1 regulates BCR induced activation[283], cell survival

and is required for protective antiviral antibody production[284]. CEACAM1 is expressed by activated neutrophils[285] and plays a role in cell survival signals that prevent apoptosis[286] and in cytokine production[287]. In NK cells, CEACAM1 is also expressed upon cell activation[288] and is required for NK cytotoxic activity[289,290]. In DCs, anti-CEACAM1 stimulation was found to promote maturation, induce chemokine secretion and increase IL-6 and IL-12 production[291]. CEACAM1 is stored in T cell intracellular compartments and activated T cells can express CEACAM1 on their surface as rapidly as 30 minutes. Expression levels can be enhanced by addition of IL-2[260], IL-7 and IL-15 following stimulation with concanavalin A (ConA) or anti-CD3 stimulation[292,293]. A few studies suggest that CEACAM1 plays a role in T cell proliferation and cytokine production. T cells from CEACAM1 deficient mice show increased proliferation and secretion of IL-2 and IFN-γ upon different stimuli both *in vitro* and *in vivo*[261]. Treatment with different anti-CEACAM1 mAb clones were found to inhibit anti-CD3-induced lymphocyte proliferation[260,294] and IL-2 production[294]. Additionally, one of these clones were also found to decrease IL-4 and increase IFN-γ secretion by antigen-primed CD4+ T cells *in vitro*[291], suggesting that CEACAM1 may play a role in Th1 differentiation. Alternatively, treatment with a different mAb clone increased T cell activation and secretion of IFN-γ and TNF-α induced by anti-CD3 stimulus[293], illustrating the complexity of determining CEACAM1's role as either a stimulatory or inhibitory receptor. Nevertheless, mechanisms of action, such as recruited ligands, and possible effects of CEACAM1 blockade on T cells during priming *in vivo* remains uncertain.

CEACAM1 is upregulated in several pathological conditions, such as viral[295] and bacterial[296,297] infections, bowel inflammation[298], vascular inflammation[299,300] and is already considered a biomarker for many kinds of cancer[301,302]. CEACAM1 is suggested as a promising therapeutic target in melanoma, lung, colorectal and pancreatic cancers[301,303,304] and has been tested in a few animal models of inflammatory diseases. In a model of myocardial infarction, mice lacking CEACAM1 had lower mortality rate and improved cardiac function in comparison to WT mice[300], although the possible attribution of these effects to T cell immune regulation was not studied. In a model of multiple sclerosis, treatment with CEACAM1-Fc fusion protein inhibited the disease severity, whereas treatment with an anti-CEACAM1 mAb increased the gravity of the pathology[305]. These therapeutic effects were found to be dependent on invariant NK cell mechanisms influencing

the secretion of IL-17 and IFN-γ cytokines. In two models of inflammatory bowel diseases (IBD), treatment with anti-CEACAM1 mAb inhibited development of TNBS or oxazolone-induced colitis[306], an effect that was most pronounced if the antibody was administered after the induction phase. This protective effect was attributed to decreased Th1 polarization suggested by a reduction in the secretion of IFN-γ and intracellular expression of T-bet by lamina propria mononuclear cells.

Preliminary work has been previously published on the effects of manipulation of CEACAM1 pathways on T cell proliferation[260,294] and cytokine secretion[291,293,294] *in vitro*. However, effects of its blockade on T cell activation, proliferation and differentiation during antigen presentation *in vivo* remain to be studied. Furthermore, preclinical studies on CEACAM1 as a potential therapeutic target for other autoimmune disorders, such as lupus and arthritis, are still unexplored. Thereby, CEACAM1 showed to be a promising target for the aims proposed in this thesis and was the first molecule to be tested.

3.2 Results

3.2.1 CEACAM1 is Expressed by DCs

Prior to analysing the effects of CEACAM1 blockade on the crosstalk between CD4+ T cells and DCs, it was important to confirm that this marker is expressed by one or both of these cell types. For that, cells from spleens and LNs of WT mice were harvested and analysed by flow cytometry as detailed in Chapter 2. First, a 12-colour panel was developed to detect CD4+ T cells, cDC1, cDC2 and pDC populations, in which markers for identification of the different subtypes of DCs were based on Ford LB, et al. reports[307]. Then, this optimised 12-colour panel was used to identify the populations of interest in a gate strategy showed in Figure 3-3A, and the expression of CEACAM1 was determined on these different populations (Figure 3-3B), in which gates were based on the fluorescence emitted by its isotype control (Figure 3-3C). The expression of CEACAM1 in these cells was also quantified (Figure 3-3D). Additionally, the expression of TIM-3, a CEACAM1 ligand described in mice[264], was determined on CD4+ T cells (Figure 3-3E), using its isotype control fluorescence intensity to determine gates (Figure 3-3F).

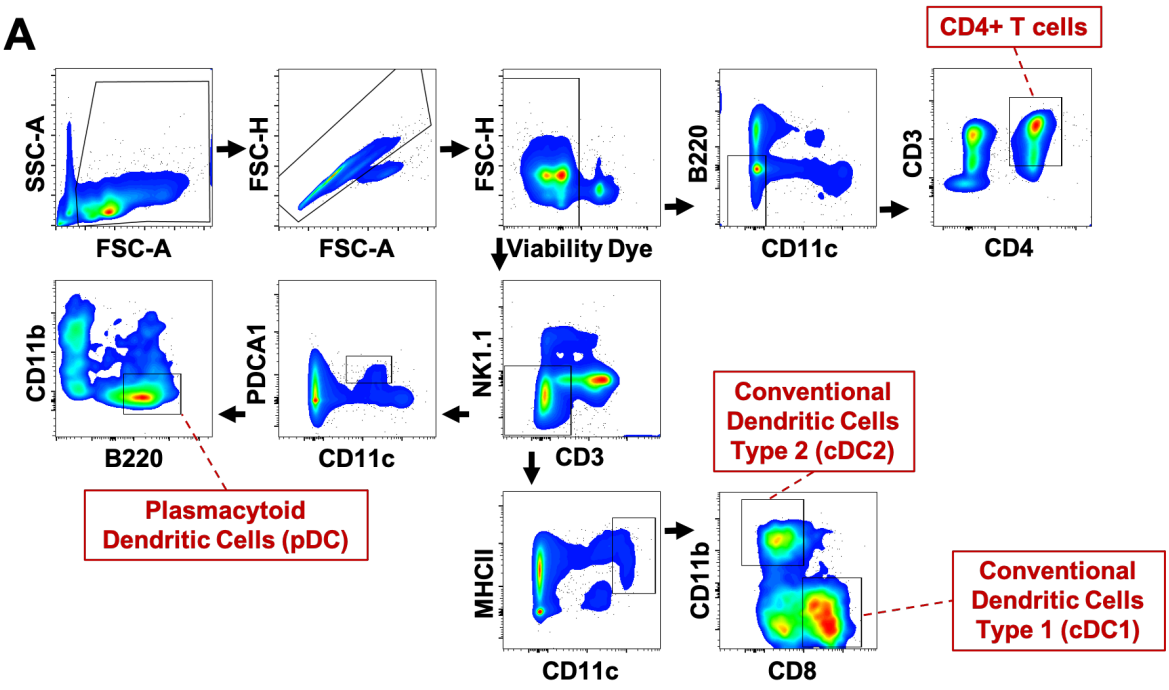
A
SSC-A
FSC-A
FSC-H
FSC-A
FSC-H
Viability Dye
B220
CD11c
CD3
CD4
CD4+ T cells
CD11b
B220
PDCA1
CD11c
NK1.1
CD3
Plasmacytoid Dendritic Cells (pDC)
Conventional Dendritic Cells Type 2 (cDC2)
MHCII
CD11c
CD11b
CD8
Conventional Dendritic Cells Type 1 (cDC1)

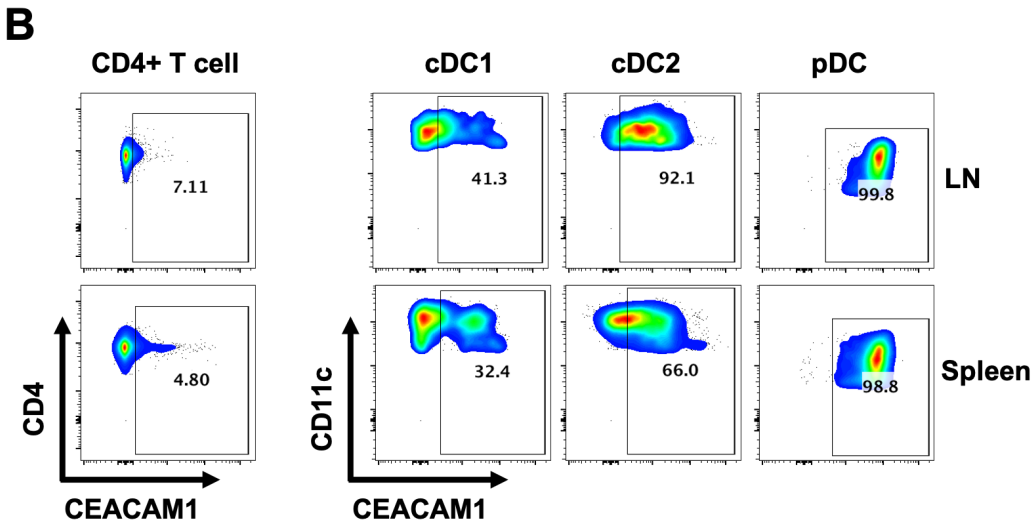
B
CD4+ T cell
cDC1
cDC2
pDC
7.11
41.3
92.1
99.8
LN
4.80
32.4
66.0
98.8
Spleen
CD4
CEACAM1
CD11c
CEACAM1

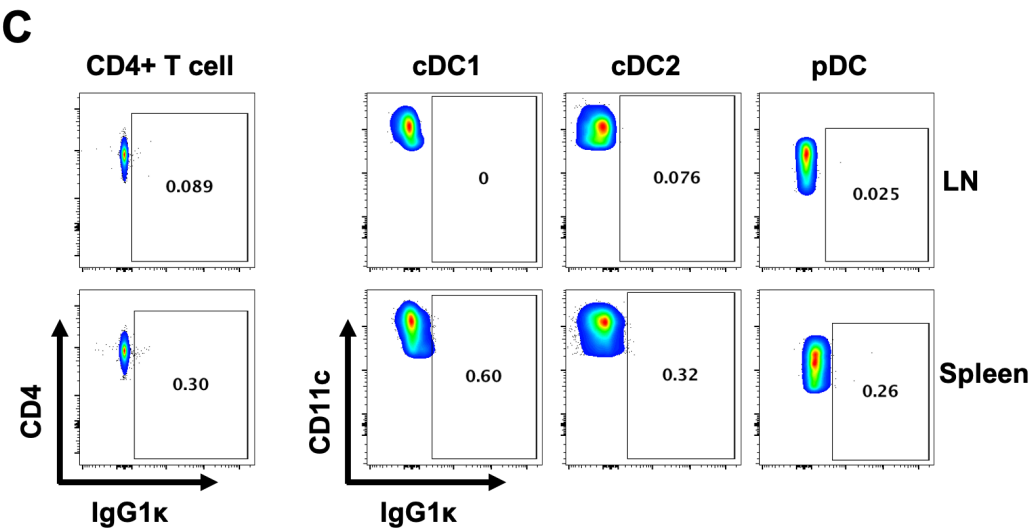
C
CD4+ T cell
cDC1
cDC2
pDC
0.089
0
0.076
0.025
LN
0.30
0.60
0.32
0.26
Spleen
CD4
IgG1κ
CD11c
IgG1κ

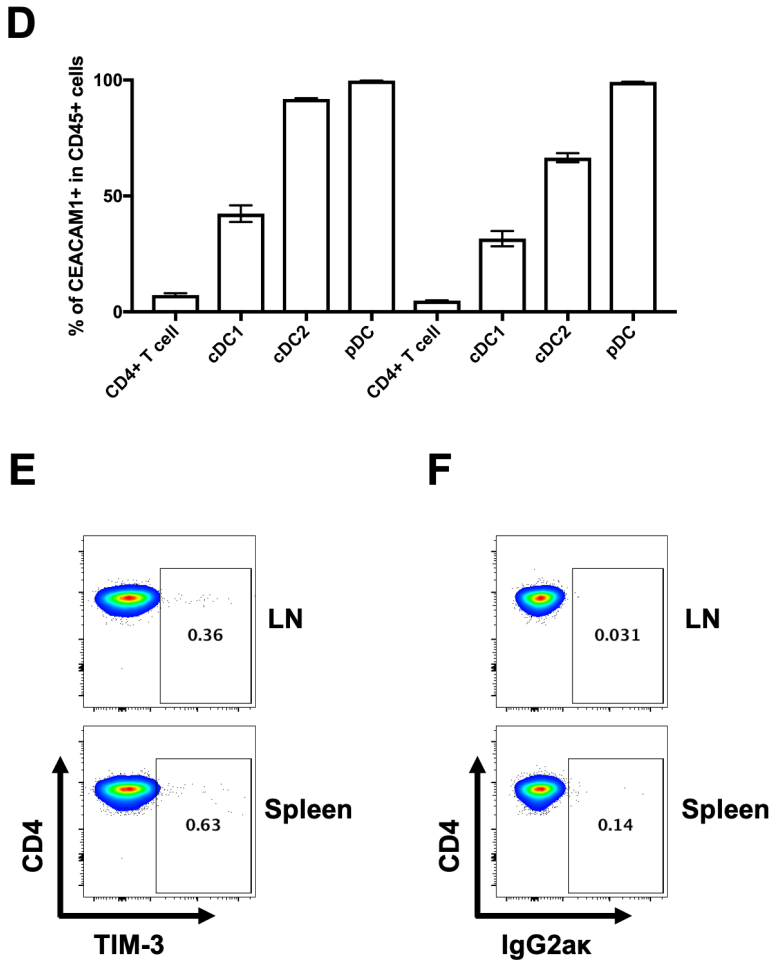

Figure 3-3. CEACAM1 expression on murine CD4+ T cells and DCs
Immune cells from C57BL/6 mice were analysed by flow cytometry for the expression of CEACAM1 and TIM-3. **(A)** Gating strategy from a 12-colour flow cytometry panel for identification of CD4+ T cells, plasmacytoid DCs (pDC), conventional DCs type 1 (cDC1) and conventional DCs type 2 (cDC2) in cells from lymph nodes (LN) gated based on fluorescence minus one (FMO) controls. After selecting leukocytes by size and granularity, doublets and dead cells were excluded. To detect CD4+ T cells, events that were negative for the B cell lineage marker B220 and the DC lineage marker CD11c were selected and CD4+ T cells were detected by expression of CD3 and CD4. To detect DCs, NK1.1- CD3- events were gated. $CD11c_{low}$ PDCA1+ B220+ CD11b- events were considered as pDCs. Conventional DCs were considered as $CD11c_{high}$ MHCII+, and events were separated between CD8+ (cDC1) and CD11b+ (cDC2) cells. **(B)** Representative dot plots of CEACAM1 expression **(C)** or its isotype control on CD4+ T cells or on different subtypes of DCs from spleens and LNs and **(D)** quantification of CEACAM1+ cells. **(E)** Representative dot plots of TIM3 expression **(F)** or its isotype control on CD4+ T cells from spleens and LNs (CD3+ CD4+). Gates on B and D show specific binding based on the fluorescence emitted from its matched isotype controls shown on C and E, respectively. Data are representative of an experiment performed in biological triplicates.

Most CEACAM1+ cells were CD11c- B220+ (84.7% ± 2.86 in LNs and 78.6% ± 1.39 in spleens), possibly reflecting B cell populations. DCs expressed different levels of CEACAM1, depending on its subtype or lymphoid organ in which they populated. Nearly all pDCs expressed high levels of CEACAM1. Conventional DCs type 2 also

expressed CEACAM1 in high proportions, especially LN resident cDC2. Populations of cDCs1 also expressed CEACAM1. On the other hand, only a small proportion of naïve CD4+ T cells expressed CEACAM1. The CEACAM1 ligand TIM-3 was not detected on naïve CD4+ T cells. I then investigated the expression of CEACAM1 and TIM-3 on primed CD4+ T cells.

3.2.2 CEACAM1 is Upregulated on Antigen-Stimulated CD4+ T cells

To investigate whether CEACAM1 is upregulated on CD4+ T cells upon antigen stimulation, mature BMDCs were cultured as described in Chapter 2 and pulsed or not with pOVA to be co-cultured with naïve OTII CD4+ T cells. CD4+ cells were then analysed by flow cytometry at co-culture set-up (0 hours) and 24, 48 and 72 hours. For the flow cytometric analysis, expression of the surface marker CD44 was used to identify activated T cells[308] (Figure 3-4A). For the detection of T cells, the CD4 marker was used. Generally, 10-20% of CD4+ T cells from naïve spleens and LNs of OTII mice are $CD44_{high}$ (Caio S. Bonilha unpublished observations), whereas cultures that have received antigen stimulation had higher proportions of $CD44_{high}$ and were considered as activated T cells. Surface expression of CEACAM1 on T cells was determined (Figure 3-4B), in which gates were based on the fluorescence emitted by its isotype control (Figure 3-4C), and its proportions were compared between T cells that have received antigen stimulation and T cells that were cultured with BMDCs that were not carrying antigen (Figure 3-4D). Expression of TIM-3 was also determined on activated CD4+ T cells in the different time points (Figure 3-4E), using its isotype control fluorescence intensity to determine gates (Figure 3-4F).

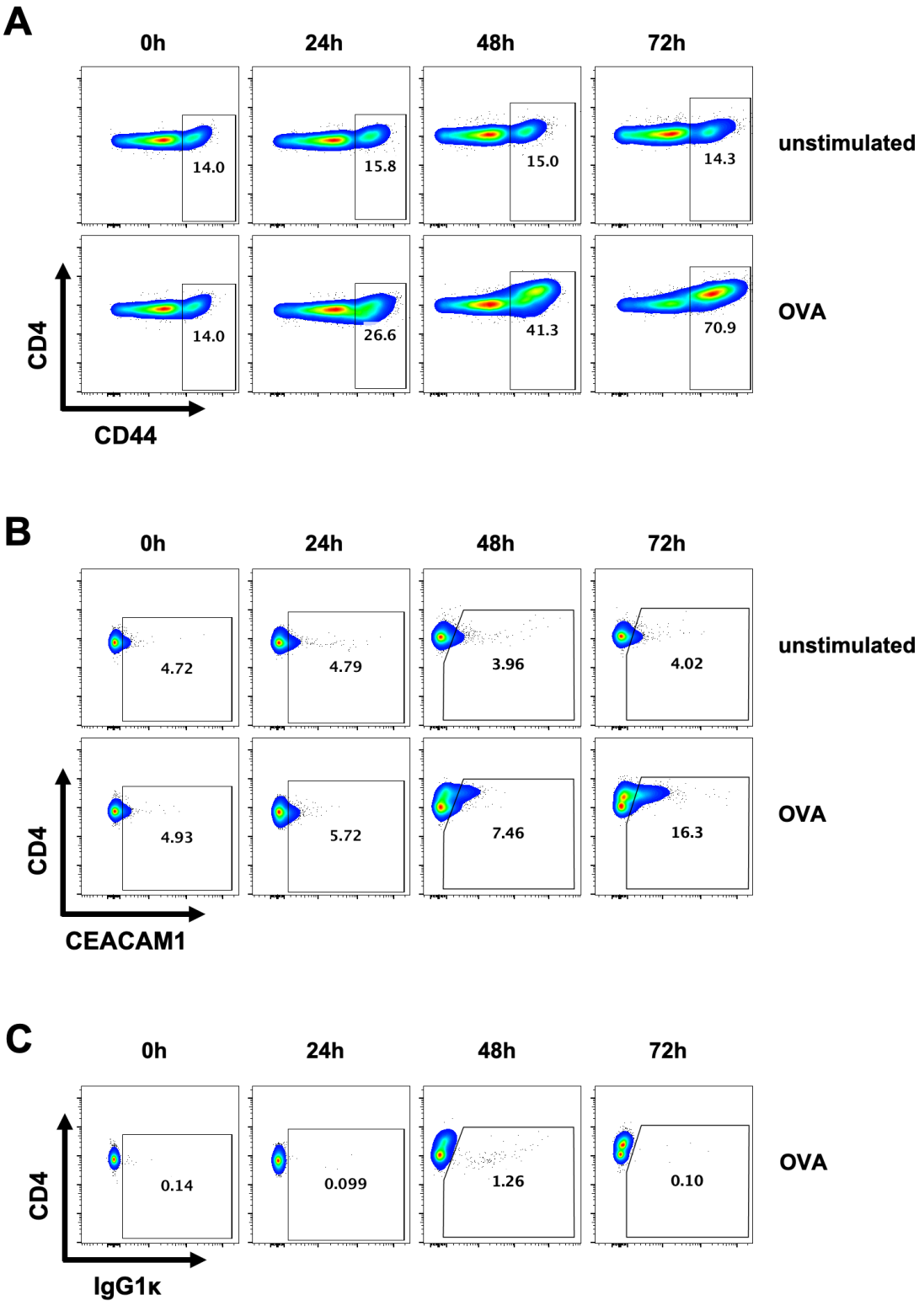
A
0h
24h
48h
72h
14.0
15.8
15.0
14.3
unstimulated
14.0
26.6
41.3
70.9
OVA
CD4
CD44
B
0h
24h
48h
72h
4.72
4.79
3.96
4.02
unstimulated
4.93
5.72
7.46
16.3
OVA
CD4
CEACAM1
C
0h
24h
48h
72h
0.14
0.099
1.26
0.10
OVA
CD4
IgG1κ

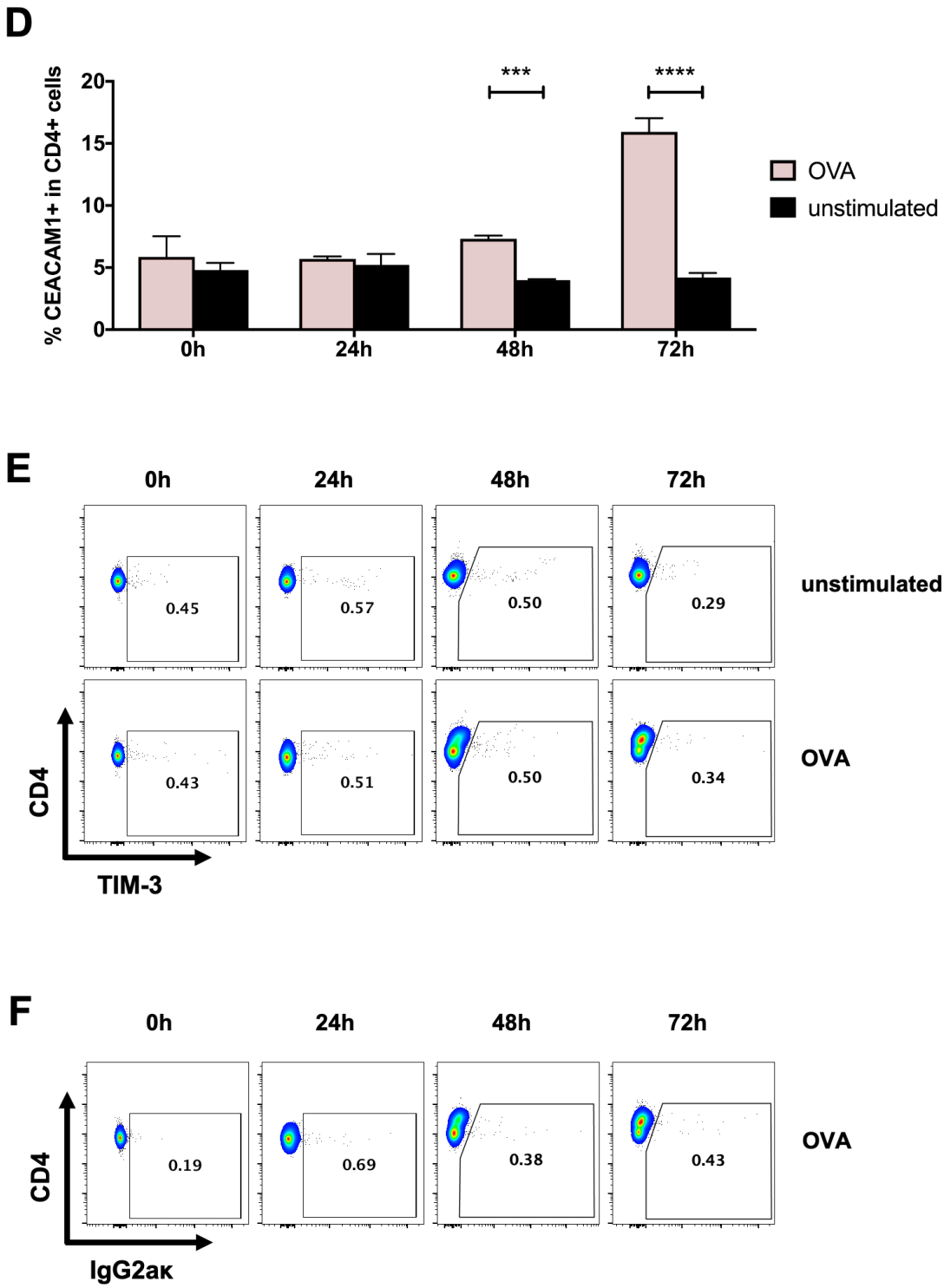

Figure 3-4. CEACAM1 and TIM-3 expression on CD4+ T cells upon priming
CD4+ T cells from OTII mice were cultured with OVA peptide (pOVA)-pre-pulsed bone marrow derived dendritic cells and analysed for the expression of CEACAM1 and TIM-3 in different time points after the co-culture set-up. **(A)** Representative dot plots of CD44 expression on unstimulated and OVA-stimulated CD4+ T cells with gating on $CD44_{high}$ cells. **(B)** Representative dot plots of CEACAM1 expression on unstimulated and OVA-stimulated CD4+ T cells **(C)** or its isotype control on OVA-stimulated CD4+ T cells and **(D)** quantification of CEACAM1+ cells with comparison between the two different groups 0, 24, 48 and 72 hours after priming. **(E)** Representative dot plots of TIM-3 expression on unstimulated and OVA-stimulated CD4+ T cells **(F)** or its isotype control on OVA-stimulated CD4+ T cells. Gates show specific binding based on its matched isotype control. Results are expressed as mean ± SD of an experiment performed in triplicates. Statistical differences were determined using a two-way ANOVA. ***$p \leq 0.001$, ****$p \leq 0.0001$.

CD4+ T cells cultured with pOVA-pre-pulsed BMDCs were successfully primed as shown by a time dependent increase in the frequency of $CD44_{high}$ populations. In contrast, T cells that didn't receive antigen stimulation failed to upregulate this marker. A low frequency of CEACAM1-expressing cells was found on CD4+ T cells cultured with BMDCs not carrying antigen and with pOVA-pulsed-BMDCs 24 hours after co-culture set-up. The proportions of CEACAM1-expressing cells on CD4+ T cells that were incubated 48 and 72 hours with antigen-pulsed-BMDCs were higher in comparison to CD4+ T cells that were incubated with BMDCs not carrying antigen for the same periods of time. TIM-3 was not detected on naïve or activated CD4+ T cells, as dot plots from cells that were incubated with fluorophore-conjugated anti-TIM-3 antibody showed a similar pattern of those that were incubated with its isotype control.

3.2.3 CEACAM1 is Highly Expressed by BMDCs

The last step before analysing the effects of CEACAM1 blockade on CD4+ T cells priming was to verify if BMDCs express this marker. BMDCs were cultured for 7 days and analysed by flow cytometry for the expression of CD86, a marker for DCs' maturity[309], and CEACAM1 (Figure 3-5A). To mature BMDCs, LPS stimulation was given from day 6 to 7, before analysis. The proportion of cells expressing CEACAM1 was quantified and compared between immature and mature BMDCs (Figure 3-5B). Isotype control antibodies for the CD86 and CEACAM1 antibody clones were used to identify specific binding.

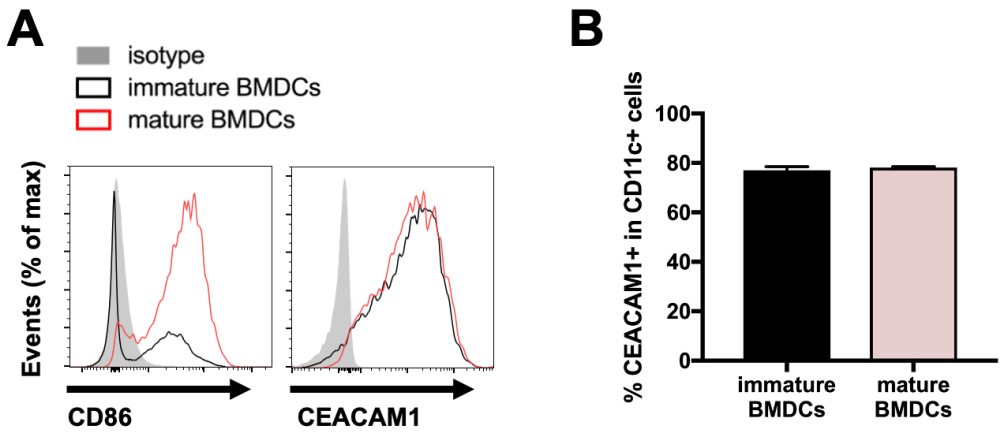

Figure 3-5. CEACAM1 expression on BMDCs
BMDCs were cultured for 7 days and analysed by flow cytometry for the expression of CEACAM1. **(A)** Representative histograms of expression of CD86 (left side) and CEACAM1 (right side) on immature (black unfilled) or mature BMDCs (red unfilled) or in BMDCs stained with matched isotype controls (grey-shaded). **(B)** Comparison of the proportion of CEACAM1+ cells from immature and mature BMDCs gated according to its isotype control. Results are expressed as mean ± SD of an experiment performed in triplicates. Statistical difference was determined using an unpaired Student's t test. p = non-significant.

The expression of CD86 showed that LPS-stimulated BMDCs achieved full maturity[310,311]. CEACAM1 was expressed on similar levels on both immature and mature BMDCs, with no significant difference between these two populations. This experiment validated the use of BMDCs for CEACAM1 functional assays, as these cells expressed similar levels as some populations of DCs found *in vivo*, such as LN cDC2.

3.2.4 Treatment with Anti-CEACAM1 Monoclonal Antibody (mAb) CC1 During Antigen Presentation has No Effect on CD4+ T Cells Priming

After demonstrating that DCs and BMDCs express CEACAM1, I could utilise my *in vitro* assay to test if blockade of CEACAM1 with anti-CEACAM1 mAb CC1 changes the outcomes of T cells upon priming. BMDCs pre-pulsed with pOVA were cultured with CFSE-labelled, naive OTII CD4+ T cells in complete medium in the presence of anti-CEACAM1 mAb CC1 or isotype control for 72 hours and analysed by flow cytometry. Cells that have divided were identified using CFSE dilution (Figure 3-6A). This is based on the rationale that daughter cells emit half of the CFSE fluorescence of the mother cell. In addition, cells that divided three times were also analysed (Figure 3-6B). To assess T cell activation, the proportion of $CD44_{high}$

cells were also determined (Figure 3-6C). In addition, supernatants from these cultures were kept for the detection of IFN-γ by ELISA (Figure 3-6D). This analysis aimed to validate the CC1 mAb for its use in functional assays by replicating results from the literature that showed that CEACAM1 manipulation with the use of another anti-CEACAM1 clone (mAb AgB10) increased IFN-γ secretion by antigen-specific T cells[291].

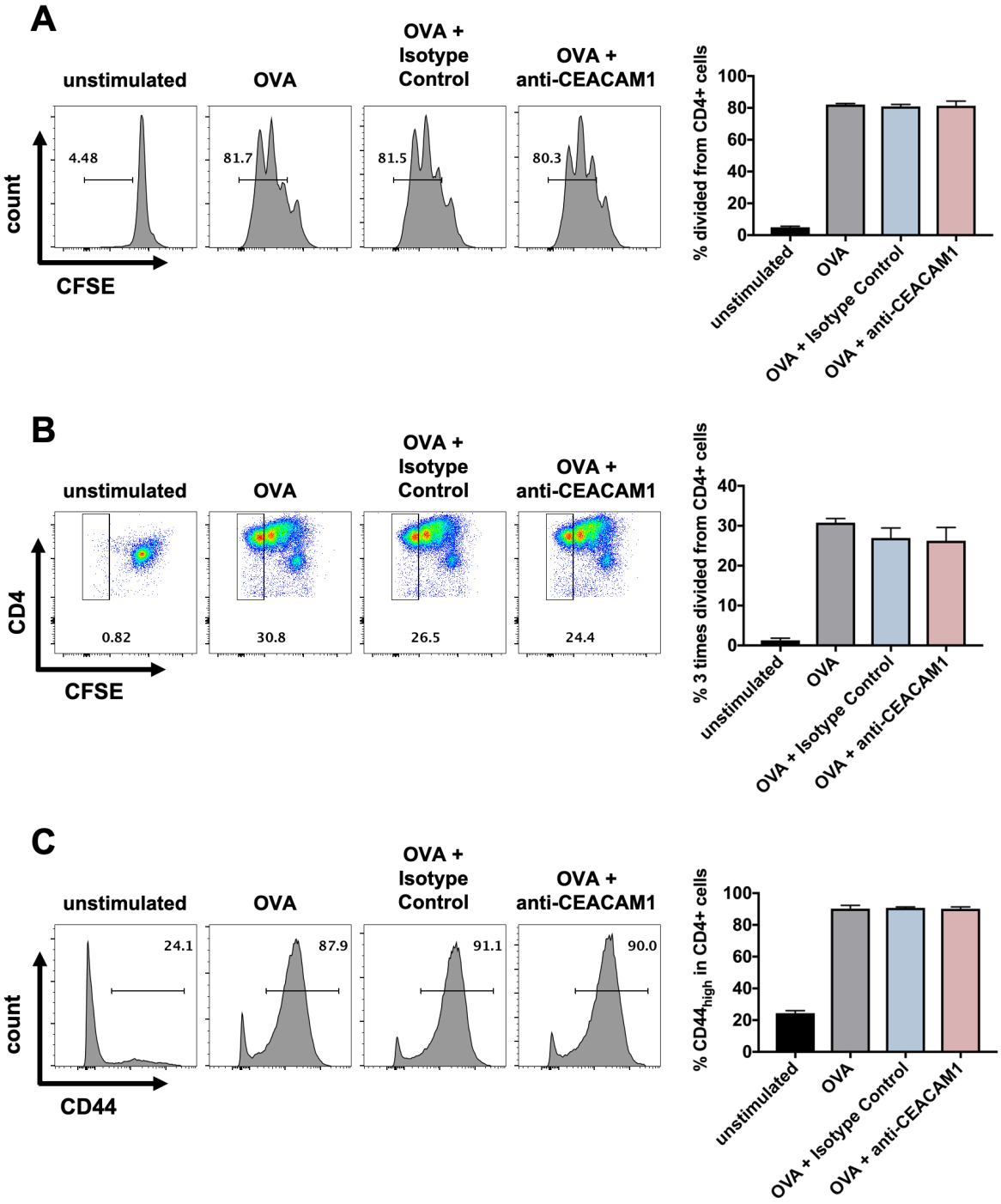
A
unstimulated
OVA
OVA + Isotype Control
OVA + anti-CEACAM1
4.48
81.7
81.5
80.3
count
CFSE
% divided from CD4+ cells
100
80
60
40
20
0
unstimulated
OVA
OVA + Isotype Control
OVA + anti-CEACAM1
B
unstimulated
OVA
OVA + Isotype Control
OVA + anti-CEACAM1
0.82
30.8
26.5
24.4
CD4
CFSE
% 3 times divided from CD4+ cells
40
30
20
10
0
unstimulated
OVA
OVA + Isotype Control
OVA + anti-CEACAM1
C
unstimulated
OVA
OVA + Isotype Control
OVA + anti-CEACAM1
24.1
87.9
91.1
90.0
count
CD44
% CD44high in CD4+ cells
100
80
60
40
20
0
unstimulated
OVA
OVA + Isotype Control
OVA + anti-CEACAM1

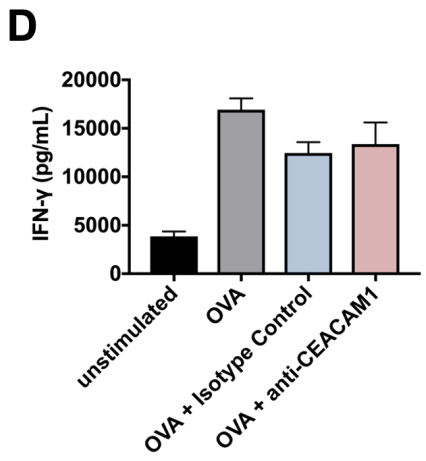

Figure 3-6. Effects of anti-CEACAM1 mAb CC1 on CD4+ T cell activation and proliferation
CFSE-labelled CD4+ T cells from OTII mice were cultured with OVA peptide (pOVA)-pre-pulsed bone marrow-derived dendritic cells in the presence of anti-CEACAM1 mAb (CC1) or its isotype control for 72 hours and analysed by flow cytometry and ELISA. **(A)** Representative histograms of CFSE fluorescence intensity on CD4+ cells (left side) and quantification of CD4+ T cells that have divided based on the gating of CFSE fluorescence intensity (right side). **(B)** Representative dot plots of CFSE fluorescence intensity on CD4+ cells with gating on fluorescence equivalent to three divisions (left side) and quantification of CD4+ T cells that have divided three times (right side). **(C)** Representative histograms of CD44 fluorescence intensity on CD4+ cells (left side) and quantification of CD4+ T cells that are $CD44_{high}$ (right side). **(D)** Quantification of IFN-γ concentration present in the co-cultures' supernatants detected with ELISA. Results are expressed as mean ± SD of an experiment performed in triplicates. Statistical differences in all graphs were determined between anti-CEACAM1-treated group and the two other groups that received antigen stimulation using a one-way ANOVA. p = non-significant for all comparisons.

The group treated with anti-CEACAM1 mAb CC1 did not show any significant difference in T cell activation and proliferation in comparison to the isotype control or to the untreated OVA-stimulated groups. In addition, no difference was found on the concentration of IFN-γ from culture supernatants. This either suggests that the antibody was not blocking CEACAM1 pathways or that it was not binding to its specific target for unknown reasons. To address the question of whether the purified CC1 mAb was binding to CEACAM1, I pre-treated BMDCs with the CC1 mAb. After 30 minutes, I incubated BMDC with a fluorophore conjugated CC1 antibody of the same clone and evaluated if the pre-treatment was able to inhibit binding of the conjugated antibody (Figure 3-7).

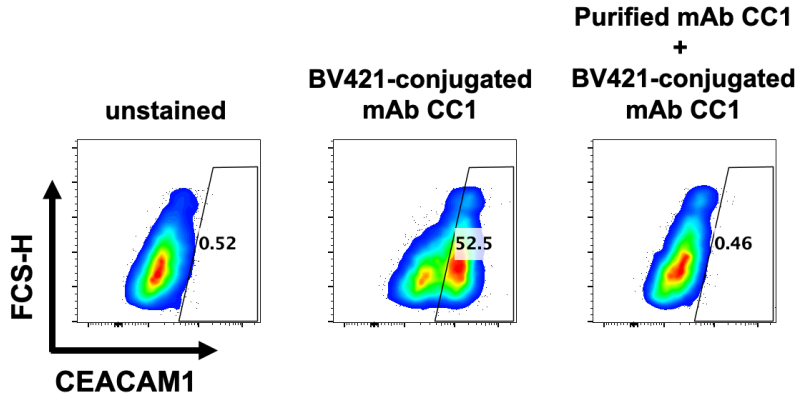

Figure 3-7. Assessment of the capacity of purified anti-CEACAM1 mAb CC1 to block fluorophore conjugated anti-CEACAM1 ligation to CEACAM1
Day-7 immature BMDCs were used to analyse if the purified anti-CEACAM1 mAb CC1 was binding to the specific target. Dot plots of CEACAM1 expression in untreated unstained control, untreated positive control stained with fluorophore-conjugated anti-CEACAM1 antibody and purified anti-CEACAM1 mAb CC1 pre-treated and stained with fluorophore-conjugated anti-CEACAM1 antibody are shown.

The purified anti-CEACAM1 mAb CC1 was able to block ligation of the fluorophore conjugated, anti-CEACAM1 CC1 mAb, indicating that the purified antibody that was being used for functional assays was able to bind to its specific target. Approaches to obtain alternative CEACAM1 reagents were tried and are described in the Discussion section of this chapter (section 3.3). I then moved to an alternative approach to manipulate CEACAM1 expression on BMDCs to use these cells in my functional assays.

3.2.5 siRNA Targeting *CEACAM1* Gene Has Minimal Impact on CEACAM1 Expression on BMDCs

As previously shown, CEACAM1 is expressed in high levels by DCs and BMDCs but in low levels by CD4+ T cells. Genetically manipulated BMDCs that express low levels of CEACAM1 could be used in functional assays aiming to determine the role of CEACAM1 in the interactions between T cells and DCs. For this genetic manipulation, I chose the siRNA technique. Immature BMDCs were transfected with CEACAM1 siRNA and different concentrations of Lipofectamine 2000, a transfection reagent that has previously been shown to work for BMDCs[312,313]. Cells were then harvested 72 hours after the transfection and analysed by flow cytometry for the expression of CEACAM1 (Figure 3-8A). CD11c was used as a DC marker to identify the target population. For the control group, siRNA targeting

GFP, a gene responsible for encoding the GFP fluorescent protein and that is not present in the system, was used. The expression of CEACAM1 on CD11c+ cells was then compared between groups (Figure 3-8B).

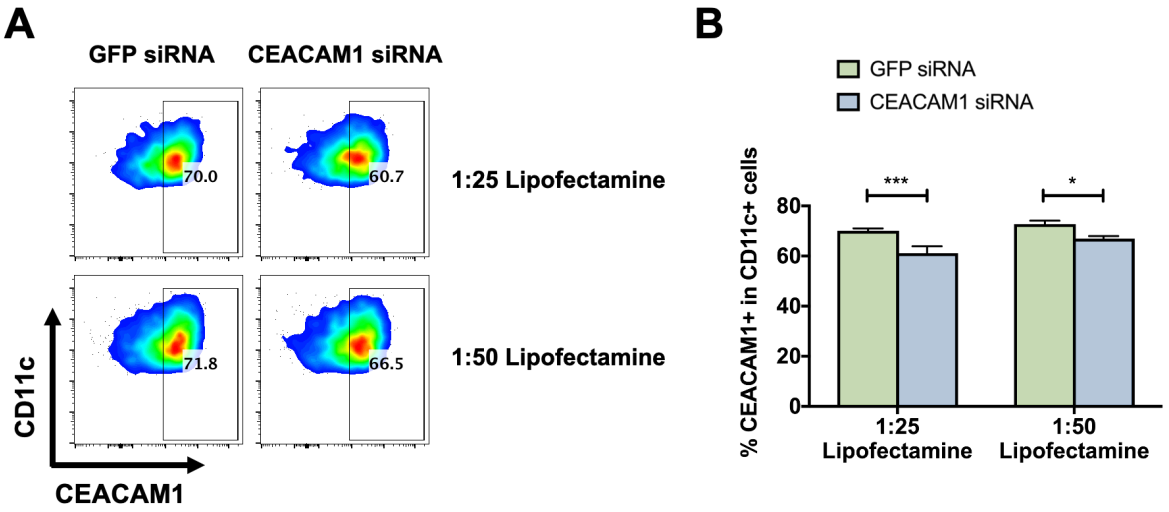

Figure 3-8. CEACAM1 siRNA effects on BMDC CEACAM1 expression
Day-7 immature BMDCs were transfected with siRNA targeting the *CEACAM1* gene or the *GFP* gene (control) and different concentrations of Lipofectamine 2000 for 72 hours to be analysed by flow cytometry for the expression of CEACAM1. **(A)** Representative dot plots of CEACAM1 expression on CD11c+ cells. **(B)** Quantification of the proportion of CEACAM1+ cells and comparison between CEACAM1 siRNA and GFP siRNA groups. Results are expressed as mean ± SD of triplicate cultures from two independent experiments. Statistical differences were determined using a two-way ANOVA. *$p \leq 0.05$, ***$p \leq 0.001$.

BMDCs transfected with siRNA targeting the *CEACAM1* gene showed a small but statistically significant reduction in expression of CEACAM1 with both concentrations of Lipofectamine 2000. However, the decrease was minimal and would be unlikely to be biologically relevant in the context of my assays. Other attempts with changes in the protocol were performed aiming to obtain a greater decrease and are discussed in the next section (3.3).

3.3 Discussion

Conventional DCs type 2 are subtype of DC that are known to have dominant role in antigen presentation in the context of MHCII molecules[6,32] and that I showed to express high levels of CEACAM1. CEACAM1 was also expressed at lower levels on cDC1 and at higher levels on pDCs. CEACAM1 could play a role in intercellular interactions between leukocytes by homophilic binding, or between CEACAM1 and other potential surface ligands, such as TIM-3[262-264]. Naïve CD4+ T cells express

CEACAM1 in low proportions, something that was previously reported[314] and confirmed by my experiments, and undetectable levels of TIM-3, the only heterophilic ligand for CEACAM1 described in mice to this date[264,301]. Although a positive control for TIM-3 staining was not used in the experiments in this thesis, the literature reports lack of TIM-3 expression on splenic CD4+ T cell of 12-week old C57BL/6 mice[315]. This study have used the same mAb clone that was used in my experiments (RMT3-23), that have proven specific ligation to TIM-3[263]. However, the expression of other ligands described in humans, such as CEACAM5, CEACAM6 or CEACAM8[261] was not investigated. Considering that the literature suggests that CEACAM1 blockade could have an impact on DC-T cell crosstalk[291,316] and that other ligands may have not been discovered yet, I pursued the investigation of whether CEACAM1 plays a role on CD4+ T cell priming. Antigen stimulated CD4+ T cells expressed higher levels of CEACAM1 in comparison with naïve cells, supporting results from the literature that showed increased CEACAM1 surface expression in T cells stimulated with anti-CD3 antibodies or ConA[292]. This upregulation may suggest that CEACAM1 may play a role in T cell effector functions and that homophilic binding could be important in secondary encounters of effector T cells with APCs carrying specific antigen.

Purified anti-CEACAM1 mAb CC1 was acquired from a commercial source that indicated this product had an impact in functional assays similar to those I wished to perform. To investigate if this mAb clone was able to block CEACAM1 intercellular interactions, I tried to replicate results from the literature that described a decreased secretion of IFN-γ upon blockade during priming *in vitro*[291]. For this, I used an assay with OTII naïve CD4+ T cells and BMDCs that I had demonstrated expressed high levels of CEACAM1. Anti-CEACAM1 mAb CC1 was not able to affect the secretion of IFN-γ measured in the co-culture supernatants. Additionally, although CEACAM1 blockade by treatment with anti-CEACAM1 mAb clones D14HD11 and 4/3/17 were previously found to inhibit anti-CD3-induced proliferation *in vitro*[260,294], no effects on proliferation or activation were found with treatment of anti-CEACAM1 mAb CC1 in my assay. To ensure that the purified antibody was binding to its specific target, I performed an experiment that showed that treatment with the purified antibody inhibited the ligation of a fluorophore conjugated anti-CEACAM1 antibody. It is possible that mAb CC1 might have a stimulatory effect in the system, as a distinct mAb (HD11) was found to increase

T cell activation mediated by an anti-CD3 mAb[293]. Perhaps, this could be addressed by repeating my *in vitro* assay with the use of a suboptimal concentration of antigen, to allow a margin for stimulation to be detected, since only an optimal concentration of antigen was used. However, before this was done, results from experiments that were being performed by other lab members were revealed.

The former lab members Drs Robert A. Benson and Catriona Prendergast performed experiments including the breach of self-tolerance model of arthritis, which is extensively discussed within this thesis, using the mAb CC1. No differences were found between anti-CEACAM1 mAb CC1 and the isotype control in any of their *in vitro* experiments (unpublished data not shown). Also, no differences were found in clinical and pathological measurements and on markers for CD4+ T cell activation from treated mice in comparison to the control group under induction of the RA murine model (unpublished data not shown). These results suggest that the mAb CC1 was not having any effect in *in vitro* or *in vivo* systems. These findings are supported by a study from 2018 that found no or minimal anti-tumour effect under treatment with mAb CC1 *in vivo*[317] but contradicted by a previous study that showed beneficial effects on a murine model of colitis under treatment of this same mAb clone in comparison to an isotype control[306]. This study from 2018 used protein and cell-based ELISA assays to show that the mAb CC1 is not able to block CEACAM1 homophilic interactions[317].

As reliable sources for reagents with proven efficacy for disruption of CEACAM1 pathways could not be identified, I tried to inhibit CEACAM1 expression on BMDCs by employing siRNA. In theory, siRNA silencing of CEACAM1 in BMDCs could have been used for *in vitro* and *in vivo* assays which could show the possible effects of blockade of CEACAM1 ligation in the interactions between T cells and BMDCs. I transfected siRNA targeting the *CEACAM1* gene to BMDCs in an attempt to silence CEACAM1 mRNA expression that would lead to a decrease in CEACAM1 surface expression. Although reverse transcription-polymerase chain reaction (RT-PCR) was not used to show that the transfection was able to affect the expression of mRNA molecules, I concluded that the transfection was successful as it could affect the expression of CEACAM1 on BMDCs. However, although CEACAM1 half-life is relatively short (26-40 hours)[318], the decrease found in my experiments was minimal, as a substantial proportion of the transfected cells were still expressing

CEACAM1. In addition, my attempts to improve these results by modifying different variables of the protocol (cell number seeded, concentration of siRNA, concentration of the transfection reagent and presence of absence of LPS treatment to induce cell maturation) were not successful. An intervention aiming for transfection at a time point earlier than 7 days after initiation of BMDCs culture could not only affect CEACAM1 surface expression but possibly other undiscovered pathways relevant to BMDCs differentiation in which this molecule may play a role. In addition, a tool that could possibly promote a bigger change on the expression of surface molecules in a short period of time that is to induce full cell maturation with 24-hour LPS stimulation after siRNA transfection was not successful for CEACAM1 siRNA on BMDCs. This tool was successful in other studies in which siRNA targeted other genes, such as genes that encode CD40[319,320], CD80 and CD86[312,313]. It is believed that this approach was successful for these molecules because they are quickly upregulated on the cells surface upon BMDC maturation, which does not occur with CEACAM1 as showed in section 3.2.3 of this chapter.

The same study that showed that anti-CEACAM1 mAb CC1 is not able to block homophilic binding demonstrated that fragment-antigen-binding (Fab) fragments generated from digestion of this antibody clone were able to block homophilic binding on a cell-based assay[317]. However, this was only performed after work with another candidate molecule was advanced, and focus was given to these studies. As such, approaches of digesting anti-CEACAM1 mAb CC1 for generation of Fab fragments could base future work.

The balance of CEACAM1 isoforms found in affected tissues from different pathological conditions are fundamental for distinguishing CEACAM1 potential targeting[263,321–323]. The possible classification of CEACAM1 as a T cell co-stimulatory/inhibitory molecule is dependent of this isoform balance, which may difficult potential therapies for cancer/autoimmune diseases. In addition, given CEACAM1 expression in different cell types, its manipulation may affect diverse pathways (endothelial cell-endothelial cell, leukocyte-endothelial cell, leukocyte-leukocyte). As such, studies utilising cell-selective CEACAM1 deletion may point important pathway-specific roles in distinct pathological conditions.

As I had taken the study of CEACAM-1 as far as possible with the reagents available I next progressed to another candidate gene identified in our screen. Considering the potential of these molecules based on the expression profiles shown in the first section of this chapter, in which *F11R* gene expression seems to be much higher on CD11b+ DCs than in neutrophils from the synovial fluid of arthritic mice, I decided to test my hypothesis and focus my study on the molecule encoded by *F11R*, which is the subject of the next chapter.

Chapter 4 JAM-A Contributes to CD4+ T cell Effector Functions During Priming *in vitro*

4.1 Introduction

The junctional adhesion molecule-A (JAM-A), also called junctional adhesion molecule-1 (JAM-1), is a molecule encoded by the *F11R* gene. The *F11R* gene was identified from the list of 15 genes relevant to leukocyte migration pathways, as explained in Chapter 3 (section 3.1). In summary, the breach of tolerance RA model was performed in WT mice and migratory and non-migratory cells from inflamed joints and pLNs were sent for transcriptomic analysis, in which differentially regulated genes were identified. The *F11R* gene was upregulated in non-migratory immune cells from the joint, suggesting that JAM-A expression by joint non-migratory immune cells could also be upregulated. Due to the nature of induction of inflammation in this disease model, as well as the fact that antigen presentation can occur in arthritic joints[106], I hypothesized that JAM-A can play a role in the interactions between T cells and APCs. Moreover, *F11R* is the only gene from the list of 15 genes that is more expressed in DCs (CD11b+ DCs from LNs) than in neutrophils from the synovial fluid of arthritic mice (see section 3.1). This data was important in the decision to choose this candidate, as immune cells sent for pathway analysis were composed of a higher proportion of neutrophils than T cells or DCs, suggesting that the different regulation found in the F11R gene was not influenced by neutrophils, but could have been influenced by a higher proportion of DCs or an upregulation of gene expression within DC populations. Studies that manipulated JAM-A *in vitro* were reviewed and I then proceeded to examine its role using the assays and approaches described in previous chapters.

4.1.1 Junctional Adhesion Molecule-A (JAM-A)

JAM-A is part of the junctional adhesion molecules (JAM) family, member of the IgSF, and received its first denomination as F11 receptor (F11R), a receptor expressed on the surface of human platelets[324]. It was only a few years later that this molecule was detected in intercellular junctions of endothelial and epithelial cells[325]. Besides these cell types, JAM-A is also expressed by immune cells, such

as monocytes[325] and DCs[326,327]. JAM-A is a transmembrane glycoprotein that is present as a homodimer on the cells surface. Homodimers are structures formed by two independent but identical chains that, in the case of JAM-A, are connected to form a domain called D1[328]. This domain is responsible for JAM-A interactions with other JAM-A molecules[328-330], whereas the membrane-proximal D2 domain attaches the molecule to the JAM-A-expressing cell surface and interacts with other ligands such as LFA-1[328]. JAM-A can undergo homophilic interactions (JAM-A-JAM-A)[331] that can occur between epithelial-epithelial cells, endothelial-endothelial cells[325,332] or platelets-endothelial cells[333,334] and heterophilic interactions. In heterophilic interactions, JAM-A can bind to other members of the JAM family (JAM-B and JAM-C)[335], LFA1[329,330] and CD9[336,337]. JAM-A-LFA1 ligation was described in interactions between LFA1-expressing human Jurkat T cells and JAM-A-expressing endothelial cells[330]. This T cell line expresses high levels of JAM-A, suggesting that JAM-A homophilic interactions can also occur between T cells and the endothelium. Evidence however shows that JAM-A-LFA1 ligation is stronger than JAM-A-JAM-A binding and that this pathway reduces the dynamic strength of JAM-A homophilic interactions[338]. Although immunoprecipitation assays revealed precipitants of JAM-A and the β3 integrin (CD61) from an endothelial cells lysates[337], suggesting a direct interaction between these molecules, it was later found that this interaction was dependent on CD9, as absence of this tetraspanin inhibited JAM-A coimmunoprecipitation with β3 integrin[337]. Other immunoprecipitation assays suggest that JAM-A could also bind to the αIIb integrin (CD41)[339]. In addition to these ligands, JAM-A also works as a receptor for a few strains of murine and human viruses[340-342].

JAM-A plays important roles in endothelial cell migration[336,337,343] and barrier functions[332], and a few studies have evaluated the effects of JAM-A blockade in the interactions between these cells and leukocytes *in vitro*. Treatment with anti-JAM-A mAb BV11 inhibited spontaneous and chemokine-induced monocyte transmigration through endothelial cell monolayers[325]. The JAM-A-LFA1 pathway was found to contribute to neutrophil and T cell transmigration. Disruption of this pathway inhibited IL-8- and chemokine-mediated neutrophil transmigration, although no impact on cell arrest was found[330,344]. Treatments with anti-JAM-A antibody and a JAM-A-Fc fusion protein were able to inhibit chemokine-induced LFA1-dependent transendothelial migration of human CD4+ CD45RO+ memory T

cells[330,345]. Treatment with anti-JAM-A mAb H202.106 decreased splenic pDCs transmigration through layers of HEV cells without affecting pDCs adhesion capacity[346]. Although these studies in monocytes, neutrophils, memory T cells and pDCs suggest that JAM-A blockade could have a negative impact on leukocyte migration, cDCs seem to respond differently. cDCs express high levels of this transmembrane protein compared with pDC[326,327], allowing JAM-A homophilic intercellular ligations to possibly occur. BMDCs treated with anti-JAM-A mAb BV11 showed increased random motility *in vitro*[326]. This same effect was found on BMDCs from JAM-A deficient mice in comparison with WT BMDCs. JAM-A disruption by gene depletion in BMDCs promoted increased transmigration across monolayers of lymphatic endothelial cells, but not through microvascular endothelial cells. These JAM-A deficient BMDCs expressed similar levels of maturation markers (CD80 and CD86), surface molecules related to DC migration (CD11a, CD11b, CD11c, CD62L, JAM-B and JAM-C) and antigen uptake capacity in comparison with WT BMDCs, suggesting that JAM-A may not participate in early stages of DCs differentiation and maturation. Another study showed higher transmigration of BMDCs expressing normal levels of JAM-A through layers of endothelial cells from JAM-A KO mice in comparison with endothelial cells from JAM-A KO mice reconstituted with full-length JAM-A cDNA[347]. These studies suggest that while DC JAM-A participates in DC trafficking through the lymphatics, JAM-A expressed by endothelial cells play a dominant role in DC migration through peripheral tissues.

JAM-A is known to be involved in the regulation of endothelial-endothelial and leukocyte-endothelial cell interactions, but its importance in interactions between leukocytes remains unclear. Although preliminary work has been published reporting unaltered IFN-γ secretion by antigen-primed CD4+ T cells in response to JAM-A KO BMDCs compared with WT BMDCs[347], JAM-A may still regulate interactions between T cells and APCs at a cell-cell level and influence their activation, proliferation and differentiation. In this chapter, the involvement of JAM-A in the interactions between CD4+ T cells and DCs during antigen presentation *in vitro* is investigated.

4.2 Results

4.2.1 JAM-A is Expressed by DCs

Before analysing the effects of JAM-A blockade on CD4+ T cells during antigen presentation, I evaluated the expression of JAM-A on CD4+ T cells and different subtypes of DCs. Spleens and LNs from WT mice were harvested, digested with Collagenase D for a higher yield of adherent cells, stained with fluorophore-conjugated antibodies and analysed by flow cytometry. The optimised 12-colour panel described in Chapter 3 (Section 3.2.1) was used to analyse JAM-A expression on populations expressing lineage markers (Figure 4-1A), or more specifically on CD4+ T cells, cDC1, cDC2 and pDC populations (Figure 4-1B), with the use of an isotype control for the detection of JAM-A specific binding (Figure 4-1C). The proportion of JAM-A+ cells from specific leukocyte subsets was quantified (Figure 4-1D), as well as from MHCII+ cells expressing different levels of CD11c (Figure 4-1E, F).

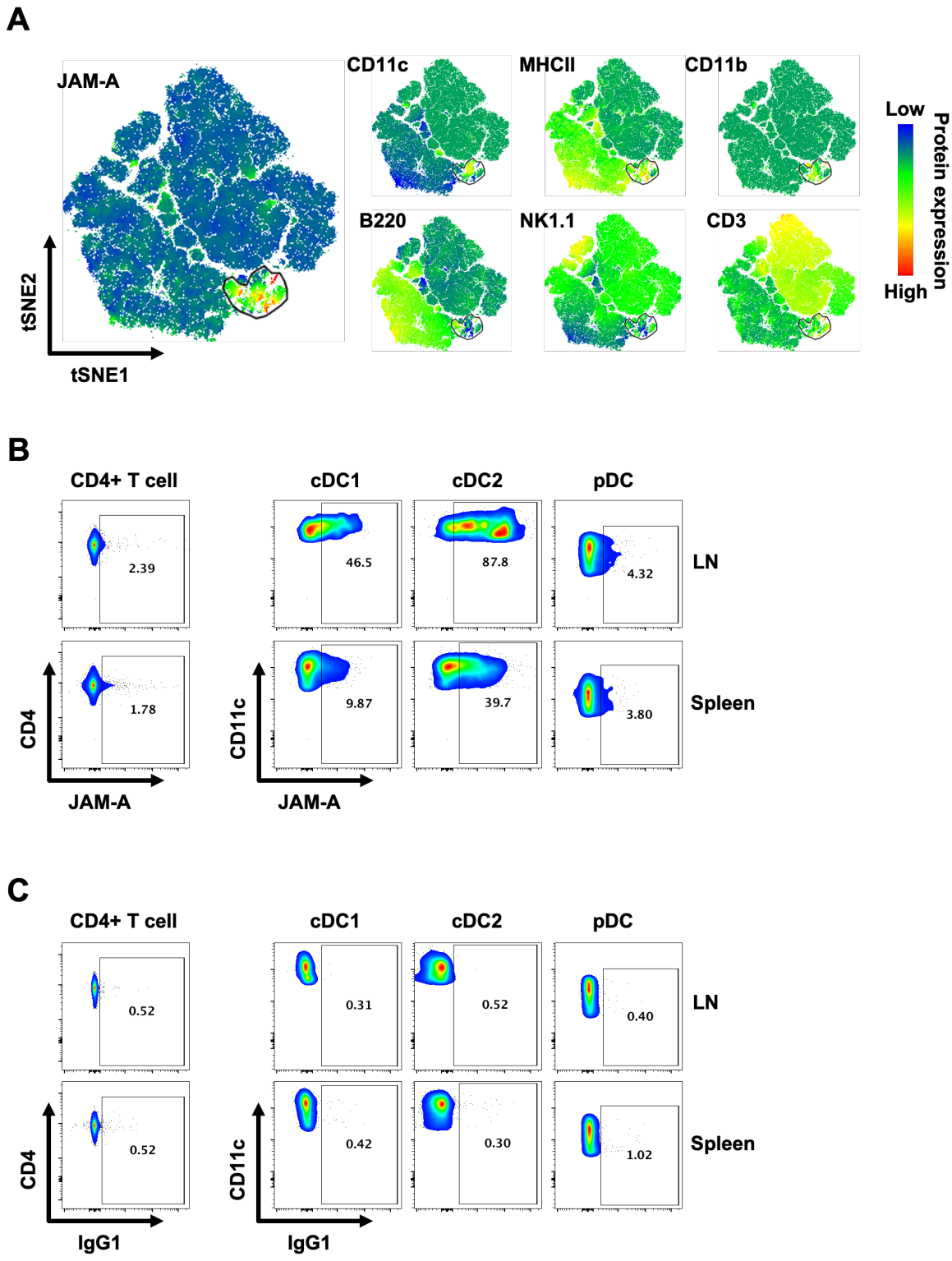
A
JAM-A
CD11c
MHCII
CD11b
B220
NK1.1
CD3
Low
High
Protein expression
tSNE2
tSNE1
B
CD4+ T cell
cDC1
cDC2
pDC
2.39
46.5
87.8
4.32
LN
1.78
9.87
39.7
3.80
Spleen
CD4
CD11c
JAM-A
JAM-A
C
CD4+ T cell
cDC1
cDC2
pDC
0.52
0.31
0.52
0.40
LN
0.52
0.42
0.30
1.02
Spleen
CD4
CD11c
IgG1
IgG1

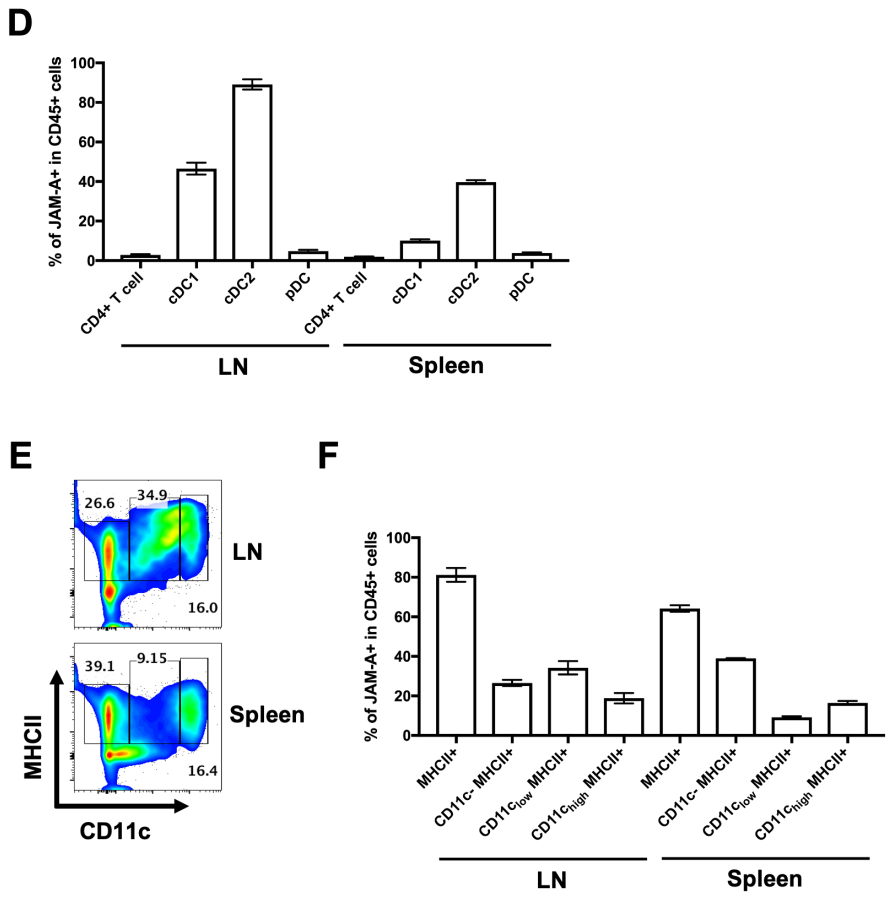

Figure 4-1. JAM-A expression on murine CD4+ T cells and DCs
Immune cells from C57BL/6 mice were analysed by flow cytometry for the expression of JAM-A. **(A)** tSNE analysis of immune cells (CD45+) from lymph nodes (LN) based on polychromatic flow cytometry data including JAM-A, CD11c, MHCII, CD11b, B220, NK1.1 and CD3 expression profiles highlighting the population expressing the highest levels of JAM-A. **(B)** Representative dot plots of JAM-A expression **(C)** or its isotype control on CD4+ T cells (B220- CD11c- CD3+ CD4+), type 1 conventional DCs (cDC1) (CD3- NK1.1- $CD11c_{high}$ MHCII+ CD8+ CD11b-), type 2 conventional DCs (cDC2) (CD3- $CD11c_{high}$ MHCII+ CD8- CD11b+) and plasmacytoid DCs (pDCs) (CD3- NK1.1- $CD11c_{low}$ PDCA1+ B220+ CD11b-), from spleens and LNs. Gates on B show populations expressing JAM-A based on the fluorescence emitted from its isotype control shown on C. **(D)** Quantification of JAM-A+ events in distinct leukocyte subsets. **(E)** Gating strategy for identification of MHCII+ cells expressing different levels of CD11c (negative, low or high) and **(F)** quantification of the proportion of JAM-A+ cells in these populations. Data are representative of an experiment performed in biological triplicates.

The tSNE analysis on immune cells from LNs showed some characteristics of the LN resident JAM-A+ population. The heatmap shows that LN resident JAM-A+ leukocytes (CD45+) are mostly composed of MHCII+, CD11c+ and CD11b+ cells, and that only a small part of B220+ cells express JAM-A, suggesting that the JAM-A-expressing population is mainly formed by DCs and partly by B cells. In addition, only a small proportion of NK (NK1.1+) and T cells (CD3+) appear to express JAM-A. JAM-A expression on specific leukocytes subsets was also analysed. CD4+ T cells from both spleens and LNs expressed low levels of JAM-A. On the other hand, all DC subsets expressed substantial levels of JAM-A. LN cDC2 was the subset that

expressed the highest levels and allowed the identification of a JAM-A_{high} cDC2 population. LN resident cDC1 and cDC2 seem to express higher levels than splenic cDC1 and cDC2, respectively. Both LN and spleen pDCs expressed low levels of JAM-A. The analysis of MHCII+ cells expressing different levels of CD11c showed that $CD11c_{low}$ MHCII+ cells that look to be present in the LNs in higher frequency than in the spleens express high levels of JAM-A. These cells also express high levels of CD11b, suggesting that they could be macrophages. However, the use of macrophage lineage markers would be necessary to distinguish these cell populations in a more reliable way.

Lymphoid organs are connected to secondary organs through lymphatic and blood vessels. The expression of some adhesion molecules were shown to vary substantially across different lymphoid organs[323]. As such, I analysed JAM-A expression on CD4+ T cells from spleens, different LNs (inguinal, brachial, superficial cervical, mesenteric) and Peyer's patches (Figure 4-2).

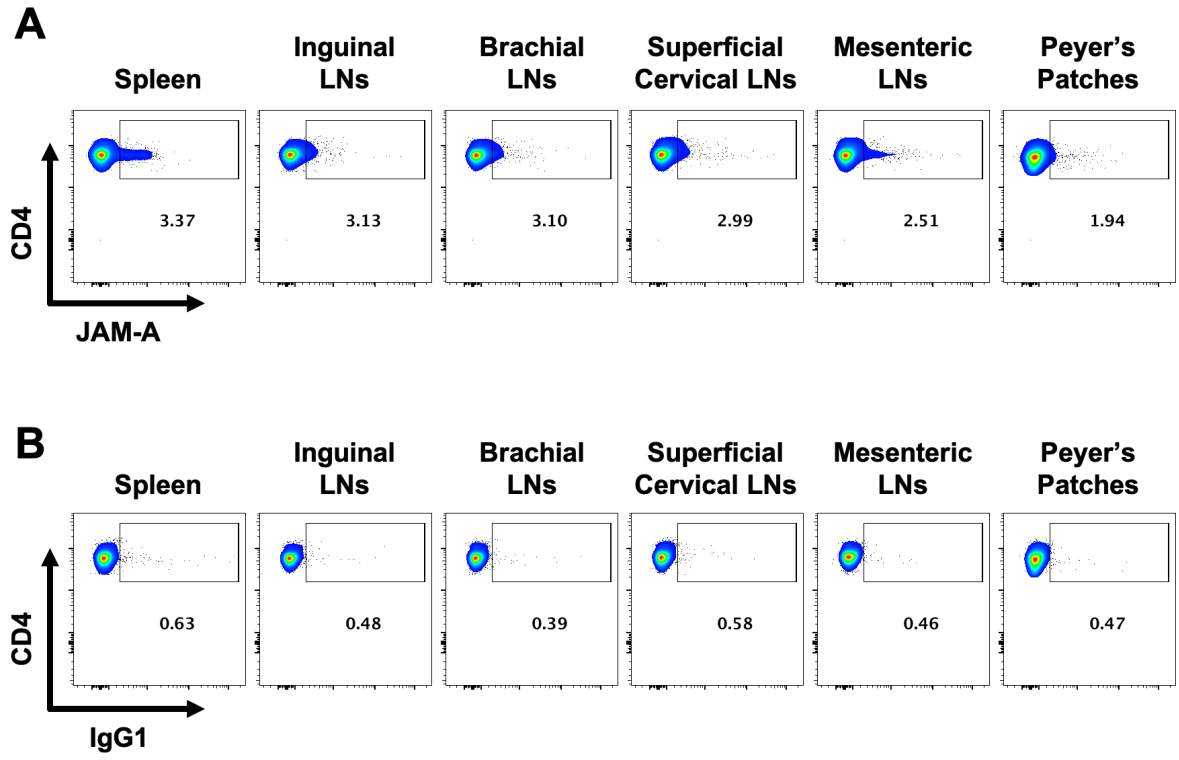

Figure 4-2. JAM-A expression on CD4+ T cells from different lymphoid organs
CD4+ T cells from different lymphoid organs of C57BL/6 mice were analysed by flow cytometry for the expression of JAM-A. **(A)** Representative dot plots of JAM-A expression **(B)** or its isotype control on CD4+ T cells (CD3+ CD4+) from spleens, inguinal, brachial, superficial cervical and mesenteric lymph nodes (LN) and Peyer's patches. Gates show populations expressing JAM-A based on the fluorescence emitted from its isotype control (not shown). Data are representative of an experiment performed in biological triplicates.

Similar proportions of JAM-A+ cells were found on CD4+ T cells populations from spleen, inguinal LN, brachial LN, superficial cervical LN, mesenteric LN and Peyer's patches. As JAM-A intercellular ligation can occur between JAM-A molecules from the different interacting cells[338] and the experiments in this Chapter section showed that, although a high proportion of DCs express JAM-A, only a small proportion of CD4+ T cells express JAM-A, I then decided to analyse if CD4+ T cells express a potential ligand for JAM-A.

4.2.2 Naïve CD4+ T Cells Express a Potential Ligand for JAM-A

As DCs express JAM-A, but only a small part of CD4+ T cells express this surface protein, I analysed the presence of a potential ligand for JAM-A on the surface of CD4+ T cells. LFA1, a known ligand for JAM-A[330], is composed by an alpha (CD11a) and a beta (CD18) chain. CD18 is also a component of MAC-1 (CD11b/CD18), a receptor that is expressed on T cell surface[348]. As CD11a is only described to be part of LFA1[349], this alpha chain was used for the detection of LFA1 on the surface of T cells. Immune cells from spleens and LNs of WT mice were stained with CD3, CD4 and CD11a (Figure 4-3). CD4+ T cells from both spleen and LNs expressed high levels of CD11a.

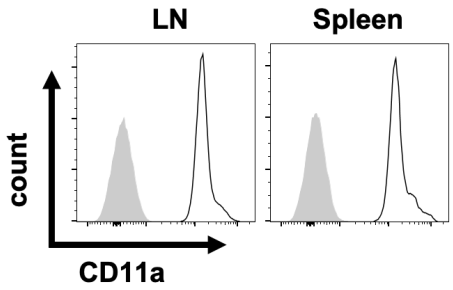

Figure 4-3. Expression of CD11a on murine CD4+ T cells
CD4+ T cells from spleens and lymph nodes of C57BL/6 mice were analysed by flow cytometry for the expression of CD11a. Histograms show CD11a expression (unfilled) or its matched isotype control (grey-shaded). Data are representative of an experiment performed in biological triplicates.

4.2.3 Antigen-Primed CD4+ T cells Express Low Levels of JAM-A

To evaluate whether activated CD4+ T cells express JAM-A, splenocytes from WT mice were incubated with soluble anti-CD3 and anti-CD28 agonistic antibodies for 72 hours. As such, after being harvested, cells were stained with CD4 for

identification of CD4+ cells, CD44 for detection of the cells' activation status (Figure 4-4A) and JAM-A (Figure 4-4B).

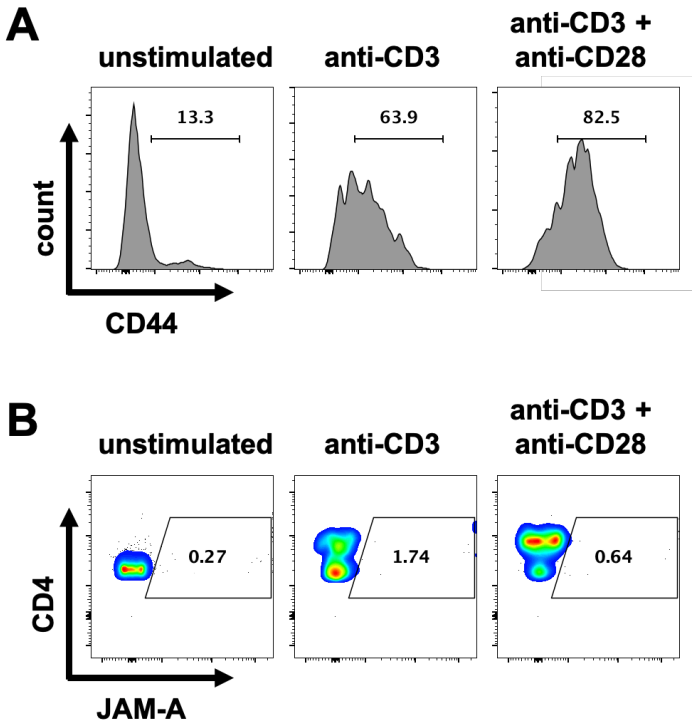

Figure 4-4. JAM-A expression on CD4+ T cells upon agonistic antibodies stimulation
Splenocytes from C57BL/6 mice were stimulated with anti-CD3 and anti-CD28 antibodies for 72 hours and CD4+ T cells were analysed by flow cytometry for the expression of JAM-A. **(A)** Representative histograms of CD44 expression on unstimulated, anti-CD3-stimulated and anti-CD3 + anti-CD28-stimulated splenocytes with gating on $CD44_{high}$ cells. **(B)** dot plots of JAM-A expression on CD4+ T cells from unstimulated, anti-CD3-stimulated and anti-CD3 + anti-CD28-stimulated splenocytes with gating on JAM-A+ cells based on the fluorescence of its isotype control (not shown). Data are representative of an experiment performed in triplicates.

Cells that were co-stimulated with anti-CD28 mAb expressed higher levels of CD44 than the group in which co-stimulation was absent. JAM-A was nearly undetectable on CD4+ T cells from all groups. As no other co-stimulation that occur during antigen presentation was present in the analysed assay, I decided to analyse JAM-A expression on antigen-primed CD4+ T cells using an APC-dependent system.

In order to analyse JAM-A expression on CD4+ T cells activated by antigen, naïve OTII CD4+ T cells were incubated for different time periods with pOVA-pre-pulsed BMDCs. CD4+ cells were then harvested and analysed by flow cytometry and antigen experienced T cells were identified by CD44 expression (Figure 4-5A). Surface expression of JAM-A on T cells was also determined (Figure 4-5B) and its

proportions were compared between T cells incubated with antigen pulsed or control BMDC (Figure 4-5D). Expression of CD11a, a potential ligand for JAM-A was also determined on cultures that received antigen stimulation at different time points (Figure 4-5E), using its isotype control fluorescence intensity to determine gates (Figure 4-5F).

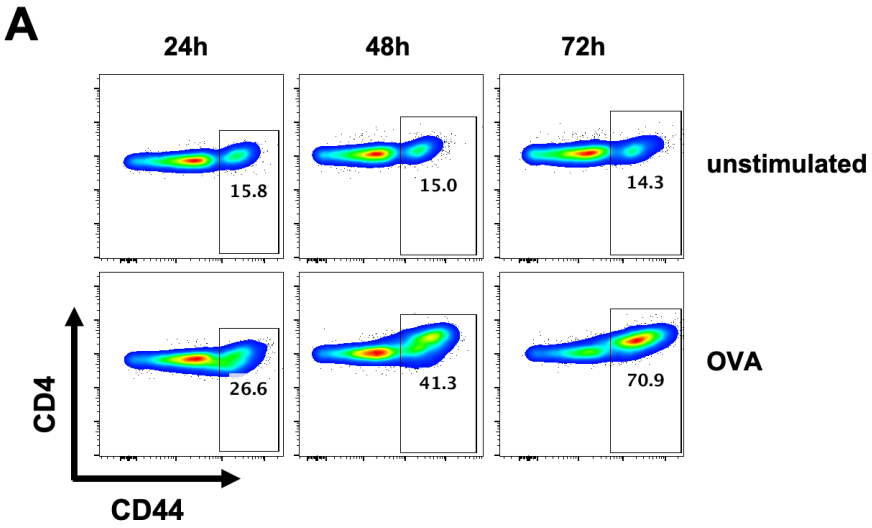
A
24h
48h
72h
15.8
15.0
14.3
unstimulated
26.6
41.3
70.9
OVA
CD4
CD44

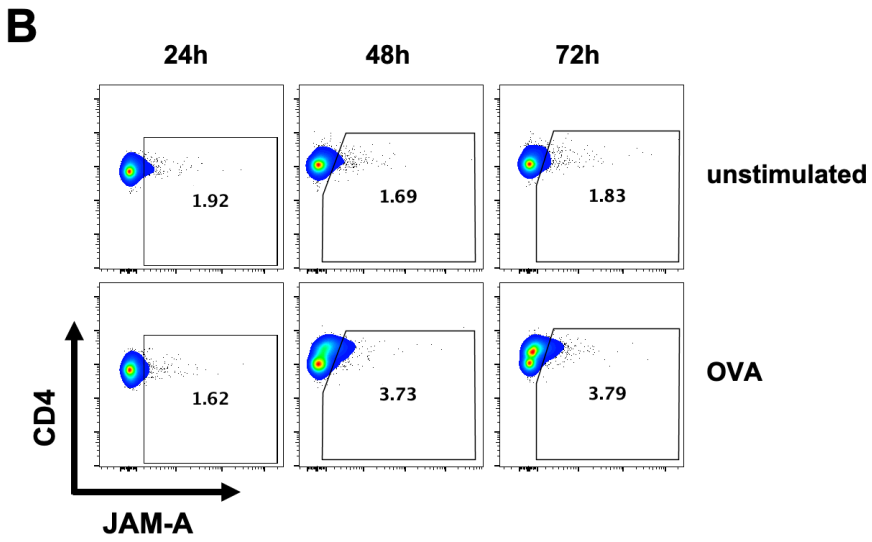
B
24h
48h
72h
1.92
1.69
1.83
unstimulated
1.62
3.73
3.79
OVA
CD4
JAM-A

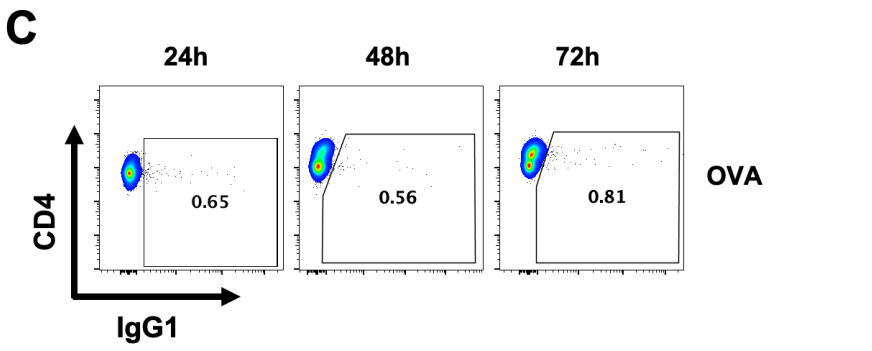
C
24h
48h
72h
0.65
0.56
0.81
OVA
CD4
IgG1

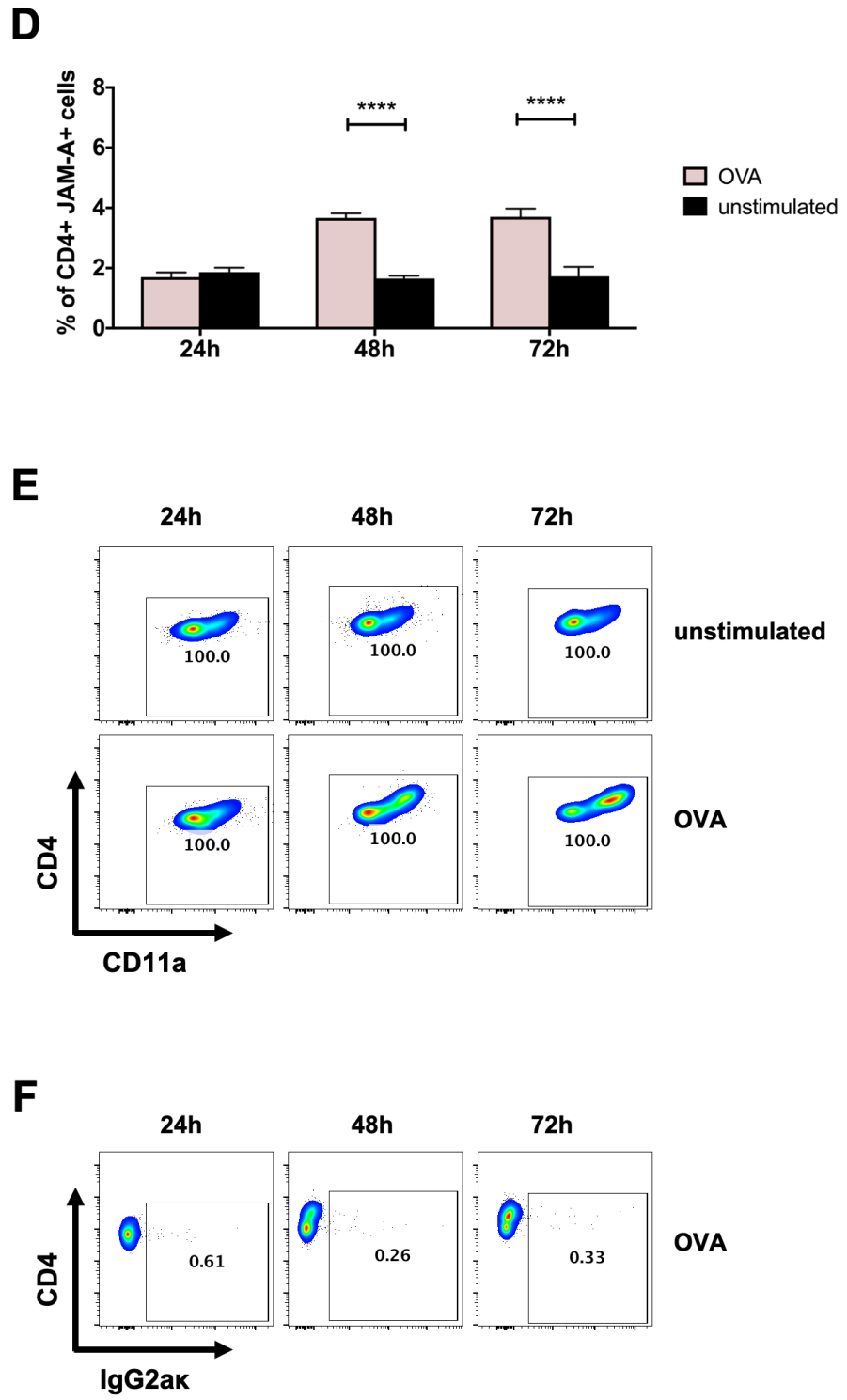

Figure 4-5. Expression of JAM-A and its potential ligands on activated CD4+ T cells
CD4+ T cells from OTII mice were cultured with OVA peptide (pOVA)-pre-pulsed bone marrow-derived dendritic cells and analysed by flow cytometry for the expression of JAM-A and CD11a are different time points following activation. **(A)** Representative dot plots of CD44 expression on unstimulated and OVA-stimulated CD4+ T cells with the percentage of $CD44_{high}$ cells indicated. **(B)** Representative dot plots of JAM-A expression on unstimulated and OVA-stimulated CD4+ T cells **(C)** or its isotype control on OVA-stimulated CD4+ T cells and **(D)** quantification of JAM-A+ cells with comparison between the two different groups 24, 48 and 72 hours after priming. **(E)** Representative dot plots of CD11a expression on unstimulated and OVA-stimulated CD4+ T cells **(F)** or its isotype control on OVA-stimulated CD4+ T cells. Gates show specific binding based on matched isotype control. Results are expressed as mean ± SD of an experiment performed in triplicates. Statistical differences were determined using a two-way ANOVA. ****$p \leq 0.0001$.

CD4+ T cells cultured with pOVA-pulsed BMDCs were successfully primed. The frequency of $CD44_{high}$ cells increased across time on the group that received antigen stimulation, reaching its peak of expression three days after initial contact between the cell types. In contrast, T cells that didn't receive antigen stimulation did not upregulate CD44. JAM-A was expressed in low levels on naïve CD4+ T cells and on early activated CD4+ T cells. However, antigen stimulation for 48 and 72 hours resulted in higher expression of JAM-A in comparison with non-antigen stimulated CD4+ T cells. Both naïve and activated CD4+ T cells expressed CD11a, and it was possible to notice an upregulation of $CD11a_{high}$ populations on cells that were exposed to antigen across time.

To analyse if the increase on JAM-A+ cells on antigen-primed CD4+ T cell cultures in comparison with unstimulated cultures could have been driven by cytokines released by these activated cells during or shortly after priming, I used a second approach in which naïve and activated cells were present in the same well. Isolated naïve CD4+ T cells from OTII and WT mice were concomitantly cultured with BMDCs pre-pulsed with pOVA, whereas other co-cultures did not receive antigen. Cells were harvested 72 hours later, stained and analysed by flow cytometry. As all immune cells from OTII mice express CD45.1, this marker was used to identify WT (CD45.1-) and OTII (CD45.1+) cells within the same culture before analysing them for CD44 expression (Figure 4-6A). Surface expression of JAM-A was also detected (Figure 4-6B) using the fluorescence intensity of its isotype control to identify specific binding (Figure 4-6C). Frequencies of JAM-A+ populations from OTII CD4+ T cells in cultures containing pOVA-pulsed BMDCs were compared to WT CD4+ T cells in cultures containing pOVA-pulsed BMDCs, to OTII CD4+ T cells in cultures containing control BMDCs or to WT CD4+ T cells in cultures containing control BMDCs (Figure 4-6D).

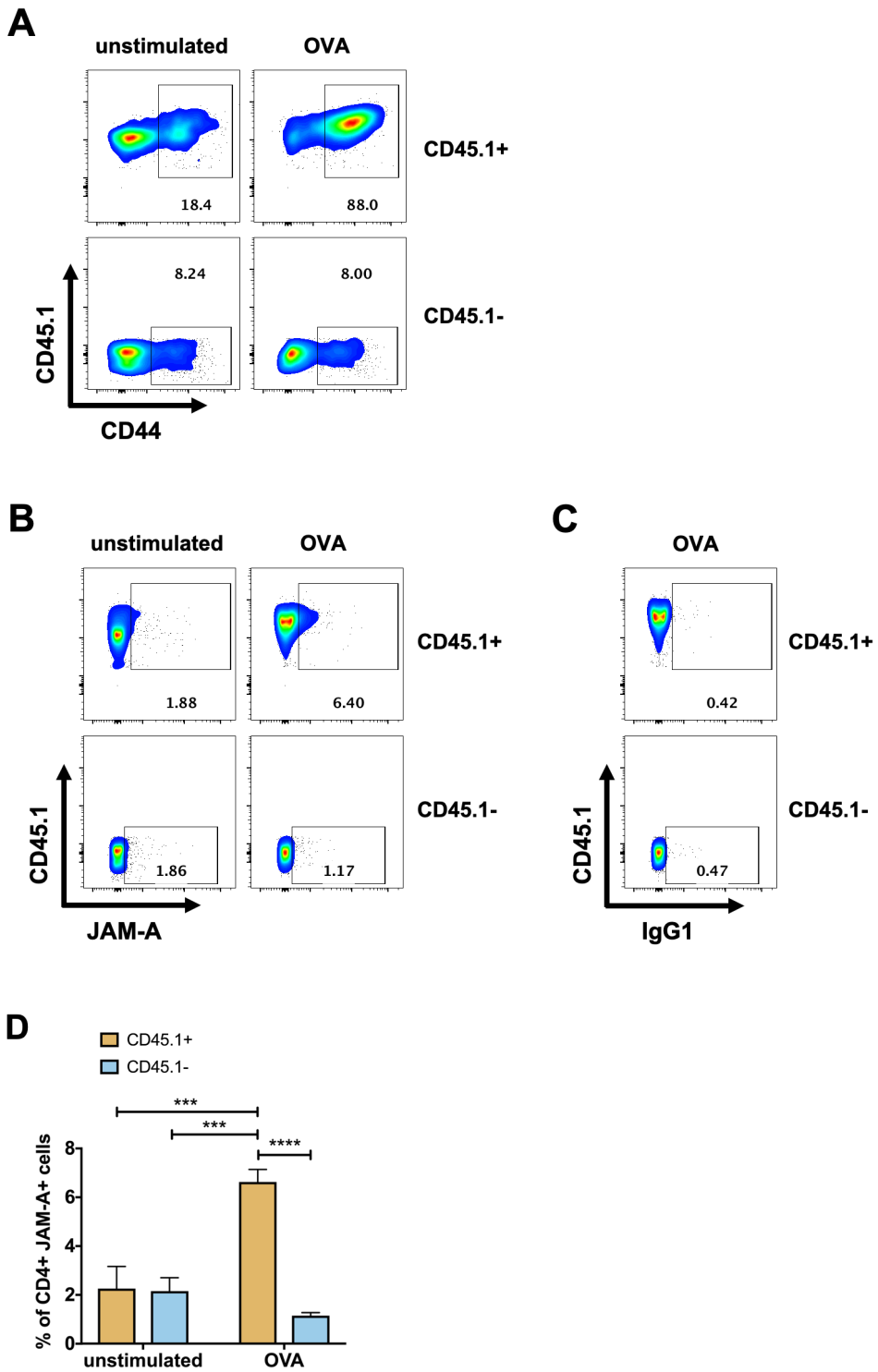

Figure 4-6. JAM-A expression on naïve or antigen-primed OTII CD4+ T cells and naïve wild-type (WT) CD4+ T cells

CD4+ T cells from OTII and C57BL/6 mice were cultured together with OVA peptide (pOVA)-pre-pulsed bone marrow-derived dendritic cells for 72 hours and analysed by flow cytometry for the expression of JAM-A. **(A)** Representative dot plots of CD44 expression on OTII (CD45.1+) or WT (CD45.1-) CD4+ T cells from co-cultures with or without OVA with gating on $CD44_{high}$ cells. **(B)** JAM-A expression **(C)** or its isotype control on OTII (CD45.1+) or WT (CD45.1-) CD4+ T cells from co-cultures with or without OVA with gating on JAM-A+ cells based on its isotype control. **(D)** Quantification of JAM-A+ cells from the CD4+ populations and comparison between the CD45.1+ OVA group and the other groups. Results are expressed as mean ± SD of an experiment performed in triplicates. Statistical differences were determined using a two-way ANOVA. ***p ≤ 0.001, ****p ≤ 0.0001.

The frequency of $CD44_{high}$ populations demonstrated that CD45.1+, but not CD45.1- CD4+ T cells, were successfully activated when present in wells with pOVA-pulsed BMDCs. In addition, both CD45.1+ and CD45.1- CD4+ T cells incubated with BMDCs that were not carrying antigen did not upregulate CD44. Activated CD45.1+ CD4+ T cells expressed higher levels of JAM-A in comparison with CD45.1+ and CD45.1- CD4+ T cells that did not receive antigen and to CD45.1- CD4+ T cells that were present in the same wells as the activated CD45.1+ T cells.

4.2.4 JAM-A is Expressed by BMDCs

Before analysing the effects of JAM-A blockade on CD4+ T cell priming, it was important to verify if BMDCs express this surface protein, as this would be the DC type to be used for functional assays. BMDCs were cultured for 7 days. Immature BMDCs were not stimulated, whereas mature BMDCs received 24-hours LPS stimulation, from day 6 to 7, before being analysed. Cells were then harvested and analysed by flow cytometry for the expression of CD86, to indicate maturation, and JAM-A (Figure 4-7A). The proportion of cells expressing JAM-A was quantified and compared between immature and mature BMDCs (Figure 4-7B).

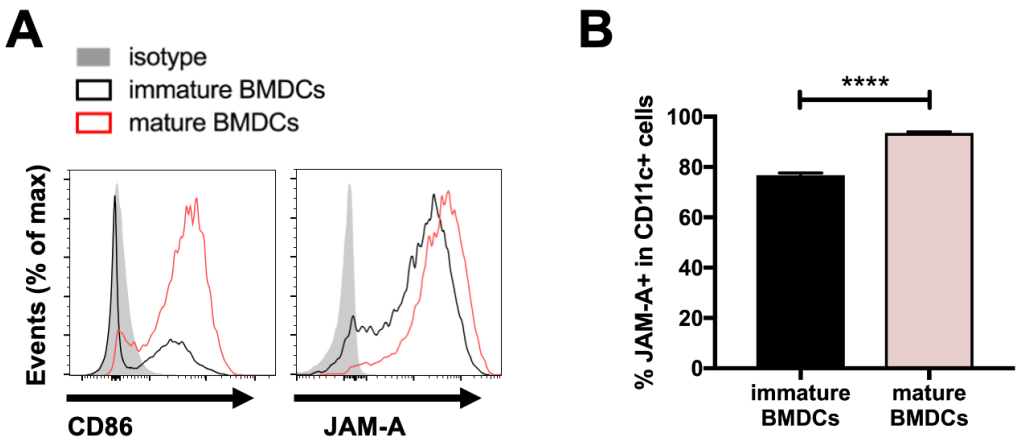

Figure 4-7. JAM-A expression on BMDCs
BMDCs were cultured for 7 days and analysed by flow cytometry for the expression of JAM-A. **(A)** Representative histograms of expression of CD86 (left side) and JAM-A (right side) on immature (black unfilled) or mature BMDCs (red unfilled) or in BMDCs stained with isotype controls (grey-shaded). **(B)** Comparison of the proportion of JAM-A+ cells from immature and mature BMDCs gated according to its isotype control. Results are expressed as mean ± SD of an experiment performed in triplicates. Statistical differences were determined using an unpaired Student's t test. ****$p \leq 0.0001$.

JAM-A was widely expressed on both immature and mature BMDCs. However, it was expressed on a higher proportion of mature BMDCs. This experiment validated the use of BMDCs for functional assays aiming to manipulate JAM-A, as these cells expressed similar levels as some populations of DCs found *in vivo*, such as LN resident cDC2.

4.2.5 JAM-A is Present on the Site of Interaction During CD4+ T Cell Priming

The analysis of the localisation of JAM-A on the DC surface during antigen presentation could suggest whether this molecule could be important in the interactions between DCs and T cells. OTII CD4+ T cells were cultured with BMDCs pulsed with pOVA for 24 hours. After being harvested, cells were stained and analysed by confocal microscopy. Cells were stained with CD4 for detection of CD4+ T cells, CD11c, MHCII and JAM-A. MHCII is known to be strongly recruited to the immune synapse [350,351], therefore cell doublets in which translocation of MHCII to the site of interaction (SI) with the T cell was evident were identified, as described in Chapter 2 (section 2.6.2), and images from a z-stack plane were acquired for the analysis of protein expression across the BMDC membrane (Figure 4-8A). Isotypes were used to detect specific binding for all markers. The ratio of the MFI between the SI and the rest of the BMDCs membrane from MHCII, CD11c and JAM-A was calculated (Figure 4-8B) and JAM-A ratio was compared with MHCII and CD11c ratios.

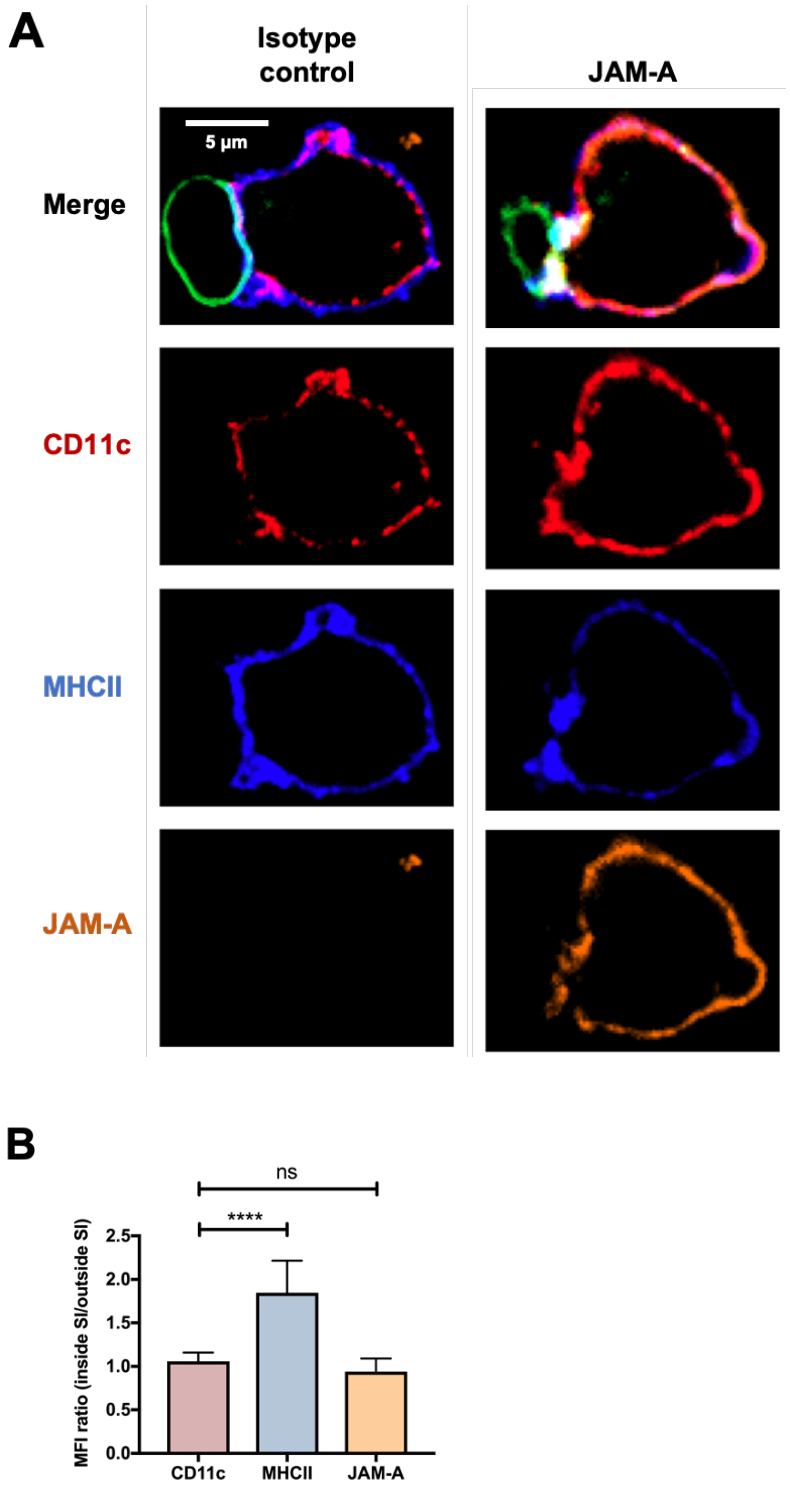

Figure 4-8. JAM-A localisation on BMDC surface during CD4+ T cells priming
CD4+ T cells from OTII mice were cultured with OVA peptide (pOVA)-pre-pulsed BMDCs for 24 hours and analysed by confocal microscopy for the expression of CD11c, MHCII and JAM-A. **(A)** Representative confocal image stacks of CD4+ T cell recorded in the green channel (CD4, mAb GK1.5) in contact with a BMDC identified by its expression of CD11c (mAb N418) recorded in the red channel and MHCII (mAb HL3) recorded in the blue channel and JAM-A (right side) (mAb H202-106) or its isotype control (left side) recorded in the yellow channel. **(B)** Quantification of the ratio between the BMDC's membrane median fluorescence intensity (MFI) from the inside and the outside of the site of interaction (SI) and comparison between JAM-A and MHCII or CD11c. Results are expressed as mean ± SD of eight doublets with translocation of MHCII to the SI from one experiment. Statistical differences were determined using a one-way ANOVA. ns = non-significant, ****$p \leq 0.0001$.

JAM-A was detected on the surface of BMDCs and not on the surface of CD4+ T cells that were interacting with these cells, supporting the findings from the previous flow cytometry-based experiments. The analysis of the MFI ratio between the inside and outside of the SI showed a higher concentration of MHCII inside the SI in comparison with CD11c, demonstrating MHCII translocation during antigen presentation. This analysis also showed that JAM-A ratio was near 1, a similar rate as CD11c. Although there is no apparent recruitment of JAM-A into the SI, this molecule is still present on the surface of BMDCs in the SI during antigen presentation.

4.2.6 Anti-JAM-A mAb Treatment During Antigen Presentation *in vitro* Attenuates CD4+ T Cell Activation and Proliferation

To allow margin for an increase in T cell activation and proliferation possibly caused by anti-JAM-A treatment to be seen, JAM-A disruption experiments were performed in optimal and suboptimal antigen stimulation conditions. To identify appropriate suboptimal and optimal concentrations of antigen and T cells-DCs ratio, pOVA and BMDC titration was performed using a co-culture assay, as described in Chapter 2 (section 2.2.4). The percentage of $CD44_{high}$ (Figure 4-9A), representing antigen-experienced cells, divided (Figure 4-9B) and four times divided (Figure 4-9C) CD4+ T cells, based on CFSE fluorescence intensities, were taken into consideration for the definition of appropriate cell ratios and suboptimal/optimal concentrations of antigen.

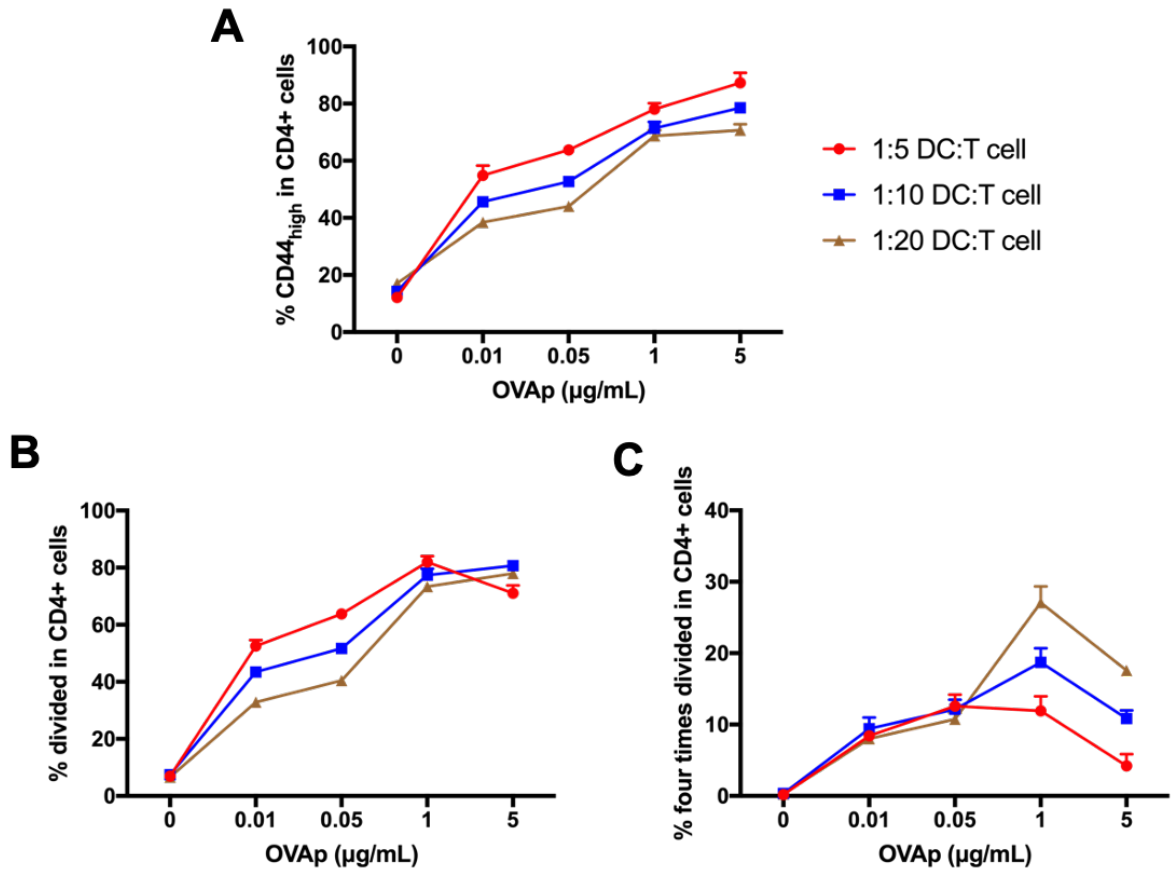

Figure 4-9. Optimisation of cell ratios and antigen concentration on CD4+ T cell activation and proliferation in BMDC-T cell co-cultures
CFSE-labelled CD4+ T cells from OTII mice were cultured with BMDCs pre-pulsed with different concentrations of OVA peptide (pOVA) and at different cells' ratio for 72 hours and analysed by flow cytometry for CD44 expression and CFSE fluorescence intensity. **(A)** Quantification of $CD44_{high}$ cells from the CD4+ populations. **(B)** Quantification of cells that have divided based on the CFSE fluorescence intensity from the CD4+ populations. **(C)** Quantification of cells that have divided four times from the CD4+ populations. Data are from an experiment performed in triplicates.

Increasing doses of antigen were able to activate CD4+ T cells in increasing proportions, and co-cultures that had more DCs seemed to activate more T cells. This was also observed when analysing cells that have divided, with exception of the highest concentration of antigen (5 µg/mL) at 1:5 BMDC:T ratio that had lower division rate in comparison with the same concentration of antigen but different cell ratios and to 1 µg/mL at 1:5 ratio. The analysis of four times divided cells showed that cultures that had less BMDCs had more cell proliferation when higher concentrations of antigen were used (1 and 5 µg/mL). To maintain the same conditions to experiments previously performed in our laboratory, the cell ratio chosen to be used for the next experiments was 1:10. The concentration of antigen chosen to reflect optimal conditions was 1 µg/mL, as it was able to achieve near maximum T cell activation and maximum T cell proliferation. For suboptimal

conditions, 0.05 µg/mL was chosen, as this concentration was able to induce roughly half of CD4+ T cells to activate and divide. For simplification, the optimal concentration of antigen is referred as OVA_{high} in this thesis, whereas the suboptimal concentration is referred as OVA_{low}.

To identify reagents to block JAM-A function, I analysed the reagents used in the literature. The anti-JAM-A mAb BV11 has been extensively used for both for *in vitro*[325,326,330] and *in vivo*[224,325,352–356] studies in mice. Recently, a novel antagonistic JAM-A peptide called peptide 4D capable of blocking JAM-A homophilic interactions has been developed[333]. This peptide was able to inhibit platelet adhesion to cytokine-inflamed endothelial cells and was also tested in *in vivo* studies[357,358], suggesting it could also be a promising reagent to be used for the experiments in this thesis. For *in vitro* work addressed in this chapter, I decided to work with the BV11 mAb clone.

After showing that DCs and BMDCs express JAM-A and CD4+ T cells express a potential ligand for JAM-A, I performed *in vitro* assays to test if blockade of JAM-A pathways during priming could promote changes in the outcome of CD4+ T cells. BMDCs pre-pulsed with optimal and suboptimal concentrations of pOVA were cultured with CFSE-labelled OTII naïve CD4+ T cells in the presence of anti-JAM-A mAb BV11 or its isotype control (purified rat IgG2bκ mAb RTK4530) for 72 hours and analysed by flow cytometry. Cells that have divided were identified using CFSE fluorescence intensity, quantified and compared between groups that have received the same concentration of antigen (Figure 4-10A). To assess T cell activation, $CD44_{high}$ cells were gated, quantified and also compared between groups that were stimulated under the same conditions (Figure 4-10B).

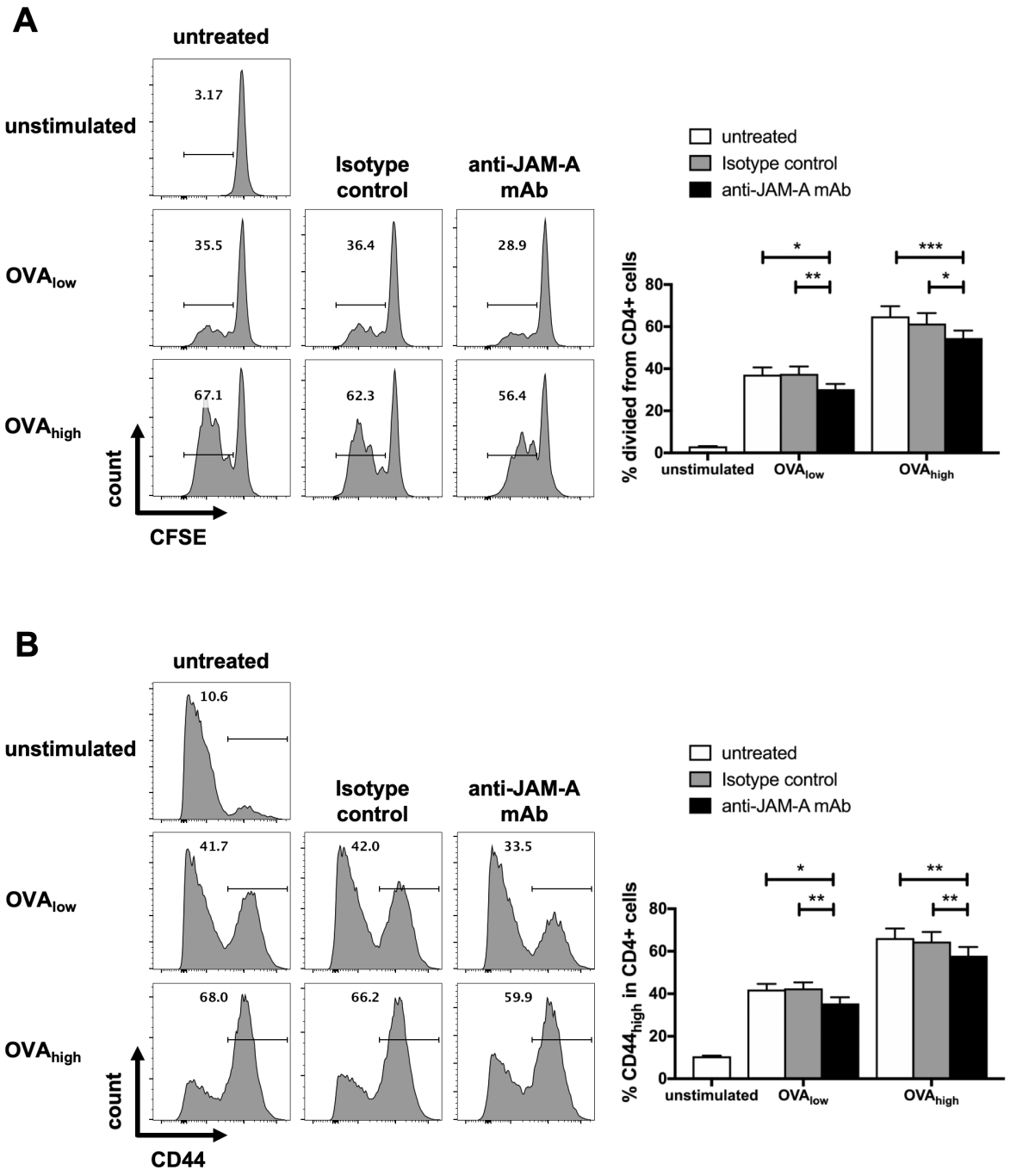

Figure 4-10. JAM-A blockade *in vitro* attenuates CD4+ T cell activation and proliferation
CFSE-labelled CD4+ T cells from OTII mice were cultured with bone marrow-derived dendritic cells pre-pulsed with suboptimal (OVA_{low}) or optimal (OVA_{high}) concentrations of OVA peptide (pOVA) in the presence of anti-JAM-A mAb (BV11) or its isotype control for 72 hours and analysed by flow cytometry for CD44 expression and CFSE fluorescence intensity. **(A)** Representative histograms of CFSE fluorescence intensity on CD4+ cells (left side) and quantification of CD4+ T cells that have divided based on the gating of CFSE fluorescence intensity (right side). **(B)** Representative histograms of CD44 fluorescence intensity on CD4+ cells (left side) and quantification of CD4+ T cells that are $CD44_{high}$ (right side). Results are expressed as mean ± SD of hexaplicate cultures from three independent experiments. Statistical differences between groups that received the same concentration of antigen were determined using a two-way ANOVA. *$p \leq 0.05$, **$p \leq 0.01$, ***$p \leq 0.001$.

CD4+ T cells under stimulation with the optimal concentration of antigen achieved nearly full activation and cells stimulated with the suboptimal concentration of pOVA were less activated, whereas T cells in groups that did not receive antigen did not upregulate CD44. Isotype-treated and untreated groups showed similar levels of T cell activation and proliferation. Treatment with anti-JAM-A mAb BV11 during antigen presentation attenuated CD4+ T cell activation and proliferation under both concentrations of antigens in comparison with the isotype control groups as well as to the untreated groups. Considering that these effects were small and might not be biologically relevant, other approaches to evaluate if JAM-A blockade impacts CD4+ T cell-DC interactions were performed. Besides T cell activation and proliferation, T cell differentiation is key for successful manipulation of T-cell responses, as different subsets secrete distinct cytokines that play specific roles in several pathological conditions[359]. Therefore, I next analysed if JAM-A plays a role on CD4+ T cell differentiation.

4.2.7 Anti-JAM-A mAb Treatment During Antigen Presentation *in vitro* Impacts T-bet expression and IL-17 secretion by CD4+ T Cells

Cell culture supernatants from the previous experiment were analysed by ELISA. The presence of cytokines that could suggest CD4+ T cell differentiation towards specific subsets was investigated. IFN-γ (Figure 4-11A), IL-4 (not shown), IL-10 (Figure 4-11B) and IL-17 (Figure 4-11C) that are secreted in high levels by Th1, Th2, Treg and Th17 cells[74], respectively, were analysed. The concentrations were quantified and compared between groups that were stimulated under the same concentrations of pOVA.

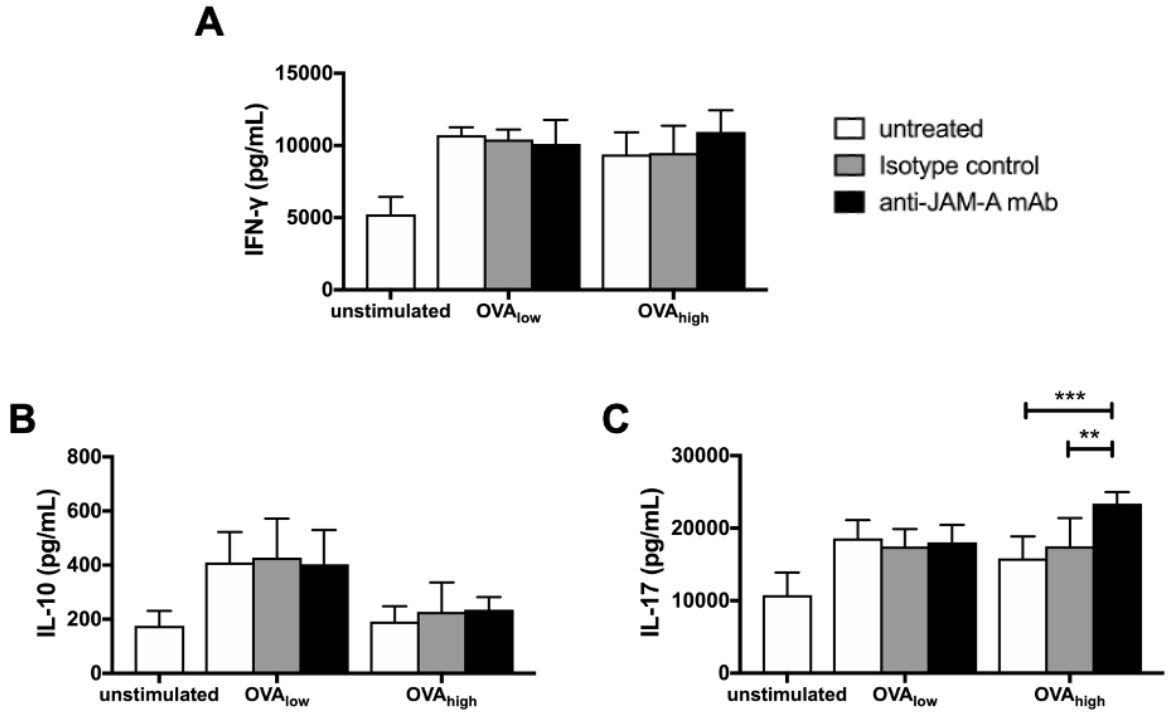

Figure 4-11. JAM-A blockade *in vitro* increases IL-17 secretion by CD4+ T cells
CD4+ T cells from OTII mice were cultured with bone marrow-derived dendritic cells pre-pulsed with suboptimal (OVA_{low}) or optimal (OVA_{high}) concentrations of OVA peptide (pOVA) in the presence of anti-JAM-A mAb (BV11) or its isotype control for 72 hours and the supernatants' co-cultures were analysed by ELISA for the presence of different cytokines. **(A)** Quantification of IFN-γ, **(B)** IL-10 and **(C)** IL-17 concentrations with comparisons between groups that received the same concentration of antigen. Results are expressed as mean ± SD of hexaplicate cultures from three independent experiments. Statistical differences were determined using a two-way ANOVA. $^{**}p \leq 0.01$, $^{***}p \leq 0.001$.

In both concentrations of antigen and for all cytokines, levels from untreated and isotype-treated groups were similar. IL-4 was not detected in the co-culture supernatants when utilising the commercial kit that has a sensitivity of 2 pg/mL. IFN-γ and IL-17 were detected in higher concentrations in the supernatants from cultures that received antigen in comparison with the ones from unstimulated cells. No differences in IFN-γ and IL-10 secretion were found between groups that received the same concentration of antigen. Although no differences in IL-17 concentrations were found between groups under the suboptimal condition, anti-JAM-A mAb BV11 treatment increased the secretion of IL-17 under the optimal concentration of pOVA in comparison with both isotype-treated and untreated groups. These findings suggested that JAM-A blockade could promote CD4+ T cell differentiation towards a Th17 subset.

To further analyse JAM-A blockade effects on CD4+ T cell differentiation, I cultured OTII CD4+ T cells with BMDCs pulsed with suboptimal and optimal

concentrations of pOVA treated with anti-JAM-A mAb BV11 or its isotype control for 72 hours and analysed the expression of transcription factors that regulate the fate of T cell subsets. After being harvested, cells were stained for CD4, CD44 (not shown) and the transcription factors that are characteristic of Th17, Th1 and Treg cells: RORγt (Figure 4-12A), T-bet (Figure 4-12B) and FoxP3 (Figure 4-12C), respectively. The frequencies of RORγt+, T-bet+ and FoxP3+ cells within the CD4+ population were quantified and compared between groups treated with anti-JAM and groups treated with the isotype control or untreated groups.

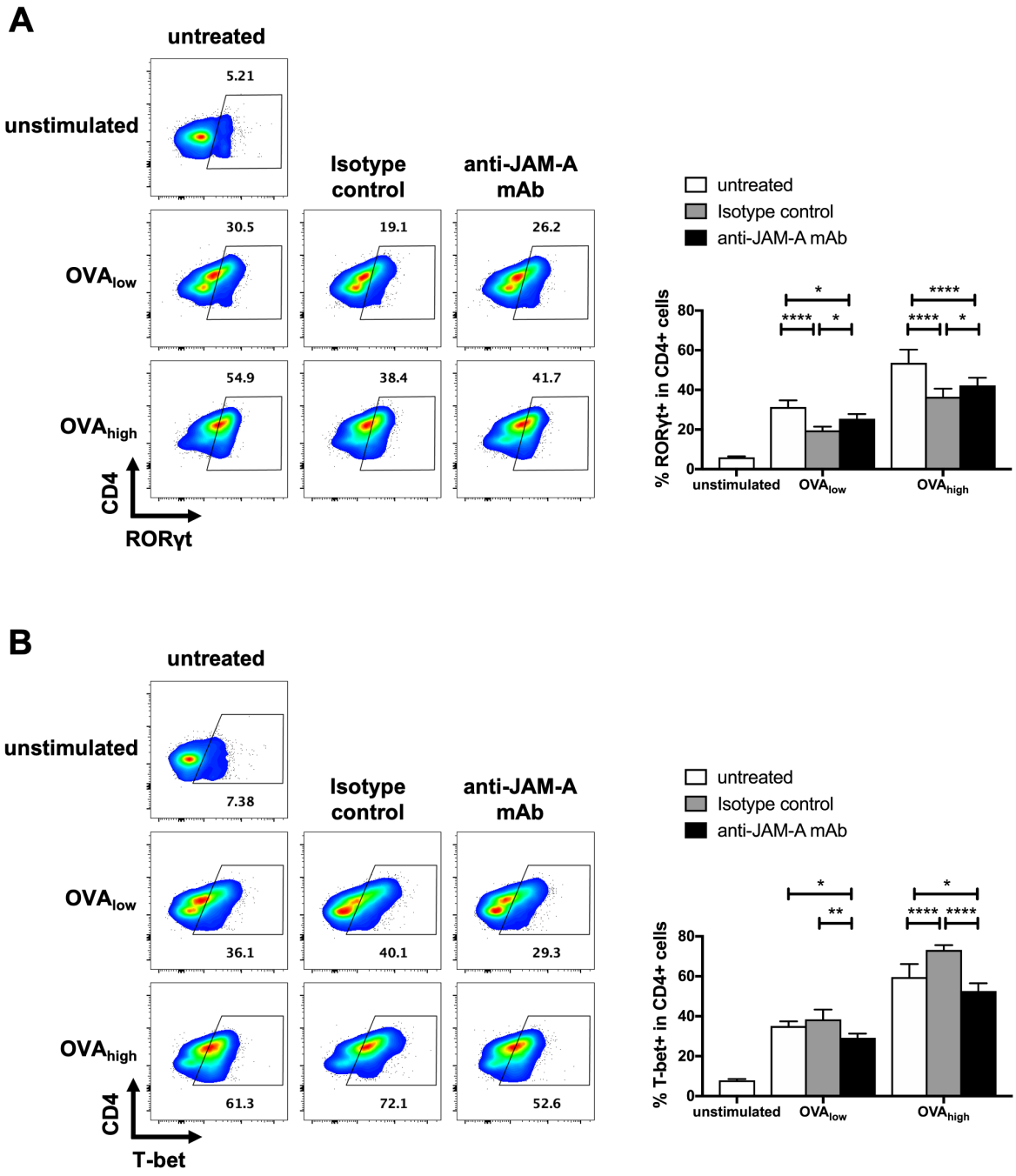
A
untreated
unstimulated
5.21
Isotype control
anti-JAM-A mAb
OVAlow
30.5
19.1
26.2
OVAhigh
54.9
38.4
41.7
CD4
RORγt
untreated
Isotype control
anti-JAM-A mAb
% RORγt+ in CD4+ cells
unstimulated
OVAlow
OVAhigh
B
untreated
unstimulated
7.38
Isotype control
anti-JAM-A mAb
OVAlow
36.1
40.1
29.3
OVAhigh
61.3
72.1
52.6
CD4
T-bet
untreated
Isotype control
anti-JAM-A mAb
% T-bet+ in CD4+ cells
unstimulated
OVAlow
OVAhigh

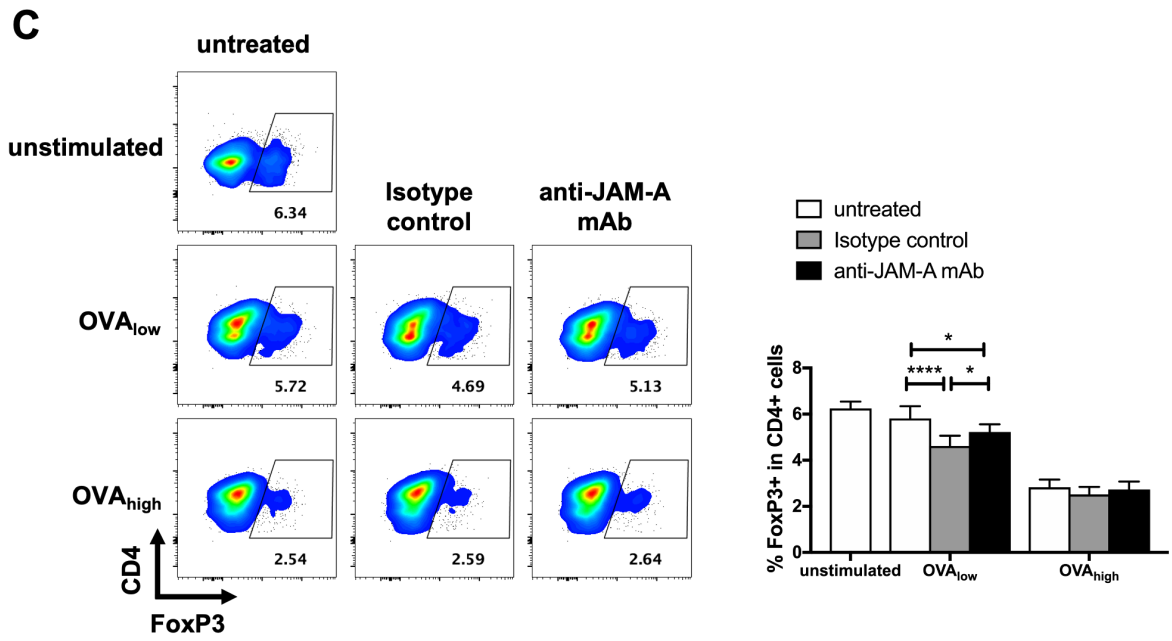

Figure 4-12. JAM-A blockade *in vitro* decreases T-bet expression in CD4+ T cells
CD4+ T cells from OTII mice were cultured with bone marrow-derived dendritic cells pre-pulsed with suboptimal (OVA_{low}) or optimal (OVA_{high}) concentrations of OVA peptide (pOVA) in the presence of anti-JAM-A mAb (BV11) or its isotype control for 72 hours and analysed by flow cytometry for the expression of different transcription factors. **(A)** Representative dot plots of RORγt, **(B)** T-bet and **(C)** FoxP3 intracellular expression on CD4+ T cells (left side) and quantification of cells with specific staining of the transcription factors based on the fluorescence emitted by its matched isotype controls (right side). Comparisons were made within groups with the same concentration of antigen between anti-JAM-A treated group and untreated or isotype-treated groups. Results are expressed as mean ± SD of an experiment performed in hexaplicates. Statistical differences were determined using a two-way ANOVA. *p ≤ 0.05, **p ≤ 0.01, ***p ≤ 0.001.

Analysis of the CD44 expression showed that antigen stimulated CD4+ T cells were successfully activated at similar levels as previous experiments, whereas cells that did not receive antigen continued to be naïve. This was reflected in a higher proportion of RORγt+ and T-bet+, but not FoxP3+ cells, in groups that received antigen in comparison with the unstimulated groups. Both treatments with isotype and anti-JAM-A antibodies decreased the proportion of CD4+ RORγt+ cells in comparison with untreated groups in both suboptimal and optimal conditions. However, anti-JAM-A mAb BV11 treatment increased the proportion of CD4+ RORγt+ cells in comparison with isotype-treated groups in both concentrations of antigen. Although isotype controls are antibodies against irrelevant antigen, they can still engage Fc receptors present on the surface of activated CD4+ T cells that participate in the differentiation of these cells into effector cell populations[360], which may explain the isotype effects found in my assay. Anti-JAM-A treatment decreased the proportion of T-bet expressing CD4+ T cells in comparison with both isotype-treated and untreated groups under both suboptimal and optimal

conditions. Under optimal conditions the level of CD4+ FoxP3+ T cells was similar among groups. Under suboptimal conditions, anti-JAM-A treatment decreased the proportion of CD4+ FoxP3+ T cells in comparison with the untreated group but increased its proportion in comparison with the isotype control group. It was also possible to notice that the isotype treatment affected the proportion of FoxP3+ cells in comparison with the untreated group. These results suggest that disruption of JAM-A pathways may play a role in Th1 differentiation by participating in upregulation of T-bet expression.

Since anti-JAM-A treatment was not able to affect IFN-γ secretion, detected in the culture supernatants, but decreased T-bet intracellular expression in CD4+ T cells, I decided to analyse if antigen-stimulated T cells produce more IFN-γ when treated with anti-JAM-A during priming. CD4+ T cells were again cultured with BMDCs carrying different amounts of antigen and treated with anti-JAM-A mAb BV11 or its isotype control for 72 hours. Cells were then harvested and stained for detection of surface CD4 and intracellular IFN-γ (Figure 4-13A). Frequencies of CD4+ IFN-γ+ T cells (Figure 4-13B) and the MFI from the IFN-γ+ populations (Figure 4-13C) were quantified and compared between anti-JAM-A-treated groups and isotype-treated or untreated groups.

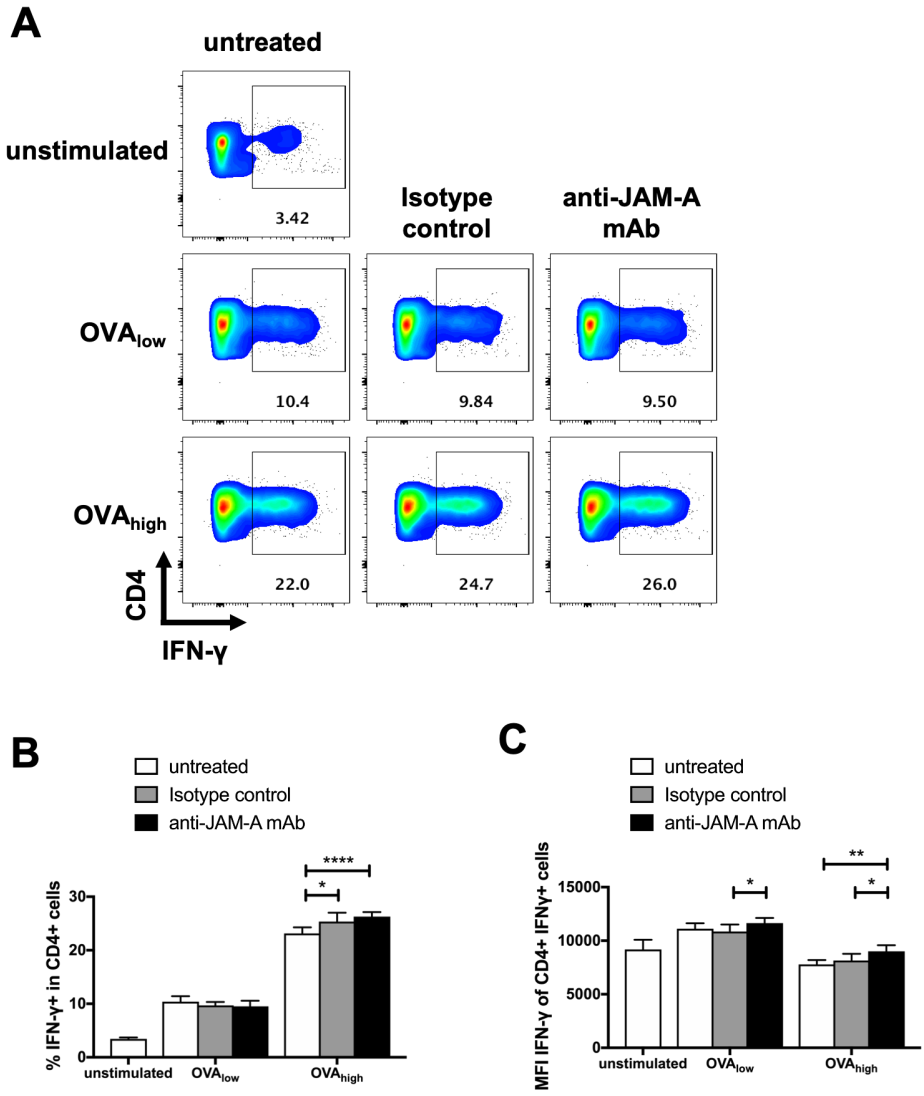

Figure 4-13. The impact of JAM-A blockade *in vitro* in CD4+ T cell IFN-γ production
CD4+ T cells from OTII mice were cultured with bone marrow-derived dendritic cells pre-pulsed with suboptimal (OVA_{low}) or optimal (OVA_{high}) concentrations of OVA peptide (pOVA) in the presence of anti-JAM-A mAb (BV11) or its isotype control for 72 hours and analysed by flow cytometry for IFN-γ intracellular expression. **(A)** Representative dot plots of IFN-γ expression on CD4+ cells gated according to its isotype control. **(B)** Quantification of the proportion of CD4+ T cells expressing IFN-γ. **(C)** Quantification of the IFN-γ median fluorescence intensity (MFI) from the IFN-γ+ population. Results are expressed as mean ± SD of hexaplicate cultures from three independent experiments. Statistical differences between anti-JAM-A-treated group and other groups that received the same concentration of antigen were determined using a two-way ANOVA. *$p \leq 0.05$, **$p \leq 0.01$, ****$p \leq 0.0001$.

The proportion of IFN-γ+ cells were higher with increasing concentrations of antigen. Under suboptimal conditions, the proportion of IFN-γ+ CD4+ T cells were similar between groups, but anti-JAM-A increased the MFI of these IFN-γ+ populations in comparison with isotype-treated cells. Under optimal conditions, the proportion of IFN-γ+ CD4+ T cells was higher in the group treated with anti-JAM-A in comparison with the untreated group but not to the isotype-treated group. In this matter, the isotype control also increased the proportion of IFN-γ+

events. However, the IFN-γ MFI from cells treated with anti-JAM-A mAb was higher than the ones from both untreated and isotype-treated groups under optimal conditions.

4.2.8 Anti-JAM-A mAb Treatment During Antigen Presentation *in vitro* Impacts DC-T cell Cluster Formation

From the fact that JAM-A is a molecule that promotes cell-cell adhesion[325], I hypothesised that JAM-A blockade could reduce DCs and T cell interactions. I first analysed the capacity of cells to form clusters under JAM-A blockade during antigen presentation. For that, OTII CD4+ T cells were cultured with BMDCs pulsed with different concentrations of pOVA and under treatment of anti-JAM-A mAb BV11 or its isotype control. A preliminary experiment was done analysing cells 24 hours after the co-cultures set-up, but there were no significant differences between the negative (unstimulated) and positive control (OVA_{low} and OVA_{high}) groups (not shown). Because cells responded better after 48 hours of the co-culture set-up, evidenced by the significant difference of number and total area of clusters from negative and positive control groups, I used this time point for the experiment in this section. Live cells were then analysed with the brightfield channel of a widefield microscope. Clusters that were defined as cell aggregates with at least 2000 μm^2 were identified (Figure 4-14A) and its numbers (Figure 4-14B), mean areas (Figure 4-14C), total area (Figure 4-14D) were quantified as described in Chapter 2 (section 2.6.4). These parameters from anti-JAM-A-treated groups were compared to the ones from isotype-treated and untreated groups that were stimulated under the same condition of antigen. The frequency distribution of clusters from anti-JAM-A- and isotype-treated groups that were submitted to a high concentration of antigen was also analysed (Figure 4-14E).

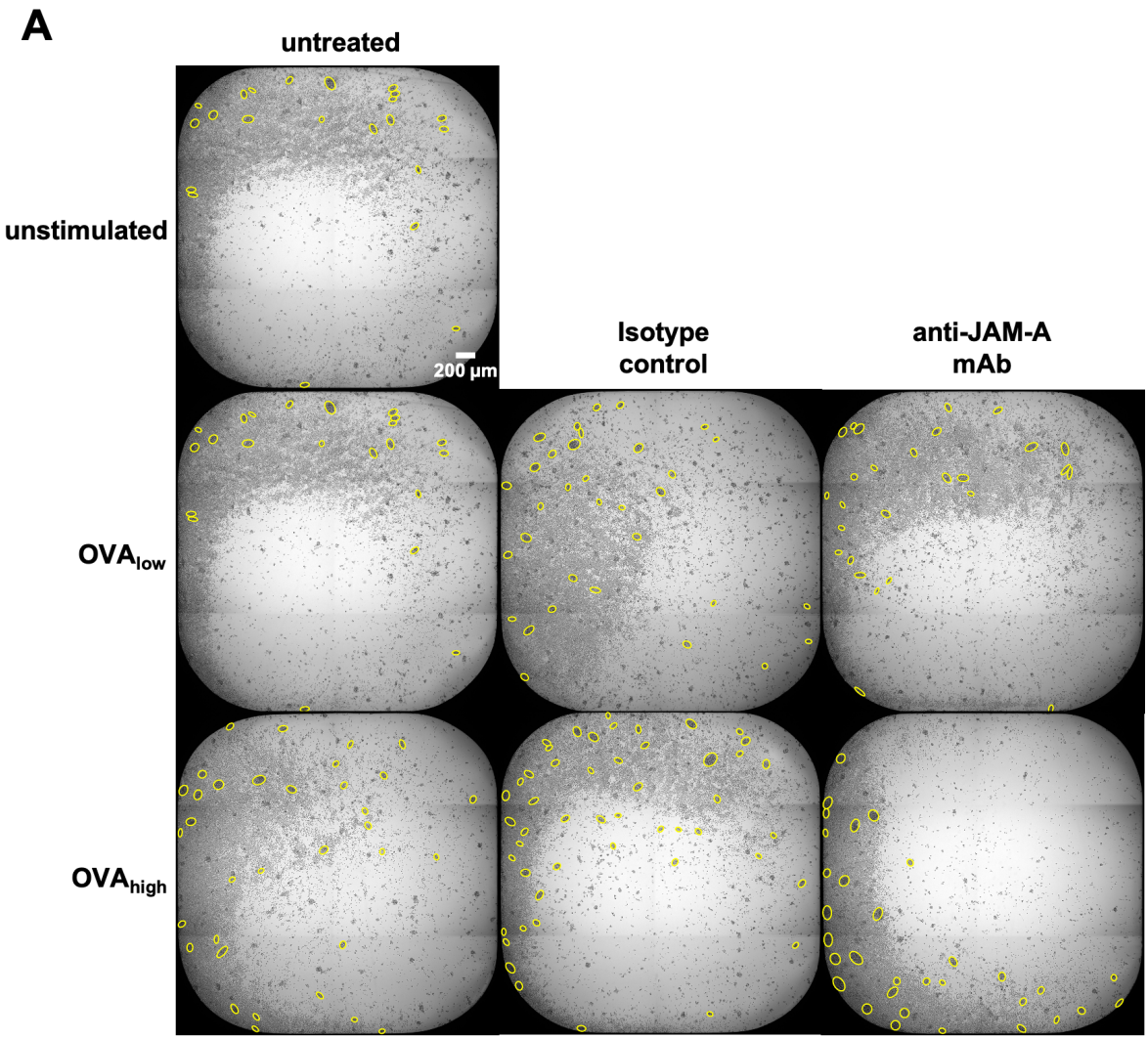
A
untreated
unstimulated
200 µm
Isotype control
anti-JAM-A mAb
OVAlow
OVAhigh

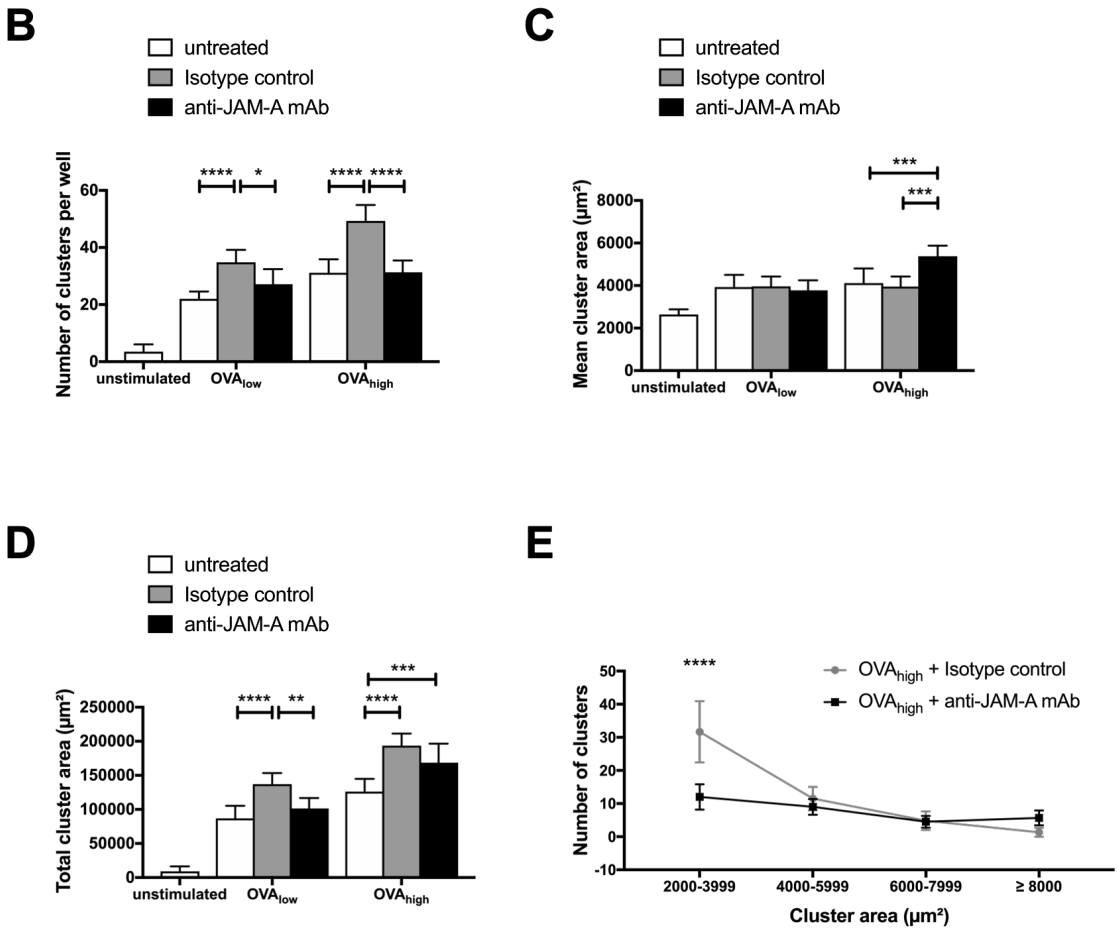

Figure 4-14. JAM-A blockade *in vitro* affects BMDC-T cell cluster formation
CD4+ T cells from OTII mice were cultured with bone marrow-derived dendritic cells pre-pulsed with suboptimal (OVA_{low}) or optimal (OVA_{high}) concentrations of OVA peptide (pOVA) in the presence of anti-JAM-A mAb (BV11) or its isotype control for 48 hours and analysed by widefield microscopy. **(A)** Representative images of whole wells containing cell cultures showing elliptical selections of cell aggregates with at least 2000 µm^2 in yellow. **(B)** Quantification of number, **(C)** mean area and **(D)** total area of clusters with comparisons within groups with the same concentration of antigen between anti-JAM-A treated group and untreated or isotype-treated groups. **(E)** Frequency distribution of the clusters area under optimal concentration of antigen and treated with anti-JAM-A mAb or its isotype control. Results are expressed as mean ± SD of an experiment performed in hexaplicates. Statistical differences were determined using a two-way ANOVA or an unpaired Student's t test. *p ≤ 0.05, **p ≤ 0.01, *** ≤ 0.001, **** ≤ 0.0001.

Cell clustering was higher in groups that were stimulated with antigen than in unstimulated groups. The isotype control increased the total number of clusters in both concentrations of antigen and the total area of clusters under suboptimal activation conditions. However, under suboptimal conditions, groups treated with anti-JAM-A had similar number and total area of clusters in comparison with untreated groups, but lower number and total area of clusters in comparison with isotype-treated groups. No differences were found between groups on the mean area of clusters under the suboptimal condition. Under optimal conditions, groups treated with anti-JAM-A treatment had similar number but higher area of clusters

in comparison with untreated groups but a lower number and similar total area of clusters in comparison with isotype-treated groups. Anti-JAM-A treated cultures had a higher mean area of clusters in comparison with both untreated and isotype-treated groups under optimal conditions. The frequency distribution analysis showed that anti-JAM-A treatment decreased the number of clusters smaller than 4000 μm^2 in comparison with the isotype-treated group. These effects in cluster formation in comparison between anti-JAM-A- and isotype-treated cells supported the hypothesis that specific disruption of JAM-A pathways in the context of the presence of IgG (e.g. recruitment of Fc receptors) could be affecting T cell-DC interactions. I then analysed the contact area of these cell types under priming after JAM-A blockade.

4.2.9 Anti-JAM-A mAb Treatment During Antigen Presentation *in vitro* Does Not Affect DC-T Cell Area of Interaction

To evaluate if disruption of JAM-A pathways during T cell priming affects the area of interaction between T cells and DCs, CFSE-labelled OTII CD4+ T cells were cultured with CMTPX-labelled BMDCs pulsed with optimal and suboptimal concentrations of antigens. Cultures were treated with anti-JAM-A mAb BV11 or its isotype control. Live cells were analysed 24 hours later using fluorescence widefield microscopy for detection of CFSE-labelled T cells in the green channel and CMTPX-labelled BMDCs in the red channel (Figure 4-15A). To evaluate the co-localization between green and red channels, two indexes were used: the Pearson's correlation index (PCC) (Figure 4-15B) that only takes into consideration the proportion of the image that has overlap between channels and the Manders' overlap coefficient (MOC) (Figure 4-15C) that takes into consideration the proportion of the area in which one colour is present but the other is not[361]. In practical terms, the MOC would consider the proportion of T cells that are not in contact with DCs, whereas the PCC would only consider the area of the DC that is in contact with T cells. This time point was chosen due to the fact that there is virtually no T cell proliferation by this point, therefore results on the co-localization analysis would reflect cell interaction only. Comparisons of PCC e MOC indexes were done between groups that received the same concentration of antigen.

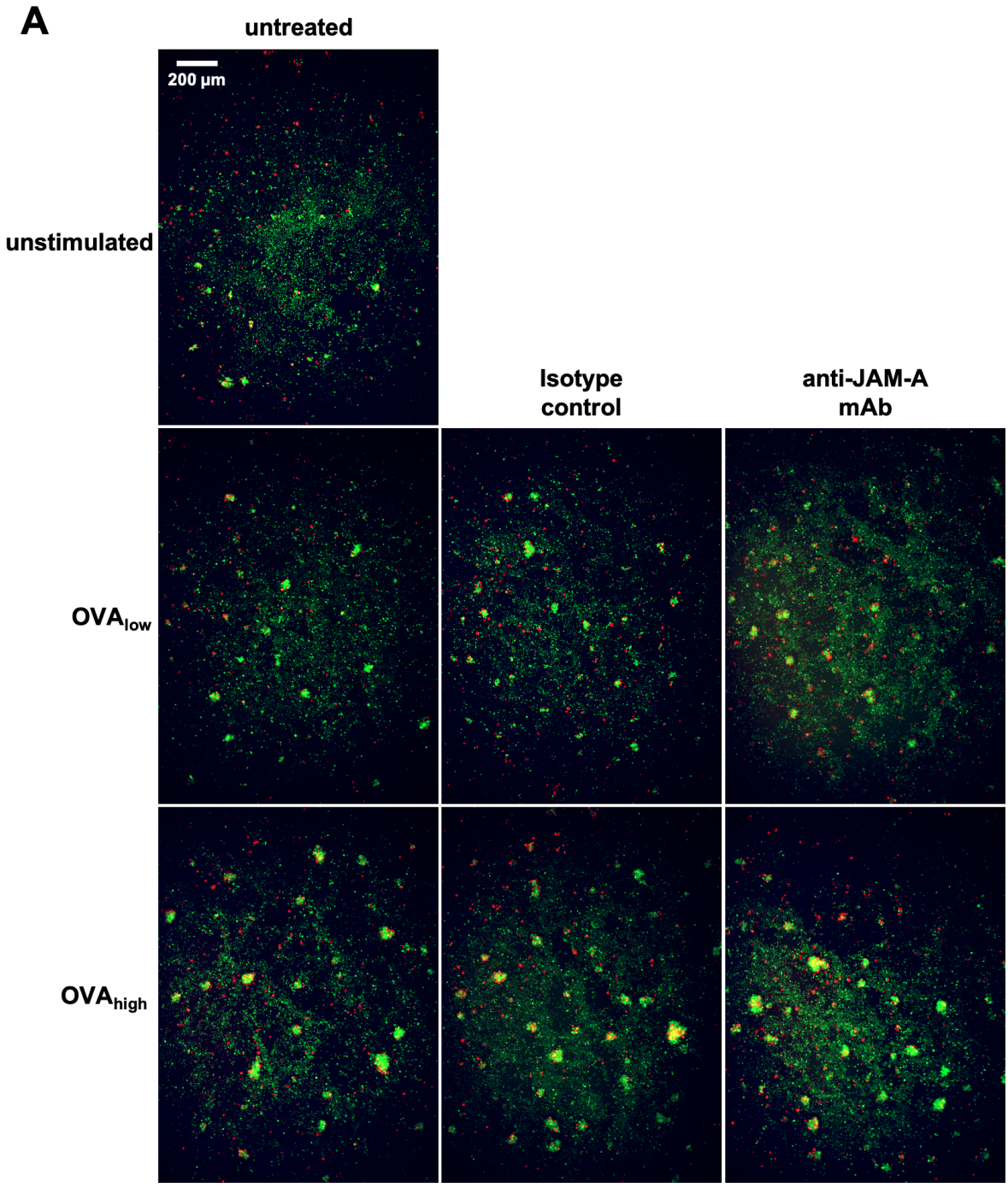
A
untreated
200 µm
unstimulated
Isotype control
anti-JAM-A mAb
OVAlow
OVAhigh

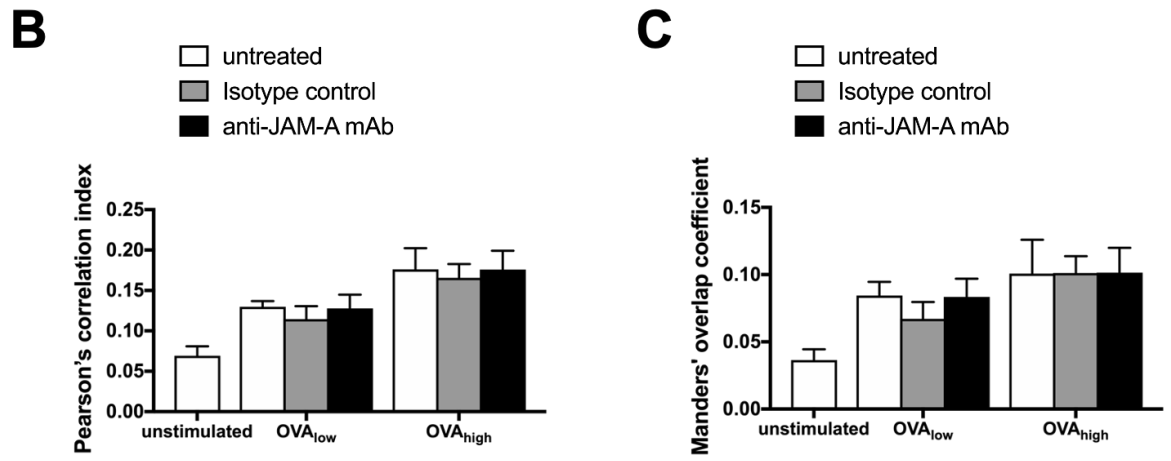

Figure 4-15. JAM-A blockade *in vitro* does not affect BMDC-T cell interactions
CFSE-labelled CD4+ T cells from OTII mice were cultured with CMTPX-labelled bone marrow-derived dendritic cells (BMDC) pre-pulsed with suboptimal (OVA_{low}) or optimal (OVA_{high}) concentrations of OVA peptide (pOVA) in the presence of anti-JAM-A mAb (BV11) or its isotype control for 24 hours and analysed by widefield fluorescence microscopy. **(A)** Representative images of regions containing the highest concentration of cells showing CD4+ T cells in the green channel and BMDCs in the red channel. **(B)** Colocalization analysis between the green and the red channels showing the Pearson's correlation index and **(C)** the Manders' overlap coefficient. Results are expressed as mean ± SD of hexaplicate cultures from two independent experiments. Statistical differences between groups that received the same concentration of antigen were determined using a two-way ANOVA. p = non-significant for all comparisons.

Both PCC and MOC indexes were higher on groups that were stimulated with antigen in comparison with unstimulated groups, suggesting increased physical interaction between T cells and BMDCs when antigen was present in the system. No significant differences were found on both co-localisation indices when comparing groups that were stimulated under the same condition.

4.3 Discussion

The analysis of JAM-A expression in immune cells *in vivo* revealed that JAM-A is expressed on a large proportion of LN cDC2, a subtype of DCs that plays a dominant role in antigen presentation[6,32]. A considerable proportion of other subtypes of DCs express JAM-A, such as LN cDC1 and splenic cDC2 and cDC1. The higher expression on cDC2 populations in comparison with cDC1 is also observed in other lymphoid organs besides LNs and spleen, such as Peyer's patches[362]. Low proportions of both splenic and LN pDCs are JAM-A+. This finding is supported by a study that showed expression of JAM-A in a small proportion of murine pDCs from spleen, mesenteric LN, peripheral LN and blood[346]. Although a high proportion of some T cell lines can express JAM-A, such as Jurkat T cells[330], I

showed that only a small proportion of naïve CD4+ T cells from spleen, LNs (inguinal, brachial, superficial cervical, mesenteric) and Peyer's patches of C57BL/6 mice express JAM-A. These findings suggest that JAM-A homophilic binding is unlikely to happen during the first encounter of antigen by the T cells.

In vitro experiments showed that CD4+ T cells express low or undetectable levels of JAM-A when stimulated with anti-CD3 and anti-CD28 agonistic antibodies for 3 days. However, a higher proportion of CD4+ T cells stimulated with antigen by BMDCs *in vitro* for 48 and 72, but not 24 hours, expressed JAM-A in comparison with unstimulated T cells. To address if this upregulation could be driven by the cytokines that were released by activated T cells or BMDCs during or after priming, I used an *in vitro* system in which both naïve and antigen specific activated CD4+ T cells were present in the same well for comparison. I analysed the expression of JAM-A on cultures containing both OTII and WT isolated CD4+ T cells and antigen-pulsed BMDCs. After 72 hours, a higher percentage of activated OTII CD4+ T cells expressed JAM-A in comparison with WT CD4+ T cells that were present in the same wells. Altogether, these findings suggest that JAM-A upregulation on activated CD4+ T cells is dependent on contact dependent signals from the APC during antigen presentation other than CD28-CD80/CD86, and that JAM-A may play a role on CD4+ T cell effector functions.

Although only a small population of naïve CD4+ T cells express JAM-A, most of them express a potential ligand for JAM-A. *In vivo* naïve CD4+ T cells express high levels of integrin CD11a, the alpha chain of LFA1, a known ligand for JAM-A[330]. Furthermore, upon activation, CD4+ T cells upregulate CD11a expression. Integrins such as LFA1 exist in an inactivated state on the cell surface and, upon stimulus, these molecules undergo a conformational change that enables them to interact with extracellular ligands[363]. However, although some mAb clones can specifically detect the active conformation of LFA1[364], the mAb clone that was used in my *in vitro* experiments to detect CD11a (M17/A) does not distinguish between activated and resting forms of LFA1. Nevertheless, the expression of active LFA1 on both naïve and memory CD4+ T cells is described in the literature[365]. While further JAM-A ligands were not investigated in this present Chapter, T cells also express other potential ligands for JAM-A. Although JAM-B is not expressed by

leukocytes[366], JAM-C is expressed by naïve and mitogen-activated human T cells[367] and CD9 is expressed by naïve murine and human CD4+ T cells[368–370].

After showing that BMDCs express JAM-A and in higher proportions on mature cells, supporting findings from the literature[326], I analysed the location of JAM-A on the SI with the T cell. Although JAM-A was not concentrated in the SI as has been observed for MHCII, the molecule was present in the SI during antigen presentation, suggesting it could be available for binding with potential ligands from the T cells surface. To analyse if JAM-A could play a role in determining T cell outcomes during priming, I cultured antigen-pulsed BMDCs with OTII naïve CD4+ T cells and analysed their activation status as well as division rate. Treatment with anti-JAM-A mAb BV11 attenuated CD4+ T cell activation and proliferation both on suboptimal and on optimal conditions of antigen, suggesting that JAM-A may play a role in T cell priming.

To analyse if JAM-A plays a role on CD4+ T cell differentiation, I first analysed cytokines from the supernatant of co-cultures from the previous experiment to identify cytokines that are mainly produced by Th1 (IFN-γ), Th2 (IL-4), Treg (IL-10) and Th17 (IL-17) cells. Although IL-4 was not detected, the levels of IFN-γ and IL-10 were similar across groups that were stimulated with the same concentrations of antigen. This is supported by a study that showed no differences on IFN-γ concentrations from the supernatant of OVA-primed OTII CD4+ T cells by BMDCs from JAM-A KO mice *in vitro* 5 days after co-culture set-up in comparison with WT BMDCs[347]. However, JAM-A blockade increased the secretion of IL-17 under the optimal concentration of antigen, suggesting an increased differentiation of Th17 cells. To address this question, I performed the same *in vitro* experiment but with focus on looking for transcription factors that control T cell differentiation. As expected, JAM-A blockade promoted a small but significant increase in the proportion of CD4+ T cells expressing RORγt, the master transcription factor of Th17 cells[74], supporting the finding of increased IL-17 secretion detected in the culture supernatants. However, this effect was only found in comparison to isotype-treated cells, as treatment with this IgG against irrelevant antigen decreased the percentage of RORγt+ cells in comparison to untreated cells. Interestingly, previous literature describes a 4.5-fold increase on absolute number of CD4+ IL-17+ T cells in the colonic lamina propria of JAM-A-

deficient mice in comparison with WT mice[371]. In addition, I also demonstrated a small increase in the proportion of CD4+ T cells expressing FoxP3, the main transcription factor of Treg cells[74], after JAM-A blockade under suboptimal conditions. Again, this effect was only found in comparison to isotype-treated cells, ad not to untreated cells. Treatment with the isotype control antibody decreased the proportion of FoxP3+ cells. In support to the increased proportion of FoxP3+ cells in anti-JAM-A groups in comparison to isotype-treated groups, previous literature showed a small but significant increase on the absolute number of FoxP3+ T cells in the lamina propria of JAM-A-deficient mice in comparison with WT mice[371], possibly suggesting that JAM-A blockade could influence pathways that supress Treg differentiation.

Induction of CD4+ T cell differentiation towards specific Th subsets is usually followed by inhibition of other subsets. T-bet, for example, is described to interact with promoters of the RORC gene, responsible for encoding RORγt, and supress Th17 differentiation[76]. As such, the expression of T-bet on T cells after JAM-A blockade during priming was also analysed. JAM-A blockade decreased the proportion of T-bet expressing CD4+ T cells, suggesting that recruitment of JAM-A intercellular ligation is required for optimal Th1 differentiation.

In contrast to the observed decrease in the proportion of T-bet-expressing cells, no differences in IFN-γ secretion measured from the co-culture supernatants between the anti-JAM-A- and the isotype-treated group were found. I further evaluated the capacity of these T cells to produce IFN-γ by intracellular measurement. Although the proportion of CD4+ IFN-γ+ T cells was not changed with treatment of anti-JAM-A, this population of IFN-γ producers showed a small but significant increased capacity to produce IFN-γ. However, in order to compare the results from the experiment that detected IFN-γ from the supernatant with the experiment that detected intracellular IFN-γ, it is important to consider the technicalities of the two different methods that were utilised. While ELISA has a high technical variation, evidenced by a higher SD that constantly follows this kind of experiment, the detection of intracellular cytokines is a more precise method. However, after being harvested, these cells were re-stimulated *in vitro* with PMA, a protein kinase C activator, and ionomycin, a calcium ionophore that increases intracellular calcium concentration, to encourage their cytokine production that

are kept in intracellular compartments driven by the treatment of a protein transport inhibitor (Brefeldin A). Although this method is widely used for the detection of the intracellular cytokine by flow cytometry, these cells are now re-stimulated, and therefore, the effects caused by the initial treatment with anti-JAM-A could be lost or diminished.

As JAM-A is an adhesion molecule that provides firm attachment to cells[325], I hypothesised that the effects seen on CD4+ T cell outcome after JAM-A blockade during antigen presentation could be driven by an impaired cell-cell interaction. First, I analysed the capacity of T cells and DCs to form clusters under treatment with anti-JAM-A mAb BV11. This analysis showed that, although the isotype control mAb increased the number and total area of clusters under suboptimal conditions, opposing effects were found when comparing the isotype-treated group with the anti-JAM-A-treated group. Under suboptimal conditions, anti-JAM-A treatment was able to decrease the number of clusters and its total area in comparison with cells treated with its isotype control mAb. Under optimal conditions, JAM-A blockade also decreased the number of clusters, but because the area of the clusters was in general larger, the total area occupied by them was unchanged in comparison with the isotype-treated group. I believe that the physical disruption caused by specific disruption of JAM-A pathways in an environment with abundant IgG could be related to a delay on cell interactions caused by JAM-A intercellular ligation blockade. After priming T cells, DCs have to detach from T cells to prime other cells or to play other immunomodulatory roles. Therefore, blockade of an adhesion molecule such as JAM-A could be modifying parameters as for example, surface or time of these intercellular interactions, consequently impairing this process and possibly delaying it. However, these live cells were analysed 48 hours after priming, when T cell proliferation already occurs. Therefore, the analysis of these clusters doesn't reflect just the physical interaction between the cell types, but also takes into consideration the number of T cells that are present in the system. To tease apart the bias of proliferation from the analysis of T cells-DC interactions, I measured cell interactions 24 hours after priming with fluorescence-dyed cells and analysed the overlap between both channels relative to each cell type. Both co-localization indexes, PCC and MOC were unchanged with treatment of anti-JAM-A mAb BV11. I considered employing confocal microscopy to analyse the area of contact with a higher precision. However, these

experiments analyse only static images of a specific moment in the co-culture, whereas JAM-A blockade could be possibly affecting the time of interaction between the cells or perhaps the quality of the crosstalk, parameters that would be difficult to measure with the instruments that are available in the laboratory.

As blockade of JAM-A during CD4+ T cell priming impacted in T cell activation and proliferation, I therefore identified JAM-A as a regulator of CD4+ T cell activation. Although effects of JAM-A blockade only attenuated but not inhibited T cell proliferation and activation, this molecule could play an important role on CD4+ T cell activation *in vivo*. In addition, JAM-A seems to drive CD4+ T cell differentiation towards Th1, a subset that is linked to the development of autoimmunity[76]. As having an attenuation effect in T cell activation, its blockade could be possibly useful as a therapeutic for inflammatory diseases, and its promotion could be studied as treatment targeting cancer cells. Before evaluating the potential of JAM-A as a therapeutic target in a disease model, I analysed the effects of JAM-A blockade on CD4+ T cell outcomes during antigen presentation in the complexity of the murine *in vivo* environment, that is the subject of the next Chapter.

Chapter 5 JAM-A Contributes to CD4+ T cell Effector Functions During Priming *in vivo*

5.1 Introduction

In the last Chapter, I demonstrated that blockade of JAM-A affects DC-T cell cluster formation, T cell activation, proliferation, differentiation and cytokine secretion. In addition to DCs and other leukocytes, JAM-A is expressed by endothelial and epithelial cells in intercellular tight junctions[325]. Moreover, TNFα- and IFNγ-stimulated endothelial cells redistribute JAM-A from these intercellular junctions to the apical surface, increasing its support for leukocyte adhesion[330,372]. Therefore, studies on disruption of JAM-A pathways aiming to investigate the interactions between leukocytes *in vivo* must also consider the effect of disrupting leukocyte-endothelial cell interactions.

A few studies have assessed the effects of JAM-A blockade *in vivo* in the interactions between leukocytes and endothelial cells. Treatment with anti-JAM-A mAb BV11 decreased leukocyte transendothelial migration through cremaster venules induced by IL-1ß, but not by the chemoattractants leukotriene B4 (LTB4) or platelet-activating factor (PAF)[354]. The same response pattern was observed in JAM-A deficient mice in comparison with WT mice. This decrease in leukocyte transendothelial migration through venous tissues was found to be mediated by JAM-A expressed by endothelial cells, but not by leukocytes. On the other hand, an increased granulocyte infiltration was found in the colonic mucosa of JAM-A KO mice in comparison with WT animals[373]. More recently, mice with selective loss of JAM-A in myelomonocytic cells, cells that can differentiate into monocytes, macrophages and CD8+ or CD8- DCs[374], were used to investigate JAM-A role on JAM-A-expressing leukocytes during inflammation. These mice showed no difference in neutrophil recruitment into the peritoneum and macrophage chemokine production in response to LPS and zymosan, in comparison with control mice[375]. However, these parameters were significantly reduced in JAM-A$^{-/-}$ mice stimulated by these inflammatory mediators. On the other hand, mice with selective loss of JAM-A in intestinal epithelial cells resulted in increased intestinal permeability, reduced peritoneal neutrophils migration and macrophage

chemokine production. These findings suggest that JAM-A expression in the epithelium is fundamental for JAM-A role in myeloid cells-mediated inflammation.

DCs migrate from inflamed tissues to specialized lymphoid organs, where antigen presentation and activation of naïve T cells occurs[6]. BMDCs from JAM-A deficient mice showed increased migration from FITC-painted skin to the draining LN[326]. In addition, a study showed higher transmigration of JAM-A-expressing BMDCs through layers of JAM-A$^{-/-}$ endothelial cells in comparison with endothelial cells from JAM-A$^{-/-}$ mice reconstituted with full-length JAM-A cDNA[347]. These studies suggest that disruption of JAM-A pathways could affect endogenous DC migration and therefore impact the amount of antigen presented in the LN. In this chapter, I aimed to investigate whether JAM-A blockade affects CD4+ T cell activation, proliferation and differentiation *in vivo* by employing an adoptive transfer model.

5.2 Results

5.2.1 JAM-A is Expressed on T Cell and Medullary Areas of Mouse Lymph Nodes (LN)

To analyse some of the factors that can influence DC entry in the LN under JAM-A blockade during CD4+ T cell priming *in vivo*, the expression of JAM-A was analysed on histological sections of murine LNs. Mesenteric LNs were harvested and cryo-sections stained for the identification of the markers B220, lymphatic vessel endothelial receptor 1 (LYVE1) and JAM-A (Figure 5-1A). Regions suggesting B cell follicles were identified by expression of B220, a B cell lineage marker. LYVE1 is found primarily on lymphatic endothelial cells[376] and was used to detect the medullary region of the LN. The MFI across a longitudinal region of the section covering all areas of the section was also analysed (Figure 5-1B).

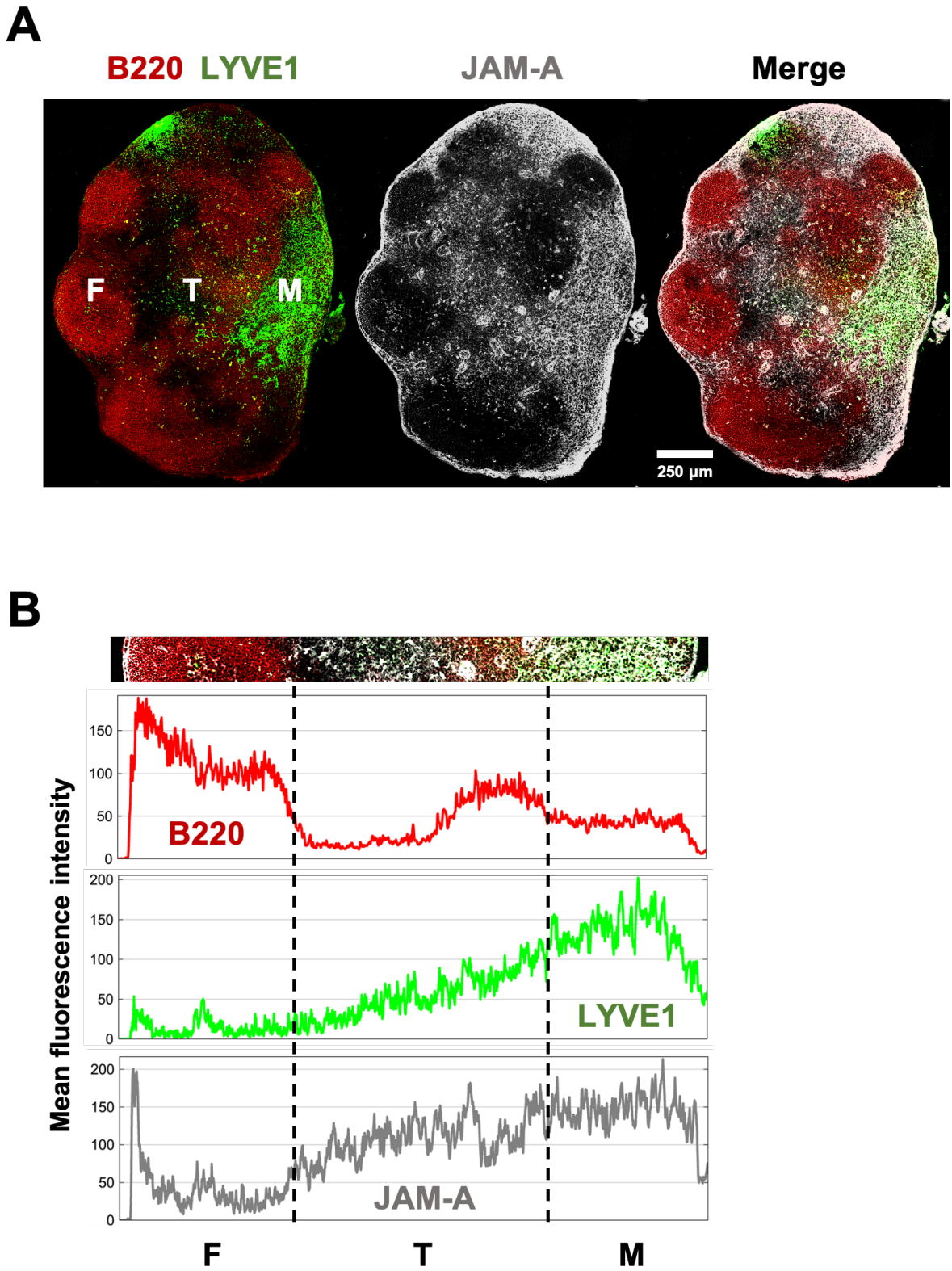

Figure 5-1. JAM-A localization in a murine lymph node (LN)
Sections from a naïve mesenteric LN from C57BL/6 mice were analysed by widefield fluorescence microscopy for the expression of JAM-A, B220 and LYVE1. **(A)** Representative image of a section through a LN indicating B cell follicles (F), T cell region (T) and the medulla (M). Regions were identified with B220 (mAb RA3-6B2) in red, LYVE1 (mAb ALY7) in green and JAM-A (mAb H202-106) in grey. **(B)** Histograms of B220, LYVE1 and JAM-A mean fluorescence intensity (MFI) from a longitudinal 8 µm section of the LN that covered all three regions. Isotype controls were used to certify specific binding. Data are representative of three independent experiments.

LYVE1 was highly expressed in the LN medulla, as well as a smaller cortical region that can possibly be the local of an insertion of an afferent lymphatic vessel. The area in which B220 and LYVE1 were less expressed was identified as the T cell area of the LN. Analysis as described in chapter 2.6.4 showed that JAM-A is expressed in the T cell area of the LN, where DCs contact T cells to present antigen. However, JAM-A is highly expressed in external areas of the LN, and in the medullary area, suggesting that JAM-A blockade *in vivo* could influence the interactions between leukocytes and endothelial cells.

5.2.2 siRNA Targeting *F11R* Gene Has Limited Impact on JAM-A Expression on BMDCs

JAM-A blockade *in vivo* could not only potentially affect the interactions between T cells and DCs, but it would also possibly disrupt leukocyte-endothelial cell interactions. To tease apart these effects, I tried to employ a technique that would influence the expression of JAM-A only on leukocytes. As JAM-A is expressed in high levels by DCs and BMDCs but in low levels by CD4+ T cells. BMDCs genetically manipulated to express low levels of JAM-A could be pulsed with antigen and be used to challenge mice, aiming to specifically disrupt JAM-A pathways during antigen presentation *in vivo*. For this genetic manipulation, the siRNA technique was used as described in detail in Chapter 2 (section 2.2.5). Cells were harvested 72 hours after the transfection to be analysed by flow cytometry for the expression of JAM-A (Figure 5-2A). CD11c was used as a DC marker to identify the target population. For the control group, I used siRNA targeting *GFP*, a gene responsible for encoding the GFP fluorescent protein, a molecule that is not present in the system. The expression of JAM-A on CD11c+ cells was then compared between groups (Figure 5-2B).

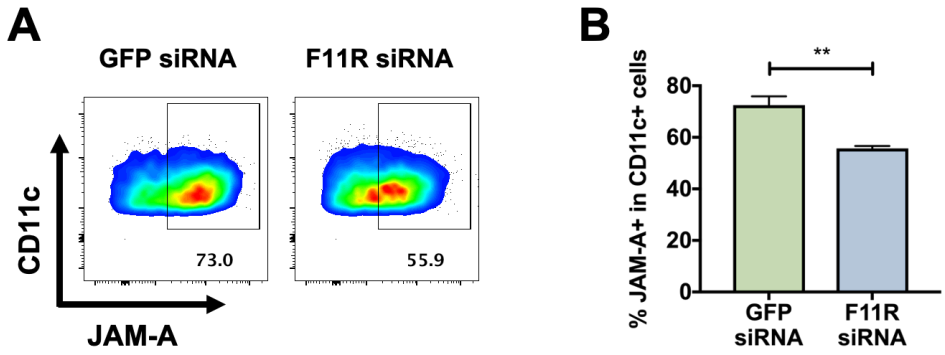

Figure 5-2. *F11R* siRNA minimally affects bone marrow-derived dendritic cells (BMDC) JAM-A expression
Day-7 immature BMDCs were transfected with siRNA targeting the *F11R* gene or the *GFP* gene (control) and Lipofectamine 2000 for 72 hours and analysed by flow cytometry for the expression of JAM-A. **(A)** Representative dot plots of JAM-A expression on CD11c+ cells. **(B)** Quantification of the proportion of JAM-A+ cells and comparison between *F11R* siRNA and *GFP* siRNA groups. Results are expressed as mean ± SD of triplicate cultures from three independent experiments. Statistical differences were determined using an unpaired Student's t test. **p ≤ 0.01.

BMDCs transfected with siRNA targeting the *F11R* gene expressed statistically significantly lower levels of surface JAM-A. However, the small decrease suggests that the use of these transfected cells would possibly not be biologically relevant in the context of *in vivo* experiments. Additional attempts with changes to the protocol were performed aiming to further reduce the expression of JAM-A, such as different concentrations of cells, transfection reagent and siRNA. All changes in the protocol however resulted in similar effects as seen in the present experiment.

5.2.3 The impact of anti-JAM-A mAb Treatment *in vivo* in CD4+ T Cell Activation and Proliferation

As an alternative approach, we assess the effects of antibody mediated JAM-A blockade on CD4+ T cell responses *in vivo*. Although I have shown in Chapter 4 that JAM-A blockade attenuated CD4+ T cell activation and proliferation *in vitro*, immunological components that are not present in *in vitro* studies, such as cell migration, have a role on antigen presentation *in vivo*. The literature reports increased migration of BMDCs generated from JAM-A-deficient mice from inflamed skin tissues to draining LNs[326]. As such, a possible increase on T cell activation and/or proliferation under conditions of JAM-A manipulation during priming *in vivo* could be expected. To allow for an increase in these parameters to be observed, I first performed an OVA titration to select a suboptimal antigen dose. CFSE-

labelled naïve CD4+ T cells from OTII mice were transferred to WT mice, as described in Chapter 2 (section 2.3.1). The next day, mice were challenged in the hind footpads with different doses of OVA (0, 0.05, 0.5 and 5 µg). LPS was also administered to induce non-specific inflammation and stimulate DC trafficking[377]. The pLNs were harvested 72 hours after challenge and analysed by flow cytometry. OTII CD4+ T cells were identified by its expression of CD45.1 and CD4 (Figure 5-3A). Cell division was assessed based on CFSE fluorescence intensity (Figure 5-3B) and cell activation was determined by the expression of CD44 (Figure 5-3C).

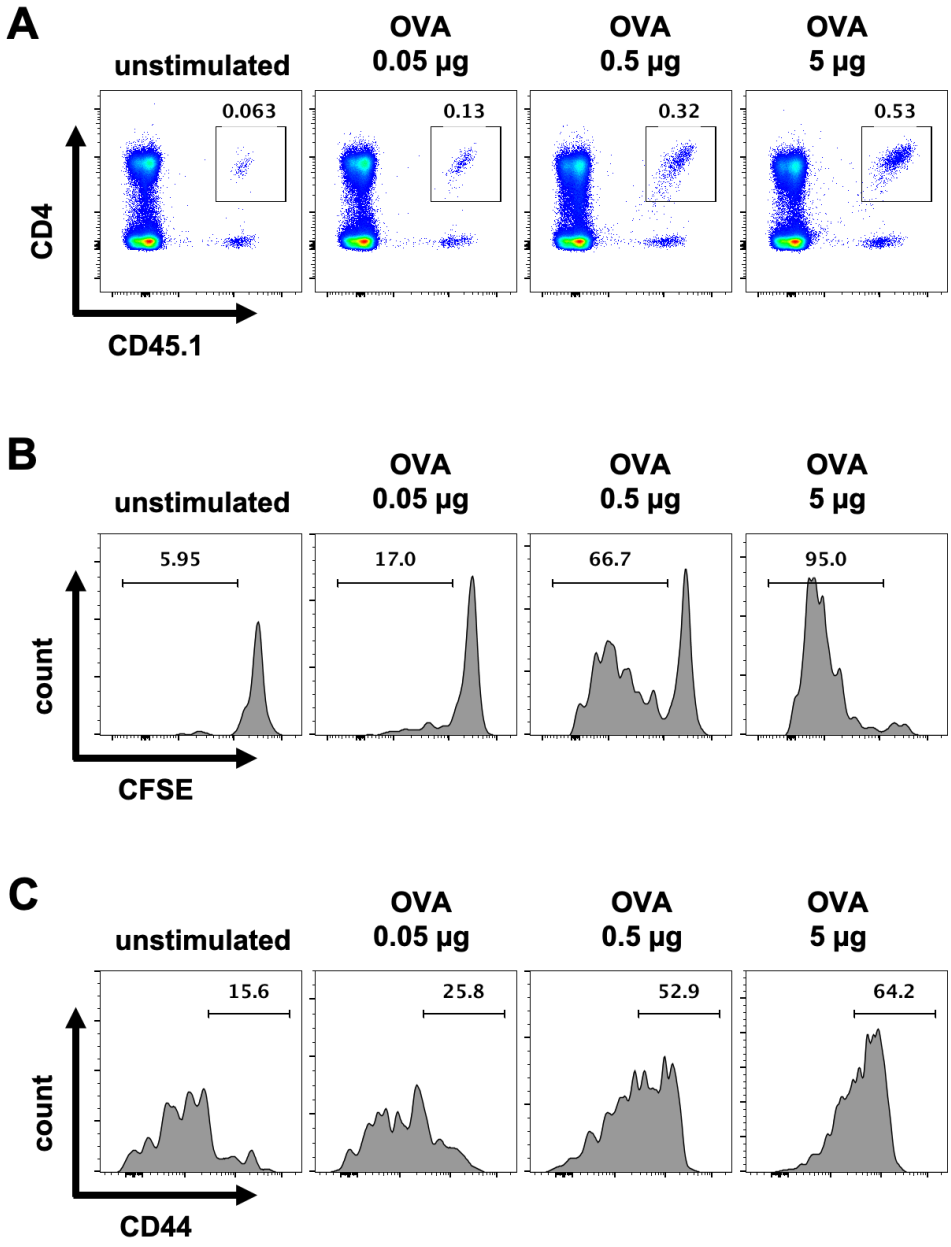

Figure 5-3. Determination of a suboptimal dose of antigen in the adoptive transfer model
CFSE-labelled immune cells from lymph nodes (LN) and spleens of OTII mice were adoptively transferred to C57BL/6 mice that were challenged with footpad injections of LPS and different doses of OVA. Popliteal lymph nodes (pLN) were harvested 72 hours later and analysed by flow cytometry for the expression of CD44 and CFSE. **(A)** Gating strategy for identification of OTII CD4+ T cells (CD4+ CD45.1+) showing the frequency of these cells when different doses of antigen are used. **(B)** Histograms of CFSE fluorescence intensity on OTII CD4+ cells with gating on divided cells. **(C)** Representative histograms of CD44 fluorescence intensity on OTII CD4+ cells with gating on $CD44_{high}$ cells. Data are representative of an experiment performed in duplicate.

The increasing doses of OVA promoted activation and proliferation of the adoptively transferred CD4+ T cells in increasing proportions, evidenced by the frequency of $CD44_{high}$ populations, the proportion of CD45.1+ CD4+ cells found in LNs and the CFSE fluorescence intensity of the OTIIs populations. Although 0.5 and 5 µg have induced T cell activation in similar proportions, T cells challenged with

the first concentration have divided in a lower proportion. As such, I chose to perform the next experiment with 0.5 µg of antigen.

To evaluate the effects of JAM-A blockade during antigen presentation on the induction of CD4+ T cell responses, the adoptive transfer model was performed again as described in Chapter 2 (section 2.3.1). CFSE-labelled, OTII naïve CD4+ T cells were adoptively transferred to WT mice, that were challenged in the hind footpads with LPS and 0.5 µg OVA. The animals were treated with anti-JAM-A mAb BV11 or its isotype control, as described in Chapter 2 (section 2.3.1). The pLNs were harvested 72 hours after challenge and had their cells counted (Figure 5-4A) and analysed by flow cytometry. OTII CD4+ T cells were identified by its expression of CD45.1 and CD4 (Figure 5-4B) and the proportion (Figure 5-4C) and absolute number (Figure 5-4D) of OTII T cells were calculated. To evaluate if the treatment promoted a change in the accumulation of adoptively transferred non-CD4 cells in the pLNs, the proportion (Figure 5-4E) and numbers (Figure 5-4F) of adoptively transferred cells that were CD4- was also analysed.

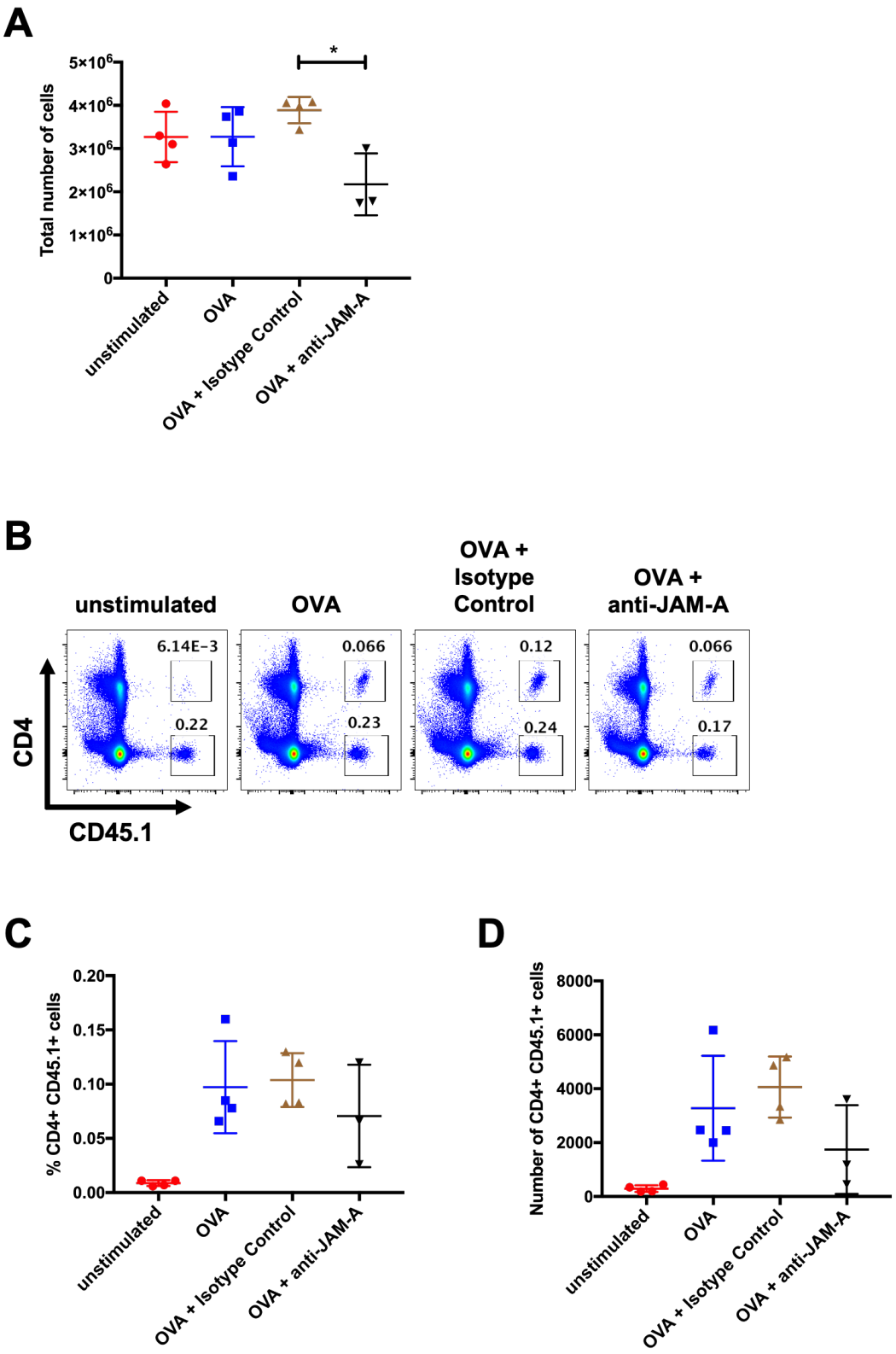
A
Total number of cells
5×10^6
4×10^6
3×10^6
2×10^6
1×10^6
0
*
unstimulated
OVA
OVA + Isotype Control
OVA + anti-JAM-A
B
unstimulated
OVA
OVA + Isotype Control
OVA + anti-JAM-A
6.14E-3
0.22
0.066
0.23
0.12
0.24
0.066
0.17
CD4
CD45.1
C
% CD4+ CD45.1+ cells
0.20
0.15
0.10
0.05
0.00
unstimulated
OVA
OVA + Isotype Control
OVA + anti-JAM-A
D
Number of CD4+ CD45.1+ cells
8000
6000
4000
2000
0
unstimulated
OVA
OVA + Isotype Control
OVA + anti-JAM-A

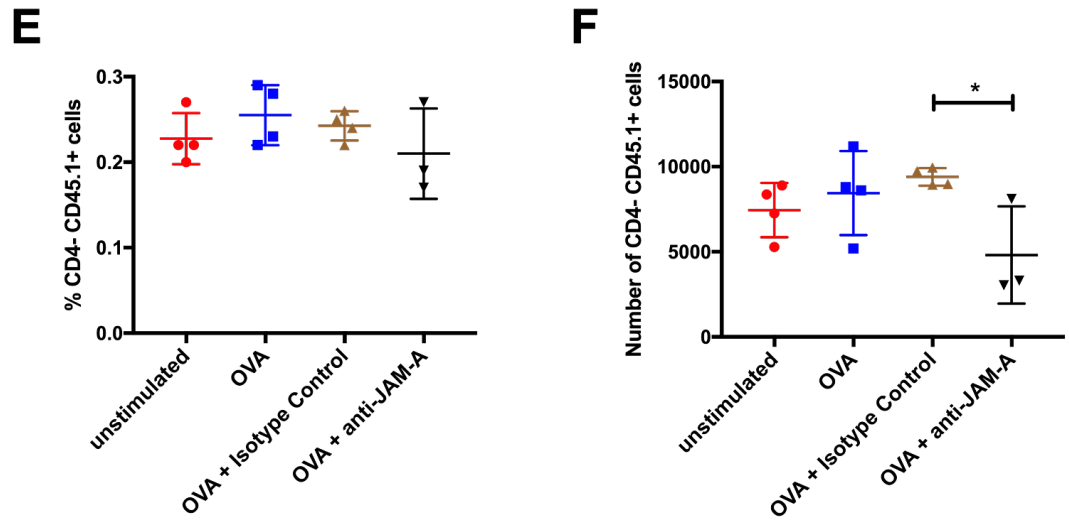

Figure 5-4. JAM-A blockade *in vivo* impact in leukocyte accumulation in the LN
CFSE-labelled immune cells from lymph nodes (LN) and spleens of OTII mice were adoptively transferred to C57BL/6 mice that were challenged with footpad injections of LPS and OVA in the presence of anti-JAM-A mAb (BV11) or its isotype control. Popliteal lymph nodes (pLN) were harvested 72 hours later and analysed by flow cytometry for the expression of CD44 and CFSE. **(A)** Quantification of cell numbers by cell counting with a haemocytometer. **(B)** Representative dot plots of CD4 and CD45.1 expression on cells with gating on adoptively transferred OTII CD4+ T cells (CD4+ CD45.1+) or CD4- (CD4- CD45.1+) cells. **(C)** Quantification of the proportion or **(D)** absolute number of OTII CD4+ cells. **(E)** Quantification of the proportion or **(F)** absolute number of adoptively transferred CD4- cells. Results are expressed as mean ± SD of an experiment performed in biological replicates (n = 4). Statistical differences between groups that received antigen were determined using a one-way or a two-way ANOVA. *p ≤ 0.05.

Anti-JAM-A mAb treatment decreased the total number of cells from pLNs, in comparison with the isotype control group, but not to the untreated group. The proportion and number of CD4+ CD45.1+ cells were unaltered under treatment with anti-JAM-A. However, although the proportions of CD4- adoptively transferred cells were not different across groups, JAM-A blockade decreased the total number of these cells in comparison with the isotype-treated group, suggesting that the treatment could impact the accumulation of non-CD4 leukocytes in the pLNs when comparing to isotype-treated cells. The viability of cells was also analysed as described in section 2.4.1 (not shown), but no differences in cell death were found.

To analyse the proliferation of the OTII cells, their CFSE fluorescence intensity was analysed (Figure 5-5A) and compared (Figure 5-5B). In addition, peaks based in the number of divisions were identified (Figure 5-5C) and compared between groups that have received antigen stimulation (Figure 5-5D).

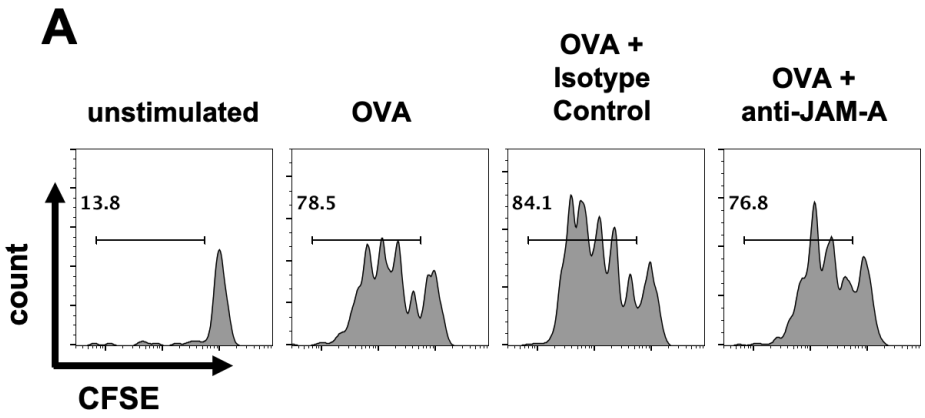
A
unstimulated
OVA
OVA + Isotype Control
OVA + anti-JAM-A
13.8
78.5
84.1
76.8
count
CFSE

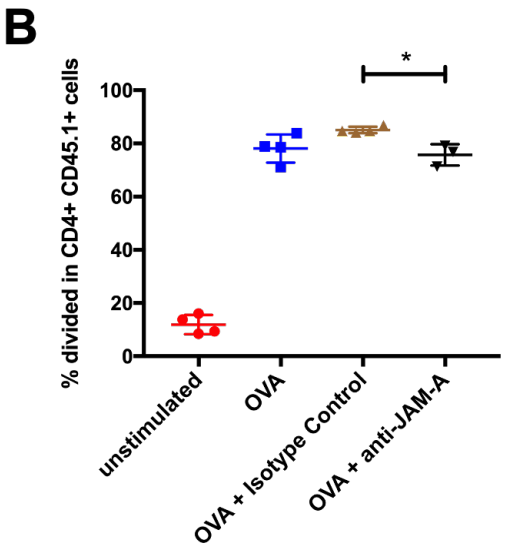
B
% divided in CD4+ CD45.1+ cells
100
80
60
40
20
0
*
unstimulated
OVA
OVA + Isotype Control
OVA + anti-JAM-A

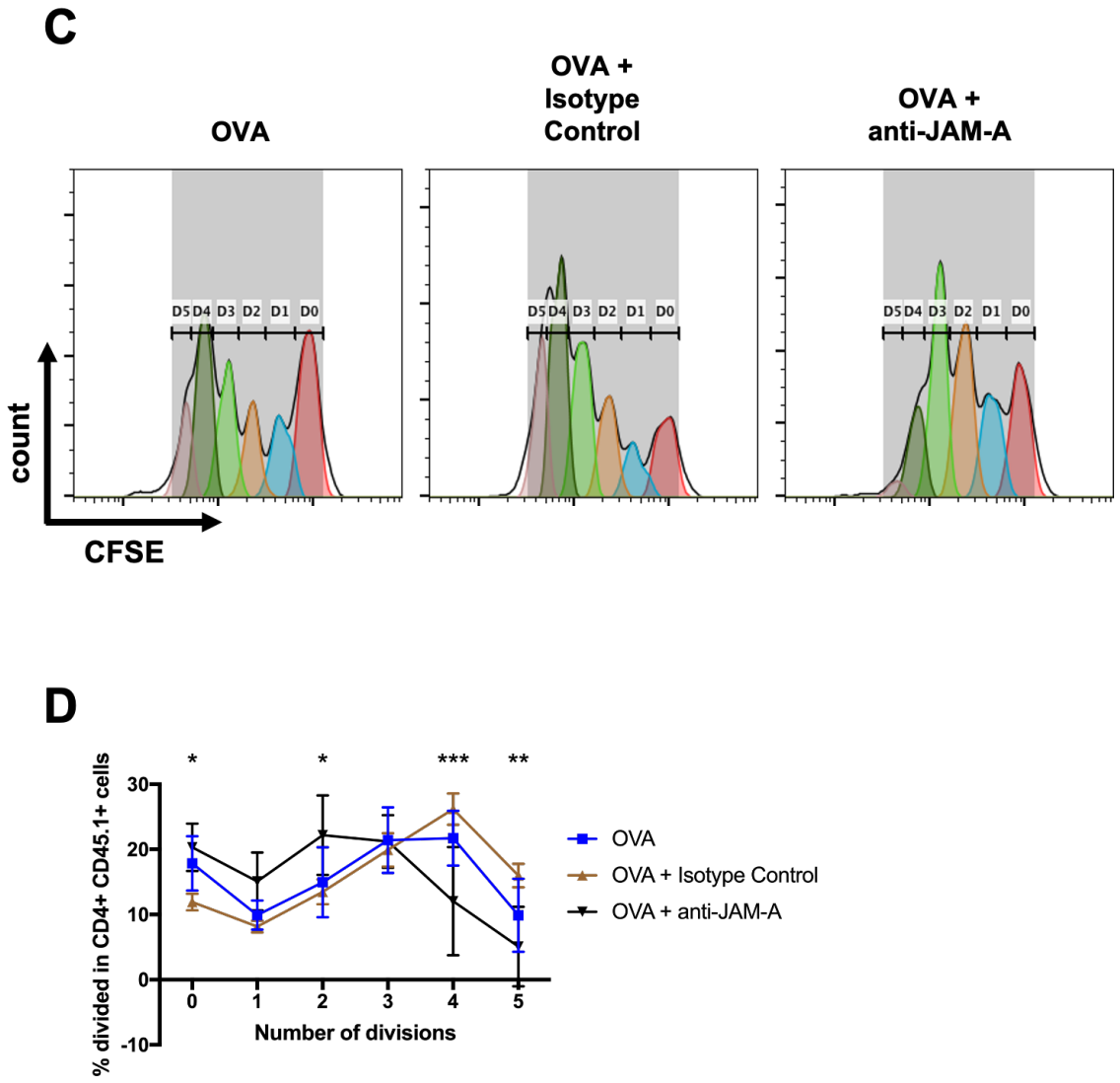

Figure 5-5. The impact of JAM-A blockade *in vivo* in CD4+ T cell proliferation
CFSE-labelled immune cells from lymph nodes (LN) and spleens of OTII mice were adoptively transferred to C57BL/6 mice that were challenged with footpad injections of LPS and OVA in the presence of anti-JAM-A mAb (BV11) or its isotype control. Popliteal lymph nodes (pLN) were harvested 72 hours later and analysed by flow cytometry for the expression of CFSE. **(A)** Representative histograms of CFSE fluorescence intensity on OTII CD4+ cells (CD4+ CD45.1+) with gating on divided cells and **(B)** quantification of OTII CD4+ T cells that have divided based on the gating of CFSE fluorescence intensity. **(C)** Representative histograms of CFSE fluorescence intensity on OTII CD4+ cells with identification of division peaks (D0 to D5). **(D)** Quantification of OTII CD4+ T cells that have divided based on its number of divisions. Results are expressed as mean ± SD of an experiment performed in biological replicates (n = 4). Statistical differences between the anti-JAM-A-treated and the isotype-treated groups were determined using a one-way or a two-way ANOVA. *p ≤ 0.05, **p ≤ 0.01, ****p ≤ 0.0001.

The administration of OVA promoted proliferation of OTII CD4+ T cells in all groups that received antigen, while only a small proportion of cells were CFSE- in the unstimulated group. JAM-A blockade decreased the overall proliferation of CD4+ T cells from pLNs of anti-JAM-A-treated mice in comparison with cells from isotype-treated animals, but not with cells from untreated mice. The detailed analysis of proliferation peaks by number of divisions showed that a higher

proportion of cells from anti-JAM-A-treated mice underwent 0 or 2 divisions in comparison with the isotype control group. Additionally, anti-JAM-A mAb treatment decreased the proportion of cells that divided 4 or 5 times when compared with cells from mice treated with the isotype control. However, no differences were found in comparison with anti-JAM-A-treated and untreated mice.

In addition to proliferation rates, the status of cell activation was also analysed in cells from the present study. For that, OTII cells were analysed for the expression of CD44 and CD62L. Phenotypes suggesting naïve ($CD44_{low}CD62L+$) and memory ($CD44_{high}CD62L-$) CD4+ T cells[378] were identified (Figure 5-6A) and their proportions (Figure 5-6B and D) and absolute numbers (Figure 5-6C and E) were compared across groups that were challenged with OVA. In addition, $CD44_{high}CD62L+$ cells, likely suggesting a recent recognition of cognate antigen by upregulation of CD44 but still maintaining normal levels of CD62L, were also analysed (Figure 5-6F and G).

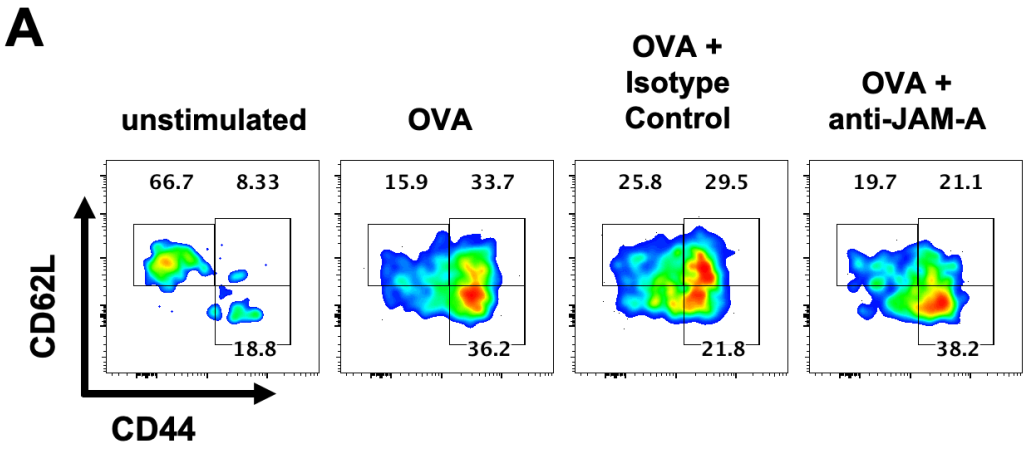
A
unstimulated
OVA
OVA + Isotype Control
OVA + anti-JAM-A
66.7
8.33
18.8
15.9
33.7
36.2
25.8
29.5
21.8
19.7
21.1
38.2
CD62L
CD44

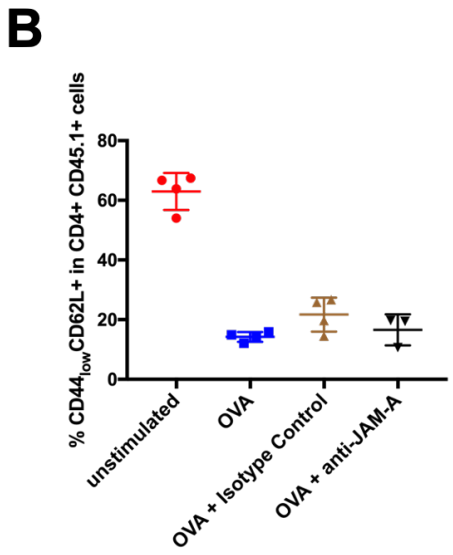
B
% CD44low CD62L+ in CD4+ CD45.1+ cells
80
60
40
20
0
unstimulated
OVA
OVA + Isotype Control
OVA + anti-JAM-A

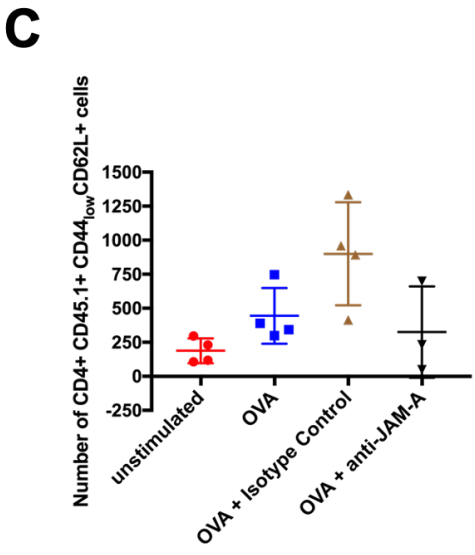
C
Number of CD4+ CD45.1+ CD44low CD62L+ cells
1500
1250
1000
750
500
250
0
-250
unstimulated
OVA
OVA + Isotype Control
OVA + anti-JAM-A

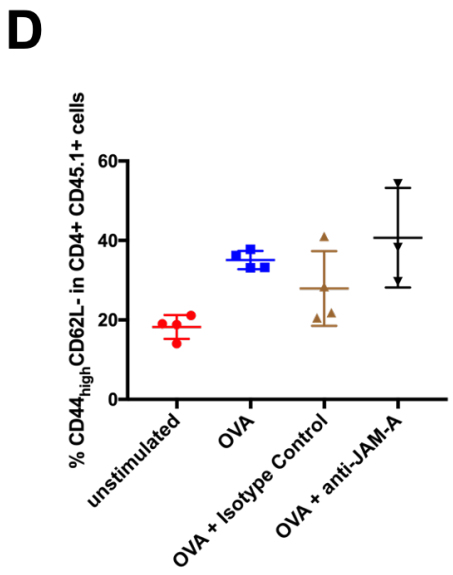
D
% CD44high CD62L- in CD4+ CD45.1+ cells
60
40
20
0
unstimulated
OVA
OVA + Isotype Control
OVA + anti-JAM-A

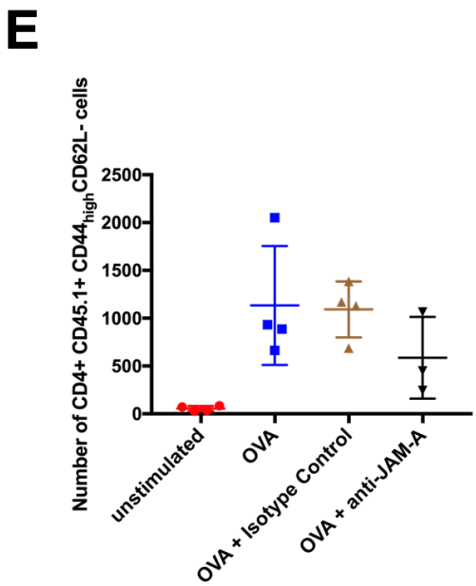
E
Number of CD4+ CD45.1+ CD44high CD62L- cells
2500
2000
1500
1000
500
0
unstimulated
OVA
OVA + Isotype Control
OVA + anti-JAM-A

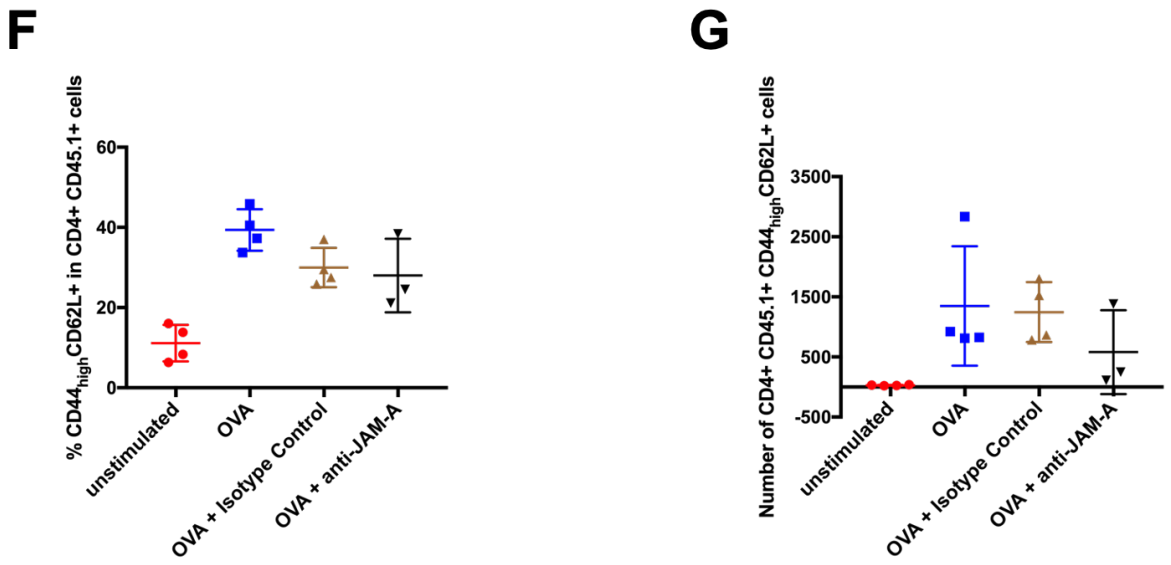

Figure 5-6. JAM-A blockade *in vivo* does not affect CD4+ T cell activation
CFSE-labelled immune cells from lymph nodes (LN) and spleens of OTII mice were adoptively transferred to C57BL/6 mice that were challenged with footpad injections of LPS and OVA in the presence of anti-JAM-A mAb (BV11) or its isotype control. Popliteal lymph nodes (pLN) were harvested 72 hours later and analysed by flow cytometry for the expression of CD44. **(A)** Representative histograms of CD44 and CD62L expression on OTII CD4+ cells (CD4+ CD45.1+). **(B)** Quantification of the proportion or **(C)** absolute number of OTII CD4+ T cells that are $CD44_{low}CD62L+$. **(D)** Quantification of the proportion or **(E)** absolute number of OTII CD4+ T cells that are $CD44_{high}CD62L-$. **(F)** Quantification of the proportion or **(G)** absolute number of OTII CD4+ T cells that are $CD44_{high}CD62L+$. Results are expressed as mean ± SD of an experiment performed in biological replicates (n = 4). Statistical differences between groups that received antigen were determined using a one-way or a two-way ANOVA. p = non-significant for all comparisons.

The administration of OVA induced activation of OTII CD4+ T cells, evidenced by the lower proportion of naïve and higher proportion of memory T cells compared to the unstimulated group. Anti-JAM-A mAb treatment did not affect the proportions nor the numbers of naïve, memory or $CD44_{high}CD62L+$ cells. As whole OVA was used for challenging mice and this, as well as other proteins, require antigen processing, a process that involves the degradation of proteins within the APCs cytoplasm[351] and that produces a range of different peptides that may react with endogenous T cells through specific antigen recognition or cross-reactivity[379,380], I also analysed the activation status of CD4+ CD45.1- cells (not shown). No differences were found in the activation status of endogenous CD4+ cells.

5.2.4 Anti-JAM-A mAb Treatment *in vivo* Does Not Affect CD4+ T Cell Differentiation

To analyse if JAM-A blockade *in vivo* can modify CD4+ T cell differentiation patterns, I analysed the expression of key transcription factors for T cell differentiation into Th17 (RORγt) (Figure 5-7A, B and C), Th1 (T-bet) (Figure 5-7D, E and F) and Treg cells (Figure 5-7G, H and I).

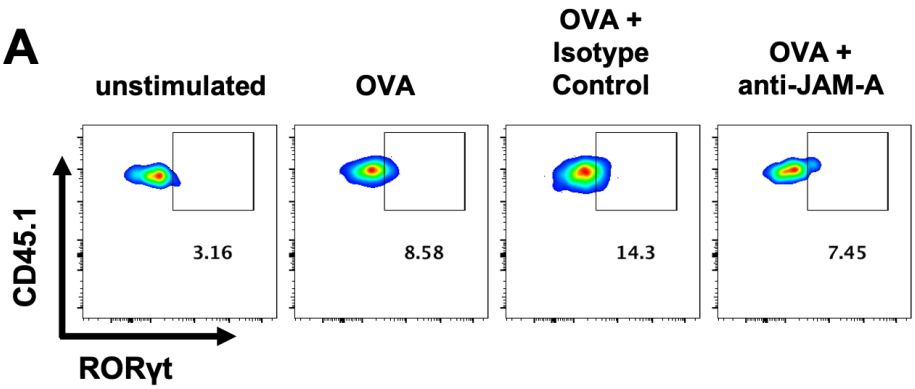
A
unstimulated
OVA
OVA + Isotype Control
OVA + anti-JAM-A
CD45.1
RORγt
3.16
8.58
14.3
7.45

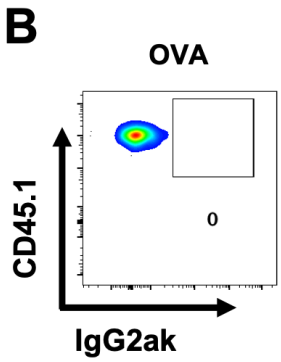
B
OVA
CD45.1
IgG2ak
0

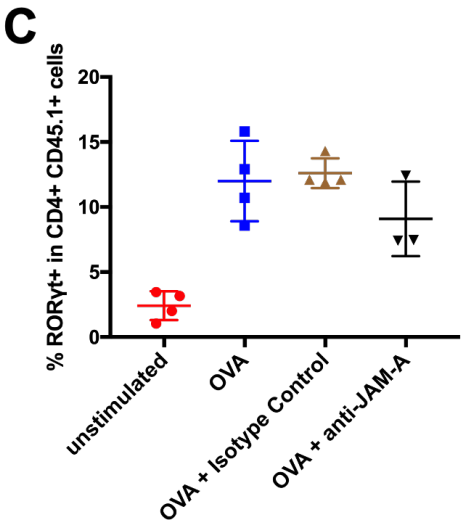
C
% RORγt+ in CD4+ CD45.1+ cells
20
15
10
5
0
unstimulated
OVA
OVA + Isotype Control
OVA + anti-JAM-A

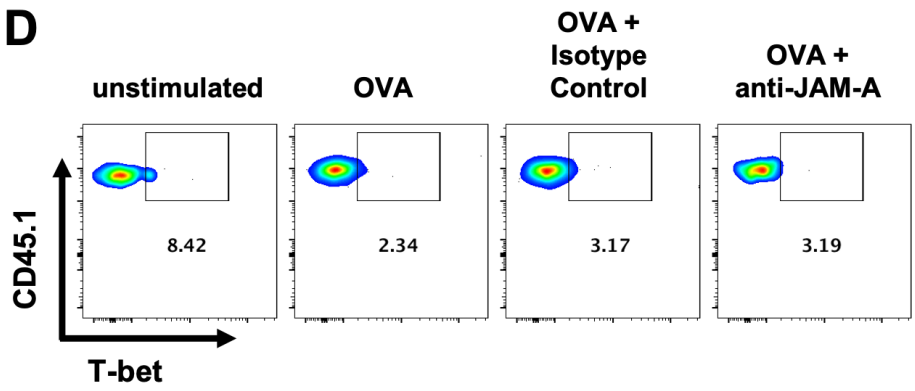
D
unstimulated
OVA
OVA + Isotype Control
OVA + anti-JAM-A
CD45.1
T-bet
8.42
2.34
3.17
3.19

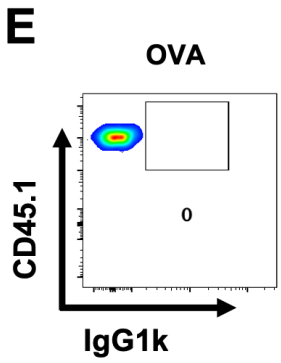
E
OVA
CD45.1
IgG1k
0

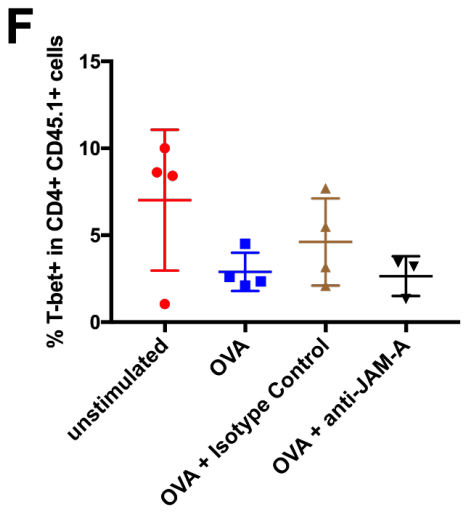
F
% T-bet+ in CD4+ CD45.1+ cells
15
10
5
0
unstimulated
OVA
OVA + Isotype Control
OVA + anti-JAM-A

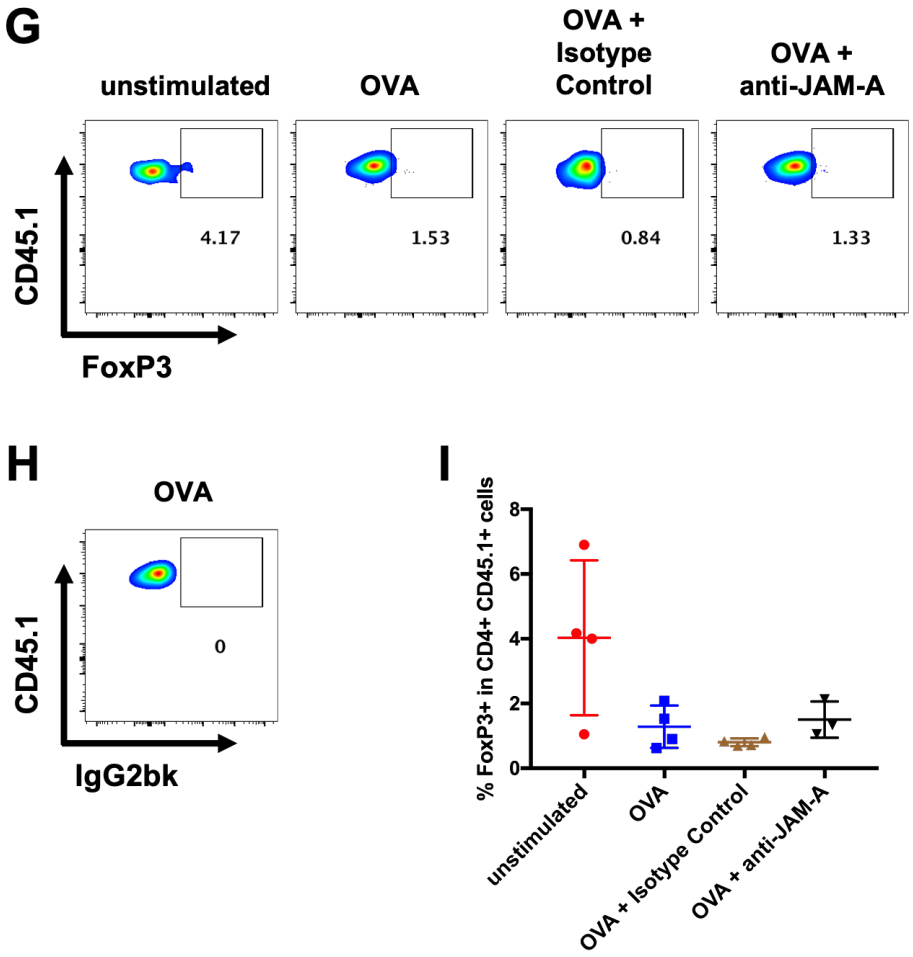

Figure 5-7. JAM-A blockade *in vivo* does not affect CD4+ T cell differentiation
CFSE-labelled immune cells from lymph nodes (LN) and spleens of OTII mice were adoptively transferred to C57BL/6 mice that were challenged with footpad injections of LPS and OVA in the presence of anti-JAM-A mAb (BV11) or its isotype control. Popliteal lymph nodes (pLN) were harvested 72 hours later and analysed by flow cytometry for the expression of different transcription factors. **(A)** Representative dot plots of RORγt expression on OTII CD4+ cells (CD4+ CD45.1+) or **(B)** its isotype control and **(C)** quantification of RORγt+ cells. **(D)** Representative dot plots of T-bet expression on OTII CD4+ cells or **(E)** its isotype control and **(F)** quantification of T-bet+ cells. **(G)** Representative dot plots of FoxP3 expression on OTII CD4+ cells or **(H)** its isotype control and **(I)** quantification of FoxP3+ cells. Gates show specific binding based on matched isotype control. Results are expressed as mean ± SD of an experiment performed in biological replicates (n = 4). Statistical differences between groups that received antigen were determined using a one-way ANOVA. p = non-significant for all comparisons.

The analysis shows that anti-JAM-A mAb treatment did not affect the proportion of OTII CD4+ T cells expressing any of the analysed transcription factors (RORγt, T-bet and FoxP3). The MFI of populations expressing the studied transcription factors was also analysed (not shown). No differences were found between the isotype-treated and the anti-JAM-A treated groups.

5.3 Discussion

In Chapter 4, I demonstrated that blockade of JAM-A pathways *in vitro* in the context of the presence of IgG (e.g. recruitment of Fc receptors) during antigen presentation disrupts cell cluster formation, attenuates T cell activation and proliferation and affects T cell differentiation and cytokine secretion. However, many factors can affect CD4+ T cell-DC interactions *in vivo*, such as interactions with other cell types and cell migration. In this chapter, I have analysed the effects of JAM-A blockade on T cell priming *in vivo*. JAM-A expression could be demonstrated in T cell and medullary areas of murine LNs. In addition, JAM-A was also detected in an area of the LN that suggests insertion of an afferent vessel. Afferent vessels might be used by the DCs to enter the LN following their migration from inflamed tissues[6]. Accordingly, treatment with an anti-JAM-A mAb *in vivo* may not only possibly affect the interactions between T cells and DCs but could also influence DC migration, by disrupting interactions between DCs and endothelial cells. To tease apart migration effects from T cell-DC interactions *in vivo*, I employed siRNA. This technique, aiming to induce downregulation of the *F11R* gene, could lead to decrease of JAM-A expression on the DCs surface. However, transfection of siRNA targeting the *F11R* gene only minimally impacted the expression of surface JAM-A on BMDCs. Technical modifications were performed in following siRNA experiments, such as attempts with different cell numbers that would influence cell confluency and could have an impact in the expression of JAM-A, however, no substantial knockdown effects were obtained. As shown in Chapter 4 (section 4.2.4), mature BMDCs express higher levels of JAM-A in comparison with immature cells. This difference was similar to that observed in the siRNA experiment between "siRNA *F11R"*-transfected BMDCs and the control group. Although I did not perform post-transfection experiments to determine mRNA levels, my findings suggest that the transfected cells maintained their JAM-A levels as when they were immature, possibly due to the lack of *F11R* mRNA for synthesis of new JAM-A molecules. Nevertheless, the effects of the JAM-A knockdown on BMDCs were considered insufficient for their use in *in vivo* experiments aiming to disrupt JAM-A pathways.

As an alternative approach to look at the effects of JAM-A blockade on CD4+ T cell priming *in vivo,* I decided to use the anti-JAM-A mAb BV11. OTII CD4+ T cells were

adoptively transferred to WT mice and OVA was given in their footpads accompanied by LPS as adjuvant to induce non-specific inflammation and stimulate DC migration[377]. Three days later, their pLNs were harvested for analysis of T cell activation and proliferation. After selecting a dose of antigen that achieved suboptimal T cell proliferation, I performed an experiment treating mice with anti-JAM-A mAb BV11 or its isotype control. Treatment with anti-JAM-A mAb decreased the total number of cells in the pLNs in comparison to treatment with its isotype control, as well as the number of CD4- adoptively transferred cells (CD45.1+). However, no differences in the proportion or number of OTII CD4+ cells were found. As only transferred cells were CFSE-labelled, it was not possible to analyse the proliferation of endogenous immune cells. These results, along with no differences in cell death being found, raise interesting points, such as whether JAM-A blockade affects leukocyte entry or exit in the LNs. These questions will motivate follow-up migration experiments using cell fate mapping tools such as Kaede mice[249].

The impact of JAM-A blockade on *in vivo* OTII CD4+ T cell proliferation, activation and differentiation was also analysed. Although a positive impact on cell proliferation could have been expected due to a report in the literature showing increased DC migration from an inflamed tissue to the draining LN[326], *in vivo* treatment with anti-JAM-A mAb attenuated the proliferation of CD4+ T cells when comparing to the isotype-treated group, as supported by my *in vitro* studies in Chapter 4. More specifically, OTII T cells from mice treated with anti-JAM-A underwent 4 or 5 divisions in lower proportions in comparison to the isotype-treated group. Although treatment with anti-JAM-A mAb decreased the number of adoptively transferred CD4- cells, the impact in CD4+ T cell proliferation was not reflected in the absolute number of OT-II CD4+ cells from pLNs. Cell accumulation, a parameter that was analysed by the proportion/number of OTII cells in the LNs is influenced by other parameters besides cell proliferation, such as cell death, apoptosis and migration. My analysis did not show differences in cell death; however, the available markers from the flow cytometry analysis did not allow an evaluation on cell apoptosis and migration. In addition, no differences in the proportions or numbers of naïve ($CD44_{low}CD62L+$), memory ($CD44_{high}CD62L-$) or recently primed ($CD44_{high}CD62L+$) T cells were found, suggesting that the treatment did not impact CD4+ T cell activation.

No effect on CD4+ T cell differentiation was found, evidenced by similar proportions of RORγt+, T-bet+ or FoxP3+ cells in the anti-JAM-A and isotype-treated groups. These findings differ from my *in vitro* experiment in Chapter 4 that showed impact of JAM-A blockade in CD4+ T cell differentiation. This difference can be explained by a few hypotheses. *In vivo* JAM-A blockade may have altered the motility and/or migration of DCs, as suggested by a report in the literature[326], and therefore indirectly induced changes in the quantity or quality of T cell-DC crosstalk during antigen presentation that could have affected T cell outcomes differently than in *in vitro* assays. In addition, BMDCs used *in vitro* express different surface markers than the heterogenous population that comprises endogenous DCs[47,54]. These, therefore, deliver distinct quantity or quality of signals that may affect CD4+ T cell differentiation differently. Lastly, danger signals induced by LPS stimulus on cells expressing TLR2 and/or TLR4, such as some endothelial cells that release IL-6 under LPS stimulation[381], may also affect CD4+ T cell differentiation differently. Further studies are needed to address these questions.

The results in this Chapter indicate that anti-JAM-A treatment *in vivo* in the context of the presence of IgG (e.g. recruitment of Fc receptors) may impact the interactions between CD4+ T cells and DCs, as differences in cell proliferation may result from changes in the quantity or quality of signals exchanged by these cell types during their interactions. However, no differences in T cell activation were found. As such, the changes observed in cell division rates might be a product of an impact in other immune components, such as in the profile of cytokines released by other immune cells that can influence cell expansion, including IL-2, a potent T cell growth factor[382], or an impact in cell apoptosis. In addition, it is important to note that there were no differences in T cell proliferation when comparing anti-JAM-A treated with untreated mice. Nevertheless, further studies will analyse the mechanisms in which JAM-A is involved in T cell priming *in vivo*.

Due to the ability of JAM-A manipulation to disrupt CD4+ T cell-DC interactions *in vitro*, as showed in Chapter 4, I analysed the impact of anti-JAM-A mAb treatment in a breach of self-tolerance model of arthritis, as shown in the next Chapter.

Chapter 6 JAM-A as a Therapeutic Target for Rheumatoid Arthritis

6.1 Introduction

The *F11R* gene, responsible for encoding the JAM-A molecule, was chosen from a list of upregulated genes on non-migratory joint immune cells in comparison with migratory immune cells in a murine RA model, as explained in Chapter 3 (section 3.1). This gene upregulation may reflect a higher expression of JAM-A protein on immune cells from these inflamed joints. I have demonstrated in Chapter 4 that JAM-A blockade *in vitro* attenuates CD4+ T cell activation and proliferation. In addition, JAM-A blockade in an adoptive transfer model decreased proliferation of adoptively transferred CD4+ T cells, as shown in Chapter 5. Several molecules involved in T cell-APC signalling have been studied as therapeutic target for inflammatory diseases and cancer, including RA, as extensively described in Chapter 1. As such, these findings suggest that JAM-A blockade in RA could affect T cell activation in the arthritic joint and/or leukocyte migration to the LNs, possibly impacting on the disease development and/or severity.

Several drugs are available for treatment of RA. These include analgesics, non-steroidal anti-inflammatory drugs (NSAID), disease-modifying antirheumatic drugs (DMARD), glucocorticoids and biological agents, such as abatacept, a blocker of the CD28-CD80/CD86 T cell co-stimulatory pathway[200,383,384]. However, no cure for RA is currently known, and many patients do not respond to conventional treatments[385]. As such, there is considerable unmet clinical need and increasing interest in the discovery of new pathways that can be targeted for treatment and management of this disease. In this chapter, I investigated JAM-A as a potential therapeutic target for RA. The data presented in the preceding chapters suggest that JAM-A can mediate the accumulation of immune cells in inflamed joints by allowing strong leukocyte adhesion to the inflamed endothelial cells, and may participate in the breach of self-tolerance found in RA through its expression by DCs (Figure 6-1). I therefore hypothesised that JAM-A blockade could affect the breach of tolerance by disrupting interactions between autoreactive T cells and DCs, and by possibly inducing migration of leukocytes out of inflamed joints,

decreasing their accumulation in the joints and ultimately leading to a faster resolution or attenuation of clinical disease. The breach of self-tolerance murine model of arthritis[170] was performed as described in Chapter 2 (Section 2.3.3) in Kaede mice for identification of JAM-A protein expression on immune cells from inflamed joints, as well as in WT mice for analysis of potential therapeutic effects following manipulation of JAM-A during the disease phase of induction.

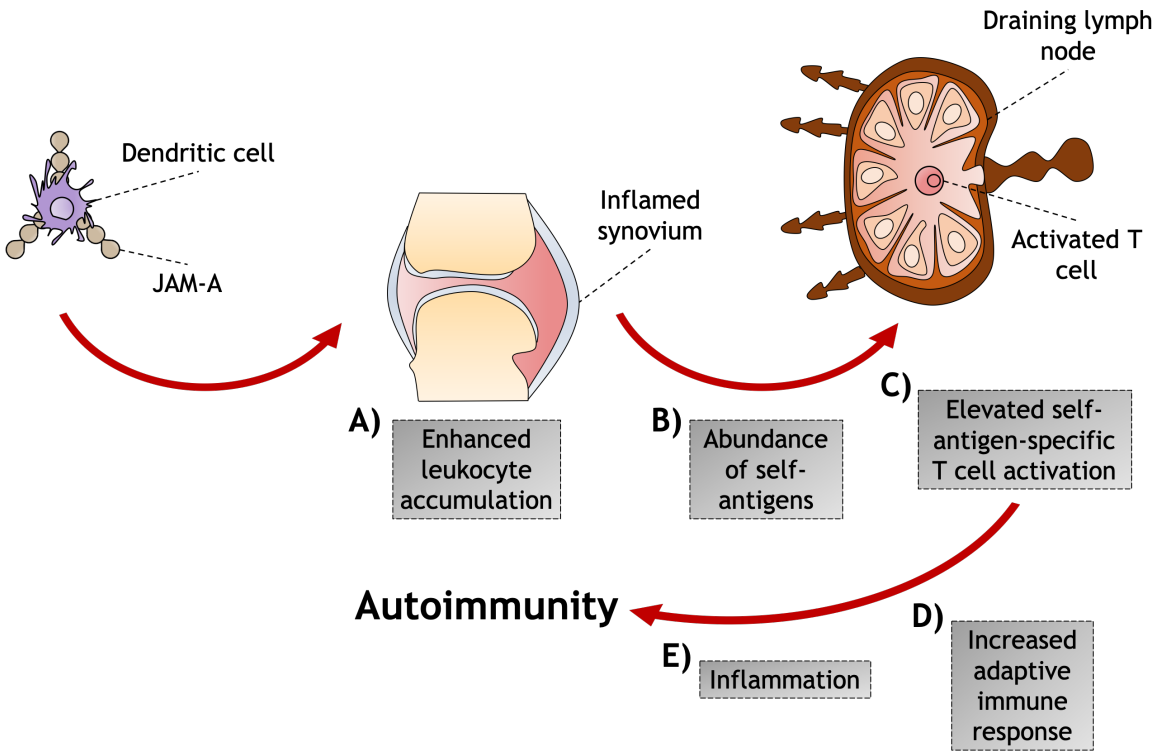

Figure 6-1. Proposed model for a functional role for JAM-A in the breach of self-tolerance in RA
Whilst JAM-A may contribute to disease through multiple cell types and signalling processes, mechanisms of DC trafficking mediated by JAM-A and their indirect effects in immune responses might play a key role in the breach of self-tolerance that occurs in the induction and/or development of RA. **(A)** JAM-A may assist the accumulation of immune cells in the inflamed synovium by enhancing leukocyte adhesion to the inflamed endothelia. **(B)** The accumulation of DCs increases the availability of self-antigen not only in the arthritic joint, where antigen presentation can occur, but also in the draining LN, by DCs carrying self-antigen captured in the affected tissue. **(C)** This abundance of self-antigens possibly leads to the activation of a higher proportion of self-antigen specific T cells. **(D)** The induction of adaptive immune responses against self-antigens leads to **(E)** inflammation and tissue destruction characteristic of autoimmune diseases.

6.2 Results

6.2.1 JAM-A is Upregulated on Non-Migratory Immune Cells from Inflamed Joints

As demonstrated in Chapter 3 (section 3.1), the *F11R* gene was found to be upregulated in non-migratory leukocytes from inflamed joints. To investigate if JAM-A protein is also upregulated on the surface of these cells, I performed the same experimental procedure that generated the gene data, as described in Chapter 2 (section 2.3.2). For this experiment, instead of using WT mice as host animals, Kaede mice expressing a photoconvertible green protein in all its cells were used[249]. Prior the harvest day, the hosts' feet were exposed to a laser for photoconversion of the green fluorescent protein (Kaede green) to red (Kaede red)[249]. Four days after the footpad challenge with HAO, joints and pLNs were harvested, digested and stained with fluorophore-conjugated antibodies. The expression of JAM-A was analysed by flow cytometry in two different panels one for myeloid cells (CD45, CD11b, CD11c, MHCII, Ly6G) and another for lymphoid cells (CD45, CD3, CD4, CD8 and CD19). Photoswitched cells (Kaede red cells, as described in section 2.3.2) were selected (Figure 6-2A) for the analysis and comparison of JAM-A expression on Kaede red cells from the joints, referred as non-migratory cells, with Kaede red cells from pLNs, referred as migratory cells (Figure 6-2B, C, D). Levels of surface JAM-A were analysed on cells expressing lineage markers (Figure 6-2E, F). JAM-A expression was also analysed in cells that were present in the joint since the photoswitch event (Kaede red) and that infiltrated in the inflamed tissue by the cull day (Kaede green) (Figure 6-2G, H).

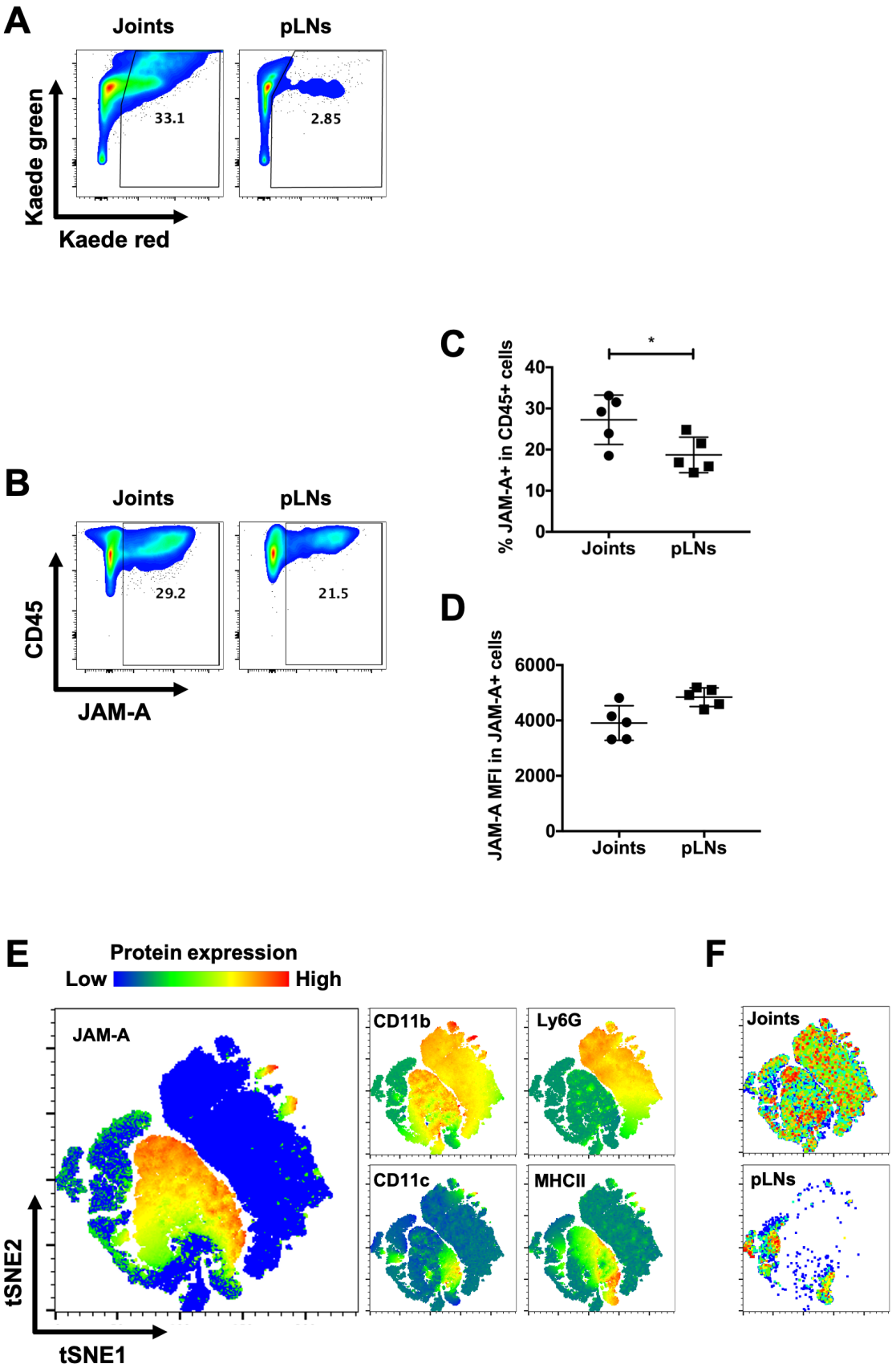
A
Joints
pLNs
33.1
2.85
Kaede green
Kaede red
B
Joints
pLNs
29.2
21.5
CD45
JAM-A
C
*
% JAM-A+ in CD45+ cells
40
30
20
10
0
Joints
pLNs
D
JAM-A MFI in JAM-A+ cells
6000
4000
2000
0
Joints
pLNs
E
Protein expression
Low
High
JAM-A
CD11b
Ly6G
CD11c
MHCII
tSNE2
tSNE1
F
Joints
pLNs

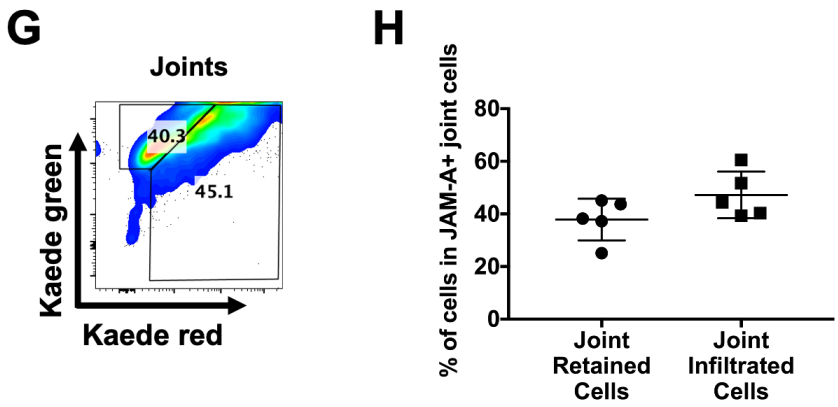

Figure 6-2. JAM-A expression on immune cells from inflamed joints and popliteal lymph nodes Immune cells from the joints and popliteal lymph nodes (pLN) of Kaede mice that were submitted to the breach of self-tolerance model of arthritis were analysed by flow cytometry for the expression of JAM-A. **(A)** Dot plots showing the identification of photoconverted (Kaede red) cells gated according to a non-photoswitched mouse (not shown). **(B)** Representative dot plots of JAM-A expression on CD45+ Kaede red cells, **(C)** quantification of the proportion JAM-A+ population and **(D)** quantification of JAM-A median fluorescence intensity (MFI) from the JAM-A+ population. **(E)** tSNE analysis of concatenated CD45+ Kaede red cells from joints and pLNs of all mice based on polychromatic flow cytometry data including JAM-A, CD11b, Ly6G, CD11c and MHCII expression profiles and **(F)** heatmap of the immune cells from joints or pLNs of a representative mouse. **(G)** Gating strategy of Kaede green or Kaede red events in cells from the joints and **(H)** quantification of JAM-A+ populations with comparison between Kaede green and Kaede red cells. Gates were made according to the fluorescence emitted by JAM-A isotype control (not shown). Results are expressed as mean ± SD of an experiment performed in biological replicates (n = 5). Statistical differences were determined using a paired Student's t test. *p ≤ 0.05.

The analysis of the JAM-A MFI showed that the amount of JAM-A expressed on the surface of leukocytes between migratory and non-migratory leukocytes was not significantly different. However, a higher proportion of non-migratory cells expressed JAM-A in comparison with migratory leukocytes. This data supports the RNAseq data mentioned in Chapter 3 (section 3.1), in which *F11R* expression was found to be increased in joint cells in comparison with cells that migrated to the LNs. The analysis of the tSNE plots indicated that the major part of the JAM-A-expressing population was composed by CD11b+ cells, partially also being MHCII and CD11c, but not Ly6G. It is possible to note that the majority of these CD11b+ cells are CD11c-, possibly reflecting macrophage populations. However, macrophage lineage markers, such as F4/80 would be necessary to classify these events in a more reliable way. It was also possible to notice that the major part of the population of JAM-A expressing Kaede red leukocytes that was present in the joints could not be seen in cells from the pLNs. The analysis of JAM-A expression on cells that were in the joint since the photoswitch event (Kaede red) in comparison to the ones that infiltrated in the joint by the cull day (Kaede green) showed no significative difference.

Following a more comprehensive analyses of JAM-A expression in specific cell types from the previous experiment, the expression of JAM-A in $CD11c_{high}$ MHCII+ cells (Figure 6-3A, B), classified as cDCs, and $CD11c_{low}$ CD11b- cells (Figure 6-3C, D), referred here as pDCs, was evaluated. In addition, I analysed the expression of JAM-A on pDCs from the migratory population and compared it with the expression on LN resident pDCs (Kaede green cells) (Figure 6-3E, F, G). For analysing CD4+ T cells, cells were gated as CD4+ CD19- and CD8-, as the CD3 staining was not satisfactory. I therefore analysed JAM-A expression on CD4+ cells (Figure 6-3H, I) and also on CD19+ cells (Figure 6-3J, K), a lineage marker for B lymphocytes, cells that can also work as APCs, as detailed in Chapter 1.

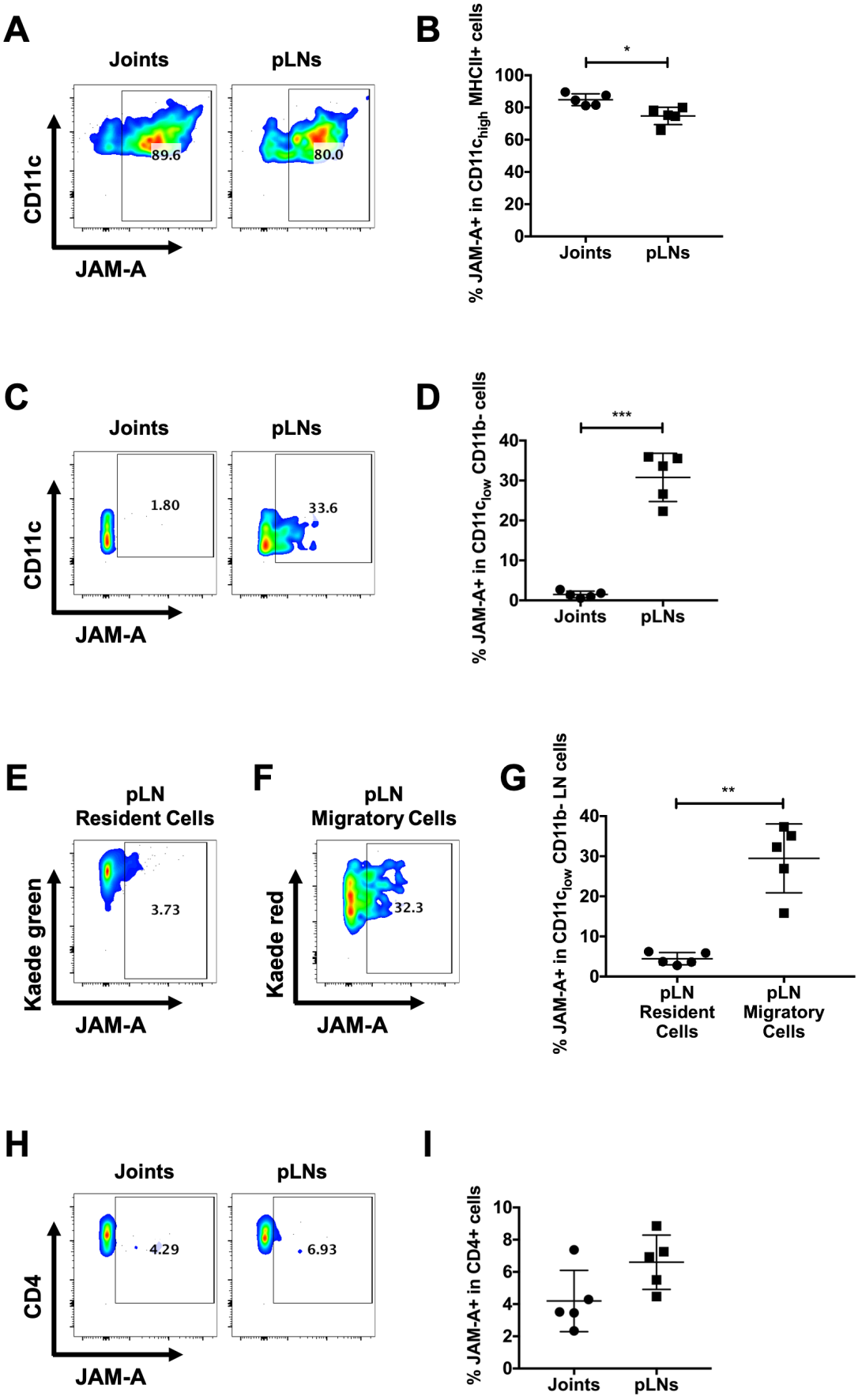
A
Joints
pLNs
89.6
80.0
CD11c
JAM-A
B
% JAM-A+ in CD11c$_{high}$ MHCII+ cells
*
100
80
60
40
20
0
Joints
pLNs
C
Joints
pLNs
1.80
33.6
CD11c
JAM-A
D
% JAM-A+ in CD11c$_{low}$ CD11b- cells
***
40
30
20
10
0
Joints
pLNs
E
pLN
Resident Cells
3.73
Kaede green
JAM-A
F
pLN
Migratory Cells
32.3
Kaede red
JAM-A
G
% JAM-A+ in CD11c$_{low}$ CD11b- LN cells
**
40
30
20
10
0
pLN
Resident
Cells
pLN
Migratory
Cells
H
Joints
pLNs
4.29
6.93
CD4
JAM-A
I
% JAM-A+ in CD4+ cells
10
8
6
4
2
0
Joints
pLNs

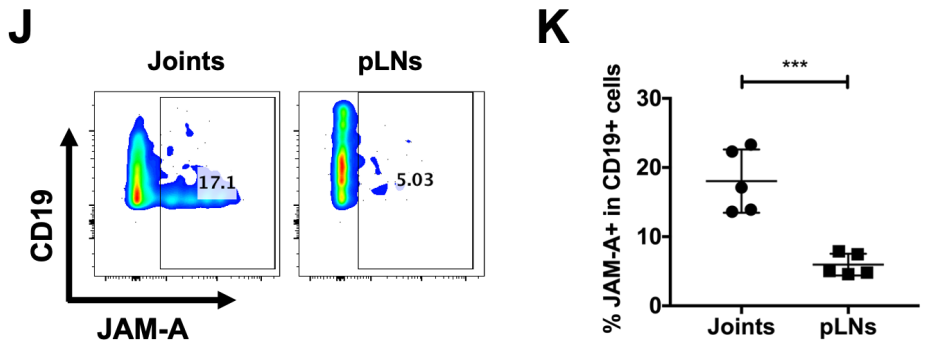

Figure 6-3. JAM-A expression on immune cell subsets from inflamed joints and popliteal lymph nodes

Immune cells from the joints and popliteal lymph nodes (pLN) of Kaede mice that were submitted to the breach of self-tolerance model of arthritis were analysed by flow cytometry for the expression of JAM-A. **(A)** Representative dot plots of JAM-A expression on $CD11c_{high}$ MHCII+ from CD45+ Kaede red cells and **(B)** quantification of JAM-A+ populations with comparison between cells found in joints and pLNs. **(C)** Representative dot plots of JAM-A expression on $CD11c_{low}$ CD11b- cells from CD45+ Kaede red cells and **(D)** quantification of JAM-A+ populations with comparison between cells found in joints and pLNs. **(E)** Representative dot plots of JAM-A expression on $CD11c_{low}$ CD11b- cells from Kaede green or **(F)** Kaede red cells and **(G)** comparison between the frequency of JAM-A+ cells on both populations. **(H)** Representative dot plots of JAM-A expression on CD4+ cells and **(I)** quantification of the JAM-A+ populations with comparison between cells found in joints and pLNs. **(J)** CD19+ cells from CD45+ Kaede red cells and **(K)** quantification of the JAM-A+ populations with comparison between cells found in joints and pLNs. Gates were made according to the fluorescence emitted by JAM-A isotype control (not shown). Results are expressed as mean ± SD of an experiment performed in biological replicates (n = 5). Statistical differences were determined using a paired Student's t test. ns = non-significant, *p ≤ 0.05, **p ≤ 0.01, ***p ≤ 0.001.

The analysis of JAM-A expression on specific DC subtypes showed that a higher proportion of non-migratory cDCs expressed JAM-A in comparison with migratory cDCs. On the other hand, the proportion of non-migratory pDCs expressing JAM-A was significantly lower than migratory pDCs. The expression of JAM-A was also analysed on LN resident pDCs. These cells expressed JAM-A in lower proportions when compared with LN migratory pDCs. It is important to note that all cells from both these populations expressed MHCII. In addition to the cell analysis, the proportion of CD4+ cells expressing JAM-A was not different when comparing migratory and non-migratory populations. However, a higher proportion of CD19+ cells from non-migratory populations expressed JAM-A in comparison with migratory cells.

6.2.2 Anti-JAM-A mAb Treatment Does Not Affect Arthritis in a Breach of Self-Tolerance Murine Model of Arthritis

The murine arthritis model was performed as described in Chapter 2 (section 2.3.2). To increase the chances of a successful induction of RA in this model, the quality of polarised cells was analysed before being adoptively transferred to WT host mice. The transferred cell population was around 85% CD4+. From this population, approximately 98% expressed the OTII transgenic TCR (Vα2+ Vß5+). 70% of these had a Th1 polarised phenotype, as assessed by T-bet expression; a rate that was considered satisfactory when taking into consideration results obtained in previous experiments performed in our laboratory (unpublished data). Clinical scores (Figure 6-4A) and paw thickness (Figure 6-4B) were measured for 7 days after the induction of joint inflammation as described in section 2.3.2.

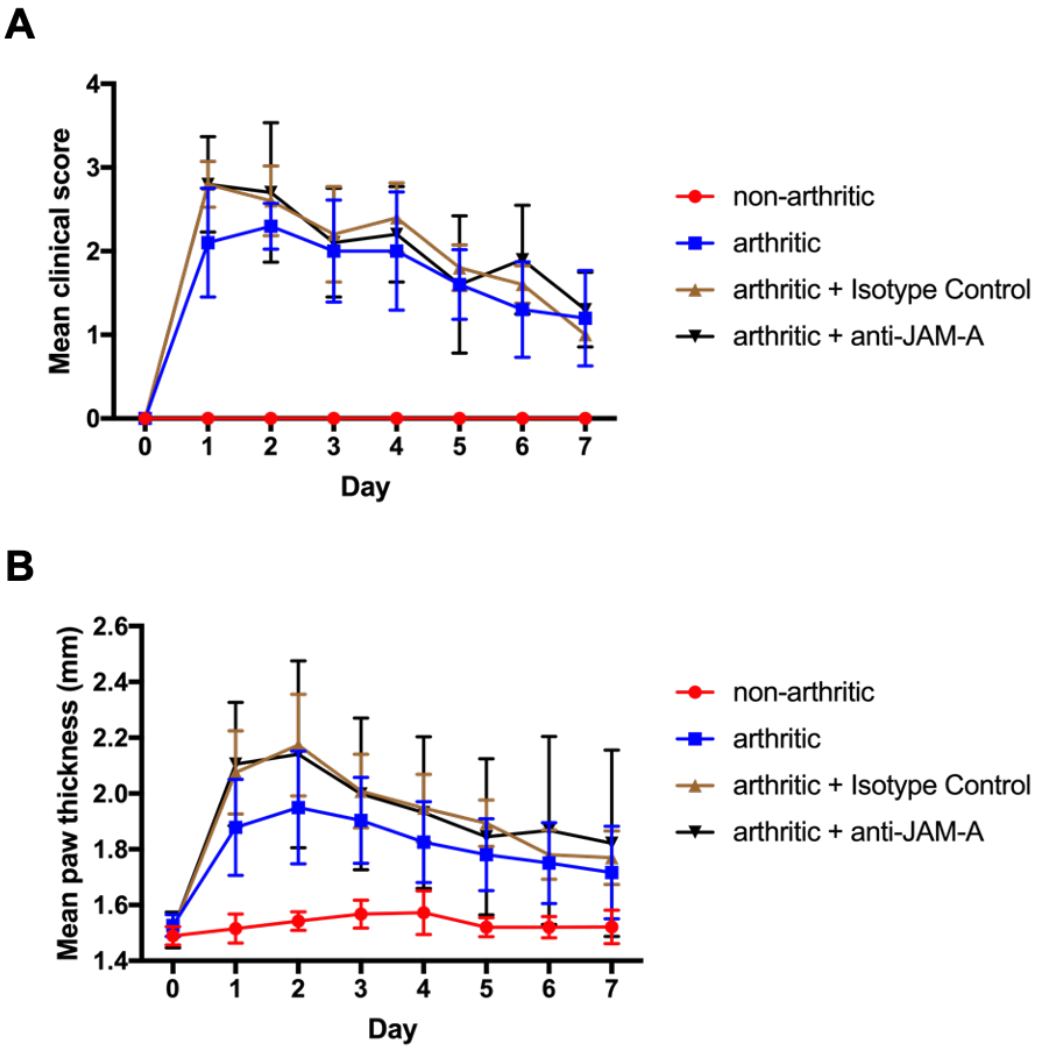

Figure 6-4. JAM-A blockade in a murine model of early arthritis does not affect clinical disease C57BL/6 mice were submitted to the breach of self-tolerance model of arthritis and treated with anti-JAM-A mAb (BV11) or its isotype control in days 0, 2, 4 and 6 after HAO injections and the clinical course of arthritis was monitored for 7 days after the footpad challenge. **(A)** Quantification of mean clinical scores. **(B)** Quantification of mean paw thickness. Results are expressed as mean ± SD of an experiment performed in biological replicates (n = 5). Statistical differences between the groups that were challenged with antigen were determined using a two-way ANOVA. p = non-significant for all comparisons.

A comparison between the negative (non-arthritic) and positive (arthritic) controls confirmed joint inflammation was induced after the HAO footpad injections[170]. Treatment with anti-JAM-A mAb did not affect mean clinical scores nor mean paw thickness in comparison to the isotype control. As no clinical effect was found in this early, acute model, we provided a second challenge, defined as a chronic model[386] (HAO footpad injections in Freund's incomplete adjuvant). This decision was based in a hypothesis that anti-JAM-A could have been affecting immune components that would be more pronounced in the context of a late model of RA,

such as the activation or proliferation of autoreactive T cells. As mice were not culled and their LNs were not available for the analysis of the activation and proliferation of CD4+ T cells, their blood was harvested for the analysis of PBMCs by flow cytometry. The activation status of peripheral blood CD4+ T cells was analysed by the expression of CD44 (Figure 6-5A) and compared between groups that received antigen (Figure 6-5B).

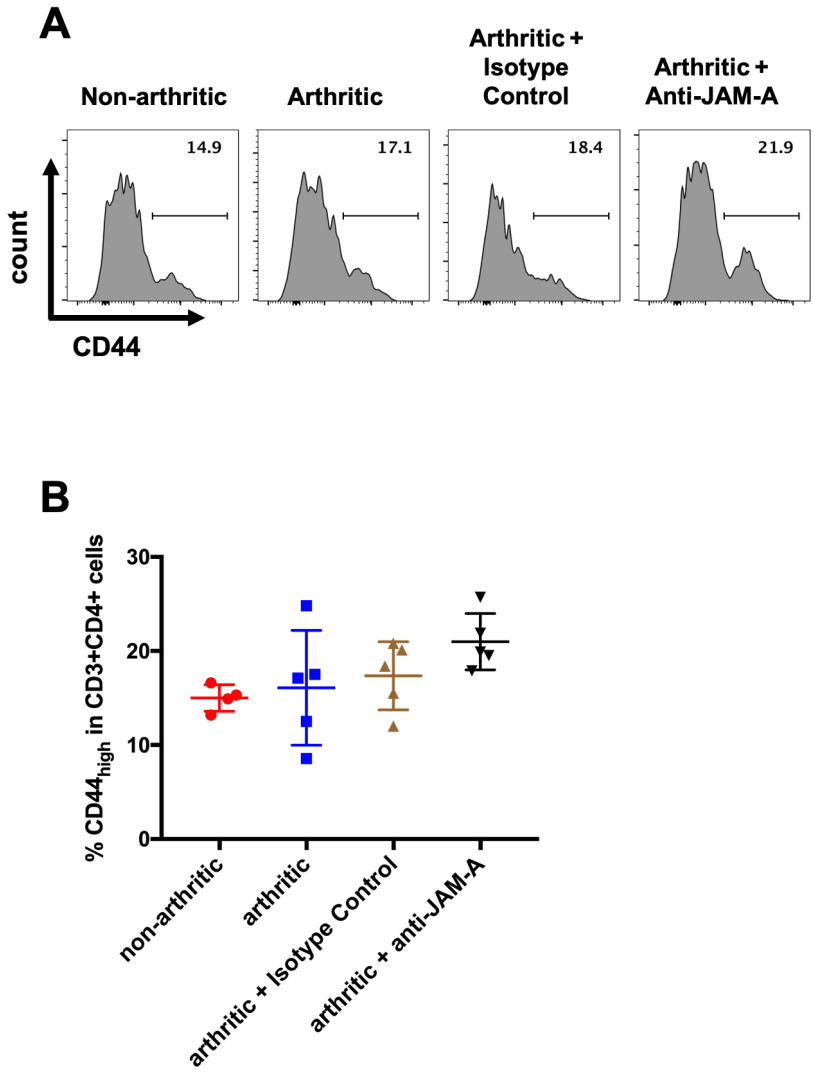

Figure 6-5. JAM-A blockade in a murine model of early arthritis does not affect the activation of peripheral blood CD4+ T cells
C57BL/6 mice were submitted to the breach of self-tolerance model of arthritis and treated with anti-JAM-A mAb (BV11) or its isotype control in days 0, 2, 4 and 6 after HAO injections and had their peripheral blood mononuclear cells (PBMC) analysed 7 days after the footpad challenge. **(A)** Representative histograms of CD44 expression on CD3+ CD4+ cells with gating on $CD44_{high}$ cells and **(B)** quantification of the proportion of CD4+ T cells that are $CD44_{high}$. Results are expressed as mean ± SD of an experiment performed in biological replicates (n = 5). Statistical differences between groups that were challenged with antigen were determined using a two-way ANOVA. p = non-significant for all comparisons.

The activation of peripheral blood CD4+ T cells was not affected by anti-JAM-A mAb treatment. Before analysing the ability of JAM-A blockade during the induction of RA to affect breach of self-tolerance, I analysed the concentration of anti-OVA antibodies in the serum. Anti-OVA secretion could indicate a potential interference of the treatment in T cell-dependent B cell responses. The concentration of serum anti-OVA IgG1 (Figure 6-6A) and IgG2c (Figure 6-6B) were analysed by ELISA, as described in Chapter 2 (section 2.5.2). Both isotypes were analysed, as IgG1 is commonly stimulated during Th2-type immune responses and IgG2a/IgG2c are associated with Th1-type responses[387]. This way, the bias of a possible shift in Th1/Th2 differentiation would be addressed.

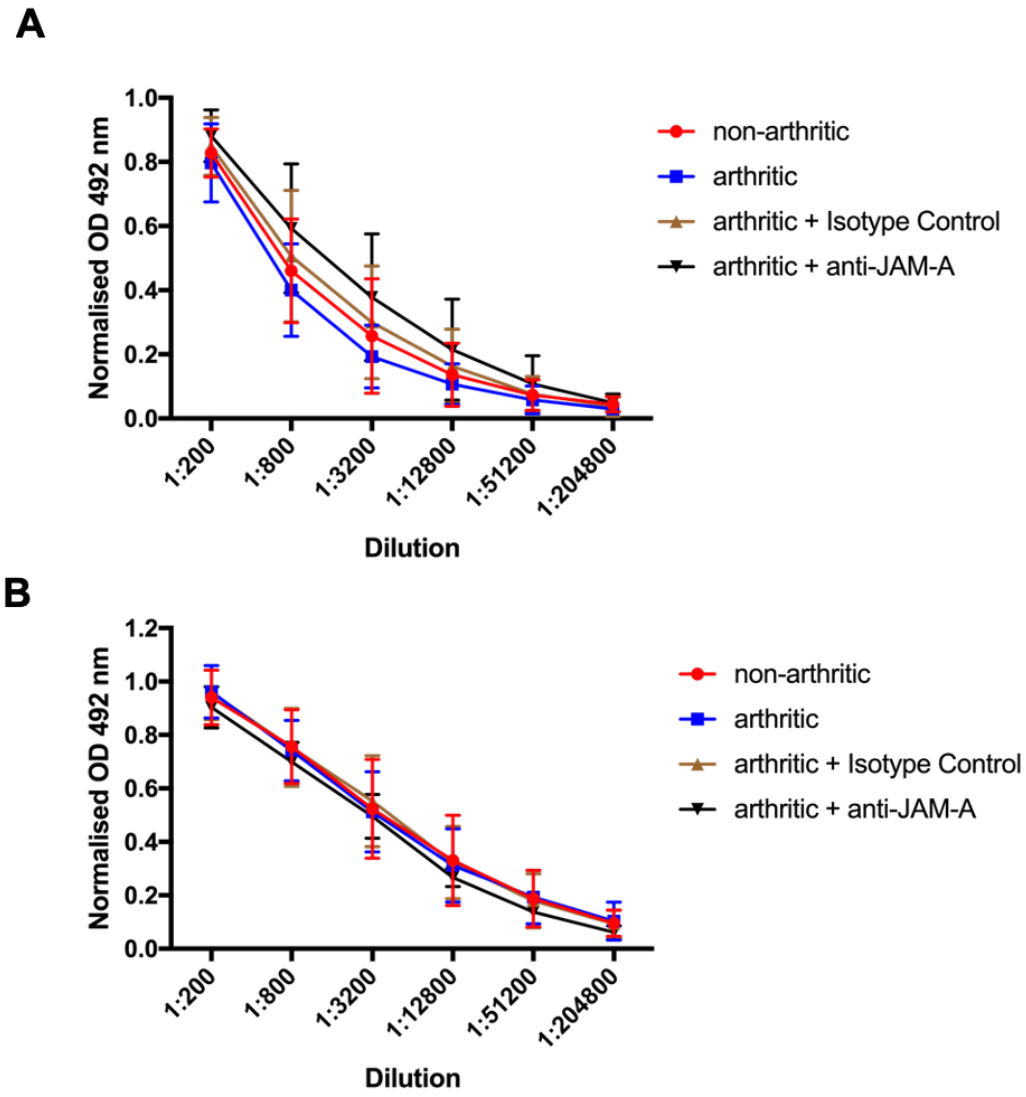

Figure 6-6. JAM-A blockade in a murine model of early arthritis does not affect the secretion of anti-OVA antibodies
C57BL/6 mice were submitted to the breach of self-tolerance model of arthritis and treated with anti-JAM-A mAb (BV11) or its isotype control in days 0, 2, 4 and 6 after HAO injections and their plasma were analysed for the presence of anti-OVA antibodies by ELISA 7 days after the footpad challenge. **(A)** Quantification of the normalised optical density (OD) of anti-OVA IgG1 or **(B)** IgG2c antibodies. Results are expressed as mean ± SD of an experiment performed in biological replicates (n = 5). Statistical differences were determined using a two-way ANOVA. p = non-significant for all comparisons.

No differences in the concentration of serum anti-OVA IgG1 or IgG2c were found between anti-JAM-A-treated and isotype-treated mice. These data support the hypothesis that JAM-A blockade does not affect T cell-dependent B cell activation. I, therefore, analysed anti-JAM-A's ability to influence breach of tolerance in this animal model. The concentration of serum anti-CII was analysed by ELISA (Figure 6-7), as described in Chapter 2 (section 2.5.2).

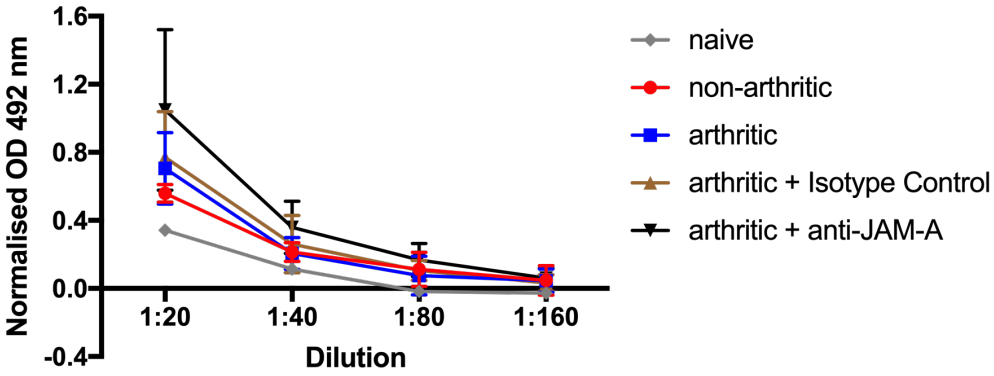

Figure 6-7. JAM-A blockade in a murine model of early arthritis does not affect the secretion of anti-collagen type II antibodies
C57BL/6 mice were submitted to the breach of self-tolerance model of arthritis and treated with anti-JAM-A mAb (BV11) or its isotype control in days 0, 2, 4 and 6 after HAO injections and their plasma were analysed for the presence of anti-collagen type II (CII) antibodies by ELISA 7 days after the footpad challenge. The graph shows the quantification of the normalised optical density (OD) of the anti-CII antibody detection. Results are expressed as mean ± SD of an experiment performed in biological replicates (n = 5). Statistical differences between the anti-JAM-A-treated and the isotype-treated groups were determined using a two-way ANOVA. p = non-significant.

The concentration of anti-CII antibodies was not affected by anti-JAM-A mAb treatment in comparison with the isotype control treatment, suggesting that JAM-A blockade did not affect breach of tolerance in this model of early RA.

6.3 Discussion

DCs and T cells play a definitive role in the pathogenesis of RA, as described in sections 1.8.3 and 6.1 and previously shown in animal studies by our research group[106,198,200,388-390], human genetic studies[391-393] and clinical trials[394-397]. In addition, the accumulation of leukocytes is a major contributor to joint swelling and pain in RA patients[398]. JAM-A has been studied as a therapeutic target in a number of preclinical models of diseases characterised by accumulation of leukocytes in affected tissues. In a model of skin inflammation, systemic treatment with an anti-JAM-A mAb BV11 was able to inhibit monocyte infiltration upon chemokine administration in subcutaneous air pouches[325]. However, in a model of ear skin antigen-induced inflammation, JAM-A$^{-/-}$ mice displayed enhanced contact hypersensitivity[326]. The increase in ear swelling was associated with a higher migration of JAM-A-deficient DCs to LNs, possibly leading to increased activation of antigen specific T cells. Anti-JAM-A mAb BV11 was also used intravenously in a model of meningitis, attenuating cytokine-induced

meningitis[353]. This therapeutic effect was attributed to an inhibition of monocyte and neutrophil accumulation in the cerebrospinal fluid and neutrophil infiltration into the brain parenchyma. In a model of ischaemia-reperfusion injury, JAM-A genetic depletion or blockade with anti-JAM-A mAb BV11, supressed leukocyte transmigration through a cremaster muscle endothelium [354]. In addition, in a serum-transfer arthritis model, treatment with anti-JAM-A mAb BV11 delayed the disease onset and partially ameliorated overall disease[224], possibly by inducing leukocyte migration out of the affected joints, consequently decreasing its accumulation in the inflamed tissue.

My findings that JAM-A has a role in the interactions between CD4+ T cells and DCs in addition to findings from the literature that JAM-A antagonism have promoted leukocyte migration out of inflamed tissues in several disease models, point to JAM-A as a potential therapeutic target for treatment of RA. *F11R* expression was upregulated in joint non-migratory leukocytes in a murine model of RA (unpublished data). To test the hypothesis that this upregulation in gene expression reflects a higher expression of JAM-A on the surface of immune cells, I performed the same experiment used for the detection of the *F11R* upregulation by using Kaede mice to allow tracking of immune cells from the joints to pLNs. Results from my experiment confirmed this hypothesis, showing a higher proportion of JAM-A+ cells from leukocytes that were arrested in the joints in comparison with immune cells that migrated to pLNs. In addition, no differences were found in the expression of JAM-A in cells that were in the joint in the moment of the photoswitch in comparison to cells that infiltrated after this event. These data suggest that JAM-A might hypothetically have a more pronounced role in retaining cells in the inflamed joint rather than in promoting leukocyte infiltration in the inflamed tissue. Evidence of JAM-A upregulation in hypoxic cells[399,400] suggest that the hypoxia present in the synovial tissue of RA patients[401–405] could potentially lead to an increased JAM-A protein expression on cells from the inflamed joints of these patients. Recently, a study described increased expression of F11R mRNA on PBMCs of RA patients[406]. However, this upregulation could have been driven by the systemic inflammation itself, as this study used healthy individuals as the control group.

The analysis of lineage markers showed that most of the JAM-A+ populations from both joints and pLNs were composed by CD11b+ cells, while part was composed by MHCII+ cells but not Ly6G+ cells. This supports the data from gene bank, that neutrophils from synovial fluid of arthritic mice expressed minimal levels of F11R mRNA (section 3.1). The analysis of JAM-A expression on cDCs showed that cells that were in the joint expressed surface JAM-A in higher proportions than cDCs that migrated to the pLNs. In addition, CD19+ cells, suggesting B cells, which can also act as APCs, mainly in the context of Tfh differentiation[100], also had their JAM-A expression analysed. A 3-fold increase was found on the proportion of CD19+ cells that were JAM-A+ in non-migratory populations in the joint, in comparison with migratory populations in the pLN. On the other hand, only a small proportion of CD4+ cells in both the joints and pLNs expressed JAM-A, in accordance with my *in vitro* findings reported in Chapter 4 that naïve and *in vitro* activated CD4+ T cells express low or undetectable levels of JAM-A. However, a T cell lineage marker (e. g. CD3) was not available in the flow cytometry analysis of this *in vivo* experiment. As such, these CD4+ cells could not only be CD4+ T cells but also other leukocytes that express CD4, such as monocytes and macrophages[32].

When analysing populations that were $CD11c_{low}$ CD11b- from the Kaede experiment, possibly suggesting populations of pDCs[307,407], I found a 20-fold increase on the percentage of JAM-A expression on cells that migrated to the pLNs compared to the ones that stayed in the joints. Plasmacytoid DCs from both LNs and spleens express low levels of JAM-A in physiological conditions, as shown in Chapter 4 (section 4.2.1). To verify the reliability of the identification of the JAM-A-expressing pDCs population, I compared the expression of JAM-A between pDCs that migrated to the LN to LN resident pDCs, which confirmed the low expression of JAM-A on LN pDCs that did not migrate from the joints. Our research group has previously reported pDCs as regulators of the breach of self-tolerance in the murine model of RA that was also used in this chapter. Selective pDC depletion *in vivo* was reported to increase lymphocyte autoimmune responses against anti-CII and enhanced the severity of the pathology[388]. While only a proportion of the pDC populations in my experiment expressed MHCII (17.68% ± 3.5 on joint non-migratory, 48.7% ± 2.7 on pLN resident cells and 62.5% ± 10.8 on pLN migratory cells), all JAM-A+ pDCs from migratory cells and from pLN resident cells were MHCII+, although JAM-A could not be reliably detected on joint pDCs.

The different results of manipulating JAM-A in disease models shown in the literature seems to be related to the mechanisms of induction of inflammation in each chosen pre-clinical model. While JAM-A blockade promoted a worsening of clinical disease in a T cell-mediated model of skin inflammation[326], JAM-A disruption ameliorated clinical disease in non-T cell-mediated models of inflammation, as mentioned in section 6.1. As such, JAM-A blockade in the murine model of RA used in this thesis could be expected to increase clinical scores by increasing the proportion of activated CD4+ T cells that play an important role in the induction of disease in this model. However, treatment with a JAM-A antagonist during the phase of induction could ameliorate disease by decreasing infiltration or retention of neutrophils that comprised the dominant leukocyte population found in the inflamed tissues and that also play a role in the induction of inflammation in arthritis. In addition, my studies in Chapters 4 and 5 showed that JAM-A blockade during priming could impact CD4+ T cell outcomes. Although a big part of the T cells in this disease model by the time when treatments were administered were already primed (Th1 polarised cells), the treatment could impact antigen presentation to autoreactive naïve CD4+ T cells. Additionally, in a model of RA in which mice receive serum from K/BxN mice, animals expressing transgenic TCR and MHCII and develop severe inflammatory arthritis[169], treatment with anti-JAM-A mAb delayed the disease onset and partially ameliorated overall disease[224].

To analyse the potential therapeutic effects of blockade of JAM-A pathways in RA, the breach of self-tolerance model of arthritis was performed in WT mice. Anti-JAM-A blockade did not affect clinical disease up to 7 days post-antigen footpad challenge. In addition, no differences were found in the activation status of peripheral blood CD4+ T cells. The analysis of T cells from pLNs would give a more precise idea of the effects of the treatment in the priming of autoreactive CD4+ T cells. However, a decision was made to extend the current experiment from an early to a late model of RA, as previously described by our research group[386]. Clinical disease will be again analysed after a second footpad challenge. Although my analysis of anti-CII antibodies suggests that the treatment did not have an impact on the breach of tolerance induced at this early stage, differences in the breach of self-tolerance may be more pronounced at later time-points. Presumably, the potential effects of anti-JAM-A treatment lies in disrupting

priming of naïve autoreactive T cells and the breach of tolerance could impact RA in later time points, as autoimmune components (e. g. anti-CII antibodies) are more pronounced following a second challenge[386] and may play a bigger role in the pathology than possible changes in leukocyte recruitment. Nevertheless, the later model that is still running at the present time, in addition to other future work, such as studies to evaluate the effects of JAM-A manipulation in leukocyte accumulation in the inflamed joint, will answer this and other questions that may point JAM-A as a therapeutic target for RA.

Chapter 7 General Discussion and Future Directions

The way a naïve CD4+ T cell encounters antigen presented by an APC for the first time dictates its fate as activated, apoptotic or anergic and influences other aspects of T cell biology (e. g. phenotype). In the centre of this crosstalk are surface molecules that support these intercellular interactions and provide stimulatory or inhibitory signals to the T cell. These molecules control not only T cell activation status but proliferation rate and differentiation into distinct T cell subsets. Additionally, disruption of pathways involving these molecules have been employed in several murine disease models and human diseases to achieve modulation of immune responses. As such, there is increasing interest in discovering new molecules that can control these cell-cell interactions. The overall aim in this thesis was to identify novel molecules that can control the interactions between T cells and DCs. This will further our understanding of disease processes and highlight new potential therapeutic targets for human disease.

7.1 Summary of Key Findings

The first aim of this study was to select candidate molecules that could be important in the interactions between T cells and DCs. To achieve this, I analysed transcriptomic data generated from previous experiments using a murine model of RA. I identified genes upregulated in immune cells that did not migrate from the joints to LNs, in comparison with migratory immune cells. I hypothesised that molecules encoded by these genes could be important for T cell-DC interactions that occur in the inflamed joint and influence T cell activation and/or differentiation[6]. From this list, the expression of genes related to leukocyte migration were analysed in a gene bank for the identification of the most promising candidates based on its expression in T cells and DCs: *CEACAM1*, *CX3CR1* and *F11R*. I started to test my second aim of evaluating if disruption of pathways involving molecules encoded by these genes could change CD4+ T cells outcomes by studying CEACAM1. CEACAM1 was found to be expressed on DCs and BMDCs and in low levels on CD4+ T cells. Treatment with anti-CEACAM1 mAb CC1 *in vitro* did

not affect the profile of T cell secreted cytokines, which contradicted the literature that showed increased IFN-γ under CEACAM1 blockade during priming[291]. As I couldn't replicate these results, I employed gene knockdown aiming downregulation of CEACAM1 surface expression on BMDCs for further use of these cells on functional assays. Small interfering RNA targeting *CEACAM1* gene was only able to minimally decrease CEACAM1 protein expression. I then moved to another candidate from out list: *F11R*.

JAM-A, a protein encoded by the *F11R* gene, was expressed on cDCs and BMDCs but only in small levels on CD4+ T cells. I showed that JAM-A was present in the site of interaction between DCs and CD4+ T cells. Treatment with anti-JAM-A mAb BV11 during priming *in vitro* affected cell cluster formation, attenuated CD4+ T cell activation and proliferation and impacted on CD4+ T cell differentiation and cytokine secretion. In support, this treatment was found to decrease CD4+ T cell proliferation *in vivo*, in comparison to cells from isotype-treated animals, addressing the second aim of the thesis to identify the potential of the chosen molecule to disrupt CD4+ T cell-DC interactions *in vivo*. The last aim of this thesis was to investigate the impact of disrupting JAM-A function on the progress of inflammation in a breach of self-tolerance murine model of arthritis. Analysis of JAM-A protein expression in this model showed that JAM-A was upregulated on the surface of non-migratory immune cells in comparison with those that migrated from the joints to the pLNs, supporting the findings from the transcriptomic data. I then tested the impact of JAM-A blockade on disease progression in this murine model of early arthritis. No changes were found in clinical disease, activation of peripheral blood CD4+ T cells or in levels of autoantibodies of mice treated with anti-JAM-A in comparison to isotype-treated animals. I then decided to extend the model to a late model of arthritis to allow possible late effects on autoimmunity to be seen. The analysis of the results from this late model will further our understanding on the effects of JAM-A blockade during the induction phase of RA.

7.2 Detection of Molecules with Potential for Controlling T cell-DC Interactions

The primary aim in Chapter 3 was to identify molecules with potential for controlling T cell-DC interactions. For that, I consulted unpublished data from experiments previously performed in our laboratory. Former members Drs Robert A. Benson and Catriona Prendergast have identified genes related to leukocyte migration that were upregulated in leukocytes arrested in inflamed joints after induction of a breach of self-tolerance murine model of arthritis, in comparison with migratory leukocytes. Presumably, these gene upregulation may reflect an upregulation on protein expression on the surface of DCs and/or CD4+ T cells and these upregulated molecules could be relevant for the crosstalk between these cells' types during antigen presentation. I hypothesized that blockade of some of these molecules during CD4+ T cell priming could modulate T cell outcomes, such as activation, proliferation, differentiation and profile of cytokine secretion. After analysing the expression profile of these genes in immune cells from a genetic database and in addition to the commercial availability of antagonistic or agonistic reagents, I identified 3 genes that encode molecules with potential to test my hypothesis: *CEACAM1*, the first chosen to be studied, *CX3CR1* and *F11R*.

I showed that CEACAM1 protein is expressed on DCs, BMDCs and in low levels on CD4+ T cells. I used anti-CEACAM1 mAb CC1, an antibody reported to be effective in functional assays, in *in vitro* to test its potential to modulate CD4+ T cell-DC interactions and therefore T cell outcomes. Treatment with this mAb during priming did not change T cell outcomes, this differs from a report in the literature where a different mAb was employed in a similar assay and modulated the profile of secreted cytokines[291]. CC1 mAb also did not have any effects in both *in vitro* and *in vivo* experiments performed by other members of our research group. Later, the CC1 mAb was found to not block CEACAM1-CEACAM1 ligation[317]. I then attempted collaboration with another research group who have reagents proven to be useful for functional assays, however, logistical problems prevented us from obtaining sufficient reagent, in a time for this thesis. In addition, I also attempted to downregulate CEACAM1 surface expression on BMDCs by siRNA gene knockdown for use of these cells in prospective assays however this was not found to be

satisfactory. Although it was not possible to study CEACAM1 role on CD4+ T cells priming, studies from the literature suggest that CEACAM1 ligation may play a role T cell activation, proliferation[260,294] and cytokine secretion[291]. However, its definition as stimulatory or inhibitory co-signalling molecule seems to be more complex as it may depend on the predominance of CEACAM1 isoforms expressed[261,279-283]. Therefore, more studies are required to investigate CEACAM1 role as a T cell co-signalling molecule and highlight its potential targeting for inflammatory diseases. For the purposes of the studies in this thesis, I moved to another candidate: *F11R*.

7.3 JAM-A Role on CD4+ T Cell Priming

The *F11R* gene was identified in a list of genes related to leukocyte migration as described in section 7.2. As the majority of the non-migratory leukocytes sent for sequencing were neutrophils, I reanalysed the expression profile of the candidate genes in a genetic database. *F11R* was the only candidate that was highly regulated in splenic and/or LN cDCs but not in neutrophils from the synovial fluid from the arthritic joints of mice. Before considering performing experiments to analyse if the gene expression correlated with surface protein expression, I have evaluated the functions of the protein encoded by this gene *in vitro* and *in vivo*.

The *F11R* gene encodes JAM-A, a protein that I showed to be expressed by cDCs and BMDCs and in lower levels by pDCs and CD4+ T cells. By utilising confocal microscopy, I demonstrated that JAM-A is physically present within the site of immunological synapse between CD4+ T cells and DCs. Treatment with anti-JAM-A mAb BV11 *in vitro* attenuated CD4+ T cell activation and proliferation in comparison with both isotype-treated and untreated cells. Based on literature reports, a positive impact on T cell activation/proliferation could have been expected under JAM-A blockade *in vivo*. JAM-A-deficient DCs showed increased migration from a skin inflamed site to draining LNs in comparison with DCs expressing normal levels of JAM-A[326]. In addition, higher transmigration of JAM-A-expressing BMDCs through layers of JAM-A-deficient lung endothelial cells in comparison with endothelial cells from JAM-A$^{-/-}$ mice reconstituted with full-length JAM-A complementary DNA (cDNA) was reported[347]. These studies indicate a complex participation of JAM-A in DC migration, dependent on the cell in which

it is expressed. While expression of JAM-A may participate in DC trafficking through the lymphatics, endothelial JAM-A may play an important role in DC arrest and migration functions through the vascular endothelium. As such, systemic blockade of JAM-A intercellular ligation could simultaneously impact different pathways that are responsible for distinct migration functions. Nevertheless, *in vivo* blockade of JAM-A pathways with anti-JAM-A mAb in my adoptive transfer model attenuated CD4+ T cell proliferation in comparison to isotype-treated animals, although no differences were found in the proportion of naïve, memory and recently primed CD4+ T cells. This finding in addition to my *in vitro* data suggest that JAM-A may play a role in the interactions between CD4+ T cells and DCs that lead to T cell proliferation. However, the disruption of JAM-A pathways may also influence other functions, such as DC migration, as schematised in Figure 7-1; or the secretion of IL-2 by other cells present in the system, an essential cytokine for T cell division[382].

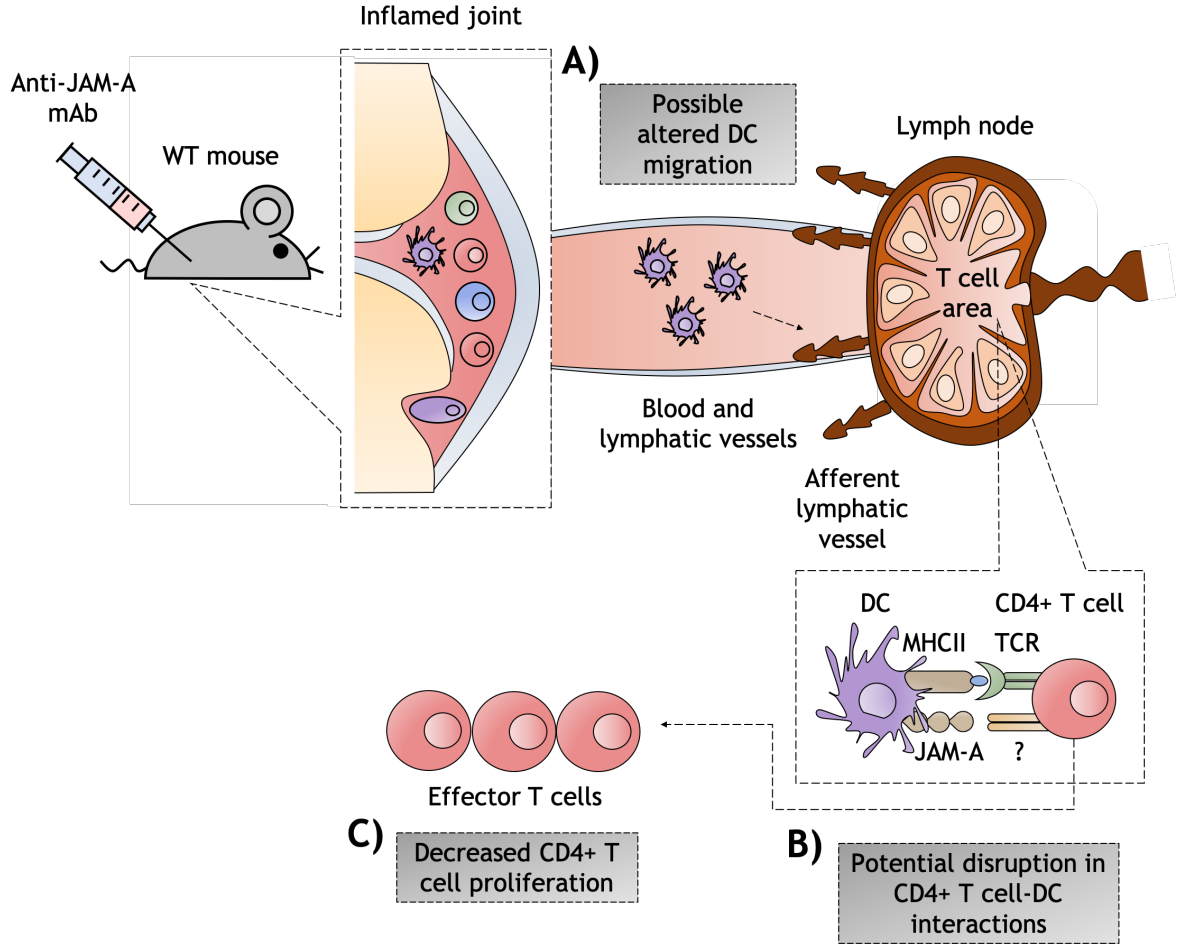

Figure 7-1. Proposed model for effects of JAM-A blockade in CD4+ T cell priming
Schematic representation of the potential effects of JAM-A blockade in CD4+ T cell priming. Treatment with anti-JAM-A mAb i*n vivo* may affect CD4+ T cell priming in distinct manners. **(A)** JAM-A blockade may affect the migration of DCs from the affected tissue to the draining LN. This potential altered kinetics may affect the time that these cells populate the LN and consequently the time or quality of their crosstalk with CD4+ T cells. **(B)** JAM-A may work as a co-signalling molecule or as an adhesion receptor that stabilise T cell-DC contacts. As such, JAM-A blockade may potentially disrupt these interactions, leading to changes in post-priming CD4+ T cell outcomes, such as **(C)** a decrease in clonal expansion of activated T cells.

Following the assessment of JAM-A blockade on T cell outcomes, I investigated the effects of anti-JAM-A mAb BV11 treatment during T cell priming on T cell differentiation and cytokine secretion. *In vitro*, JAM-A blockade did not affect IL10 and IFN-γ secretion 72 hours after initiation of priming, supporting results from the literature that found no differences in IFN-γ secretion in 5-day co-cultures in a similar CD4+ T cell-DC assay[347]. In the meantime, I demonstrated that JAM-A blockade *in vitro* increased the secretion of IL-17. A study from the literature demonstrated that cells from the colonic lamina propria of JAM-A KO mice stimulated *in vitro* with PMA/ionomycin had significantly higher absolute numbers of CD4+ IL17+ T cells in comparison with WT mice, with no differences

in IFN-γ-expressing CD4+ T cells numbers reported[371]. To investigate if disruption of JAM-A pathways during antigen presentation could lead to enhanced Th17 differentiation, I performed a T cell-DC *in vitro* assay and investigated intracellular expression of RORγt, the major Th17 transcription factor. JAM-A blockade during priming *in vitro* increased the proportion of RORγt+ T cells in comparison to isotype-treated cells. Additionally, JAM-A blockade decreased the proportion of T-bet+ T cells, as induction of differentiation into specific subsets can inhibit the differentiation to other subsets[76]. Under suboptimal concentrations of antigen, anti-JAM-A treatment during priming *in vitro* also increased the proportion of FoxP3-expressing T cells when compared to cells treated with its isotype control. Findings in the literature describe an increase in the absolute numbers of CD4+ FoxP3+ T cells from the colonic mucosa of JAM-A-deficient mice in comparison with WT mice[371]. Altogether, these data suggest that JAM-A ligation may influence pathways that can promote Th1 differentiation. As I showed that anti-JAM-A treatment during antigen stimulation *in vitro* produced normal levels of IFN-γ but decreased proportions of T-bet+ T cells, I evaluated the capacity of anti-JAM-A-treated cells to produce IFN-γ. Although no differences on the proportion of IFN-γ+ T cells on cells re-stimulated with PMA/ionomycin were found, the populations of IFN-γ producers had increased capacity to produce IFN-γ, supporting my previous findings of normal levels of IFN-γ secretion but lower proportions of T-bet+ T cells under JAM-A blockade during priming. *In vivo*, however, different components could impact T cell differentiation, such as a disruption in DC migration patterns that could indirectly influence the time or quality of cell-cell crosstalk and different inflammatory mediators that could be present under LPS stimulus, such as IL-6 that are secreted by some TLR4-expressing endothelial cells[381]. In addition, endogenous DCs comprise a heterogenous population with different profile of surface ligands/receptors that also differ from the ones found on BMDCs that were used in my *in vitro* assays[47,54]. As such, antigen presentation from endogenous DCs or BMDCs to CD4+ T cells involve different quality and/or quantity of signals. In this adoptive transfer model, no differences were found in the expression of key transcription factors of Th1, Th17 and Treg cells.

To understand the mechanisms where the adhesion molecule JAM-A could be involved in interactions between T cells and DCs, I first studied the ability of cells

treated with anti-JAM-A mAb BV11 to form clusters. Treatment with anti-JAM-A under suboptimal and optimal antigen concentrations disrupted DC-T cell cluster formation when cells were analysed 48 hours after priming. Anti-JAM-A treatment decreased the number of clusters in both conditions in comparison to isotype-treated cells. The analysis of clusters from suboptimal conditions showed that the treatment also decreased the total area occupied by them. Under optimal conditions, however, anti-JAM-A treatment did not affect the total area of clusters, which I attributed to an increase in the mean area of individual clusters. As clusters were analysed 48 hours after initiation of priming, these results don't reflect only cell interaction, but also take into account T cells proliferation, as these cells have already started to divide at this point. To analyse cell interaction only, I analysed clusters 24 hours after the initiation of antigen presentation. Analyses of T cell-DC colocalization with fluorescent dyed-cells utilising widefield microscopy showed that anti-JAM-A treatment did not affect interactions between these two cell types. However, even if cells are not touching each other, colocalization indexes based on widefield images might still count them as contacting cells. Follow-up experiments using confocal microscopy that would allow a more specific definition of membrane interaction will help our understanding on the mechanisms in which JAM-A blockade during priming affects CD4+ T cell outcomes.

7.4 JAM-A-Targeted Therapy in Rheumatoid Arthritis

The higher expression of *F11R* mRNA found in the experiment previously performed by our research group as described in Chapter 3 (section 3.1) suggests that JAM-A protein expression could be upregulated on non-migratory leukocytes arrested in inflamed joints in comparison with migratory immune cells. To test that, I performed the breach of self-tolerance model of arthritis in Kaede mice. By tracking the non-migratory and migratory Kaede red cells, I confirmed that JAM-A is upregulated on the surface of immune cells arrested in the joints. When analysing the expression of JAM-A in APCs from these two populations, I reported a higher proportion of JAM-A-expressing cells on non-migratory cDCs and B cells compared to migratory cells. However, a significantly higher proportion of migratory pDCs expressed JAM-A compared with non-migratory and pLN-resident pDCs. The population of JAM-A-expressing pDCs also expressed high levels of MHCII,

suggesting that JAM-A+ pDCs may play a role on carrying joint antigen and possibly presenting it to CD4+ T cells in the pLNs during RA.

To evaluate JAM-A-targeted therapy in RA, the breach of self-tolerance model of arthritis was performed in WT mice. While studies in antigen-independent models of inflammatory diseases suggest that JAM-A blockade may ameliorate clinical disease by a possible decrease in accumulation of leukocytes in inflamed tissues, studies using antigen-dependent models suggest that disruption of JAM-A pathways could promote a worsen in clinical disease, possibly by increasing activation of T cells. In spite of that, no effects were found in clinical disease up to 7 days after post-challenge in my RA model. This was evidenced by similar mean clinical scores and paw thickness in groups that received antigen footpad injections. In addition, no differences were found in the concentration of serum anti-OVA and anti-CII antibodies, suggesting that the treatment did not impact T cell-dependent B cell activation or humoral immune responses to CII. Furthermore, the treatment did not change the proportion of peripheral blood activated CD4+ T cells in comparison to cells from isotype-treated mice. Considering the costs of the blocking antibody, I did not perform experiments to investigate if the antibody was reaching the inflammation site, such as with the use of kit to conjugate it to a fluorophore and track it *in vivo*. As such, it was not possible to affirm that the antibody was blocking JAM-A pathways locally. Although no impact in the breach of self-tolerance was reported up to 7 days post-challenge, I hypothesised that JAM-A blockade during the phase of RA induction could have an impact in late stages. As such, I decided to postpone the experiment closure to allow an analysis of the effects of prophylactic JAM-A blockade in late time points. The future analysis of this late model of RA , as well as experiments aiming JAM-A manipulation during the phase of induction or after disease onset in other models of inflammatory diseases will further our knowledge of the participation of this molecule in the context of inflammation.

Antagonistic JAM-A targeting in preclinical models of inflammatory diseases show promising results for controlling inflammation caused by leukocyte or platelet accumulation. Disruption of JAM-A intercellular ligation may decrease the accumulation of leukocytes in these inflamed tissues and affect T cell outcomes that promote/enhance pathology. However, the possible disruption in multiple

pathways (endothelial cell-endothelial cell, leukocyte-endothelial cell, leukocyte-leukocyte) caused by JAM-A targeting suggests precaution in the interpretation of results from preclinical model studies. Disruption of JAM-A pathways may affect epithelial barrier integrity that may ultimately increase susceptibility to infections caused by facilitated infiltration of pathogens to affected tissues. In support, drugs targeting some T cell co-stimulation molecules such as LFA-1, a JAM-A ligand, resulted in its withdrawn from the market due to fatal brain infections [408]. As such, studies with cell-selective JAM-A disruption that aim to distinguish pathway-specific effects in different pathological conditions are essential for furthering our understanding of JAM-A role in inflammatory diseases. These studies may point to pathway-specific therapies with a high therapeutic potential but diminished adverse effects.

7.5 Final Conclusions

The data provided in this thesis has identified JAM-A as a novel molecule controlling CD4+ T cell-DC interactions. JAM-A provides support to CD4+ T cell activation, proliferation, differentiation and profile of secreted cytokines. JAM-A manipulation with an antagonistic mAb in an adoptive transfer model attenuated CD4+ T cell proliferation in comparison to cells from isotype-treated animals. These findings highlight the relevance of JAM-A in regulating immune responses in the context of inflammation. However, disruption of JAM-A pathways by prophylactic treatment with anti-JAM-A mAb did not affect arthritis in a breach of self-tolerance murine model of arthritis. Further work will investigate possible therapeutic effects of JAM-A manipulation in late models of RA, as well as in other inflammatory disease animal models, which may ultimately highlight JAM-A as a potential therapeutic target for human diseases.

References

1. Boehm, T. Design principles of adaptive immune systems. *Nat. Rev. Immunol.* **11**, 307–317 (2011).

2. Dranoff, G. Cytokines in cancer pathogenesis and cancer therapy. *Nat. Rev. Cancer* **4**, 11–22 (2004).

3. Jain, A. & Pasare, C. Innate control of adaptive immunity: beyond the three-signal paradigm. *J. Immunol.* **198**, 3791–3800 (2017).

4. Marshall, J. S., Warrington, R., Watson, W. & Kim, H. L. An introduction to immunology and immunopathology. *Allergy, Asthma Clin. Immunol.* **14**, 1–10 (2018).

5. Ademokun, A. A. & Dunn-Walters, D. Immune responses: primary and secondary. *eLS* (2010) doi:10.1002/9780470015902.a0000947.pub2.

6. Worbs, T., Hammerschmidt, S. I. & Förster, R. Dendritic cell migration in health and disease. *Nat. Rev. Immunol.* **17**, 30–48 (2017).

7. Hughes, C. E., Benson, R. A., Bedaj, M. & Maffia, P. Antigen-presenting cells and antigen presentation in tertiary lymphoid organs. *Front. Immunol.* **7**, (2016).

8. Wieczorek, M. *et al.* Major histocompatibility complex (MHC) class I and MHC class II proteins: conformational plasticity in antigen presentation. *Front. Immunol.* **8**, 1–16 (2017).

9. Kambayashi, T. & Laufer, T. M. Atypical MHC class II-expressing antigen-presenting cells: can anything replace a dendritic cell? *Nat. Rev. Immunol.* **14**, 719–730 (2014).

10. Benson, R. A. *et al.* Antigen presentation kinetics control T cell/dendritic cell interactions and follicular helper T cell generation in vivo. *Elife* **4**, 1–16 (2015).

11. Hogquist, K. A., Baldwin, T. A. & Jameson, S. C. Central tolerance: learning self-control in the thymus. *Nat. Rev. Immunol.* **5**, 772–782 (2005).

12. Klein, L., Kyewski, B., Allen, P. M. & Hogquist, K. A. Positive and negative selection of the T cell repertoire: what thymocytes see (and don't see). *Nat. Rev. Immunol.* **14**, 377–391 (2014).

13. Fink, P. J. & Hendricks, D. W. Post-thymic maturation: young T cells assert their individuality. *Nat. Rev. Immunol.* **11**, 544–549 (2011).

14. Taniuchi, I. CD4 helper and CD8 cytotoxic T cell differentiation. *Annu. Rev. Immunol.* **36**, 579–601 (2018).

15. Legut, M., Cole, D. K. & Sewell, A. K. The promise of γδT cells and the γδT cell receptor for cancer immunotherapy. *Cell. Mol. Immunol.* **12**, 656–658 (2015).

16. Kreslavsky, T., Gleimer, M., Garbe, A. I. & von Boehmer, H. αβ versus γδ fate choice: counting the T-cell lineages at the branch point. *Immunol. Rev.* **238**, 169–181 (2010).

17. Lefranc, M.-P. *et al.* IMGT, the international ImMunoGeneTics database. *Nucleic Acids Res.* **27**, 209–212 (1999).

18. Lefranc, M. P. Immunoglobulin and T cell receptor genes: IMGT® and the birth and rise of immunoinformatics. *Front. Immunol.* **5**, 1–22 (2014).

19. Mahe, E., Pugh, T. & Kamel-Reid, S. T cell clonality assessment: past, present and future. *J. Clin. Pathol.* **71**, 195–200 (2018).

20. Masopust, D. & Schenkel, J. M. The integration of T cell migration, differentiation and function. *Nat. Rev. Immunol.* **13**, 309–320 (2013).

21. Chien, Y., Zeng, X. & Prinz, I. The natural and the inducible: IL-17 producing gamma delta T cells. *Trends Immunol.* **34**, 151–154 (2013).

22. Omilusik, K. D. & Goldrath, A. W. The origins of memory T cells. *Nature* **552**, 337–339 (2017).

23. Zhao, E. *et al*. Bone marrow and the control of immunity. *Cell. Mol. Immunol*. **9**, 11–19 (2012).

24. Proverb, G. *B cell development, activation and effector functions. Primer to the Immune Response* (2014). doi:10.1016/b978-0-12-385245-8.00005-4.

25. Bergmann, B. *et al*. Memory B cells in mouse models. *Scand. J. Immunol*. **78**, 149–156 (2013).

26. Maity, P. C., Datta, M., Nicolò, A. & Jumaa, H. Isotype specific assembly of B cell antigen receptors and synergism with chemokine receptor CXCR4. *Front. Immunol*. **9**, 2988 (2018).

27. Liao, W. *et al*. Characterization of T-dependent and T-independent B cell responses to a virus-like particle. *J. Immunol*. **198**, 3846–3856 (2017).

28. Schroeder, H. W. J. & Cavacini, L. Structure and function of immunoglobulins. *J. Allergy Clin. Immunol*. **125**, S41–S52 (2010).

29. Chen, X. & Jensen, P. E. The role of B lymphocytes as antigen-presenting cells. *Arch. Immunol. Ther. Exp. (Warsz)*. **56**, 77–83 (2008).

30. Li, S., Wu, J., Zhu, S., Liu, Y. J. & Chen, J. Disease-associated plasmacytoid dendritic cells. *Front. Immunol*. **8**, 1–12 (2017).

31. Patente, T. A. *et al*. Human dendritic cells: their heterogeneity and clinical application potential in cancer immunotherapy. *Front. Immunol*. **10**, 1–18 (2019).

32. Eisenbarth, S. C. Dendritic cell subsets in T cell programming: location dictates function. *Nat. Rev. Immunol*. **19**, 89–103 (2019).

33. Sisirak, V. *et al*. CCR6/CCR10-mediated plasmacytoid dendritic cell

recruitment to inflamed epithelia after instruction in lymphoid tissues. *Blood* **118**, 5130–5140 (2011).

34. Yrlid, U. *et al*. Regulation of intestinal dendritic cell migration and activation by plasmacytoid dendritic cells, TNF-α and Type 1 IFNs after feeding a TLR7/8 ligand. *J. Immunol*. **176**, 5205–5212 (2006).

35. Uto, T. *et al*. Critical role of plasmacytoid dendritic cells in induction of oral tolerance. *J. Allergy Clin. Immunol*. **141**, 2156-2167.e9 (2018).

36. De Heer, H. J. *et al*. Essential role of lung plasmacytoid dendritic cells in preventing asthmatic reactions to harmless inhaled antigen. *J. Exp. Med.* **200**, 89–98 (2004).

37. Lutz, M. B., Strobl, H., Schuler, G. & Romani, N. GM-CSF monocyte-derived cells and langerhans cells as part of the dendritic cell family. *Front. Immunol*. **8**, 1–11 (2017).

38. Tamoutounour, S. *et al*. Origins and functional specialization of macrophages and of conventional and monocyte-derived dendritic cells in mouse skin. *Immunity* **39**, 925–938 (2013).

39. Wang, Y. *et al*. IL-34 is a tissue-restricted ligand of CSF1R required for the development of Langerhans cells and microglia. *Nat. Immunol*. **13**, 753–760 (2012).

40. Bittner-Eddy, P. D., Fischer, L. A., Kaplan, D. H., Thieu, K. & Costalonga, M. Mucosal Langerhans cells promote differentiation of Th17 cells in a murine model of periodontitis but are not required for porphyromonas gingivalis –driven alveolar bone destruction. *J. Immunol*. **197**, 1435–1446 (2016).

41. Igyártó, B. Z. *et al*. Skin-resident murine dendritic cell subsets promote distinct and opposing antigen-specific T helper cell responses. *Immunity* **35**, 260–272 (2011).

42. Lutz, M. B. *et al*. An advanced culture method for generating large quantities of highly pure dendritic cells from mouse bone marrow. *J. Immunol. Methods* **223**, 77–92 (1999).

43. Inba, K. *et al*. Generation of large numbers of dendritic cells from mouse bone marrow cultures supplemented with granulocyte/macrophage colony-stimulating factor. *J. Exp. Med.* **176**, 1693–1702 (1992).

44. Harry, R. A., Anderson, A. E., Isaacs, J. D. & Hilkens, C. M. U. Generation and characterisation of therapeutic tolerogenic dendritic cells for rheumatoid arthritis. *Ann. Rheum. Dis.* **69**, 2042–2050 (2010).

45. Funes, S. C. *et al*. Tolerogenic dendritic cell transfer ameliorates systemic lupus erythematosus in mice. *Immunology* **158**, 322–339 (2019).

46. Moreau, A. *et al*. Generation and in vivo evaluation of IL10-treated dendritic cells in a nonhuman primate model of AAV-based gene transfer. *Mol. Ther. - Methods Clin. Dev.* **1**, 14028 (2014).

47. Helft, J. *et al*. GM-CSF mouse bone marrow cultures comprise a heterogeneous population of CD11c+MHCII+ macrophages and dendritic dells. *Immunity* **42**, 1197–1211 (2015).

48. Tiberio, L. *et al*. Chemokine and chemotactic signals in dendritic cell migration. *Cell. Mol. Immunol.* **15**, (2018).

49. Banchereau, J. *et al*. Immunobiology of Dendritic Cells. *Annu. Rev. Immunol.* **18**, 767–811 (2000).

50. Winzler, C. *et al*. Maturation stages of mouse dendritic cells in growth factor-dependent long-term cultures. *J. Exp. Med.* **185**, 317–328 (1997).

51. Tomura, M. *et al*. Tracking and quantification of dendritic cell migration and antigen trafficking between the skin and lymph nodes. *Sci. Rep.* **4**, 1–11 (2014).

52. Hayes, A. J. *et al*. Spatiotemporal modeling of the key migratory events during the initiation of adaptive immunity. *Front. Immunol.* **10**, 1–12 (2019).

53. Eastman, A. J., Osterholzer, J. J., Olszewski, M. A., Arbor, A. & Arbor, A. Role of dendritic cell–pathogen interactions in the immune response to pulmonary cryptococcal infection. *Future Microbiol.* **10**, 1837–1857 (2015).

54. Liu, Z. & Roche, P. A. Macropinocytosis in phagocytes: Regulation of MHC class-II-restricted antigen presentation in dendritic cells. *Front. Physiol.* **6**, 1–6 (2015).

55. Dixon, J. F. P., Law, J. L. & Favero, J. J. Activation of human T lymphocytes by crosslinking of anti-CD3 monoclonal antibodies. *J. Leukoc. Biol.* **46**, 214–220 (1989).

56. Al-Aghbar, M. A., Chu, Y. S., Chen, B. M. & Roffler, S. R. High-affinity ligands can trigger T cell receptor signaling without CD45 segregation. *Front. Immunol.* **9**, (2018).

57. Charles A. Janeway, J. The T cell receptor as a multicomponent signalling machine: CD4/CD8 coreceptors and CD45 in T cell activation. *Annu. Rev. Immunol.* **10**, 645–674 (1992).

58. Glatzová, D. & Cebecauer, M. Dual role of CD4 in peripheral T lymphocytes. *Front. Immunol.* **10**, (2019).

59. Abbas, A. K., Lohr, J., Knoechel, B. & Nagabhushanam, V. T cell tolerance and autoimmunity. *Autoimmun. Rev.* **3**, 471–475 (2004).

60. Wei, J., Raynor, J., Nguyen, T. L. M. & Chi, H. Nutrient and metabolic sensing in T cell responses. *Front. Immunol.* **8**, 1–14 (2017).

61. Schoonhoven, A. van, Huylebroeck, D., Hendriks, R. W. & Stadhouders, R. 3D genome organization during lymphocyte development and activation. *Brief. Funct. Genomics* **00**, 1–12 (2019).

62. Shiow, L. R. *et al*. CD69 acts downstream of interferon-α/β to inhibit S1P 1 and lymphocyte egress from lymphoid organs. *Nature* **440**, 540–544 (2006).

63. DeGrendele, H. C., Estess, P. & Siegelman, M. H. Requirement for CD44 in activated T cell extravasation into an inflammatory site. *Science (80-.).* **278**, 672–675 (1997).

64. Obst, R. The timing of T cell priming and cycling. *Front. Immunol.* **6**, 1–10 (2015).

65. Au-Yeung, B. B. *et al*. A sharp T-cell antigen receptor signaling threshold for T-cell proliferation. *Proc. Natl. Acad. Sci. U. S. A.* **111**, (2014).

66. Athie-Morales, V., Smits, H. H., Cantrell, D. A. & Hilkens, C. M. U. Sustained IL-12 signaling is required for Th1 development. *J. Immunol.* **172**, 61–69 (2004).

67. Zwirner, N. W. & Ziblat, A. Regulation of NK cell activation and effector functions by the IL-12 family of cytokines: the case of IL-27. *Front. Immunol.* **8**, (2017).

68. Girart, M. V., Fuertes, M. B., Domaica, C. I., Rossi, L. E. & Zwirner, N. W. Engagement of TLR3, TLR7, and NKG2D regulate IFN-γ secretion but not NKG2D-mediated cytotoxicity by human NK cells stimulated with suboptimal doses of IL-12. *J. Immunol.* **179**, 3472–3479 (2007).

69. Kallies, A. & Good-Jacobson, K. L. Transcription factor T-bet orchestrates lineage development and function in the immune system. *Trends Immunol.* **38**, 287–297 (2017).

70. Kak, G., Raza, M. & Tiwari, B. K. Interferon-gamma (IFN-γ): exploring its implications in infectious diseases. *Biomol. Concepts* **9**, 64–79 (2018).

71. Miller, C. H. T., Maher, S. G. & Young, H. A. Clinical use of Interferon-γ. *Ann. N. Y. Acad. Sci.* **1182**, 69–79 (2009).

72. Siebert, S., Tsoukas, A., Robertson, J. & McInnes, I. Cytokines as therapeutic targets in rheumatoid arthritis and other inflammatory diseases. *Pharmacol. Rev.* **67**, 280–309 (2015).

73. Swain, S. L., McKinstry, K. K. & Strutt, T. M. Expanding roles for CD4 + T cells in immunity to viruses. *Nat. Rev. Immunol.* **12**, 136–148 (2012).

74. Tripathi, S. K. & Lahesmaa, R. Transcriptional and epigenetic regulation of T-helper lineage specification. *Immunol. Rev.* **261**, 62–83 (2014).

75. Kanhere, A. *et al.* T-bet and GATA3 orchestrate Th1 and Th2 differentiation through lineage-specific targeting of distal regulatory elements. *Nat. Commun.* **3**, (2012).

76. Lazarevic, V. *et al.* Transcription factor T-bet represses Th17 differentiation by preventing Runx1-mediated activation of the RORγt gene. *Nat. Immunol.* **12**, 96–104 (2011).

77. Zhu, J., Yamane, H., Cote-Sierra, J., Guo, L. & Paul, W. E. GATA-3 promotes Th2 responses through three different mechanisms: Induction of Th2 cytokine production, selective growth of Th2 cells and inhibition of Th1 cell-specific factors. *Cell Res.* **16**, 3–10 (2006).

78. Kopf, M. *et al.* Disruption of the murine IL-4 gene blocks Th2 cytokine responses. *Nature* **362**, 245–248 (1993).

79. Cote-Sierra, J. *et al.* Interleukin 2 plays a central role in Th2 differentiation. *Proc. Natl. Acad. Sci. U. S. A.* **101**, 3880–3885 (2004).

80. Diehl, S. *et al.* Inhibition of Th1 differentiation by IL-6 is mediated by SOCS1. *Immunity* **13**, 805–815 (2000).

81. Couper, K. N., Blount, D. G. & Riley, E. M. IL-10: the master regulator of immunity to infection. *J. Immunol.* **180**, 5771–5777 (2008).

82. Liu, Y., Shao, Z., Shangguan, G., Bie, Q. & Zhang, B. Biological properties

and the role of IL-25 in disease pathogenesis. *J. Immunol. Res.* **2018**, (2018).

83. Moreno, C., Prieto, P., Macías, Á., Cruz, A. De & Través, P. G. IgE enhances Fcε receptor I expression and IgE-dependent release of histamine and lipid mediators from human umbilical cord blood-derived mast cells: synergistic effect of IL-4 and IgE on human mast cell Fcε eeceptor I expression and mediator release. *J. Immunol.* **162**, 5455–5465 (1999).

84. Kaplan, M. H. Th9 cells: differentiation and disease Mark. *Immunol. Rev.* **252**, 104–115 (2013).

85. Tamiya, T. *et al.* Smad2/3 and IRF4 play a cooperative role in IL-9–producing T cell induction. *J. Immunol.* **191**, 2360–2371 (2013).

86. Malik, S. *et al.* Transcription factor Foxo1 is essential for IL-9 induction in T helper cells. *Nat. Commun.* **8**, 1–13 (2017).

87. Cheng, G. *et al.* Anti-interleukin-9 antibody treatment inhibits airway inflammation and hyperreactivity in mouse asthma model. *Am. J. Respir. Crit. Care Med.* **166**, 409–416 (2002).

88. Soussi-Gounni, A., Kontolemos, M. & Hamid, Q. Role of IL-9 in the pathophysiology of allergic diseases. *J. Allergy Clin. Immunol.* **107**, 575–582 (2001).

89. Chowdhury, K. *et al.* Synovial IL-9 facilitates neutrophil survival, function and differentiation of Th17 cells in rheumatoid arthritis. *Arthritis Res. Ther.* **20**, 1–12 (2018).

90. Zhong, W., Zhao, L., Liu, T. & Jiang, Z. IL-22-producing CD4+T cells in the treatment response of rheumatoid arthritis to combination therapy with methotrexate and leflunomide. *Sci. Rep.* **7**, 1–11 (2017).

91. Kuwabara, T., Ishikawa, F., Kondo, M. & Kakiuchi, T. The role of IL-17 and related cytokines in inflammatory autoimmune diseases. *Mediators Inflamm.* **2017**, (2017).

92. Duhen, T., Geiger, R., Jarrossay, D., Lanzavecchia, A. & Sallusto, F. Production of interleukin 22 but not interleukin 17 by a subset of human skin-homing memory T cells. *Nat. Immunol.* **10**, 857–863 (2009).

93. Beringer, A., Thiam, N., Molle, J., Bartosch, B. & Miossec, P. Synergistic effect of interleukin-17 and tumour necrosis factor-α on inflammatory response in hepatocytes through interleukin-6-dependent and independent pathways. *Clin. Exp. Immunol.* **193**, 221–233 (2018).

94. Adeegbe, D. O. & Nishikawa, H. Natural and induced T regulatory cells in cancer. *Front. Immunol.* **4**, 1–14 (2013).

95. Kimura, A. & Kishimoto, T. IL-6: regulator of Treg/Th17 balance. *Eur. J. Immunol.* **40**, 1830–1835 (2010).

96. Zhou, L. *et al.* TGF-B-induced Foxp3 inhibits TH17 cell differentiation by antagonizing RORγt function. *Nature* **453**, 236–240 (2008).

97. Koutsakos, M., Nguyen, T. H. O. & Kedzierska, K. With a little help from T follicular helper friends: humoral immunity to influenza vaccination. *J. Immunol.* **202**, 360–367 (2019).

98. Bai, X. *et al.* T follicular helper cells regulate humoral response for host protection against intestinal Citrobacter rodentium infection. *J. Immunol.* **204**, 2754–2761 (2020).

99. Jang, E. *et al.* Splenic long-lived plasma cells promote the development of follicular helper T cells during autoimmune responses. *J. Immunol.* **196**, 1026–1035 (2016).

100. Tangye, S. G., Ma, C. S., Brink, R. & Deenick, E. K. The good, the bad and the ugly - Tfh cells in human health and disease. *Nat. Rev. Immunol.* **13**, 412–426 (2013).

101. Jogdand, G. M., Mohanty, S. & Devadas, S. Regulators of Tfh cell differentiation. *Front. Immunol.* **7**, 1–14 (2016).

102. Hatzi, K. *et al*. BCL6 orchestrates Tfh cell differentiation via multiple distinct mechanisms. *J. Exp. Med.* **212**, 539–553 (2015).

103. Barker, R. N. *et al*. Antigen presentation by macrophages is enhanced by the uptake of necrotic, but not apoptotic, cells. *Clin. Exp. Immunol.* **127**, 220–225 (2002).

104. Martinez-Pomares, L. & Gordon, S. Antigen presentation the macrophage way. *Cell* **131**, 641–643 (2007).

105. Morhardt, T. L. *et al*. IL-10 produced by macrophages regulates epithelial integrity in the small intestine. *Sci. Rep.* **9**, 1–10 (2019).

106. Prendergast, C. T. *et al*. Visualising the interaction of CD4 T cells and DCs in the evolution of inflammatory arthritis. *Ann. Rheum. Dis.* **77**, 579–588 (2018).

107. Benson, R. A., McInnes, I. B., Brewer, J. M. & Garside, P. Cellular imaging in rheumatic diseases. *Nat. Rev. Rheumatol.* **11**, 357–367 (2015).

108. Couillault, C., Germain, C., Dubois, B. & Kaplon, H. Identification of Tertiary Lymphoid Structure-Associated Follicular Helper T Cells in Human Tumors and Tissues. *Methods Mol. Biol.* **1845**, 205–222 (2018).

109. Aloisi, F. & Pujol-Borrell, R. Lymphoid neogenesis in chronic inflammatory diseases. *Nat. Rev. Immunol.* **6**, 205–217 (2006).

110. Alegre, M. L., Frauwirth, K. A. & Thompson, C. B. T-cell regulation by CD28 and CTLA-4. *Nat. Rev. Immunol.* **1**, 220–228 (2001).

111. Guo, F., Iclozan, C., Suh, W.-K., Anasetti, C. & Yu, X.-Z. CD28 controls differentiation of regulatory T cells from naive CD4 T cells. *J. Immunol.* **181**, 2285–2291 (2008).

112. Simpson, T. R., Quezada, S. A. & Allison, J. P. Regulation of CD4 T cell activation and effector function by inducible costimulator (ICOS). *Curr. Opin.*

Immunol. **22**, 326–332 (2010).

113. Chen, Q. *et al*. ICOS signal facilitates Foxp3 transcription to favor suppressive function of regulatory T cells. *Int*. *J*. *Med*. *Sci*. **15**, 666–673 (2018).

114. Chen, L. & Flies, D. B. Molecular mechanisms of T cell co-stimulation and co-inhibition. *Nat*. *Rev*. *Immunol*. **13**, 227–242 (2013).

115. Simons, K. H. *et al*. T cell co-stimulation and co-inhibition in cardiovascular disease: a double-edged sword. *Nat*. *Rev*. *Cardiol*. **16**, 325–343 (2019).

116. Green, J. M., Karpitskiy, V., Kimzey, S. L. & Shaw, A. S. Coordinate regulation of T cell activation by CD2 and CD28. *J*. *Immunol*. **164**, 3591–3595 (2000).

117. Huang, Y.-H. *et al*. SLAM–SAP signaling promotes differentiation of IL-17–producing T cells and progression of experimental autoimmune encephalomyelitis. *J*. *Immunol*. **193**, 5841–5853 (2014).

118. Hu, T. *et al*. TIM4-TIM1 interaction modulates Th2 pattern inflammation through enhancing SIRT1 expression. *Int*. *J*. *Mol*. *Med*. **40**, 1504–1510 (2017).

119. Kumanogoh, A. *et al*. Class IV semaphorin Sema4A enhances T-cell activation and interacts with Tim-2. *Nature* **419**, 629–633 (2002).

120. Verma, N. K. *et al*. LFA-1/ICAM-1 ligation in human T cells promotes Th1 polarization through a GSK3β signaling–dependent notch pathway. *J*. *Immunol*. **197**, 108–118 (2016).

121. Kandula, S. & Abraham, C. LFA-1 on CD4 + T cells is required for optimal antigen-dependent activation in vivo. *J*. *Immunol*. **173**, 4443–4451 (2004).

122. Jiang, X., Bjorkstrom, N. K. & Melum, E. Intact CD100-CD72 interaction necessary for TCR-induced T cell proliferation. *Front*. *Immunol*. **8**, 4–11 (2017).

123. Kikutani, H. & Kumanogoh, A. Semaphorins in interactions between T cells and antigen-presenting cells. *Nat. Rev. Immunol.* **3**, 159–167 (2003).

124. Croft, M. The role of TNF superfamily members in T-cell function and diseases. *Nat. Rev. Immunol.* **9**, 271–285 (2009).

125. van Oosterwijk, M. F. *et al.* CD27-CD70 interactions sensitise naive CD4+ T cells for IL-12-induced Th1 cell development. *Int. Immunol.* **19**, 713–718 (2007).

126. Coquet, J. M. *et al.* The CD27 and CD70 costimulatory pathway inhibits effector function of T helper 17 cells and attenuates associated autoimmunity. *Immunity* **38**, 53–65 (2013).

127. Hendriks, J., Gravestein, L. A., Tesselaar, K. & Lier, R. A. W. Van. CD27 is required for generation and long-term maintenance of T cell immunity. *Nat. Immunol.* **1**, 433–440 (2000).

128. Arens, R. *et al.* Constitutive CD27/CD70 interaction induces expansion of effector-type T cells and results in IFNγ-mediated B cell depletion. *Immunity* **15**, 801–812 (2001).

129. Redmond, W. L., Ruby, C. E. & Weinberg, A. D. The role of OX40-mediated co-stimulation in T cell activation and survival. *Crit. Rev. Immunol.* **29**, 187–201 (2009).

130. Xiao, X. *et al.* OX40 signaling favors the induction of TH9 cells and airway inflammation. *Nat. Immunol.* **13**, 981–990 (2012).

131. Dawicki, W. & Watts, T. H. Expression and function of 4-IBB during CD4 versus CD8 T cell responses in vivo. *Eur. J. Immunol.* **34**, 743–751 (2004).

132. Zhang, P. *et al.* Agonistic anti-4-1BB antibody promotes the expansion of natural regulatory T cells while maintaining Foxp3 expression. *Scand. J. Immunol.* **66**, 435–440 (2007).

133. Ruby, C. E. *et al*. OX40 agonists can drive Treg expansion if the cytokine milieu is right. *J. Immunol*. **183**, 4853–4857 (2009).

134. Nocentini, G., Ronchetti, S., Cuzzocrea, S. & Riccardi, C. GITR/GITRL: more than an effector T cell co-stimulatory system. *Eur. J. Immunol*. **37**, 1165–1169 (2007).

135. van Olffen, R. W. *et al*. GITR triggering induces expansion of both effector and regulatory CD4 + T cells in vivo. *J. Immunol*. **182**, 7490–7500 (2009).

136. Iezzi, G. *et al*. CD40-CD40L cross-talk integrates strong antigenic signals and microbial stimuli to induce development of IL-17-producing CD4+ T cells. *Proc. Natl. Acad. Sci. U. S. A*. **106**, 876–881 (2009).

137. del Rio, M. L., Lucas, C. L., Buhler, L., Rayat, G. & Rodriguez-Barbosa, J. I. HVEM/LIGHT/BTLA/CD160 cosignaling pathways as targets for immune regulation. *J. Leukoc. Biol*. **87**, 223–235 (2010).

138. Akiyama, T., Shinzawa, M. & Akiyama, N. RANKL-RANK interaction in immune regulatory systems. *World J. Orthop*. **3**, 142–150 (2012).

139. Corse, E. & Allison, J. P. Cutting edge: CTLA-4 on effector T cells inhibits in Trans. *J. Immunol*. **189**, 1123–1127 (2012).

140. Sheng Yao *et al*. B7-H2 is a costimulatory ligand for CD28 in human. *Immunity* **34**, 729–740 (2011).

141. Ovcinnikovs, V. *et al*. CTLA-4-mediated transendocytosis of costimulatory molecules primarily targets migratory dendritic cells. *Sci. Immunol*. **4**, (2019).

142. Qureshi, O. S. *et al*. Trans-endocytosis of CD80 and CD86: a molecular basis for the cell extrinsic function of CTLA-4. *Science (80-.).* **332**, 600–603 (2011).

143. Parry, R. V. *et al*. CTLA-4 and PD-1 receptors inhibit T-cell activation by distinct mechanisms. *Mol. Cell. Biol*. **25**, 9543–9553 (2005).

144. Negishi, N. *et al*. CD155-transducing signaling through TIGIT plays an important role in transmission of tolerant state and suppression capacity. *ImmunoHorizons* **2**, 338–348 (2018).

145. Lozano, E., Dominguez-Villar, M., Kuchroo, V. & Hafler, D. A. The TIGIT/CD226 axis regulates human T cell function. *J. Immunol*. **188**, 3869–3875 (2012).

146. Yu, X. *et al*. The surface protein TIGIT suppresses T cell activation by promoting the generation of mature immunoregulatory dendritic cells. *Nat. Immunol*. **10**, 48–57 (2009).

147. Kane, L. P. T cell Ig and mucin domain proteins and immunity. *J. Immunol*. **184**, 2743–2749 (2010).

148. Lebbink, R. J. *et al*. Collagens are functional, high affinity ligands for the inhibitory immune receptor LAIR-1. *J. Exp. Med*. **203**, 1419–1425 (2006).

149. Meyaard, L. LAIR and collagens in immune regulation. *Immunol. Lett*. **128**, 26–28 (2010).

150. He, C. *et al*. Anti-CII antibody as a novel indicator to assess disease activity in systemic lupus erythematosus. *Lupus* **24**, 1370–1376 (2015).

151. Yoshida, M. *et al*. Autoimmunity to citrullinated type II collagen in rheumatoid arthritis. *Mod. Rheumatol*. **16**, 276–281 (2006).

152. Bates, J. P., Derakhshandeh, R., Jones, L. & Webb, T. J. Mechanisms of immune evasion in breast cancer. *BMC Cancer* **18**, 1–14 (2018).

153. Ahrends, T. & Borst, J. The opposing roles of CD4+ T cells in anti-tumour immunity. *Immunology* **154**, 582–592 (2018).

154. Nurieva, R. I. *et al*. Function of T follicular helper cells in anti-tumor immunity. *J. Immunol*. **202**, 138.18 LP-138.18 (2019).

155. Singh, D. *et al*. CD4+ follicular helper-like T cells are key players in anti-tumor immunity. *bioRxiv* 2020.01.08.898346 (2020) doi:10.1101/2020.01.08.898346.

156. Choi, Y. E., Yu, H. N., Yoon, C. H. & Bae, Y. S. Tumor-mediated down-regulation of MHC class II in DC development is attributable to the epigenetic control of the CIITA type I promoter. *Eur. J. Immunol.* **39**, 858–868 (2009).

157. Kah-Wai, L., Jacek, T. & Jacek, R. Dendritic cells heterogeneity and its role in cancer immunity. *J. Cancer Res. Ther.* **2**, 35–40 (2006).

158. Mueller, D. L. & Jenkins, M. K. Autoimmunity: when self-tolerance breaks down. *Curr. Biol.* **7**, 255–257 (1997).

159. Song, Y. W. & Kang, E. H. Autoantibodies in rheumatoid arthritis: rheumatoid factors and anticitrullinated protein antibodies. *QJM* **103**, 139–146 (2010).

160. Mil, A. H. M. V. D. H., Verpoort, K. N., Breedveld, F. C., Toes, R. E. M. & Huizinga, T. W. J. Antibodies to citrullinated proteins and differences in clinical progression of rheumatoid arthritis. *Arthritis Res. Ther.* **7**, R949–R958 (2005).

161. Kroot, J. A. E. J. *et al*. The prognostic value of anti-cyclic citrullinated peptide antibody in patients with recent-onset rheumatoid arthritis. *Arthritis Rheum.* **43**, 1831–1835 (2000).

162. Derksen, V. F. A. M., Huizinga, T. W. J. & van der Woude, D. The role of autoantibodies in the pathophysiology of rheumatoid arthritis. *Semin. Immunopathol.* **39**, 437–446 (2017).

163. Moschovakis, G. L. *et al*. T cell specific Cxcr5 deficiency prevents rheumatoid arthritis. *Sci. Rep.* **7**, 1–13 (2017).

164. Cao, G., Chi, S., Wang, X., Sun, J. & Zhang, Y. CD4+CXCR5+PD-1+ T follicular

helper cells play a pivotal role in the development of rheumatoid arthritis. *Med. Sci. Monit.* **25**, 3032–3040 (2019).

165. Ma, J. *et al.* Increased frequency of circulating follicular helper T cells in patients with rheumatoid arthritis. *Clin. Dev. Immunol.* **2012**, (2012).

166. Newton, J. L., Harney, S. M. J., Wordsworth, B. P. & Brown, M. A. A review of the MHC genetics of rheumatoid arthritis. *Genes Immun.* **5**, 151–157 (2004).

167. Thomas, R., Davis, L. S. & Lipsky, P. E. Rheumatoid synovium is enriched in mature antigen-presenting dendritic cells. *J. Immunol.* **152**, 2613–2623 (1994).

168. Caplazi, P. *et al.* Mouse Models of Rheumatoid Arthritis. *Vet. Pathol.* **52**, 819–826 (2015).

169. Christensen, A. D., Haase, C., Cook, A. D. & Hamilton, J. A. K/BxN serum-transfer arthritis as a model for human inflammatory arthritis. *Front. Immunol.* **7**, 213 (2016).

170. Maffia, P. *et al.* Inducing experimental arthritis and breaking self-tolerance to joint-specific antigens with trackable, ovalbumin-specific T cells. *J. Immunol.* **173**, 151–6 (2004).

171. Smolen, J. S., Aletaha, D. & McInnes, I. B. Rheumatoid arthritis. *Lancet* **388**, 2023–2038 (2016).

172. Soldevilla, M. M. *et al.* ICOS costimulation at the tumor site in combination with CTLA-4 blockade therapy elicits strong tumor immunity. *Mol. Ther.* **27**, 1878–1891 (2019).

173. French, R. R. *et al.* Eradication of lymphoma by CD8 T cells following anti-CD40 monoclonal antibody therapy is critically dependent on CD27 costimulation. *Blood* **109**, 4810–4815 (2007).

174. Roberts, D. J. *et al*. Control of established melanoma by CD27 stimulation is associated with enhanced effector function and persistence, and reduced PD-1 expression, of tumor infiltrating CD8+ T cells. *J. Immunother*. **33**, 769–779 (2010).

175. Turaj, A. H. *et al*. Antibody tumor targeting is enhanced by CD27 agonists through myeloid recruitment. *Cancer Cell* **32**, 777-791.e6 (2017).

176. Sanborn, R. E. *et al*. Anti-CD27 agonist antibody varlilumab (varli) with nivolumab (nivo) for colorectal (CRC) and ovarian (OVA) cancer: Phase (Ph) 1/2 clinical trial results. *J. Clin. Oncol*. **36**, 3001 (2018).

177. Aspeslagh, S. *et al*. Rationale for anti-OX40 cancer immunotherapy. *Eur. J. Cancer* **52**, 50–66 (2016).

178. Zhang, J., Medeiros, L. J. & Young, K. H. Cancer immunotherapy in diffuse large B-cell lymphoma. *Front. Oncol*. **8**, 1–12 (2018).

179. Chen, T. H., Chang, P. M. H. & Yang, M. H. Novel immune-modulating drugs for advanced head and neck cancer. *Head Neck* **41**, 46–56 (2019).

180. Bell, R. B. *et al*. Neoadjuvant anti-OX40 (MEDI6469) prior to surgery in head and neck squamous cell carcinoma. *J. Clin. Oncol*. **36**, 6011 (2018).

181. Chin, S. M. *et al*. Structure of the 4-1BB/4-1BBL complex and distinct binding and functional properties of utomilumab and urelumab. *Nat. Commun*. **9**, (2018).

182. Deng, C., Pan, B. & O'Connor, O. A. Brentuximab Vedotin. *Clin. Cancer Res*. **19**, 22–27 (2013).

183. Younes, A., Yasothan, U. & Kirkpatrick, P. Brentuximab vedotin. *Nat. Rev. Drug Discov*. **11**, 19–20 (2012).

184. Cohen, A. D. *et al*. Agonist anti-GITR antibody enhances vaccine-induced CD8+ T-cell responses and tumor immunity. *Cancer Res*. **66**, 4904–4912

(2006).

185. Cohen, A. D. *et al*. Agonist anti-GITR monoclonal antibody induces melanoma tumor immunity in mice by altering regulatory T cell stability and intra-tumor accumulation. *PLoS One* **5**, (2010).

186. Pedroza-Gonzalez, A. *et al*. GITR engagement in combination with CTLA-4 blockade completely abrogates immunosuppression mediated by human liver tumor-derived regulatory T cells ex vivo. *Oncoimmunology* **4**, (2015).

187. Piechutta, M. & Berghoff, A. S. New emerging targets in cancer immunotherapy: The role of Cluster of Differentiation 40 (CD40/TNFR5). *ESMO Open* **4**, (2019).

188. Sondak, V. K., Smalley, K. S. M., Kudchadkar, R., Grippon, S. & Kirkpatrick, P. Ipilimumab. *Nat. Rev. Drug Discov.* **10**, 411–412 (2011).

189. Xu, H. *et al*. Antitumor activity and treatment-related toxicity associated with nivolumab plus ipilimumab in advanced malignancies: a systematic review and meta-analysis. *Front. Pharmacol.* **10**, (2019).

190. Yang, Y. *et al*. Comparative efficacy and safety of Nivolumab and Nivolumab plus Ipilimumab in advanced cancer: a systematic review and meta-analysis. *Front. Pharmacol.* **11**, 1–10 (2020).

191. Gao, J. *et al*. Loss of IFN-γ pathway genes in tumor cells as a mechanism of resistance to anti-CTLA-4 therapy. *Cell* **167**, 397–404 (2016).

192. Shah, N. J., Kelly, W. J., Liu, S. V., Choquette, K. & Spira, A. Product review on the anti-PD-L1 antibody atezolizumab. *Hum. Vaccines Immunother.* **14**, 269–276 (2018).

193. Zuazo, M. *et al*. Functional systemic CD4 immunity is required for clinical responses to PD-L1/PD-1 blockade therapy. *EMBO Mol. Med.* **11**, 1–14 (2019).

194. Kagamu, H. *et al*. CD4+ T-cell immunity in the peripheral blood correlates

with response to anti-PD-1 therapy. *Cancer Immunol. Res.* **8**, 334–344 (2020).

195. Wu, L. *et al.* Blockade of TIGIT/CD155 signaling reverses T-cell exhaustion and enhances antitumor capability in head and neck squamous cell carcinoma. *Cancer Immunol. Res.* **7**, 1700–1713 (2019).

196. Grosso, J. F. *et al.* LAG-3 regulates CD8+ T cell accumulation and effector function in murine self- and tumor-tolerance systems. *J. Clin. Invest.* **117**, 3383–3392 (2007).

197. Das, M., Zhu, C. & Kuchroo, V. K. TIM-3 and its role in regulating anti-tumor immunity. *Immunol. Rev.* **276**, 97–111 (2017).

198. Patakas, A. *et al.* Abatacept Inhibition of T Cell Priming in Mice by Induction of a Unique Transcriptional Profile That Reduces Their Ability to Activate Antigen-Presenting Cells. *Arthritis Rheumatol.* **68**, 627–638 (2016).

199. Moreland, L., Bate, G. & Kirkpatrick, P. Abatacept. *Nat. Rev. Drug Discov.* **5**, 185–186 (2006).

200. Platt, A. M. *et al.* Abatacept limits breach of self-tolerance in a murine model of arthritis via effects on the generation of T follicular helper cells. *J. Immunol.* **185**, 1558–1567 (2010).

201. Jansen, D. T. S. L. *et al.* Abatacept decreases disease activity in a absence of CD4+ T cells in a collagen-induced arthritis model. *Arthritis Res. Ther.* **17**, 1–11 (2015).

202. Weisman, M. H. *et al.* Reduction of inflammatory biomarker response by abatacept in treatment of rheumatoid arthritis. *J. Rheumatol.* **33**, 2162–2166 (2006).

203. Kallikourdis, M. *et al.* T cell costimulation blockade blunts pressure overload-induced heart failure. *Nat. Commun.* **8**, (2017).

204. Nahas, M. R. *et al.* Phase 1 clinical trial evaluating abatacept in patients

with steroid-refractory chronic graft-versus-host disease. *Blood* **131**, 2836–2845 (2018).

205. Penack, O. *et al*. Prophylaxis and management of graft versus host disease after stem-cell transplantation for haematological malignancies: updated consensus recommendations of the European Society for Blood and Marrow Transplantation. *Lancet Haematol*. **7**, e157–e167 (2020).

206. Kadkhoda, K. *et al*. ICOS ligand expression is essential for allergic airway hyperresponsiveness. *Int. Immunol*. **23**, 239–249 (2011).

207. Uwadiae, F. I., Pyle, C. J., Walker, S. A., Lloyd, C. M. & Harker, J. A. Targeting the ICOS/ICOS-L pathway in a mouse model of established allergic asthma disrupts T follicular helper cell responses and ameliorates disease. *Allergy Eur. J. Allergy Clin. Immunol*. **74**, 650–662 (2019).

208. Ma, X. *et al*. Effect of follicular helper T cells on the pathogenesis of asthma. *Exp. Ther. Med*. **14**, 967–972 (2017).

209. O'Dwyer, R. *et al*. Anti-ICOSL new antigen receptor domains inhibit T cell proliferation and reduce the development of inflammation in the collagen-induced mouse model of rheumatoid arthritis. *J. Immunol. Res*. **2018**, (2018).

210. Odobasic, D., Kitching, A. R., Semple, T. J. & Holdsworth, S. R. Inducible co-stimulatory molecule ligand is protective during the induction and effector phases of crescentic glomerulonephritis. *J. Am. Soc. Nephrol*. **17**, 1044–1053 (2006).

211. Afek, A., Harats, D., Roth, A., Keren, G. & George, J. A functional role for inducible costimulator (ICOS) in atherosclerosis. *Atherosclerosis* **183**, 57–63 (2005).

212. Pawlowski, N. N. *et al*. αcD2 mAb treatment safely attenuates adoptive transfer colitis. *Lab. Investig*. **85**, 1013–1023 (2005).

213. Munitz, A., Bachelet, I., Finkelman, F. D., Rothenberg, M. E. & Levi-Schaffer, F. CD48 Is critically involved in allergic eosinophilic airway inflammation. *Am. J. Respir. Crit. Care Med.* **175**, 911–918 (2007).

214. McArdel, S. L., Brown, D. R., Sobel, R. A. & Sharpe, A. H. Anti-CD48 monoclonal antibody attenuates experimental autoimmune encephalomyelitis by limiting the number of pathogenic CD4+ T Cells. *J. Immunol.* **197**, 3038–3048 (2016).

215. Foks, A. C. *et al.* Blockade of Tim-1 and Tim-4 enhances atherosclerosis in LDL receptor-deficient mice. *Arterioscler. Thromb. Vasc. Biol.* **36**, 456–465 (2016).

216. Abe, Y. *et al.* TIM-4 has dual function in the induction and effector phases of murine arthritis. *J. Immunol.* **191**, 4562–4572 (2013).

217. Shanks, K. *et al.* Neuroimmune semaphorin 4D is necessary for optimal lung allergic inflammation. *Mol. Immunol.* **56**, 480–487 (2013).

218. Smith, E. S. *et al.* SEMA4D compromises blood-brain barrier, activates microglia, and inhibits remyelination in neurodegenerative disease. *Neurobiol. Dis.* **73**, 254–268 (2015).

219. Zhu, L. *et al.* Disruption of SEMA4D ameliorates platelet hypersensitivity in dyslipidemia and confers protection against the development of atherosclerosis. *Arterioscler. Thromb. Vasc. Biol.* **29**, 1039–1045 (2009).

220. Yoshida, Y. *et al.* Semaphorin 4D contributes to rheumatoid arthritis by inducing inflammatory cytokine production: pathogenic and therapeutic implications. *Arthritis Rheumatol.* **67**, 1481–1490 (2015).

221. Newton, A. H., Danahy, D. B., Chan, M. A. & Benedict, S. H. Timely blockade of ICAM-1.LFA-1 interaction prevents disease onset in a mouse model of emphysema. *Immunotherapy* **7**, 621–629 (2015).

222. Whitcup, S. M., Chan, C. C., Kozhich, A. T. & Magone, M. T. Blocking ICAM-

1 (CD54) and LFA-1 (CD11a) inhibits experimental allergic conjunctivitis. *Clin. Immunol.* **93**, 107–113 (1999).

223. Burns, R. C. *et al.* Antibody blockade of ICAM-1 and VCAM-1 ameliorates inflammation in the SAMP-1/Yit adoptive transfer model of Crohn's disease in mice. *Gastroenterology* **121**, 1428–1436 (2001).

224. Watts, G. M. *et al.* Manifestations of inflammatory arthritis are critically dependent on LFA-1. *J. Immunol.* **174**, 3668–3675 (2005).

225. Winkels, H. *et al.* CD70 limits atherosclerosis and promotes macrophage function. *Thromb. Haemost.* **117**, 164–175 (2017).

226. Makino, F. *et al.* Blockade of CD70-CD27 interaction inhibits induction of allergic lung inflammation in mice. *Am. J. Respir. Cell Mol. Biol.* **47**, 298–305 (2012).

227. Manocha, M. *et al.* Blocking CD27-CD70 costimulatory pathway suppresses experimental colitis. *J. Immunolgy* **183**, 270–276 (2009).

228. Oflazoglu, E. *et al.* Blocking of CD27-CD70 pathway by anti-CD70 antibody ameliorates joint disease in murine collagen-induced arthritis. *J. Immunol.* **183**, 3770–3777 (2009).

229. Fukushima, A. *et al.* Roles of OX40 in the development of murine experimental allergic conjunctivitis: exacerbation and attenuation by stimulation and blocking of OX40. *Investig. Ophthalmol. Vis. Sci.* **47**, 657–663 (2006).

230. Obermeier, F. *et al.* OX40/OX40L interaction induces the expression of CXCR5 and contributes to chronic colitis induced by dextran sulfate sodium in mice. *Eur. J. Immunol.* **33**, 3265–3274 (2003).

231. Foks, A. C. *et al.* Interruption of the OX40–OX40 ligand pathway in LDL receptor–deficient mice causes regression of atherosclerosis. *J. Immunol.* **191**, 4573–4580 (2013).

232. Nakano, M. *et al*. OX40 ligand plays an important role in the development of atherosclerosis through vasa vasorum neovascularization. *Cardiovasc. Res.* **88**, 539–546 (2010).

233. Findlay, E. G. *et al*. OX40L blockade is therapeutic in arthritis, despite promoting osteoclastogenesis. *Proc. Natl. Acad. Sci. U. S. A.* **111**, 2289–2294 (2014).

234. Kurata, I. *et al*. Potential involvement of OX40 in the regulation of autoantibody sialylation in arthritis. *Ann. Rheum. Dis.* **78**, 1488–1496 (2019).

235. Jeon, H. J. *et al*. CD137 (4-1BB) deficiency reduces atherosclerosis in hyperlipidemic mice. *Circulation* **121**, 1124–1133 (2010).

236. Seo, S. K. *et al*. 4-1BB-mediated immunotherapy of rheumatoid arthritis. *Nat. Med.* **10**, 1088–1094 (2004).

237. Foks, A. C. *et al*. Interference of the CD30-CD30L pathway reduces atherosclerosis development. *Arterioscler. Thromb. Vasc. Biol.* **32**, 2862–2868 (2012).

238. Somada, S. *et al*. CD30 ligand/CD30 interaction is involved in pathogenesis of inflammatory bowel disease. *Dig. Dis. Sci.* **57**, 2031–2037 (2012).

239. Sun, X. *et al*. CD30 ligand Is a target for a novel biological therapy against colitis associated with Th17 responses. *J. Immunol.* **185**, 7671–7680 (2010).

240. Santucci, L. *et al*. GITR modulates innate and adaptive mucosal immunity during the development of experimental colitis in mice. *Gut* **56**, 52–60 (2007).

241. Ma, J. *et al*. Blockade of glucocorticoid-induced tumor necrosis factor-receptor-related protein signaling ameliorates murine collagen-induced arthritis by modulating follicular helper T cells. *Am. J. Pathol.* **186**, 1559–1567 (2016).

242. Bull, M. J. *et al*. The death receptor 3-TNF-like protein 1A pathway drives adverse bone pathology in inflammatory arthritis. *J. Exp. Med.* **205**, 2457–2464 (2008).

243. Takedatsu, H. *et al*. TL1A (TNFSF15) regulates the development of chronic colitis by modulating both T-helper 1 and T-helper 17 activation. *Gastroenterology* **135**, 552–567 (2008).

244. Meylan, F. *et al*. The TNF-family cytokine TL1A drives IL-13-dependent small intestinal inflammation. *Mucosal Immunol.* **4**, 172–185 (2011).

245. Fang, L., Adkins, B., Deyev, V. & Podack, E. R. Essential role of TNF receptor superfamily 25 (TNFRSF25) in the development of allergic lung inflammation. *J. Exp. Med.* **205**, 1037–1048 (2008).

246. Karnell, J. L., Rieder, S. A., Ettinger, R. & Kolbeck, R. Targeting the CD40-CD40L pathway in autoimmune diseases: Humoral immunity and beyond. *Adv. Drug Deliv. Rev.* **141**, 92–103 (2019).

247. Foks, A. C. *et al*. Agonistic anti-TIGIT treatment inhibits T cell responses in LDLr deficient mice without affecting atherosclerotic lesion development. *PLoS One* **8**, 6–12 (2013).

248. Barnden, M. J., Allison, J., Heath, W. R. & Carbone, F. R. Defective TCR expression in transgenic mice constructed using cDNA- based α- and ß-chain genes under the control of heterologous regulatory elements. *Immunol. Cell Biol.* **76**, 34–40 (1998).

249. Tomura, M. *et al*. Monitoring cellular movement in vivo with photoconvertible fluorescence protein 'Kaede' transgenic mice. *Proc. Natl. Acad. Sci. U. S. A.* **105**, 10871–10876 (2008).

250. Goncalves-Alves, E. *et al*. MicroRNA-155 controls T helper cell activation during viral infection. *Front. Immunol.* **10**, 4–13 (2019).

251. Benson, R. A., Brewer, J. M. & Garside, P. Visualizing and Tracking T Cell

Motility In Vivo. *Methods Mol. Biol.* **1591**, 27–41 (2017).

252. Schindelin, J. *et al.* Fiji: an open-source platform for biological-image analysis. *Nat. Methods* **9**, 676–682 (2012).

253. Stauffer, W., Sheng, H. & Lim, H. N. EzColocalization: an ImageJ plugin for visualizing and measuring colocalization in cells and organisms. *Sci. Rep.* **8**, 1–13 (2018).

254. Shay, T. & Kang, J. Immunological Genome project and systems immunology. *Trends Immunol.* **34**, 602–609 (2013).

255. Paxton, R. J., Mooser, G., Pande, H., Lee, T. D. & Shively, J. E. Sequence analysis of carcinoembryonic antigen: identification of glycosylation sites and homology with the immunoglobulin supergene family. *Proc. Natl. Acad. Sci. U. S. A.* **84**, 920–924 (1987).

256. Aurivillius, M., Hansen, O. C., Lazrek, M. B. S., Bock, E. & Öbrink, B. The cell adhesion molecule Cell-CAM 105 is an ecto-ATPase and a member of the immunoglobulin superfamily. *FEBS Lett.* **264**, 267–269 (1990).

257. Horst, A. K., Najjar, S. M., Wagener, C. & Tiegs, G. CEACAM1 in liver injury, metabolic and immune regulation. *Int. J. Mol. Sci.* **19**, (2018).

258. Svenberg, T. Carcinoembryonic antigen-like substances of human bile. Isolation and partial characterization. *Int. J. Cancer* **17**, 588–596 (1976).

259. Prall, F. *et al.* Cd66a (BGP), an adhesion molecule of the carcinoembryonic antigen family, is expressed in epithelium, endothelium, and myeloid cells in a wide range of normal human tissues. *J. Histochem. Cytochem.* **44**, 35–41 (1996).

260. Kammerer, R., Hahn, S., Singer, B. B., Luo, J. S. & Von Kleist, S. Biliary glycoprotein (CD66a), a cell adhesion molecule of the immunoglobulin superfamily, on human lymphocytes: Structure, expression and involvement in T cell activation. *Eur. J. Immunol.* **28**, 3664–3674 (1998).

261. Gray-Owen, S. D. & Blumberg, R. S. CEACAM1: Contact-dependent control of immunity. *Nat. Rev. Immunol.* **6**, 433–446 (2006).

262. Beauchemin, N. *et al.* Redefined nomenclature for members of the carcinoembryonic antigen family. *Exp. Cell Res.* **252**, 243–249 (1999).

263. Sabatos-Peyton, C. A. *et al.* Blockade of Tim-3 binding to phosphatidylserine and CEACAM1 is a shared feature of anti-Tim-3 antibodies that have functional efficacy. *Oncoimmunology* **7**, 1–9 (2018).

264. Huang, Y. H. *et al.* CEACAM1 regulates TIM-3-mediated tolerance and exhaustion. *Nature* **517**, 386–390 (2015).

265. Hemmila, E. *et al.* Ceacam1a−/− mice are completely resistant to infection by murine coronavirus mouse hepatitis virus A59. *J. Virol.* **78**, 10156–10165 (2004).

266. Chen, B. T., Grunert, F., Medina-marino, A. & Gotschlich, E. C. Several Carcinoembryonic Antigens (CD66) serve as receptors for Gonococcal opacity proteins. *J. Exp. Med.* **185**, 1557–1564 (1997).

267. Islam, E. A. *et al.* Specific binding to differentially expressed human carcinoembryonic antigenrelated cell adhesion molecules determines the outcome of Neisseria gonorrhoeae infections along the female reproductive tract. *Infect. Immun.* **86**, 1–19 (2018).

268. Sauter, S. L., Rutherfurd, S. M., Wagener, C., Shively, J. E. & Hefta, S. A. Binding of nonspecific cross-reacting antigen, a granulocyte membraned glycoprotein, to Escherichia coli expressing type 1 fimbriae. *Infect. Immun.* **59**, 2485–2493 (1991).

269. Virji, M. *et al.* Carcinoembryonic antigens are targeted by diverse strains of typable and non-typable Haemophilus influenzae. *Mol. Microbiol.* **36**, 784–795 (2000).

270. Hill, D. J., Edwards, A. M., Rowe, H. A. & Virji, M. Carcinoembryonic

antigen-related cell adhesion molecule (CEACAM)-binding recombinant polypeptide confers protection against infection by respiratory and urogenital pathogens. *Mol. Microbiol.* **55**, 1515–1527 (2005).

271. Blau, D. M. *et al.* Targeted disruption of the Ceacam1(MHVR) gene leads to reduced susceptibility of mice to mouse hepatitis virus infection. *J. Virol.* **75**, 8173–8186 (2001).

272. Klaile, E. *et al.* Binding of candida albicans to human CEACAM1 and CEACAM6 modulates the inflammatory response of intestinal epithelial cells. *MBio* **8**, e02142-16 (2017).

273. Javaheri, A. *et al.* Helicobacter pylori adhesin HopQ engages in a virulence-enhancing interaction with human CEACAMs. *Nat. Microbiol.* **2**, (2016).

274. Boulton, I. C. & Gray-Owen, S. D. Neisserial binding to CEACAM1 arrests the activation and proliferation of CD4+ T lymphocytes. *Nat. Immunol.* **3**, 229–236 (2002).

275. Rojas, M., Fuks, A. & Stanners, C. P. Biliary glycoprotein, a member of the immunoglobulin supergene family, functions in vitro as a Ca2(+)-dependent intercellular adhesion molecule. *Cell Growth Differ.* **1**, 527–533 (1990).

276. Turbide, C., Kunath, T., Daniels, E. & Beauchemin, N. Optimal ratios of biliary glycoprotein isoforms required for inhibition of colonic tumor cell growth. *Cancer Res.* **57**, 2781–2788 (1997).

277. Olsson, H., Wikström, K., Kjellström, G. & Öbrink, B. Cell adhesion activity of the short cytoplasmic domain isoform of C-CAM (C-CAM2) in CHO cells. *FEBS Lett.* **365**, 51–56 (1995).

278. Watt, S. M. *et al.* Homophilic adhesion of human CEACAM1 involves N-terminal domain interactions: Structural analysis of the binding site. *Blood* **98**, 1469–1479 (2001).

279. Edlund, M., Blikstad, I. & Öbrink, B. Calmodulin binds to specific sequences

in the cytoplasmic domain of C-CAM and down-regulates C-CAM self-association. *J. Biol. Chem.* **271**, 1393–1399 (1996).

280. Schumann, D., Chen, C. J., Kaplan, B. & Shively, J. E. Carcinoembryonic antigen cell adhesion molecule 1 directly associates with cytoskeleton proteins actin and tropomyosin. *J. Biol. Chem.* **276**, 47421–47433 (2001).

281. Patel, P. C. *et al.* Inside-out signaling promotes dynamic changes in the carcinoembryonic antigen-related cellular adhesion molecule 1 (CEACAM1) oligomeric state to control its cell adhesion properties. *J. Biol. Chem.* **288**, 29654–29669 (2013).

282. Singer, B. B., Scheffrahn, I. & Öbrink, B. The tumor growth-inhibiting cell adhesion molecule CEACAM1 (C-CAM) is differently expressed in proliferating and quiescent epithelial cells and regulates cell proliferation. *Cancer Res.* **60**, 1236–1244 (2000).

283. Greicius, G. *et al.* CEACAM1 is a potent regulator of B cell receptor complex-induced activation. *J. Leukoc. Biol.* **74**, 126–134 (2003).

284. Khairnar, V. *et al.* CEACAM1 induces B-cell survival and is essential for protective antiviral antibody production. *Nat. Commun.* **6**, (2015).

285. Kuroki, M., Matsuo, Y., Kinugasa, T. & Matsuoka, Y. Augmented expression and release of nonspecific cross-reacting antigens (NCAs), members of the CEA family, by human neutrophils during cell activation. *J. Leukoc. Biol.* **52**, 551–557 (1992).

286. Singer, B. B. *et al.* CEACAM1 (CD66a) mediates delay of spontaneous and Fas ligand-induced apoptosis in granulocytes. *Eur. J. Immunol.* **35**, 1949–1959 (2005).

287. Lu, R., Pan, H. & Shively, J. E. CEACAM1 negatively regulates IL-1ß production in LPS activated neutrophils by recruiting SHP-1 to a SYK-TLR4-CEACAM1 complex. *PLoS Pathog.* **8**, 12–13 (2012).

288. Möller, M. J., Kammerer, R., Grunert, F. & Kleist, S. von. Biliary glycoprotein (BGP) expression on T cells and on a natural-killer-cell sub-population. *Int. J. Cancer* **65**, 740–745 (1996).

289. Hosomi, S. *et al*. CEACAM1 on activated NK cells inhibits NKG2D-mediated cytolytic function and signaling. *Eur. J. Immunol.* **43**, 2473–2483 (2013).

290. Markel, G. *et al*. Pivotal role of CEACAM1 protein in the inhibition of activated decidual lymphocyte functions. *J. Clin. Invest.* **110**, 943–953 (2002).

291. Kammerer, R., Stober, D., Singer, B. B., Öbrink, B. & Reimann, J. Carcinoembryonic antigen-related cell adhesion molecule 1 on murine dendritic cells is a potent regulator of T cell stimulation. *J. Immunol.* **166**, 6537–6544 (2001).

292. Nakajima, A. *et al*. Activation-Induced Expression of Carcinoembryonic Antigen-Cell Adhesion Molecule 1 Regulates Mouse T Lymphocyte Function. *J. Immunol.* **168**, 1028–1035 (2002).

293. Donda, A. *et al*. Locally inducible CD66a (CEACAM1) as an amplifier of the human intestinal T cell response. *Eur. J. Immunol.* **30**, 2593–2603 (2000).

294. Chen, C.-J. & Shively, J. E. The cell-cell adhesion molecule Carcinoembryonic antigen-related cellular adhesion molecule 1 inhibits IL-2 production and proliferation in human T cells by association with Src homology potein-1 and down-regulates IL-2 Receptor. *J. Immunol.* **172**, 3544–3552 (2004).

295. Ye, S., Cowled, C. J., Yap, C. H. & Stambas, J. Deep sequencing of primary human lung epithelial cells challenged with H5N1 influenza virus reveals a proviral role for CEACAM1. *Sci. Rep.* **8**, 1–13 (2018).

296. Klaile, E. *et al*. Carcinoembryonic antigen (CEA)-related cell adhesion molecules are co-expressed in the human lung and their expression can be modulated in bronchial epithelial cells by non-typable Haemophilus

influenzae, Moraxella catarrhalis, TLR3, and type I and II int. *Respir. Res.* **14**, 1–17 (2013).

297. Muenzner, P., Billker, O., Meyer, T. F. & Naumann, M. Nuclear factor-κB directs carcinoembryonic antigen-related cellular adhesion molecule 1 receptor expression in Neisseria gonorrhoeae-infected epithelial cells. *J. Biol. Chem.* **277**, 7438–7446 (2002).

298. Schirbel, A. *et al.* Mutual regulation of TLR/NLR and CEACAM1 in the intestinal microvasculature: implications for IBD pathogenesis and therapy. *Inflamm. Bowel Dis.* **25**, 294–305 (2019).

299. Kleefeldt, F. *et al.* Aging-related carcinoembryonic antigen-related cell adhesion molecule 1 signaling promotes vascular dysfunction. *Aging Cell* **18**, 1–13 (2019).

300. Wang, Y. *et al.* Loss of CEACAM1, a Tumor-Associated Factor, Attenuates Post-infarction Cardiac Remodeling by Inhibiting Apoptosis. *Sci. Rep.* **6**, 1–14 (2016).

301. Dankner, M., Gray-Owen, S. D., Huang, Y. H., Blumberg, R. S. & Beauchemin, N. CEACAM1 as a multi-purpose target for cancer immunotherapy. *Oncoimmunology* **6**, 1–16 (2017).

302. Takeuchi, A. *et al.* Loss of CEACAM1 is associated with poor prognosis and peritoneal dissemination of patients with gastric cancer. *Sci. Rep.* **9**, 1–9 (2019).

303. Beauchemin, N. & Arabzadeh, A. Carcinoembryonic antigen-related cell adhesion molecules (CEACAMs) in cancer progression and metastasis. *Cancer Metastasis Rev.* **32**, 643–671 (2013).

304. Hayashi, S., Osada, Y., Miura, K. & Simizu, S. Cell-dependent regulation of vasculogenic mimicry by carcinoembryonic antigen cell adhesion molecule 1 (CEACAM1). *Biochem. Biophys. Reports* **21**, 100734 (2020).

305. Fujita, M. *et al*. Carcinoembryonic antigen-related cell adhesion molecule 1 modulates experimental autoimmune encephalomyelitis via an iNKT cell-dependent mechanism. *Am. J. Pathol.* **175**, 1116–1123 (2009).

306. Iijima, H. *et al*. Specific Regulation of T Helper Cell 1–mediated Murine Colitis by CEACAM1. *J. Exp. Med.* **199**, 471–482 (2004).

307. Ford, L. B. *et al*. Characterization of conventional and atypical receptors for the Chemokine CCL2 on mouse leukocytes. *J. Immunol.* **193**, 400–411 (2014).

308. Baaten, B. J. G., Tinoco, R., Chen, A. T. & Bradley, L. M. Regulation of antigen-experienced T cells: lessons from the quintessential memory marker CD44. *Front. Immunol.* **3**, 1–12 (2012).

309. Inaba, B. K. *et al*. The tissue distribution of the B7-2 costimulator in mice: abundant expression on dendritic cells in situ and during maturation in vitro. *J. Exp. Med.* **180**, 1849–1860 (1994).

310. Takekoshi, T. *et al*. Identification of a novel marker for dendritic cell maturation, mouse transmembrane protein 123. *J. Biol. Chem.* **285**, 31876–31884 (2010).

311. Dudek, A. M., Martin, S., Garg, A. D. & Agostinis, P. Immature, semi-mature, and fully mature dendritic cells: toward a DC-cancer cells interface that augments anticancer immunity. *Front. Immunol.* **4**, 1–14 (2013).

312. Li, J. G. *et al*. CD80 and CD86 knockdown in dendritic cells regulates Th1/Th2 cytokine production in asthmatic mice. *Exp. Ther. Med.* **11**, 878–884 (2016).

313. Gu, X., Xiang, J., Yao, Y. & Chen, Z. Effects of RNA interference on CD80 and CD86 expression in bone marrow-derived murine dendritic cells. *Scand. J. Immunol.* **64**, 588–594 (2006).

314. Coutelier, J. -P *et al*. B lymphocyte and macrophage expression of

carcinoembryonic antigen-related adhesion molecules that serve as receptors for murine coronavirus. *Eur. J. Immunol.* **24**, 1383–1390 (1994).

315. Lee, K. A. *et al.* Characterization of age-associated exhausted CD8+ T cells defined by increased expression of Tim-3 and PD-1. *Aging Cell* **15**, 291–300 (2016).

316. Nagaishi, T., Iijima, H., Nakajima, A., Chen, D. & Blumberg, R. S. Role of CEACAM1 as a regulator of T cells. *Ann. N. Y. Acad. Sci.* **1072**, 155–175 (2006).

317. McLeod, R. L. *et al.* Characterization of murine CEACAM1 in vivo reveals low expression on CD8+ T cells and no tumor growth modulating activity by anti-CEACAM1 mAb CC1. *Oncotarget* **9**, 34459–34470 (2018).

318. Horstkorte, R. *et al.* Biochemical engineering of the side chain of sialic acids increases the biological stability of the highly sialylated cell adhesion molecule CEACAM1. *Biochem. Biophys. Res. Commun.* **283**, 31–35 (2001).

319. Katakowski, J. A. *et al.* Delivery of siRNAs to dendritic cells using DEC205-targeted lipid nanoparticles to inhibit immune responses. *Mol. Ther.* **24**, 146–155 (2016).

320. Suzuki, M. *et al.* A novel allergen-specific therapy for allergy using CD40-silenced dendritic cells. *J. Allergy Clin. Immunol.* **125**, 737-743.e6 (2010).

321. Ueshima, C. *et al.* CEACAM1 long isoform has opposite effects on the growth of human mastocytosis and medullary thyroid carcinoma cells. *Cancer Med.* **6**, 845–856 (2017).

322. Chen, D. *et al.* Carcinoembryonic antigen-related cellular adhesion molecule 1 isoforms alternatively inhibit and costimulate human T cell function. *J. Immunol.* **172**, 3535–3543 (2004).

323. Chen, L. *et al.* The short isoform of the CEACAM1 receptor in intestinal T cells regulates mucosal immunity and homeostasis via Tfh cell induction.

Immunity **37**, 930–946 (2012).

324. Kornecki, E., Walkowiak, B., Naik, U. & Ehrlich, Y. Activation of human platelets by a stimulatory monoclonal antibody. *The Journal of Biological Chemistry* vol. 265 10042–10048 (1990).

325. Martìn-Padura, I. *et al*. Junctional adhesion molecule, a novel member of the immunoglobulin superfamily that distributes at intercellular junctions and modulates monocyte transmigration. *J. Cell Biol*. **142**, 117–127 (1998).

326. Cera, M. R. *et al*. Increased DC trafficking to lymph nodes and contact hypersensitivity in junctional adhesion molecule-A–deficient mice. *J. Clin. Invest*. **114**, 729–738 (2004).

327. Ogasawara, N. *et al*. Induction of JAM-A during differentiation of human THP-1 dendritic cells. *Biochem. Biophys. Res. Commun*. **389**, 543–549 (2009).

328. Prota, A. E. *et al*. Crystal structure of human junctional adhesion molecule 1: Implications for reovirus binding. *Proc. Natl. Acad. Sci*. **100**, 5366–5371 (2003).

329. Fraemohs, L. *et al*. The functional interaction of the β2 integrin lymphocyte function-associated antigen-1 with junctional adhesion molecule-A is mediated by the I domain. *J. Immunol*. **173**, 6259–6264 (2004).

330. Ostermann, G., Weber, K. S. C., Zernecke, A., Schröder, A. & Weber, C. JAM-I is a ligand of the β2 integrin LFA-I involved in transendothelial migration of leukocytes. *Nat. Immunol*. **3**, 151–158 (2002).

331. Bazzoni, G. *et al*. Homophilic interaction of junctional adhesion molecule. *J. Biol. Chem*. **275**, 30970–30976 (2000).

332. Mandell, K. J., McCall, I. C. & Parkos, C. A. Involvement of the junctional adhesion molecule-1 (JAM1) homodimer interface in regulation of epithelial barrier function. *J. Biol. Chem*. **279**, 16254–16262 (2004).

333. Babinska, A. *et al*. Development of new antiatherosclerotic and antithrombotic drugs utilizing F11 receptor (F11r/JAM-A) peptides. *Biopolymers* **102**, 322–334 (2014).

334. Babinska, A. *et al*. F11-receptor (F11R/JAM) mediates platelet adhesion to endothelial cells: role in inflammatory thrombosis. *Thromb. Haemost.* **88**, 843–850 (2002).

335. Ebnet, K. Junctional adhesion molecules (JAMs): cell adhesion receptors with pleiotropic functions in cell physiology and development. *Physiol. Rev.* **97**, 1529–1554 (2017).

336. Peddibhotla, S. S. D., Brinkmann, B. F., Kummer, D. & Tuncay, H. Tetraspanin CD9 links junctional adhesion molecule-A to αvβ3 integrin to mediate basic fibroblast growth factor-specific angiogenic signaling. *Mol. Biol. Cell* **24**, 933–944 (2013).

337. Naik, M. U. & Naik, U. P. Junctional adhesion molecule-A-induced endothelial cell migration on vitronectin is integrin αVβ3 specific. *J. Cell Sci.* **119**, 490–499 (2006).

338. Wojcikiewicz, E. P. *et al*. LFA-1 binding destabilizes the JAM-A homophilic interaction during leukocyte transmigration. *Biophys. J.* **96**, 285–293 (2009).

339. Naik, M. U., Caplan, J. L. & Naik, U. P. Junctional adhesion molecule-A suppresses platelet integrin αIIbβ3 signaling by recruiting Csk to the integrin-c-Src complex. *Blood* **123**, 1393–1402 (2014).

340. Campbell, J. A. *et al*. Junctional adhesion molecule A serves as a receptor for prototype and field-isolate strains of mammalian reovirus. *J. Virol.* **79**, 7967–7978 (2005).

341. Sosnovtsev, S. V. *et al*. Identification of human junctional adhesion molecule 1 as a functional receptor for the hom-1 calicivirus on human cells. *MBio* **8**, 1–19 (2017).

342. Barton, E. S. *et al*. Junction adhesion molecule is a receptor for reovirus. *Cell* **104**, 441–451 (2001).

343. Naik, M. U., Vuppalanchi, D. & Naik, U. P. Essential role of Junctional adhesion molecule-1 in basic fibroblast growth factor-induced endothelial cell migration. *Arterioscler. Thromb. Vasc. Biol.* **23**, 2165–2171 (2003).

344. Corada, M. *et al*. Junctional adhesion molecule-A-deficient polymorphonuclear cells show reduced diapedesis in peritonitis and heart ischemia-reperfusion injury. *Proc. Natl. Acad. Sci. U. S. A.* **102**, 10634–10639 (2005).

345. Ostermann, G. *et al*. Involvement of JAM-A in mononuclear cell recruitment on inflamed or atherosclerotic endothelium inhibition by soluble JAM-A. *Arterioscler. Thromb. Vasc. Biol.* **25**, 729–735 (2005).

346. Matsutani, T. *et al*. Plasmacytoid dendritic cells employ multiple cell adhesion molecules sequentially to interact with high endothelial venule cells - molecular basis of their trafficking to lymph nodes. *Int. Immunol.* **19**, 1031–1037 (2007).

347. Murakami, M. *et al*. Inactivation of junctional adhesion molecule-A enhances antitumoral immune response by promoting dendritic cell and T lymphocyte infiltration. *Cancer Res.* **70**, 1759–1765 (2010).

348. Bullard, D. C. *et al*. Critical requirement of CD11b (Mac-1) on T cells and accessory cells for development of experimental autoimmune encephalomyelitis. *J. Immunol.* **175**, 6327–6333 (2005).

349. Fagerholm, S. C., Guenther, C., Asens, M. L., Savinko, T. & Uotila, L. M. Beta2-Integins and interacting proteins in leukocyte trafficking, immune supression, and immunodeficiency disease. *Front. Immunol.* **10**, 1–10 (2019).

350. Stephen, T. L. *et al*. Transport of Streptococcus pneumoniae capsular polysaccharide in MHC class II tubules. *PLoS Pathog.* **3**, (2007).

351. Blum, J. S., Wearsch, P. A. & Cresswell, P. *Pathways of antigen processing*. *Annual Review of Immunology* vol. 31 (2013).

352. Cera, M. R. *et al*. JAM-A promotes neutrophil chemotaxis by controlling integrin internalization and recycling. *J. Cell Sci.* **122**, 268–277 (2009).

353. Maschio, A. Del *et al*. Leukocyte recruitment in the cerebrospinal fluid of mice with experimental meningitis is inhibited by an antibody to junctional adhesion molecule (JAM). *J. Exp. Med.* **190**, 1351–1356 (1999).

354. Woodfin, A. *et al*. JAM-A mediates neutrophil transmigration in a stimulus-specific manner in vivo: evidence for sequential roles for JAM-A and PECAM-1 in neutrophil transmigration. *Blood* **110**, 1848–1856 (2007).

355. Murakami, M. *et al*. Abrogation of junctional adhesion molecule-A expression induces cell apoptosis and reduces breast cancer progression. *PLoS One* **6**, (2011).

356. Khandoga, A. *et al*. Junctional adhesion molecule-A deficiency increases hepatic ischemia-reperfusion injury despite reduction of neutrophil transendothelial migration. *Blood* **106**, 725–734 (2019).

357. Bednarek, R. *et al*. Functional inhibition of F11 receptor (F11R/junctional adhesion molecule-A/JAM-A) activity by a F11R-derived peptide in breast cancer and its microenvironment. *Breast Cancer Res. Treat.* **179**, 325–335 (2020).

358. Babinska, A. *et al*. A peptide antagonist of F11R/JAM-A reduces plaque formation and prolongs survival in an animal model of atherosclerosis. *Atherosclerosis* **284**, 92–101 (2019).

359. Kallies, A. Distinct regulation of effector and memory T-cell differentiation. *Immunol. Cell Biol.* **86**, 325–332 (2008).

360. Chauhan, A. K. Human CD4+ T-cells: A role for low-affinity Fc receptors. *Front. Immunol.* **7**, (2016).

361. Adler, J. & Parmryd, I. Quantifying colocalization: the MOC is a hybrid coefficient - an uninformative mix of co-occurrence and correlation. *J. Cell Sci.* **132**, 1–3 (2019).

362. Da Silva, C., Wagner, C., Bonnardel, J., Gorvel, J. P. & Lelouard, H. The Peyer's patch mononuclear phagocyte system at steady state and during infection. *Front. Immunol.* **8**, (2017).

363. Shen,B., Delaney, M., K., Du, X. Inside-out, outside-in, and inside-outside-in: G protein signaling. *Curr. Opin. Cell Biol.* **24**, 600–606 (2012).

364. DiFranco, K. M. *et al.* Leukotoxin (Leukothera®) targets active Leukocyte Function Antigen-1 (LFA-1) protein and triggers a lysosomal mediated cell death pathway. *J. Biol. Chem.* **287**, 17618–17627 (2012).

365. Puigdomènech, I. *et al.* HIV transfer between CD4 T cells does not require LFA-1 binding to ICAM-1 and is governed by the interaction of HIV envelope glycoprotein with CD4. *Retrovirology* **5**, 1–13 (2008).

366. Weber, C., Fraemohs, L. & Dejana, E. The role of junctional adhesion molecules in vascular inflammation. *Nat. Rev. Immunol.* **7**, 467–477 (2007).

367. Immenschuh, S. *et al.* Transcriptional induction of junctional adhesion molecule-C gene expression in activated T cells. *J. Leukoc. Biol.* **85**, 796–803 (2009).

368. Kobayashi, H. *et al.* The tetraspanin CD9 is preferentially expressed on the human CD4 +CD45RA+ naive T cell population and is involved in T cell activation. *Clin. Exp. Immunol.* **137**, 101–108 (2004).

369. Pugholm, L. H. *et al.* Phenotyping of leukocytes and leukocyte-derived extracellular vesicles. *J. Immunol. Res.* (2016) doi:10.1155/2016/6391264.

370. Tai, X. G. *et al.* A role for CD9 molecules in T cell activation. *J. Exp. Med.* **184**, 753–758 (1996).

371. Khounlotham, M. *et al*. Compromised intestinal epithelial barrier induces adaptive immune compensation that protects from colitis. *Immunity* **37**, 563–573 (2012).

372. Ozaki, H. *et al*. Cutting edge: combined treatment of TNF-alpha and IFN-gamma causes redistribution of junctional adhesion molecule in human endothelial cells. *J. Immunol.* **163**, 553–7 (1999).

373. Laukoetter, M. G. *et al*. JAM-A regulates permeability and inflammation in the intestine in vivo. *J. Exp. Med.* **204**, 3067–3076 (2007).

374. Ardavín, C. Origin, precursors and differentiation of mouse dendritic cells. *Nat. Rev. Immunol.* **3**, 582–590 (2003).

375. Luissint, A. C. *et al*. Macrophage-dependent neutrophil recruitment is impaired under conditions of increased intestinal permeability in JAM-A-deficient mice. *Mucosal Immunol.* **12**, 668–678 (2019).

376. Jalkanen, S. & Salmi, M. Lymphatic endothelial cells of the lymph node. *Nat. Rev. Immunol.* **Feb 24**, (2020).

377. Gröbner, S., Lukowski, R., Autenrieth, I. B. & Ruth, P. Lipopolysaccharide induces cell volume increase and migration of dendritic cells. *Microbiol. Immunol.* **58**, 61–67 (2014).

378. Hu, J. & August, A. Naive and Innate Memory Phenotype CD4 + T Cells Have Different Requirements for Active Itk for Their Development . *J. Immunol.* **180**, 6544–6552 (2008).

379. Antunes, D. A. *et al*. Interpreting T-Cell cross-reactivity through structure: Implications for TCR-based cancer immunotherapy. *Front. Immunol.* **8**, 1–16 (2017).

380. Sun, L. Z. *et al*. Comparison between ovalbumin and ovalbumin peptide 323-339 responses in allergic mice: Humoral and cellular aspects. *Scand. J. Immunol.* **71**, 329–335 (2010).

381. Lu, Z. *et al*. Toll-like receptor 4 activation in microvascular endothelial cells triggers a robust inflammatory response and cross talk with mononuclear cells via interleukin-6. *Arterioscler. Thromb. Vasc. Biol*. **32**, 1696–1706 (2012).

382. Bachmann, M. F. & Oxenius, A. Interleukin 2: From immunostimulation to immunoregulation and back again. *EMBO Rep.* **8**, 1142–1148 (2007).

383. Smolen, J. S. & Aletaha, D. Rheumatoid arthritis therapy reappraisal: Strategies, opportunities and challenges. *Nat. Rev. Rheumatol*. **11**, 276–289 (2015).

384. Scott, D. L., Wolfe, F. & Huizinga, T. W. J. Rheumatoid arthritis. *Lancet* **376**, 1094–1108 (2010).

385. Farutin, V. *et al*. Molecular profiling of rheumatoid arthritis patients reveals an association between innate and adaptive cell populations and response to anti-tumor necrosis factor. *Arthritis Res. Ther*. **21**, 1–14 (2019).

386. Conigliaro, P. *et al*. Characterization of the anticollagen antibody response in a new model of chronic polyarthritis. *Arthritis Rheum.* **63**, 2299–2308 (2011).

387. Padden, M. *et al*. Differences in expression of junctional adhesion molecule-A and ß-catenin in multiple sclerosis brain tissue: Increasing evidence for the role of tight junction pathology. *Acta Neuropathol*. **113**, 177–186 (2007).

388. Jongbloed, S. L. *et al*. Plasmacytoid dendritic cells regulate breach of self-tolerance in autoimmune arthritis. *J. Immunol*. **182**, 963–968 (2009).

389. Benson, R. A. *et al*. Identifying the Cells Breaching Self-Tolerance in Autoimmunity. *J. Immunol*. **184**, 6378–6385 (2010).

390. Nickdel, M. B. *et al*. Dissecting the contribution of innate and antigen-specific pathways to the breach of self-tolerance observed in a murine model of arthritis. *Ann. Rheum. Dis.* **68**, 1059–1066 (2009).

391. Kanaan, S. B. *et al*. Immunogenicity of a rheumatoid arthritis protective sequence when acquired through microchimerism. *Proc. Natl. Acad. Sci. U. S. A.* **116**, 19600–19608 (2019).

392. O'Dell, J. R. *et al*. HLA-DRB1 typing in rheumatoid arthritis: Predicting response to specific treatments. *Ann. Rheum. Dis.* **57**, 209–213 (1998).

393. Hinks, A. *et al*. Association between the PTPN22 gene and rheumatoid arthritis and juvenile idiopathic arthritis in a UK population: Further support that PTPN22 is an autoimmunity gene. *Arthritis Rheum.* **52**, 1694–1699 (2005).

394. Al-Laith, M. *et al*. Arthritis prevention in the pre-clinical phase of RA with abatacept (the APIPPRA study): A multi-centre, randomised, double-blind, parallel-group, placebo-controlled clinical trial protocol. *Trials* **20**, 1–15 (2019).

395. Fleischmann, R. *et al*. Efficacy of Abatacept and Adalimumab in Patients with Early Rheumatoid Arthritis With Multiple Poor Prognostic Factors: Post Hoc Analysis of a Randomized Controlled Clinical Trial (AMPLE). *Rheumatol. Ther.* **6**, 559–571 (2019).

396. Weinblatt, M. E. *et al*. Safety of abatacept administered intravenously in treatment of rheumatoid arthritis: Integrated analyses of up to 8 years of treatment from the abatacept clinical trial program. *J. Rheumatol.* **40**, 787–797 (2013).

397. Schiff, M., Poncet, C. & Bars, M. Le. Efficacy and safety of abatacept therapy for rheumatoid arthritis in routine clinical practice. *Int. J. Clin. Rheumtol.* **5**, 581–591 (2010).

398. Palmer, G., Gabay, C. & Imhof, B. A. Leukocyte migration to rheumatoid joints: enzymes take over. *Arthritis Rheum.* **54**, 2707–2710 (2006).

399. Mense, S. M. *et al*. Gene expression profiling reveals the profound upregulation of hypoxia-responsive genes in primary human astrocytes.

Physiol. Genomics **25**, 435–449 (2006).

400. Ben-Zvi, M., Amariglio, N., Paret, G. & Nevo-Caspi, Y. F11R expression upon hypoxia is regulated by RNA editing. *PLoS One* **8**, 1–12 (2013).

401. Akhavani, M. A. *et al*. Hypoxia upregulates angiogenesis and synovial cell migration in rheumatoid arthritis. *Arthritis Res. Ther.* **11**, 1–11 (2009).

402. Ng, C. T. *et al*. Synovial tissue hypoxia and inflammation in vivo. *Ann. Rheum. Dis.* **69**, 1389–1395 (2010).

403. Sivakumar, B. *et al*. Synovial hypoxia as a cause of tendon rupture in rheumatoid arthritis. *J. Hand Surg. Am.* **33**, 49–58 (2008).

404. Lund-Olesen, K. Oxygen tension in synovial fluids. *Arthritis Rheum.* **13**, 769–776 (1970).

405. Falchuk, K. H., Goetzl, E. J. & Kulka, J. P. Respiratory gases of synovial fluids. *Am. J. Med.* **49**, 223–231 (1970).

406. Fang, T.-J. *et al*. F11R mRNA expression and promoter polymorphisms in patients with rheumatoid arthritis. *Int. J. Rheum. Dis.* **19**, 127–133 (2016).

407. Merad, M., Sathe, P., Helft, J., Miller, J. & Mortha, A. The Dendritic Cell Lineage: Ontogeny and Function of Dendritic Cells and Their Subsets in the Steady State and the Inflamed Setting. *Annu. Rev. Immunol.* **31**, 563–604 (2013).

408. Major, E. O. Progressive multifocal leukoencephalopathy in patients on immunomodulatory therapies. *Annu. Rev. Med.* **61**, 35–47 (2010).